University of Oxford

Department of Biology

Avian influenza H9N2-specific changes in the adaptive immune receptor repertoire of *Gallus gallus domesticus* following vaccination and infectious challenge

Ștefan Dascălu

University College

A thesis submitted for the degree of

Doctor of Philosophy (DPhil)

Hilary Term 2023

Avian influenza H9N2-specific changes in the adaptive immune receptor repertoire of *Gallus gallus domesticus* following vaccination and infectious challenge

Ștefan Dascălu, University College

DPhil in Interdisciplinary Bioscience, Hilary Term 2023

Thesis Abstract

Avian influenza viruses cause major losses to the poultry sector each year and also pose a significant risk for cross-species transmission to humans, where the disease manifestations can be very severe. However, within avian hosts, there is still a limited understanding of the adaptive immune system in the contexts of both health and disease, and the immunological mechanisms which underpin vaccine-induced protective responses against infectious challenge with pathogens such as avian influenza. As the ability of the adaptive immune system to recognise specific antigens is dependent on the T and B cell receptors which together comprise the adaptive immune receptor repertoire, understanding the determinants which shape its specificities and diversity is paramount for both improving our knowledge of the avian immune system and improving current prevention and control strategies such as vaccination. In this thesis, I present a comprehensive analysis of the domestic chicken (*Gallus gallus domesticus*) adaptive immune receptor repertoire upon infection and/or vaccination with H9N2 avian influenza – a pathogen that is widely prevalent across the world and poses significant risk both to the poultry sector and to human health and wellbeing. At the time of writing, no published research has examined the avian adaptive immune repertoire using high throughput sequencing, and no repertoire studies have been performed in birds that were infected with and/or vaccinated against avian influenza. My analyses thus provide valuable information on the avian adaptive immune system and the impacts of H9N2 infection and/or vaccination on the avian adaptive immune receptor repertoires.

Declaration

I herewith declare that I have produced this thesis without the prohibited assistance of third parties and without making use of aids other than those specified in the text and acknowledgements section; notions taken over directly or indirectly from other sources have been identified as such.

This thesis has not previously been presented in identical or similar form to any other English or foreign examination board. The thesis work was conducted from October 2018 to January 2023 under the supervision of Associate Professor Adrian L. Smith and Professor Michael B. Bonsall from The University of Oxford and Professor Munir Iqbal at The Pirbright Institute.

Ștefan Dascălu

University of Oxford, January 2023

Acknowledgements

I am grateful for all the help, supervision, and guidance received by my thesis advisors Adrian L. Smith, Michael B. Bonsall, and Munir Iqbal. I am also grateful for the funding received from the Biotechnology and Biological Sciences Research Council (BBSRC), The University of Oxford, and The Pirbright Institute. At the same time, I am thankful to my colleagues and friends at Oxford and Pirbright that have provided help and advice, particularly Patrik Flammer, Steven Fiddaman, Robert Dixon, Stephen Preston, Joshua E. Sealy, and Jean-Remy Sadeyen.

On a personal note, I dedicate this doctoral thesis to my wonderful family who have always supported me during my academic endeavours and beyond. I am very grateful to have been blessed with my loving parents, Mihai and Rodica, who have been the two pillars of strength throughout my life. My grandparents, Mery, Mircea, Olga, and my late grandfather Zaharia who passed away during the COVID pandemic helped raise me and have always motivated me to become a better person. My wonderful and beloved wife Andreea was always at my side during my journey at the University of Oxford, and I am very grateful for the happiness, the love, and the support which she offered me throughout.

Last but not least, I deeply treasure the friendship and help which I received from Vlad Bădeliță, Alex Beeton, Mahan Ghafari, Eva Polaki, Hamideh Rimaz, Assen Rizov, Vlad Smochină, Cristian Apetrei, Oana and Ovidiu Strugaru, Cătălin Raiu, Emilian Popovici, Cristian Onuț and many others who were always there for me.

Vă mulțumesc!

Table of Contents

List of Figures and Tables

Chapter I:

Chapter II:

Chapter III:

Chapter IV:

Chapter V:

Appendix:

Chapter I: Introduction

I.1. Abstract

Influenza A viruses are single-stranded RNA viruses that infect a wide variety of hosts. Avian influenza viruses (AIVs) have their natural reservoir in wild aquatic birds and pose major concerns due to their wide prevalence, and their propensity to infect other species including domestic animals and humans. A high disease severity can accompany infection, and AIVs cause major economic losses to the agricultural sector each year. As avian species serve as the main hosts for these viruses, the study of their immune responses to infection provides important information for implementing prevention and control strategies. In response to infectious challenge, the innate and adaptive branches of the avian immune system contribute to protection, with species-specific differences being present regarding both components of immunity. As for influenza A virus infection in humans, the intrinsic abilities of AIVs to evade host immune responses through antigenic drift and antigenic shift renders the vaccination of birds against these pathogens extremely challenging. Understanding the changes in the adaptive immune receptor repertoire in response to AIV infection and vaccination may provide important information about these phenomena, as previous research was able to show in species such as mice or humans. To date, there have been very limited attempts to characterise the avian adaptive immune receptor repertoire, and no studies have used high throughput sequencing technology to examine the repertoire changes of avian hosts, following AIV infection. The chapter concludes by stating the aims and objectives of the thesis, which focuses on the avian adaptive immune repertoire in the context of AIV vaccination and infectious challenge.

I.2. Outline

In this chapter, I will explore the avian adaptive immune responses to influenza A virus infection, with emphasis on the adaptive immune receptor repertoires in birds. To date, very limited work has been carried out on the adaptive immune repertoire of birds, in spite of the fruitful results that such endeavours have provided in species such as mice and

humans. I will first introduce influenza A viruses and describe their biology, to then contextualise their ecological impact on humans and other animal species. Emphasis will be put on avian influenza viruses, which are used throughout this thesis to illustrate how infectious agents can develop and alter the adaptive immune responses of avian hosts. I will then describe the innate and adaptive components of avian immunity to influenza A viruses, and present both avian-specific and species-specific factors that influence susceptibility and disease progression. Subsequently, I provide information on the adaptive immune receptor repertoire, the analysis of which constitutes the main focus of the thesis. Finally, the chapter concludes by defining the aims and objectives of the thesis and presenting the structure of the following chapters, whilst also underlining the potential of the research for increasing our understanding of the avian adaptive immune system in the contexts of both health and disease.

I.3. Influenza A viruses

I.3.1. Background

Infectious diseases cause a major medical, economic, and social burden each year, resulting in significant morbidity and mortality. Historical records dating as far back as ancient times indicate that humanity has been facing the threat of pathogenic organisms since the dawn of our species on this planet. Moreover, infectious diseases have had dramatic manifestations throughout history, causing devastating effects and loss of life, especially when in the form of epidemics and pandemics. Out of the many different types of infectious biological organisms that are causative agents of diseases, viruses stand out due to their relative biological simplicity, obligate dependence on and intimate associations with their hosts.

Influenza or flu is a well-known and familiar infection with its history dating back as to the early days of humankind [1,2]. The first records of a flu-like epidemics date back to antiquity, although the exact nature of the illnesses in question are still up for debate [3]. The term "influenza" originated in the 15th century from the "influence of the stars" – a large and severe epidemic that affected Europe and possibly Asia and Africa [2]. The first

official record of influenza is the 1918 "Spanish flu" pandemic which caused a very high death toll across the world. Although not as dramatic as the pandemic manifestations of the disease, the seasonal epidemics of influenza are also major causes of concern, given the substantial morbidity and mortality associated with infection.

The causative agents of influenza disease are the influenza viruses, which are single-stranded, negative-sense, segmented RNA viruses, comprised of four distinct genera (A, B, C, and D) of the *Orthomyxoviridae* family [1]. Influenza A viruses exhibit a wide range of host species, including poultry, swine, horses, bats, and humans [4]. By contrast, influenza B and C viruses have their primary reservoir in humans, and influenza D has only recently been identified in even-toed ungulates such as pigs, goats and cattle [5,6]. Of these viruses, influenza A represents a major concern due to their broad host specificity and ability to jump from one host species to another. Indeed, influenza A viruses cause severe economic losses due to infection of domestic animal hosts, and also pose a significant zoonotic risk when they cross the species barrier into humans [1,6–8].

I.3.2. Virion structure and infection mechanism

The influenza A virion has an elaborate structure comprised of the segmented genome alongside several proteins and a lipid envelope derived from the cellular membrane of the host cell [5]. The centre of the virion contains 8 single-stranded, negative-sense RNA (vRNA) segments which code for 10 viral proteins. This segmented viral genome forms the ribonucleoprotein (RNP) complex alongside nucleoproteins (NP) and three polymerase proteins – polymerase basic 1 (PB1), polymerase basic 2 (PB2) and polymerase acid (PA). The matrix protein (M1) connects the RNP complex with the lipid envelope, which contains three viral proteins: haemagglutinin (HA), neuraminidase (NA), and matrix protein 2 (M2). The NP, HA, NA, and polymerase subunit proteins are each encoded by a separate RNA segment. By contrast, the matrix proteins M1 and M2 are encoded by the same RNA segment using different reading frames [5]. Similarly, two more non-structural proteins present in the virion are encoded from a single RNA segment: the non-structural protein 1 (NS1) and the nuclear export protein (NEP) [9]. These structural characteristics of the

influenza A virus have profound implications on the processes of infection and pathogenesis.

The entry of Influenza A viruses into cells is (generally) through receptor-mediated endocytosis, after the virion attaches to the sialic acids (SA) present on the cellular surface (**Figure 1.1**) [5,6]. This process is facilitated by the HA proteins which specifically bind SA moieties of the host cells. Importantly, the type of linkage between the SA moiety and subterminal galactose of glycans dictates the ability of the HA proteins to infect specific hosts [6]. For instance, avian-adapted influenza A viruses show preference for α2,3-linked SA (SAα2,3Gal), as this is the predominant type of SA linkage found in avian hosts. By contrast, human-adapted strains bind α2,6-linked SA (SAα2,6Gal), which is the predominant linkage found in the human bronchus epithelia [6]. However, most species contain both types of linkages, and thus the host-specificity imposed by SA linkages is not absolute. After attachment to the cellular surface, influenza A virions are internalised to the endocytic compartments, where the low pH triggers conformational changes in the HA molecule, resulting in cleavage [1,5]. The joint action of the cleaved HA subunits then opens a pore in the endosomal membrane and releases the virion contents into the cytoplasm. Once inside the cellular cytoplasm, the RNPs are transported into the nucleus as they contain nuclear localisation signals. Inside the nucleus, transcription and replication occur, as the genomic RNA is accessed by the RNA-dependent RNA polymerase complex formed by the PB1, PB2, and PA proteins [1,5]. Following transcription and replication, the influenza RNA molecules begin to associate with the viral proteins which were produced by the host cell's ribosomes and imported back into the nucleus, resulting in the formation of RNPs. These are then transported into the cytoplasm through the nuclear export machinery of the host cell and are subsequently localised near the cellular membrane [1,5].

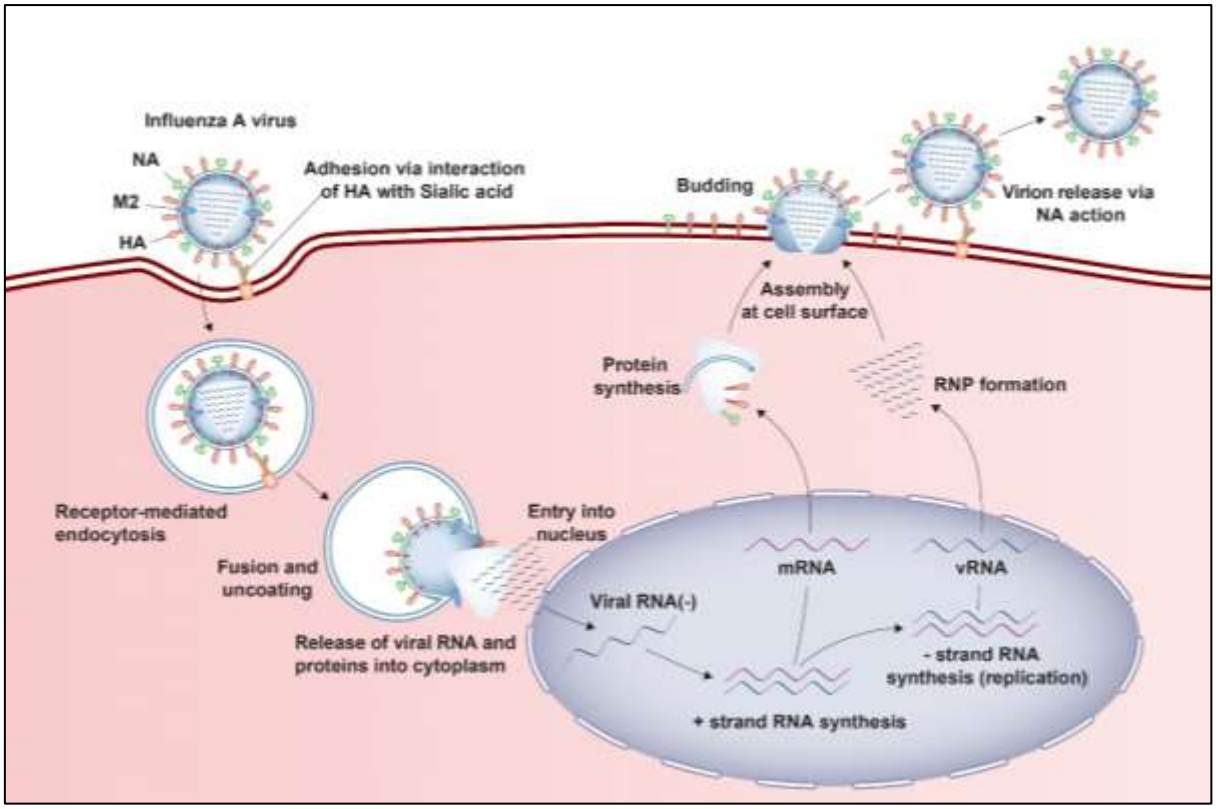

Figure 1.1: Mechanism of infection and replication of Influenza A viruses.

The virus enters the cell via receptor mediated endocytosis following attachment of the haemagglutinin (HA) molecules to the sialic acid moieties on the cell surface. Subsequent fusion with the endosomal membrane and release of the virion contents into the cytoplasm occurs, which are then transported to the nucleus. Following transcription and replication, the viral RNA (vRNA) is exported into the cytoplasm where it forms ribonucleoprotein complexes with the viral proteins that were produced by the host ribosomes. Budding occurs at the membrane surface, with the virion's release being mainly mediated by the activity of the neuraminidase (NA) protein. Adapted from Herold et al. (2015) [10].

The formation of buds on the cellular membrane represents one of the last steps before the mature virions are released from the cells. It is believed that several viral proteins are involved in this process, including the HA, NA, M1, and M2 proteins, with their conjoined action culminating in membrane scission [1,5]. The final release of influenza virions from the cell requires an energy-driven process catalysed by the NA protein which cleaves the SA moieties from the host cell, thus countering the anchoring effect of the HA proteins to the cellular membrane. As these viral proteins both interact with SA residues but have

opposite effects, a careful balance exists between their functions in order maximise their ability to attach to and infect host cells and to facilitate their release [1,5]. Furthermore, not only are these two proteins essential for the infectious cycle itself, but they also contribute to the ability of influenza A viruses to evade host immunity.

I.3.3. Classification and mechanisms of immune evasion

Influenza A viruses are classified with respect to their HA and NA surface glycoproteins, which also represent the major antigenic targets against which the adaptive immune response is mounted [5,6]. To date, at least 18 HA (H1-H18) and 11 NA (N1-N11) subtypes have been identified in various animal species [6]. Both glycoproteins contribute to the evasion of host immune responses, and this inherent feature poses considerable challenges to controlling the spread of influenza A in both human and non-human animal hosts [5–7,11]. Two phenomena play a key role in the ability of influenza A to evade host immunity. The first is a consequence of the relatively high replication error rate of RNA viruses and the selective pressure imposed by the immune system. The process – termed antigenic drift – results in the rapid accumulation of mutations in the HA and NA and facilitates viral persistence and reinfections of hosts, being responsible for the seasonal epidemics of influenza A in humans [5,6]. The other, more dramatic mechanism of immune escape refers to the phenomenon of antigenic shift [5,6]. This is made possible by the segmented nature of the influenza genome which allows for reassortment to occur between different viruses when coinfection is present. Although viral reassortment was not yet observed between influenza viruses belonging to distinct genera, antigenic shift is responsible for the pandemic strains of influenza A which result from coinfection with different subtypes. From the perspective of the host immune system, these reassorted influenza A viruses can be essentially regarded as novel pathogens, thereby posing a major threat worldwide.

I.3.4. Influenza A infections in humans: seasonal epidemics and pandemics

In humans, the current circulating strains of influenza A are H1N2 and H3N2, being responsible for the seasonal flu epidemics each year, alongside two influenza lineages

belonging to the B genus [1,5]. However, there have been many instances when influenza A viruses from other species were able to infect human hosts. Although these events are worrisome as they can be accompanied by high mortality, the inability of efficient human-to-human transmission generally results in the outbreaks being contained. For instance, there are numerous documented cases of H5N1 avian influenza infections in humans since it was first detected in Chinese geese farms in 1996 [1]. As this subtype causes around 60% mortality in humans, many of these infections had fatal outcomes. However, although there are some documented cases of limited human-to-human transmission (usually within households), its inability to spread efficiently within human populations did not allow for H5N1 influenza to trigger a pandemic. By contrast, the zoonotic influenza subtypes which gained the ability of human-to-human transmission were responsible for all influenza pandemics, causing substantial morbidity and mortality worldwide [1,5].

Based on the records from recent years, influenza A pandemics occur at an interval of 10-40 years and affect 20-40% of the world population [1,5]. From the 1900s onwards, humanity was faced by four influenza pandemics: the 1918 "Spanish" influenza, the 1957 "Asian flu", the 1968 "Hong Kong" influenza, and the 2009 "swine flu" [5,12]. Cross-species transmission coupled with viral reassortment events were responsible for each of these pandemics, as the causative viruses contained fragments of both human and animal origin. For instance, the 1918 H1N1 influenza contains both avian- and human-adapted signatures [13], and there is evidence of non-human mammalian circulation for multiple years before effective human transmission occurred [14]. Similarly, the 1957 H2N2 virus had avian-like HA and NA genes [15,16], and the 1968 H3N2 had PB1 and HA related to the Eurasian avian lineages of influenza [17]. In 2009, the H1N1 pandemic influenza is believed to have originated following multiple reassortment events involving human-, avian-, and swine-adapted viruses [17]. Indeed, there have been many documented cases of zoonotic influenza infections, particularly from domestic animals. Of these, avian influenza viruses are the most worrisome, as there have been many cases with a fatal outcome.

I.3.5. Avian influenza viruses

The broad host specificity of influenza A viruses coupled with its abilities of immune evasion via antigenic shift and antigenic drift allow for circulation to occur in a wide range of species across the planet. However, the natural reservoir of influenza A viruses is in wild aquatic birds, where the infections cause little to no mortality and are usually limited to the gastrointestinal tract which serves as the primary site of infection [1,5,6,8]. From these hosts, viruses can readily transmit to domestic birds, where the disease severity is often much higher. Indeed, domestic birds are of particular importance as these animals represent a virus reservoir where avian influenza A viruses are enzootic. Furthermore, avian influenza A viruses, hereafter referred to as avian influenza viruses (AIVs), readily evolve and diversify within poultry which often serve as intermediates from which the viruses can spread to other domestic animals, wild birds and humans [5,6,18,19]. Indeed, not only are poultry readily infected by AIVs, but these events are associated with significant economic losses each year [8,20–23].

AIVs are further classified based on the disease severity which they cause when infecting avian hosts into low pathogenic and high pathogenic avian influenza (LPAI and HPAI, respectively) [24,25]. The LPAI strains often cause mild symptoms of infection whereas the HPAI strains cause severe disease manifestations, with up to 100% mortality [25,26]. This difference in pathogenicity relates to the ability of the HA precursor protein to be cleaved by host proteases [24]. For LPAI strains, the presence of a monobasic cleavage site in the HA precursor allows only trypsin-like host proteases to cleave the protein, therefore restricting viral replication to the respiratory and gastrointestinal tracts. However, HPAI strains possess a polybasic cleavage site which allows for ubiquitous proteases (e.g. furin) to cleave the HA protein, thus enabling systemic replication and a much more severe disease manifestation [25,26]. The ability of some strains of AIV to switch from LPAI to HPAI phenotype relates to the acquisition of a polybasic cleavage site in the HA through mutation, insertions, or genetic reassortment [27]. So far, the only AIVs possessing the ability to evolve from LPAI into HPAI viruses are the H5 and H7 subtypes, which have been responsible for highly severe disease outbreaks in poultry and human infections with a high fatality rates [26,28–31].

I.3.6. H9N2 avian influenza

LPAI strains also pose major economic and public health concerns, although the disease manifestations which they cause are less severe [32]. Importantly, their high prevalence in poultry farms across the world increases the likelihood of transmission to humans, and their high propensity for mutation, coupled with the ability to reassort with HPAI strains provide major threats at a global level. One particularly prominent LPAI strain is subtype H9N2 which has become endemic in many countries across Asia, the Middle East, northern and western Africa, and some parts of Europe [33–36]. Furthermore, H9N2 AIVs have been causing yearly zoonotic infections, with half of these having occurred over the past 5 years; there is also evidence of increased H9N2 seropositivity among agricultural workers [33,37–41]. As such, given the substantial economic impact on the poultry sector, the continued evidence of zoonotic infections, and the potential for AIVs to undergo reassortment and generate novel strains, several countries have deployed national strategies in order to contain viral spread and prevent possible human outbreaks.

I.3.7. Prevention and control

To date, vaccination against influenza viruses remains the only method of offering protection against disease in humans. Similarly, veterinary vaccination against influenza is routinely administered under agricultural settings in many countries, especially for poultry and pigs [42].

Vaccination of domestic birds against AIVs dates back to the early parts of the 20th century, when chickens that recovered from "fowl plague" (now known to be H7 HPAI) were found to be resistant after subsequent exposure to the disease [28,42,43]. Early attempts of creating a vaccine involved inactivating the virus contained in biological material from birds through various physical processes such as heating or drying, or chemical processes such as using formalin or phenol glycerine. The unrefined implementation of such mechanisms usually resulted in vaccine failures, either because the HPAI was incompletely inactivated or due to insufficient antigenic stimulation following vaccination [44]. As such, the efficient use of epidemiological control measures such as the culling of poultry during outbreaks

substituted the need to implement HPAI vaccines until the mid-1990s. By contrast, LPAI vaccine development started in the 1960s, and the first vaccines were approved in the USA in 1978, as the infection of poultry (especially turkeys) resulted in severe losses in egg production, even though the disease itself did not cause severe symptoms [42,44].

According to the Food and Agriculture Organisation (FAO), poultry represents the major and most accessible source of meat, being expected to represent 41% of global meat production by 2030 [45]. Moreover, the global egg production from chickens alone was estimated at more than 86.67 billion tonnes in 2020 and it is projected to increase in the upcoming years [46]. The health status of these birds is thus a vital issue, having implications for both industrial and non-industrial settings. The global economic impact of AIV, including both low and highly pathogenic strains is extremely high, as epidemics are extinguished mainly through the culling of birds. In addition, improved diagnostic capabilities and changes in farming practices have been implemented in many countries in order to enhance the surveillance and control of AIV outbreaks in domestic animals. However, influenza veterinary vaccination remains the main strategy for preventing infectious outbreaks and minimising the burden of the disease [42] and some countries (e.g. China) have successfully implemented national veterinary vaccination against AIV which were effective in controlling the disease [47].

Just as for the seasonal influenza vaccines in humans (for a review, see [48]), the effectiveness of vaccine-induced immune memory decreases rapidly in non-human animals due to the emergence of escape variants [11,49–51]. Indeed, both antigenic drift and antigenic shift phenomena have profound implications for vaccine-induced immunity in both humans and domestic animals. What's more, the implementation of influenza A vaccines for veterinary use is poorly regulated, with reduced coordination within and between countries and frequent use of vaccines with sub-optimal homology to circulating [52]. However, these efforts involve the use of inactivated vaccines, and there is still a limited understanding about both the infectious process itself and the immunological effects of vaccination within avian hosts. Indeed, more information is required on the avian immune responses to AIVs for the efficient control of these pathogens [32,53].

I.4. Immune responses to AIV infection in birds

I.4.1. Innate responses

The avian immune system provides a fascinating and important research model in the context of both health and disease. Although birds and mammals diverged approximately 200 million years ago from a common reptilian ancestor, many functions of the innate and adaptive branches of the immune system are shared between these lineages [54]. The first lines of defence against pathogens such as AIVs are provided by the innate components of immunity, which consist of nonspecific inflammatory and cellular responses.

The innate responses to AIV can broadly be classified into two main types, based on the nature of the inflammatory response triggered by infection [55]. On the one hand, a protective type I and type III interferon response has been suggested to control a hyper-inflammation and induce an antiviral state that limits AIV replication and associated pathology. On the other hand, an uncontrolled inflammatory response involving the secretion of pro-inflammatory cytokines results in a "cytokine storm" which greatly contributes to the morbidity and mortality of AIV infection. The protective interferon (IFN) response is characteristic of species that are less prone to suffer severe forms of HPAI infection, as is the case for ducks. By contrast, gallinaceous poultry exhibit a severe hyperinflammatory response to HPAI viruses, which can result in up to 100% mortality in a matter of days [25,26]. Of note is that the interferon response was first described in chick embryos that were immunised inactivated influenza virus and produced a substance that interfered with viral replication upon infectious challenge [56,57]. The striking contrasts between different species of bird in their interferon responses to influenza A relate to species-specific immunological differences, predominantly in the signalling cascades which are triggered by infection [55].

Upon infection, a very fast induction of an antiviral response is generally apparent, being mostly triggered by the detection of intracellular dsRNA which is produced during AIV replication [58]. Pattern recognition receptors (PRRs) such as Toll-like receptor 3 (TLR-3), TLR-7, retinoic acid-inducible gene-I (RIG-I) and RIG-I-like factors such as melanoma differentiation protein-5 (MDA-5) are activated by AIV-derived RNA and initiate a cascade

of intracellular signalling which ultimately results in the production of type I interferons and the induction of an antiviral state [55,58–60]. Importantly, birds lack TLR-8 from their genome, and thus the signalling through this receptor and the protective functions which it offers in response to AIV ssRNA do not take place [61,62]. Of particular importance in controlling AIV infection in the absence of a hyperinflammatory response is the RIG-I receptor. Species-specific susceptibility to AIV pathology is provided by the contrast between ducks and chickens, as the latter species lacks RIG-I in its genome [55,59]. Although chickens do possess the MDA-5 receptor and the signalling cascade includes some overlapping downstream components with RIG-I, its expression alone is suggested to be insufficient in the induction of IFN responses to influenza infection in knockout mice [63–66]. Furthermore, transfected chicken cells expressing the duck RIG-I gene were found to reduce the viral titre by 50% when compared to controls [67]. As such, the increased susceptibility in chickens to HPAI infection and its associated severe pathology is considered to be, at least in part, due to the absence of a functional RIG-I receptor gene in its genome.

These differences, alongside other intracellular components of the innate immune response which are activated upon infection, cumulatively influence the progression, severity, and outcome of the AIV disease in avian hosts. Following the activation of PRRs during AIV challenge, cytokines and chemokines are secreted which promote the recruitment of leukocytes to the site of infection [58]. These specialised innate immune cells are important host defence mechanisms against infection, and species-specific differences have also been observed in their responses which correlated with disease severity. For instance, polymorphonuclear (PMN) cells are recruited to the sites of infection and contribute to the control of AIV through mechanisms such as phagocytosis and the production of antimicrobial enzymes, defensins, and reactive oxygen species (ROS) such as nitric oxide (NO) [58]. Although the production of NO has potent antiviral effects during the acute phases of the inflammatory response, excessive production of this highly reactive radical can have profound negative effects on the affected tissues and contribute to pathology [68]. For instance, an increased production of inducible nitric-oxide synthase (iNOS) mRNA and higher sera NO concentrations were found in chickens as opposed to ducks infected

by a H5N1 HPAI virus, and this has been suggested to correlate with the disease severity in these two species [69].

Other innate cells such as Natural killer (NK) lymphocytes have been shown to be a requirement for viral clearance of AIV in mice models [70,71]. These innate lymphocytes are known to provide early protection against infectious challenge through their cytotoxic abilities, without prior sensitisation (i.e. are MHC-unrestricted) [72]. Interestingly, when challenged with a LPAI H9N2 strain, chickens exhibited activated NK cell responses in the lungs [73]. By contrast, when challenged with a HPAI H5N1 strain, there was a decreased activation of NK cells in the lungs, thus indicating that insufficient activation of NK cells contributes to the pathology of HPAI strains. Although the involvement of NK cells during AIV infection in avian hosts remains ill-defined, these findings suggest the contribution of these innate lymphocytes may act in a strain-specific manner, which directly correlates with disease severity.

Major histocompatibility complex (MHC) class II antigen presenting cells (APCs) including macrophages and dendritic cells (DCs) also exhibit important protective functions during AIV challenge [58]. As resident populations of these cells are present in the respiratory tract, they constitute some of the first responders to AIV infection through phagocytosis and cytokine secretion. For example, infection of chicken DCs with either LPAI or HPAI strains induced differential upregulation of PRRs, which was correlated with different profiles of cytokine secretion and suggested to relate to a higher inflammatory response observed HPAI strains [74]. In addition to their innate protective functions during AIV infection, APCs take up foreign antigen and migrate to secondary lymphoid organs where they stimulate cells of the adaptive immune system. However, as opposed to mammals, where lymph nodes serve as major sites for concentrating these interactions between the innate and adaptive branches of immunity, these secondary lymphoid organs are absent from many bird species, including chickens (although they have been described in ducks) [42]. Furthermore, mammalian lymph nodes also facilitate migration of lymphocytes to and from the sites of infection. Instead, chickens contain aggregates of non-encapsulated lymphoid tissue containing small lymphocytes throughout the body which are capable of fulfilling (at least to a certain extent) some of the roles of mammalian lymph nodes. This defining anatomical feature of the avian immune system is likely to have consequences

during the initiation of the adaptive immune system, especially regarding pathogens such as AIV, which require rapid responses in order to control infection [42,75].

As described above, the innate avian immune responses to AIV infection generally follow the same principles as for other viral infectious diseases, in a manner similar to mammalian species. As rapid mortality can ensue following the infection with HPAI strains, the innate responses are particularly important in dictating the outcome of the infectious challenge [55,58]. However, the adaptive immune responses to AIVs are also key components to both recovery after infection and long-term protection.

I.4.2. Adaptive responses

The adaptive component of immunity through thymus-derived (T) cells and bursa-derived (B) cells is key to the resolution of many infections, including AIVs, and the protection against future challenge through immunological memory [76,77]. The interaction between APCs and naïve T cells initiates the adaptive branch of the immune system. For this to occur, small peptides (antigens) are loaded on major histocompatibility complex (MHC) proteins, and presented to T cell receptors (TCRs), in what has been termed as the "immunological synapse". There are two main lineages of T cells, based on the chains which they possess as part of their functional TCR receptor: αβ T cells, with a TCRα light chain and a TCRβ heavy chain; and γδ T cells, with a TCRγ light chain and a TCRδ heavy chain.

Unlike mice or humans, species on which most of the immunological research to date has focused, birds are species with a high frequency of circulating γδ T cells [76,78,79]. T cells of the γδ lineage are present at much lower circulating levels in mice and humans than αβ T cells, and many γδ T cell subsets are restricted to particular tissues (e.g. gut or skin) based on specific T cell receptor (TCR) rearrangements which occur during development. In these species T cells are known fulfil a wide variety of roles throughout the lifetime of the individual, under both physiological and pathological conditions (for reviews, see [80] and [81]). Relatedly, TCRγ gene expression was recently found to be elevated in the spleen and thymus of both young and adult chickens [82] and the γδ T cell lineage has been shown to exhibit important functions during bacterial or viral infections in chickens, including

cytokine secretion and cytotoxicity [78,83–85]. However, their functions in avian species remains poorly understood and it is yet unknown if γδ T cells recognise classical antigen-MHC complexes, or if they interact with non-classical molecules as was described in mice and humans [76,86].

The paradigms of the αβ T cell immune response in birds are similar to the mammalian adaptive immune systems [76]. Once naïve αβ T cells have been activated, they proliferate and participate in the cellular or humoral components of adaptive immunity, based on their cluster of differentiation (CD) molecule expression. CD4+ αβ T cells differentiate into T helper (Th) cells which stimulate antigen-specific B cells to produce antibodies and are thus classically associated with humoral (antibody-mediated) immunity, but they also assist cell mediated immunity. Furthermore, CD4+ αβ T cells can differentiate into other subtypes such as regulatory T (Treg) cells which modulate the immune responses. By contrast, CD8+ αβ T cells differentiate into cytotoxic T lymphocytes (CTLs) which exhibit cytotoxic functions through cell-mediated immunity, thus being able to specifically target infected cells in order to clear infection.

Antigens derived from within the cell are loaded onto MHC class I receptors, which are found on the majority of cells in the body. However, antigens from the extracellular space are loaded on MHC class II proteins, which are predominantly found on professional APCs such as dendritic cells, macrophages, or B cells. The interaction between an MHC receptor and peptide is not rigid, with many peptides having the ability to be loaded and presented to αβ T cells. Antigen presentation through the MHC class I or class II pathways facilitates the expansion of CD8+ or CD4+ effector αβ T cells, respectively. In mammals, there is substantial polymorphism of the MHC cluster, and several different class I and class II receptors (6 for each in humans, with 3 per haplotype) can be present on cells [87]. This allows for a plethora of antigens to be presented to the adaptive immune system and thus the immune system can efficiently recognise antigenic challenge from a wide variety of pathogens. However, as opposed to mammals, most birds express single dominant MHC class I and class II molecules [86,88]. Furthermore, different types of MHC molecules have evolved in birds such as chickens, with different levels of expression and affinities for antigen [88]. At one end of the spectrum, the 'promiscuous' (generalist) molecules which

are poorly expressed bind a broad variety of peptides and provide protection against multiple types of pathogens. At the opposite end, the 'fastidious' (specialist) MHC molecules which are highly expressed bind a more restricted repertoire of antigens and offer increased protection against novel and dangerous infectious agents (for a review, see [88]). Although these opposite evolutionary strategies of antigen presentation are efficient in providing protection against different types of pathogens, the expression of a single dominant MHC molecule may also have other implications for the adaptive immune response. As the interaction between αβ T cells and antigen presenting cells requires an intimate association between the TCR, antigen, and MHC molecule, the presence of a single MHC may impose constraints during avian T cell development (discussed below in more detail) and response to antigenic challenge, including AIV infection.

Cell mediated immunity through CD8+ αβ T cell responses is essential for viral clearance in birds following AIV infection [89,90] as antibody responses alone were found to be insufficient in preventing AIV transmission in avian hosts [91–93]. Species specific differences between birds have also been observed with regards to the CD8+ responses which related to disease susceptibility. For instance, duck CD8+ T cells are retained longer at the site of infection than in chickens when challenged with HPAI strains, which was suggested to indicate a deregulated cellular response in chickens and thus a better control of AIV infection in ducks [94]. This is supported by studies in mice which revealed that CD8+ T cell responses in the lungs are an essential requirement for controlling infection in that tissue [95,96]. As CD8+ αβ T cells respond to intracellularly derived antigens, they can also target internal proteins of AIVs which are more conserved between different subtypes [97]. Indeed, heterologous studies in humans and other mammalian species showed that CD8+ αβ T cell immunity against one subtype of AIV can cross-react with other strains [97–101]. This has also been observed in chickens, where H9N2-specific CD8+ αβ T cells were able to protect against HPAI H5N1 when transferred to naïve individuals [90]. For these reasons, vaccine-induced CD8+ αβ T cell responses are a major focus of current research given their potential for generating both homologous and heterologous protection against different strains of AIVs [48,102].

The humoral immune system is comprised of antigen-specific antibody-secreting B cells which receive help from CD4+ αβ T cells that have been activated through the MHC class II pathway. Evidence of the protective role of antibodies during avian host infection with AIVs comes from studies of bursectomised chickens which lacked B cell responses and were unable to mount protective responses against the viral challenge, even when a vaccine against AIV was administered prior to infectious challenge [58]. The majority of antibody responses against AIVs is directed against the HA and NA surface proteins of the virus which constitute immunodominant targets for the humoral responses in both mammals and birds [7,53,55]. Initially, naïve B cells produce express immunoglobulin (Ig) M antibodies, which are of lower antigenic affinity. Upon stimulation, antigen-specific B cells proliferate and class switch, producing higher-affinity antibodies, with some cells differentiating into antibody-secreting plasma cells.

Class switching of B cells occurs in germinal centres (GCs), which are specialised microstructures in secondary lymphoid organs [77,103]. Furthermore, within GCs, B cells undergo somatic hypermutation (discussed below in more detail), a phenomenon which increases the affinities of their antibodies for antigens. In the absence of lymph nodes, germinal centre formation in birds occurs in the spleen and other specialised secondary lymphoid organs such as Peyer's patches, Meckel's diverticulum, caecal tonsils, or the Harderian gland, depending on the proximity to and nature of the infectious challenge [104].

At mucosal sites, antibodies are secreted in the form of IgA, whereas IgY (sometimes referred to avian IgG) is produced at systemic locations [77]. As AIV replication occurs predominantly at mucosal sites in the respiratory and intestinal tracts, IgA antibody responses are essential for controlling the virus at the site of infection [58]. As the commonly used inactivated AIV vaccines generate poor responses at mucosal surfaces, vaccination strategies aimed at stimulating mucosal immunity and the generation of IgA responses have been receiving increased focus in recent years [42,105,106]. However, AIV-specific IgY can successfully neutralize the virus, prevent systemic spread, and contribute to viral clearance. Avian species possess no equivalent forms to the mammalian IgD, IgG or IgE antibodies, with the IgY form being considered an intermediate between the latter

two [77] . Ducks also exhibit a truncated form of IgY, in addition to the normal length form of this antibody [107], but the protective functions of the truncated IgY against AIVs have not been assessed. As ducks have been shown to mount a weaker response than chickens to AIV challenge or vaccination [108], it has been postulated that this could be partly due to the presence of this truncated form of IgY [55].

As in mammals, the adaptive immune system is essential for the protection of avian species against subsequent challenge, as a subset of the antigen-specific T and B cells differentiate into long-lived memory cells [106]. Upon reinfection, memory T and B cells become activated and proliferate, thus providing much faster cellular and humoral responses against the infectious agent. This essential property of the adaptive immune system of vertebrate species constitutes the immunological basis for vaccination, which can provide the host with immunological memory in the absence of infection [42,106]. Furthermore, as different T and B cells respond specifically to particular antigenic stimuli, immunological memory can be developed against a multitude of pathogen-derived antigens. This property stems from the enormous diversity of T and B cells and their surface receptors, which allows for the identification of a wide variety of exogenous and endogenous antigens which are present under pathological conditions.

I.5. The avian adaptive immune receptor repertoire

One of the defining features of adaptive immunity of jawed vertebrates is the remarkable diversity of B and T lymphocytes, with each unique 'clone' being able to specifically respond to a particular antigen [87]. This discriminative ability is attributable to the unique T and B cell receptors (i.e. the TCRs and BCRs/immunoglobulins, respectively) that are expressed by each lymphocyte with the diversity of the avian TCRs and BCRs (i.e. the adaptive immune repertoire) being genetically encoded during T and B cell development.

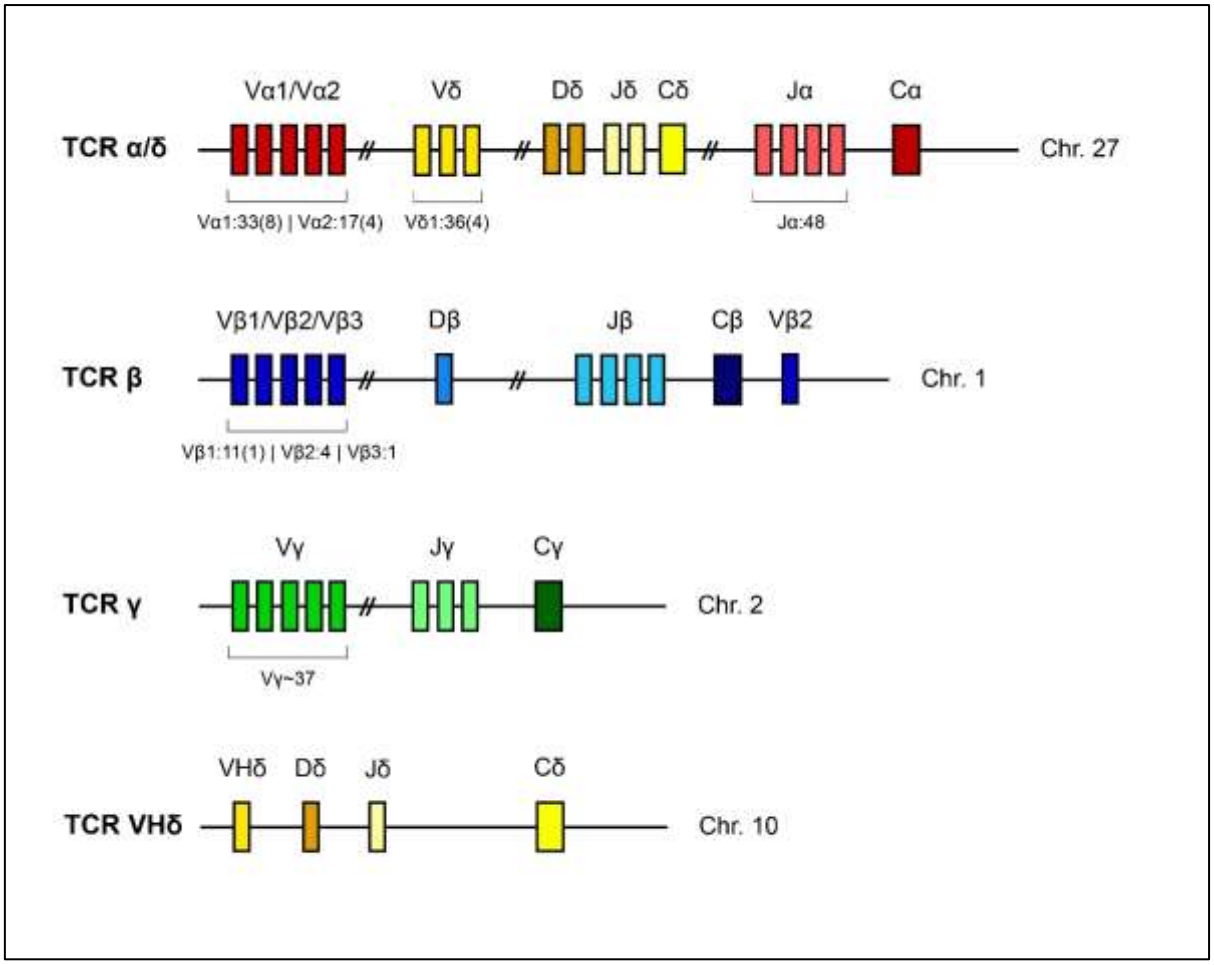

Figure 1.2: The TCR genomic organisation in chickens.

The gene boxes represent the relative position of the elements but are not illustrative of the exact number for each of the gene segments when it exceeds four. In those situations, the numbers of functional genes are indicated below and the number of pseudogenes is placed within brackets. Adapted from Smith and Göbel (2022) in Avian Immunology, 3rd edition [76].

I.5.1. The TCR repertoire

As for mammals, avian T cell development occurs in the thymus, from which they migrate to the spleen and other tissues throughout the body and the generation of TCR diversity is achieved by somatic rearrangement using Recombination-activating Gene (RAG) proteins [76]. This phenomenon occurs for both the αβ and γδ T cell lineages and involves the random genetic rearrangement variable (V), joining (J), and – in the case of the heavy chains – diversity (D) gene segments to produce a functional TCR [54,76,109]. As opposed to

humans or mice, fewer TCR genes are available for rearrangement in most birds such as chickens (**Figure 1.2**).

For example, for the TCRβ, there are 16 Vβ genes belonging to 3 distinct families (11 Vβ1, 4 Vβ2, and 1 Vβ3), 4 Jβ genes, one Dβ and one constant (Cβ) genes. [110,111]. Additionally, other processes such as the modifications at the VDJ junctions involving the substitution, addition, or deletion of nucleotides further contribute to the diversity of TCR receptor rearrangements. The resulting hypervariable region is termed the complementarity-determining region (CDR) 3, and functions in recognising and binding specific antigens presented by the MHC molecules of APCs. The pairing of light and heavy TCR chains further increases the diversity potential of the T cell repertoire, which could reach comparable numbers to the theoretical diversity potential of mice or humans [76].

I.5.2. The antibody repertoire

As opposed to mammals, where B cell development occurs in the bone marrow, a specialised organ – the bursa of Fabricius – serves as the primary lymphoid organ carrying out this function in avian species [77,112]. The process of BCR diversification also involves the somatic rearrangement of V and J genes in light (L) chains, and V, D, and J genes for the heavy (H) chains of the immunoglobulins [77]. The phenomenon of V(D)J rearrangement is not exclusive to the bursa, as it can be detected during embryonic development in other organs, with the earliest being the spleen [103]. Unlike mammals, the V(D)J recombination process itself results in very limited IgL and IgH diversity because of the often-unique gene segments involved in somatic rearrangement. For example, chickens only possess one functional V gene and one functional J gene for both the IgL and IgH chains of the BCR. Although chickens possess 15 D genes for the IgH chain, their amino acid sequences are mostly identical, and thus their potential for contributing to the BCR diversity is limited [113]. However, a high number of pseudogenes (Ψ) exists upstream of the V genes of the IgH (~60 ΨVH) and IgL (~25 ΨVL) [77]. These pseudogenes are involved in generating the diversity of the BCR through the process of gene conversion (**Figure 1.3**) [77,114]. This process is mediated by the activation-induced cytidine deaminase (AID) enzyme, which classically participates in somatic hypermutation (see

below). Gene conversion does not simply imply replacing one V gene with another, as conversion events ranging from several nucleotides to almost all the V gene sequence have been identified.

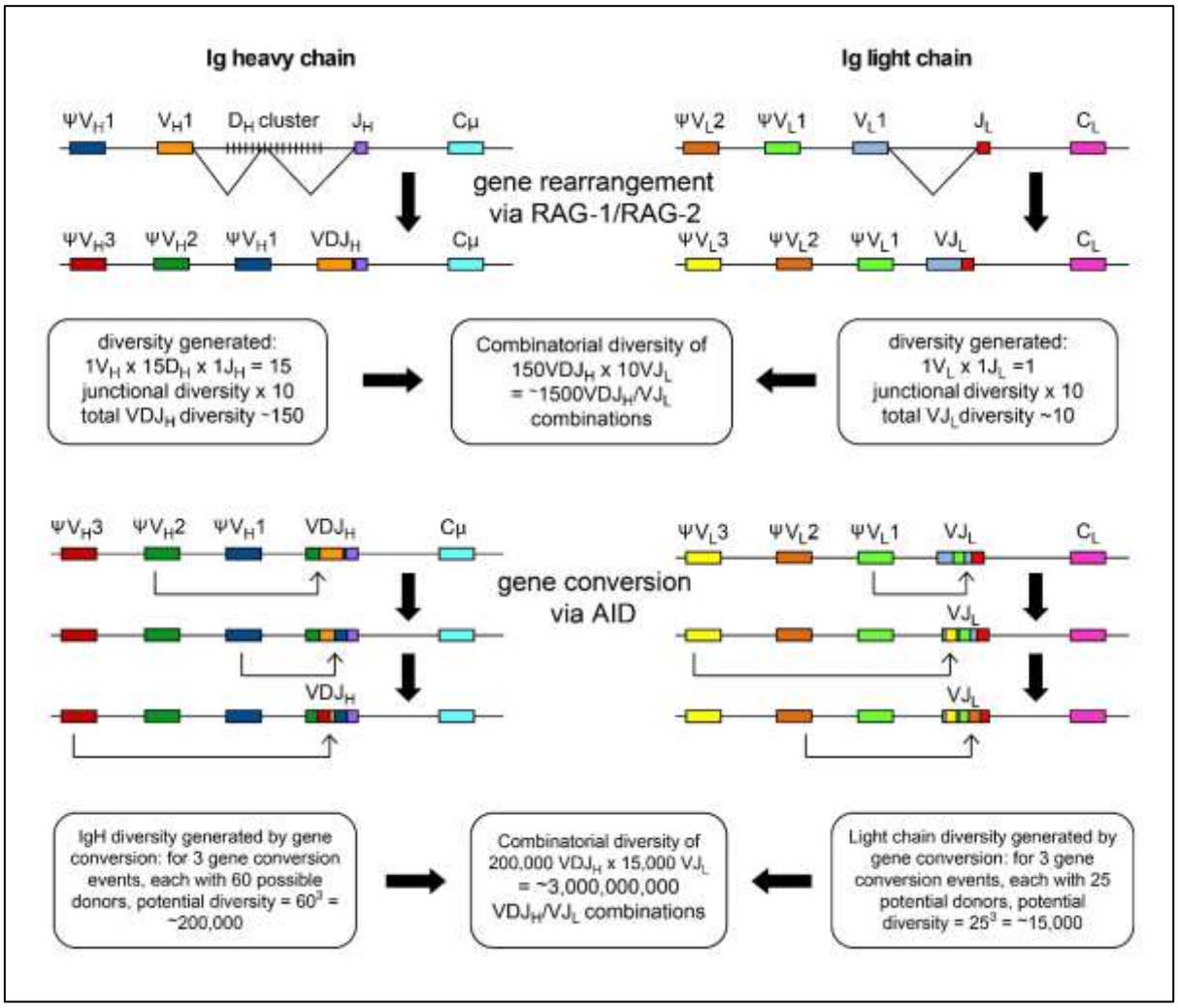

Figure 1.3: The generation of the antibody repertoire diversity in chickens.

RAG-dependent gene rearrangement generates limited diversities in the IgL and IgH repertoires. The process of gene conversion mediated by AID greatly increases the diversity of the immunoglobulin repertoire by inserting fragments of variable length from the V pseudogenes located upstream of the V(D)J rearrangement. Figure adapted from Ratcliffe and Härtle (2014) in Avian Immunology, 2nd edition [77].

As such, although the genomic diversity of avian immunoglobulins is not stored in functional V genes as it is for mammals, it is maintained within V pseudogenes which are capable of generating very high levels of functional diversity in the BCR repertoire through the process of gene conversion [77]. The pairing of light and heavy chains of the BCR further contributes to the repertoire diversity, in a manner similar to T cells. However, upon antigenic stimulation, B cells are also able to modify their existing CDR3 sequences within germinal centres (described in the above section) through the process of somatic hypermutation [77]. This phenomenon is mediated by AID and involves point mutations which are selected based on higher affinity to antigen, in a manner that is very similar to mammalian immune systems.

I.5.3. Avian-specific features and the current understanding of the immune repertoire

Although many similarities exist between the immune systems of birds and mammals, the avian immune system possesses some unique features in terms of genetic organisation (e.g. TCR or immunoglobulin gene clusters), certain processes (e.g. gene conversion in B cells), or even the relative importance of some cell subsets (e.g. γδT cells) [54]. Other distinctive features of the avian immune system include the expression of single dominant MHC class I and class II molecules [86,88] and the absence of genes involved in immunological functions in some avian species (e.g. RIG-I in chickens). While these features are known to influence the physiology of the avian immune system, there is a limited understanding of the exact mechanisms which underpin them, and their consequences on the host's ability to respond to foreign antigenic challenge. Therefore, although many similarities exist between the avian and mammalian immune systems, the differences raise interesting questions, especially when considering the diversity of the adaptive immune repertoire and its role in health and disease. As many current agricultural practices in the poultry sector are known to either directly or indirectly influence the adaptive component of immunity, in-depth analyses of how they affect the immune repertoire have the potential to shed light not only on fundamental avian biology, but also on how to better exploit certain factors in the context of health and disease.

The rapid advancements in laboratory methods, high-throughput sequencing (HTS) technologies, and the development of new bioinformatical tools have opened promising avenues for immune repertoire research [115–117]. As such, recent attention has been directed towards performing in-depth repertoire analyses in various contexts, such as infections, cancer, vaccinations, and even the effect of the microbiota on the immune system [118]. However, most of these studies were either performed in mice or in humans, with only a few focusing on the avian immune repertoire.

I.5.4. Repertoire studies during influenza infection and vaccination

To date, no studies have attempted to assess the effects of influenza infection and/or vaccination on the avian adaptive immune repertoire, in spite of the fruitful outcomes of such research in mammalian hosts. For example, studies in humans revealed that influenza exposures either through vaccination or infectious challenge have major influences on both the B and T cell repertoire [119–122]. Analyses of the antibody responses found that some B cell clones may be more predisposed than others to adopt a memory phenotype following antigen-exposure [121]. Moreover, age was shown to play a significant role regarding antigen-specific T cells, with expanded public (i.e. shared between individuals) clones being more predominant in the young, while the older subjects displayed higher expansions of 'private' (i.e. individual-specific) clonotypes [119,120]. At the same time, a decrease in the clonal diversity of both influenza-specific T [119,120] and B cells [122] was observed in older individuals. Furthermore, the repertoire diversity of both T and B cells was found to be a good predictor of the outcome of infections with influenza A viruses [123]. Although these studies have provided important insights into the effects of influenza infections or vaccinations in humans, none of this work has yet been mirrored in poultry, in spite of their importance in AIV infections [8]. Therefore, assessing the changes in the avian adaptive immune repertoire following AIV infection or vaccination will not only increase our understanding of the biology of these viruses in relation to their avian hosts, but also help in designing better prevention and control strategies [32,53].

I.6. Thesis aims and objectives

In this thesis, AIV-specific avian immune responses will be evaluated in response to vaccination, infection, and a combination between these two treatments. The model organism used throughout the analyses is the domestic chicken (*Gallus gallus domesticus*), both for its economic relevance and because of the higher susceptibility of this species to severe AIV infection. The chosen strain of AIV is H9N2, as this virus has increased in prevalence and is enzootic in many countries worldwide. Although a low pathogenic strain of AIV, the H9N2 mechanism of infection and pathogenesis is similar to HPAI strains without exhibiting the high degree of associated mortality which would prevent post-infection experimental analyses of the immune responses. The focus of the current work is the avian adaptive immune repertoire and the modifications which occur following infection and/or vaccination.

In the following chapter of the thesis, a description is provided regarding the reagents and the general experimental methods used for the analyses. At the same time, Chapter II also presents the custom laboratory and computational techniques which were used for repertoire analysis and flow cytometry and discusses the results of the analyses performed as part of protocol development and optimisation. Chapter III examines the splenic lymphocyte frequency changes and the dynamics of the antibody responses following H9N2 vaccination and/or infection. In Chapter IV, the IgM and IgY repertories are analysed, while Chapter V examines the TCRβ repertoire changes under the same immunisation scenarios. The thesis concludes with a general discussion in Chapter VI, where the cumulative implications of the findings from the data chapters of the thesis are presented. As little is known about the repertoire of avian hosts, the main aim of the thesis is to characterise the changes during both H9N2 avian vaccination and challenge, in order to improve our current understanding of these phenomena and to better inform future prevention and control strategies.

Chapter II: Materials, General Methods, and Protocol Development

II.1. Sample processing for repertoire analysis

II.1.1. RNA extraction

Tissue samples preserved in RNAlater were weighed and 15 mg of each was transferred into tubes containing 600 µl of RLT lysis buffer (Qiagen) and 100 µl of 0.2 mm sillica beads. Subsequently, they were subjected to 5 cycles of 1-minute homogenisation in a Mini-Beadbeater-24 (BioSpec) and 30 seconds of cooling on ice. Subsequently, RNA was extracted using the RNeasy Mini kit (Qiagen) by following the manufacturer's protocol. For all samples, the on-column genomic DNA digestion step was performed, with the RNase-Free DNase Set (Qiagen) being used in accordance with the manufacturer's instructions. The extracted RNA was eluted in 40 µl of nuclease-free water. RNA quality of random samples was tested using an RNA ScreenTape (Agilent Technologies) on the 4200 TapeStation (Agilent Technologies) to assess integrity. The samples were then stored at -80°C until further processing.

II.1.2. 5'RACE-ready cDNA generation

5'RACE-ready cDNA was generated using the SMARTer kit (Takara). For each reaction mastermix, 2 µl of 5X First-Strand Buffer, 1 µl of 20 mM dithiothreitol (DTT, and 1 µl of 10 µM deoxynucleoside triphosphates (dNTPs) were added alongside 0.25 µl of 40U/µl RNase inhibitor enzyme, 1 µl of 24 µM SMARTer IIA oligonucleotides, and 1 µl of 100 U of RT enzyme. The resulting 6.25 µl were then added to a mix of 1 µl of 10 µM 5'RACE CDS primer A and 2.75 µl of RNA which was previously placed in a thermocycler for 3 minutes at 72°C and 2 minutes at 42°C. Each of the 10µl reverse transcription (RT) reactions were carried out in 96 well plates using the recommended thermocycler program (90 minutes at 42°C followed by 10 minutes at 72°C). The resulting complementary DNA

(cDNA) samples were then diluted by adding 150 µl of 10 mM Tris-HCl and 1 mM disodium ethylenediaminetetraacetic acid (EDTA) (pH 8.0) and stored at -20°C.

II.1.3. 5'RACE PCRs

For each cDNA sample, specific 7-bp barcoded primers for the chicken T and B cell receptor genes (**Table 2.1**) were used for the 5'RACE PCRs. Universal reverse primers were used for all samples, specific to the common 5' adapter that was added during the cDNA synthesis step. Briefly, for each 25 µl reaction, 5 µl of Phusion 5X Buffer (New England Biolabs), 0.5 µl of 10 mM dNTP, 0.5 µl of 10 µM UPA-short primer, 0.5 µl of 2 µM UPA-long and 0.25 µl Phusion Hot Start Flex DNA Polymerase (New England Biolabs) were added to 15.25 µl nuclease-free water, for a total of 22 µl volume. To this, 0.5µl of the 10µM gene-specific 7bp-barcoded primer and 2.5 µl of cDNA were added. The individual 25 µl volume 5'RACE PCR reactions were then carried out in 96-well plates using the thermocycler program recommended by the 5'RACE kit (Takara), with 35 cycles of gene-specific amplification with an annealing temperature of 60°C.

After PCR amplification, barcoded samples were pooled and subjected to electrophoresis on a 1.4% agarose in 45 mM Tris-Borate/ 1mM EDTA (TBE) buffer gel containing 1:10,000 SYBR green (Sigma-Aldrich) at 120 V for 35 minutes. The bands of the expected lengths were gel extracted and purified using the QIAquick Gel Extraction Kit (Qiagen).

Primer Name	DNA sequence (5'→3')	Target
UPA short	CTAATACGACTCACTATAGGGC	SMARTer cDNA sequence
UPA long	CTAATACGACTCACTATAGGGCAAGCAGTGGTATCAACGCAGAGT	SMARTer cDNA sequence
T cell receptor C_β	NNNNNNNGAAAAGATGACCACATCTGGTTC	TCRβ heavy chain
Immunoglobulin C_μ	NNNNNNNCACAGAACCAACGGGAAG	IgM heavy chain
Immunoglobulin C_Υ	NNNNNNNCGGAACAACAGGCGGATAG	IgY heavy chain

Table 2. 1: Primer sequences for 5'RACE PCR amplification of chicken lymphocyte receptor genes.

Nucleotides of gene-specific primers denoted by the letter 'N' and coloured in red are variable bases used for barcoding the amplified products.

II.1.4. DNA Library preparation and sequencing

DNA libraries of the pooled barcoded PCR samples were generated using the NEBNext Ultra II DNA Library Prep Kit for Illumina (New England Biolabs), following the manufacturer's instructions. The quantity and quality of the DNA libraries were analysed using the NEBNext Library Quant Kit for Illumina (New England Biolabs) and a D1000 DNA tape (Agilent Technologies) on the 4200 TapeStation (Agilent Technologies). Sequencing was carried out using an Illumina MiSeq platform at the Department of Biology (for the germ-free experiment – see section II.3), University of Oxford and at the Pirbright Institute (for the AIV experiment – Chapters IV and V). Of note is that the library preparation and sequencing at the Pirbright Institute was not carried out by the Candidate. Instead, the Bioinformatics, Sequencing & Proteomics group using the same steps as described above.

II.2. Repertoire sequence data processing and analysis

The raw sequence data was processed by using an in-house python package (available on GitHub: https://github.com/sgp79/reptools) [124]. Briefly, the software assigns the V and J gene IDs to the sequences by BLAST [125] comparing them to a database of known reference sequences. Subsequently, the algorithm extracts the CDR3 after a Smith-Waterman alignment [126], thus allowing for higher precision at the junctions [127]. The output was then analysed using R [128].

II.2.1. Linear mixed-effects models

Linear mixed-effects models were constructed to assess the tissue-specific contribution of TCRβ clones from the microbial treatment groups. In order to account for individual-specific variability, the effect of each bird was incorporated as a random intercept. The parameters, tissue and status (i.e. treatment group), were incorporated as explanatory variables in all the models.

Due to the proportional nature of the observations, several data transformations were compared in order to select the most appropriate model. Following exploratory analyses which examined the normality of residuals and homoscedasticity, logit transformations were used when the data were represented by proportions [129]. Square root transformations were applied for the Hill numbers used to analyse the repertoire diversity. The models were implemented using the lme4 package in R using Satterthwaite's approximation, with p values and 95% bootstrap confidence intervals for the model estimates being computed using the lmerTest package [130,131].

II.2.1.1. Repertoire diversity

The suggested patterns of expansion with respect to the tissue type and microbial colonisation status were further investigated by analysing the diversity present within the samples. Although the diversity measures are commonly used in ecology to measure species diversity within an ecosystem or defined territory, they can readily be used to measure the diversity of the repertoire if unique T and B cell clones are treated as "species". For this, the effective number of species, here equating the "effective number of clones" (D) can be calculated using the weighted abundance of unique reads in each sample [132,133]. In ecology, three common measurements of diversity are used: the species richness (D_0 – the total number of species found regardless of abundance), the Shannon entropy (D_1 – a measurement which weighs the abundance of species and rare species are less important), and the Simpson concentration (D_2 – a measurement where the abundance of species weighs more and rare clones are even less important). As such, corresponding values for species richness (D_0 – defined here as "clonal richness"), the exponential of the Shannon entropy (D_1 – defined here as "typical clones") and the inverse Simpson concentration (D_2 – defined here as "dominant clones") diversity measures were computed, thus incorporating the effect of clonal expansions at different levels. This was achieved using the iNEXT package [134] in R, and interpolation or extrapolation was carried out in order to standardise between samples at a value of 10,000 total reads [134]. Individual measurements were then incorporated into a linear mixed effects model, with the *response* representing the estimated effective number of species at the particular diversity

measurements (D_0, D_1, or D_2) for the samples, as a function of microbial colonisation status and tissue type.

II.2.1.2. Public and private clonal compartments

Based on their CDR3 nucleotide sequence, V family, and J gene usage, clones were divided into the private or public compartments if they were found shared between individuals. The percent contribution to the private or public clonal compartment was estimated as a function of microbial treatment group, tissue type, and clonal compartment (private or public). At first, all clones which were found in more than one individual were regarded as public, irrespective of the number of individuals which shared them. Subsequently, a new model was constructed where public clones were divided into multiple categories based on their presence across the 10 birds: rare publics (between 2 and 5 birds), common publics (between 5 and 9), and ubiquitous clones (shared between all individuals).

II.2.1.3. V family and J gene usage

The contribution of the V gene families and the J genes to the TCRβ repertoire was assessed with regards to the microbial colonisation status and tissue identity. Since there is a high sequence similarity (>90%) within each V family [76], a significant proportion (close to 10%) of the identified reads could not be identified and assigned correctly with a specific V gene within the respective families. In order to overcome this issue, only the V family identity was used for the analysis. There were no assignment issues with regard to the J genes, as out of the total sequences only 12 reads were ambiguously assigned, and the corresponding clones were disregarded from the analysis. Subsequently, an extension of this model was used to calculate the mean estimates for V family and J gene usage in the private and public clonal compartments. For this, two versions of the model were incorporated. First, the private and the total public compartment were used. Subsequently, the public compartment was divided based on different degrees of clonal sharing between birds. Both models incorporated *clonal compartment* as an additional explanatory variable for the publicness of clones.

II.3. Protocol Development – The influences of microbial colonisation and germ-free status on the chicken TCRβ repertoire

This subchapter served as a basis for the publication (2023) "The influences of microbial colonisation and germ-free status on the chicken TCRβ repertoire" by Dascalu S, Preston SG, Dixon RJ, Flammer PG, Fiddaman S, Boyd A, Sealy JE, Sadeyen JR, Kaspers B, Velge P, Iqbal M, Bonsall M, and Smith AL in *Frontiers in Immunology* **13**:7761. https://doi.org/10.3389/FIMMU.2022.1052297
The relevant statement of authorship is found at the the end of this subsection, as per the regulations of the University of Oxford.

II.3.1. Background and rationale

The interactions between the microbiome and the host are important for many processes such as nutrition, mucosal physiology as well as protection against pathogens via competitive exclusion and the stimulation of the immune system [135–138]. Among the different compartments of the host microbiome, the gastrointestinal tract deserves special attention, as it harbours the largest microbial abundance and diversity [138,139]. To date, most studies exploring the influence of the gut microbiota on the immune system have focused on rodents and humans [140,141]. It is, therefore, important to consider the impact of the microbiota on immune processes in other species to evaluate if findings from these systems apply more generally.

The domestic chicken (*Gallus gallus domesticus*) represents both a model organism for biological research and an economically important source of protein at a global scale [136,138,142]. As in mammals, the chicken gut represents a major route for exogenous antigen uptake, and thus is extremely relevant to the normal development of both the innate and adaptive components of immunity [136–138] (for a general overview of avian gut immunology see [143]). Regarding the latter, the relations between the microbiome and the enormous diversity of unique lymphocyte receptors (i.e. the adaptive immune repertoire) raise important questions, as the chicken gut microbiota has previously been shown to be an important driver of both T and B cell responses [136,138].

The processes involved in the diversification of the T cell receptor (TCR) repertoire in birds are similar to those reported in mammals involving RAG-dependent rearrangement with

junctional modification. The TCR loci are arranged similarly in birds and mammals although the numbers of TCRVβ segments are fewer in the chicken compared with mammals (reviewed in [76]). Moreover, the chicken TCRVβ gene segments fall into just three families (called Vβ1, Vβ2 and Vβ3) which is many fewer than seen in any mammal [76]. By contrast, the TCRγ locus is expanded compared with most mammals; as such, chickens have a greater number of TCRVγ gene segments although not all Vγ gene segments in the genome are utilised with equal frequency [79]. Hence the complexity of the locus does not relate to the available repertoire and to understand the function of chicken T cells, the diversity of TCR needs to be considered. In addition to the limited V gene availability in the TCRβ locus, other features of the avian immune system that may affect the TCRβ repertoire include the relative simplicity of the chicken MHC and the expression of single dominant MHC class I and II genes [54]. Therefore, although many similarities exist between the avian and mammalian immune systems, the differences raise interesting questions, especially when considering the diversity of the adaptive immune repertoire and its role in health and disease.

Previous studies of chickens have investigated the influence of germ-free conditions on the immune repertoire using methods such CDR3 length profiles alongside molecular cloning and subsequent Sanger sequencing of products to evaluate TCR identity [144]. However, the use of high-throughput sequencing (HTS), offers a unique opportunity for comparisons to be made at the level of individual clones [115–118,145]. Therefore, such HTS approaches can shed light on different mechanisms of immune development, regulation, defence against pathogens, and other factors which underpin these phenomena.

The aims of this research were to apply and optimise the HTS-based methodology using 5'RACE PCRs (described in section II.1) TCRβ receptor diversity in chickens, and the extent to which these influences become apparent in different tissues. For optimising the bioinformatical pipeline, focus was put on the β chain of the T cell receptor (i.e. the TCRβ) because it exhibits higher combinatorial potential due to the D gene segment usage, and because of its unique expression on cells via allelic exclusion (as opposed TCRα which can be co-expressed) [109,145–147]. In the following sections, the methods and results of this analysis are presented in more detail.

II.3.2. Animal tissue samples and experimental design

Tissue samples (spleen, bursa of Fabricius, jejunum, caecum and colon) were derived from a larger in vivo study carried out at the infectiology platform PFIE (INRA, Val de Loire) in accordance with the national and international regulations specific to the research facility as part of the Development of Immune Function and Avian Gut Health (DIFAGH) consortium. One group of PA12 white leghorn chickens (n=5) was hatched and reared under germ-free conditions, whilst another group (n=5) of PA12 chickens was reared under conventional specific pathogen-free (SPF) conditions. For the germ-free birds, the eggs were collected immediately after laying and surface sterilized by an immersion in 1.5% Divosan Plus VT53 (Johnson Diversey, France) for 5 minutes at room temperature. Subsequently, these eggs were transferred into HEPA-filtered incubator. After 18 days at 37°C, the surface of the eggs was sterilized in 1.25% Divosan for 4 min at 37 °C. After hatching, the temperature of the isolator was maintained at 37.5 °C for 7 days, then reduced by 1 °C per day until reaching a stable temperature of 25 °C. Chickens were offered X ray-irradiated starter diet (Special Diets Services; Dietex, Argenteuil, France) and sterilized water ad libitum. The sterility of chickens was confirmed weekly by incubating fresh faecal droppings in 10 mL of sterile brain–heart infusion broth under both aerobic and anaerobic conditions, which allows for bacterial, yeast, and fungal growth. The absence of non-culturable bacteria in faecal and caecal samples of germ-free chickens was confirmed by quantitative PCR of a conserved region of the bacterial ribosomal 16S gene. Individuals from both groups were culled at day 55 post-hatch, when tissue samples were harvested and preserved in RNAlater (Thermo Fisher Scientific) according to manufacturer's instructions. Samples were stored at –80°C prior to processing. The experimental and computational work proceeded as described in sections II.1 and II.2).

II.3.3. Repertoire computational analysis and results

II.3.3.1. Recovered sequences and productively rearranged TCRβ chains

Following library generation and sequencing, a total of 1,052,190 TCRβ reads were obtained, of which 980,606 (~93.2%) were productively rearranged (in frame with no

premature stop codons) (Figure 1). Importantly, within tissue type, there were no apparent differences in the total reads acquired or the proportions of productive reads between the germ-free and conventional birds. However, high levels of heterogeneity were observed between different tissues in terms of total sequences. Although the bursa is considered an organ associated with B cell diversification, this site does include T cells and was therefore included in the analyses [104,148]. Of note, substantially fewer TCRβ sequences were recovered from the bursa than from the other tissues. By contrast, the other tissue samples provided a much higher number of productive reads per sample (average of 24,000). For the subsequent parts of the analysis, only the productively rearranged TCRβ sequences were examined.

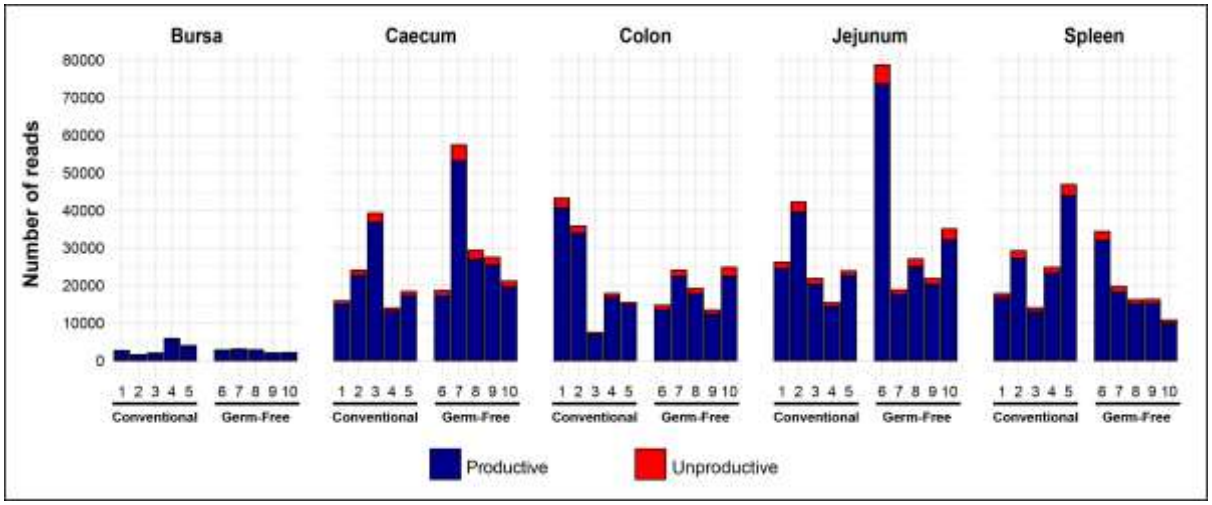

Figure 2. 1: *Total chicken TCRβ reads identified in different tissues of chickens reared under germ-free or conventional (SPF) conditions.*

Bird numbers and their corresponding microbial colonisation status are displayed on the x axis. Productive and unproductive reads are shown in blue and red, respectively.

II.3.3.2. Tissue-specific clonal homeostasis

In order to examine the T cells in each tissue, clonal homeostasis plots were generated using the proportion of individual clones within each sample. When the proportions between two or more clones in the sample were equal, the highest rank among them was assigned to the group, and the smaller ranks were skipped. This method was chosen to emphasise the differences in abundance between the clones, whilst still capturing the diversity of the

clonotype composition. As such, patterns were revealed based both on tissue type and the microbial colonisation status.

Broadly, the intestinal tissues and the bursa exhibit greater proportions of clonal expansions than the spleen (**Figure 2.2**). This is indicated by the proportion of the total being represented by the most abundant ranked clones. The pattern in the spleen with lower ranked clones making up >75% of total reads may reflect a large proportion of unexpanded (naïve) T cells (noting that chickens have no lymph nodes). Since read numbers across tissues (apart from the bursa) were broadly comparable, the patterns of expansion were not simply a product of systematically different sequencing depth or coverage.

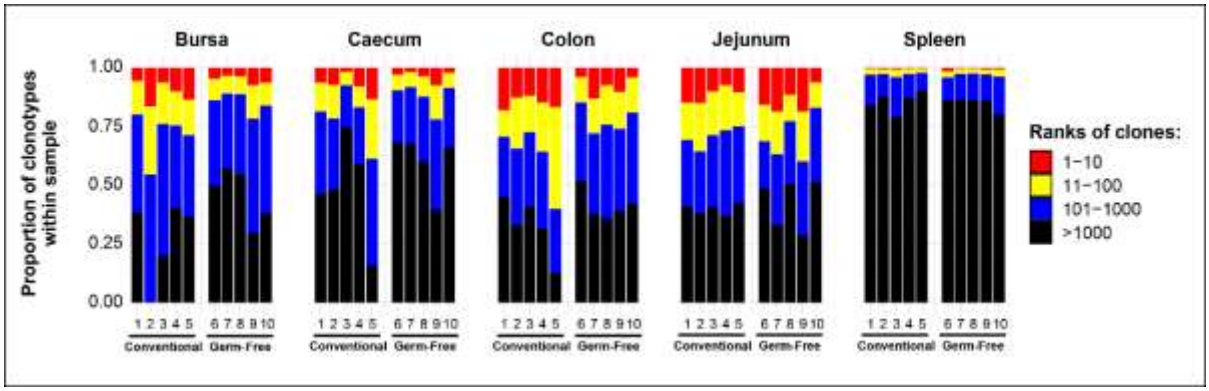

Figure 2. 2: *TCRβ clonal homeostasis plots of individual tissue samples.*
Bird numbers and their corresponding microbial colonisation status are displayed on the x axis. Clones were ranked based on their abundance into four categories: first 10 most abundant (red), from 11-100 (yellow), 101-1000 (blue), and above 1000 (black) in terms of total abundance within each sample. The proportions of clonotypes are displayed on the y axis.

When comparing the tissue-specific repertoires between the treatment groups, the spleen and jejunum exhibited no marked differences between germ-free and conventional groups. Conversely, the colon, caecum, and bursa seem to have more clonal expansions (a greater proportion of the total made up by the highest ranked clones) in the conventional chickens than in the germ-free group.

II.3.3.3. CDR3 lengths and distance the from germline configuration

Clonal expansion patterns were further explored by calculating the total length of the CDR3 and generating histograms with the densities of the observed amino acid lengths. Furthermore, for each unique CDR3 sequence, the Levenshtein distance was calculated to a 'germline' VDJ rearrangement. This theoretical sequence lacks any nucleotide modifications which could arise during recombination, thereby providing a reference for how much the CDR3 has changed following this process. The Levenshtein distance is a simple measurement of string similarity (here, sequence similarity) where insertions, deletions, and substitutions are treated the same. For every one such modifications to the reference sequence, the distance increases by the value of 1. Density histograms were then generated in order to observe specific CDR3 expansions based on the germline distance.

The length distributions (**Figure 2.3**) generally follow a normal distribution with some deviations from normality being present in specific samples. As expected, there are no noticeable deviations from normality in the spleens, which indicates that no large expansions of specific lengths are present. By contrast, all conventional birds display some type of expansion in the colon, whereas only two germ-free birds exhibit this trait. Interestingly, 4/5 germ-free birds exhbit very large expansions in the jejunum, corresponding to the CDR3 lengths of 14 and 15 amino acids. These CDR3 lengths correspond to the patterns observed in the conventional jejunal samples, although only 3/5 birds exhibit this pattern. The bursal samples and the caecum (with the exception of one conventional bird) do not show any marked expansions of specific CDR3 lengths.

Density plots of the Levenshtein distance from the germline configuration (**Figure 2.4**) support the observed patterns of CDR3 length distributions in the samples, although the deviations from normality are more heterogeneous. No pronounced biases are suggested in the spleen, corresponding to the results revealed by the CDR3 lengths. Furthermore, in the jejunum, with the exception of one bird from each group, clear patterns of expansion are present, generally favouring configurations which are closer to germline.

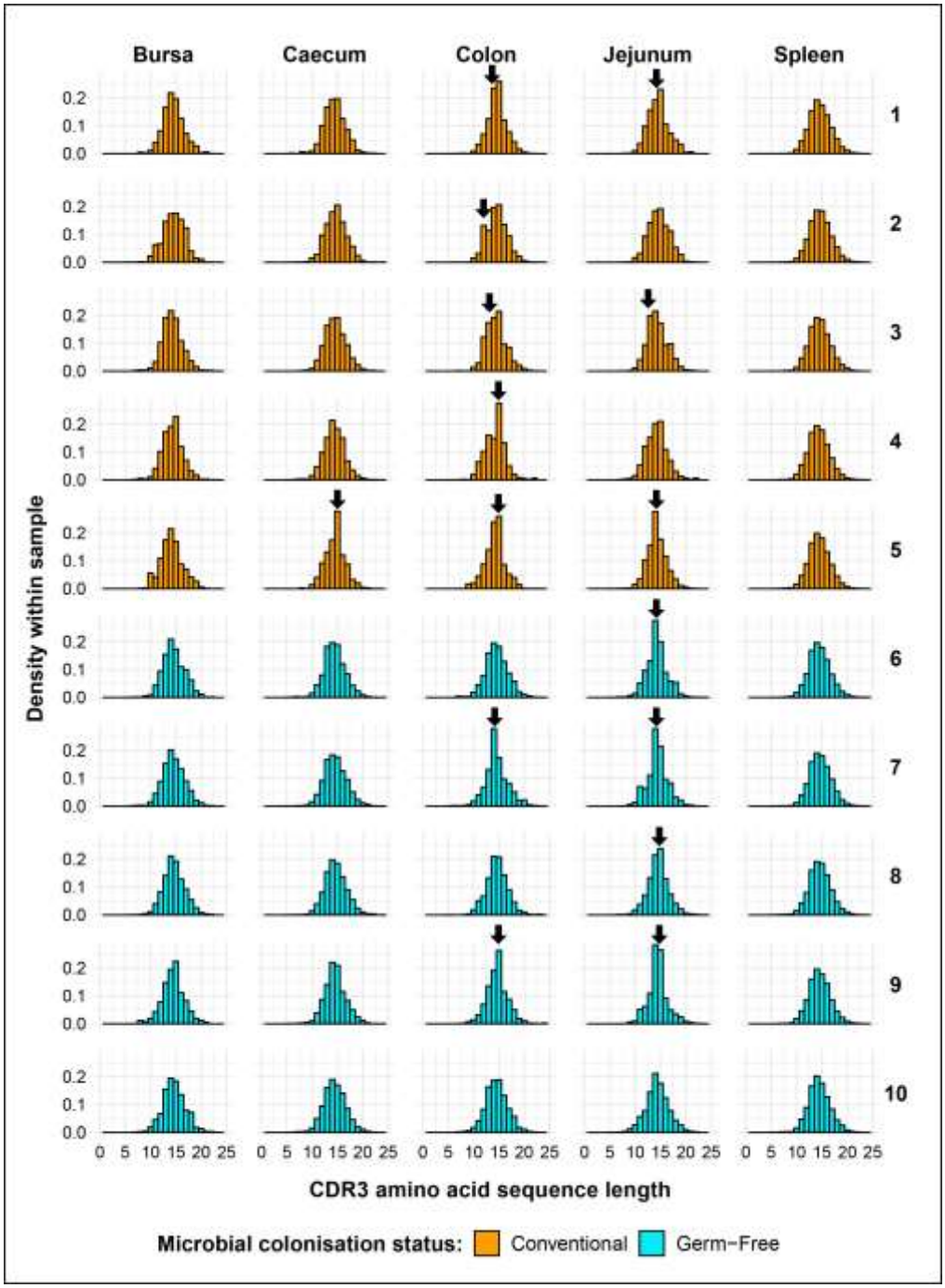

Figure 2. 3: TCRβ CDR3 length distribution by tissue and bird.

CDR3 length densities are displayed on the y axes of the plots. Each row displays the tissues of an individual bird for which the corresponding number is shown on the right side of the plots. Colours denote the microbial colonisation status of chickens for conventional flora (orange) and germ-free (light blue). Black arrows illustrate deviations from normality which suggest potential clonal biases. For visualisation purposes, the long tails of the CDR3 distributions were not included in the plots.

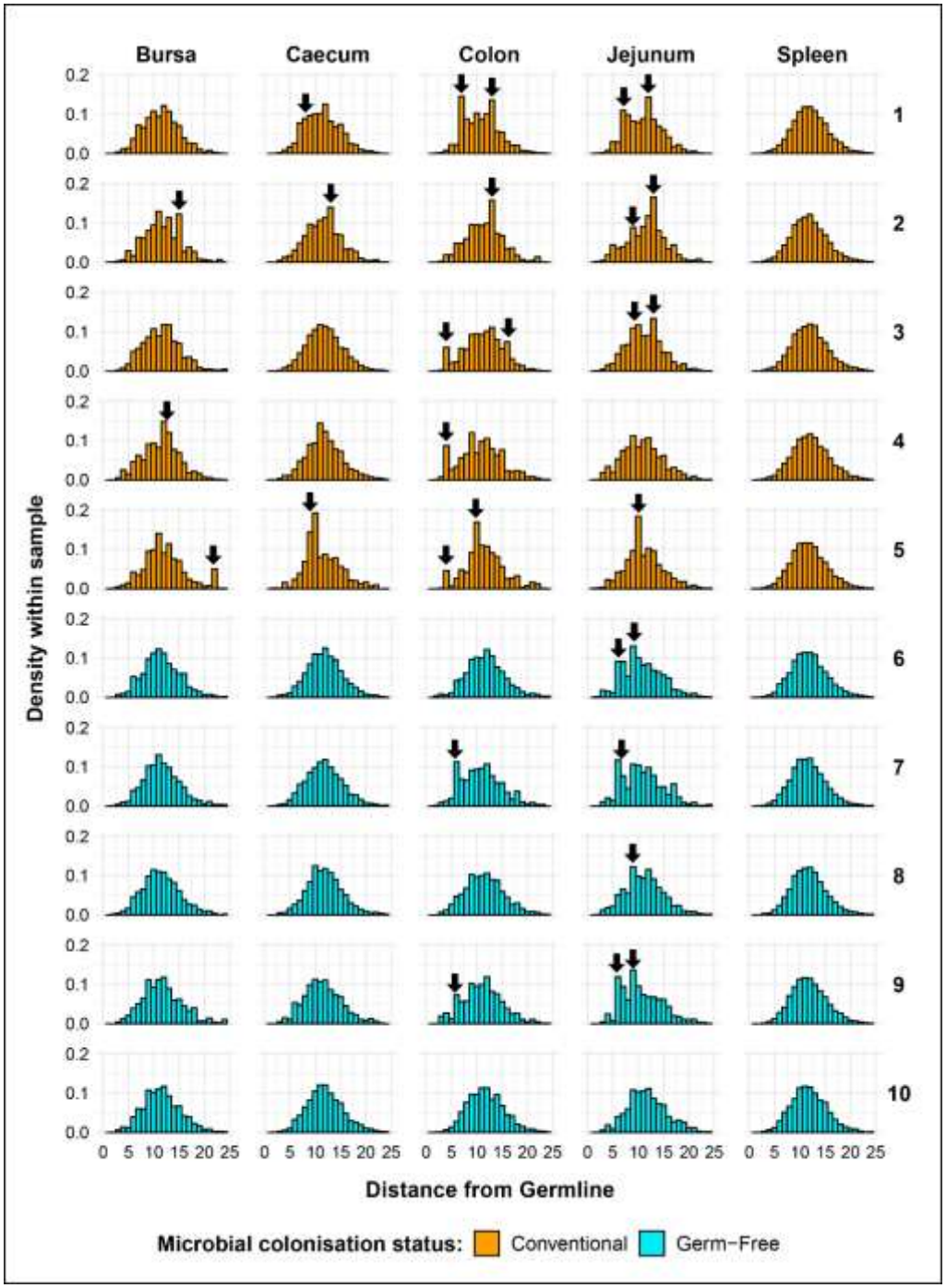

Figure 2. 4: *TCRβ CDR3 germline distance distribution by tissue and bird.*

The densities of CDR3 Levenshtein distances (see main text) to a theoretical VDJ rearrangement are displayed on the y axes of the plots. Each row displays the tissues of an individual bird for which the corresponding number is shown on the right side of the plots. Colours denote the microbial colonisation status of chickens for conventional flora (orange) and germ-free (light blue). Black arrows illustrate deviations from normality which suggest potential clonal biases. For visualisation purposes, the long tails of the CDR3 distributions were not included in the plots.

Similar to the CDR3 length distribution patterns, all conventional flora colon samples exhibit deviations from normality which indicate an increased proportion of clones with specific rearrangements. Moreover, the two germ-free chickens that displayed length-specific expansions in the colon (birds 7 and 9) also have marked expansions in terms of germline distance. However, by contrast to the CDR3 lengths when only one conventional bird had a suggested expansion in the caecum, all of the birds in this group show expansions in the bursal and/or caecal samples. These patterns are not observable in the germ-free birds, which show little to no deviations from normality just as for the CDR3 length distributions.

Together, the results of the CDR3 lengths and distances from germline analysis suggest that the birds may exhibit clonal biases which are dependent both on tissue type and microbial colonisation status.

II.3.3.4. CDR3 amino acid physicochemical properties

Since the TCRβ interactions with peptides are based upon the physicochemical properties of the CDR3 amino acid residues, these were explored in the repertoires obtained with germ-free and conventionally reared chickens. The values for each measurement was obtained from the IMGT online database (www.imgt.org/ IMGTeducation/Aide-memoire/_UK/aminoacids/IMGTclasses.html) [149,150]. The total volume (Å3) for each TCRβ CDR3 was calculated by summing the corresponding volumes of the individual amino acids constituting the sequence [151]. For the hydropathy, polarity, and charge of the amino acids, the net scores for individual CDR3 sequences were calculated by summing the values for each residue and dividing by the total number of amino acids [152,153].

Several observations are apparent regarding the physicochemical properties of the CDR3s in the observed tissue samples. First, the specific tissue types have characteristic distribution patterns which are not profoundly influenced by the microbial colonisation status. Second, heterogeneity among tissues of different individuals is an important component of the

observed patterns. As such, if specific peaks are present in one bird, the same features are not necessarily represented in others, irrespective of microbial status. Third, the physicochemical properties of CDR3 amino acids seem to be consistent among all spleen samples, in a similar manner to the CDR3 length and germline distance distributions (see above).

The distribution patterns of the CDR3 amino acid volumes (**Figure 2.5**) show no marked differences between individuals when considering the spleen, bursa, and caecum samples. However, several density peaks are observable in jejunum and colon, where the influences of the microbial treatment group become apparent. In the colon, the germ-free birds generally do not have pronounced peaks in CDR3 volumes whereas the conventional flora birds show multiple peaks of variable volumes. By contrast, the jejunal samples exhibit pronounced peaks irrespective of treatment group, although smaller-volume CDR3s seem to be more pronounced in the germ-free chickens.

Similar observations can be made regarding the CDR3 net polarity score (**Figure 2.6**), with the spleen, bursa, and caecum showing no specific patterns in the distributions that could be distinguished from individual-specific variability. However, just as for the CDR3 volume distributions, the jejunum exhibits the most pronounced net polarity peaks across both treatment groups. Furthermore, whereas the conventional flora chickens seem to favour clones with increased polarity, the jejunal samples of germ-free birds have more pronounced peaks of slightly less polar CDR3s. Concerning the colon samples, the distributions are noisier in conventional flora birds, with more peaks being present than in the germ-free birds.

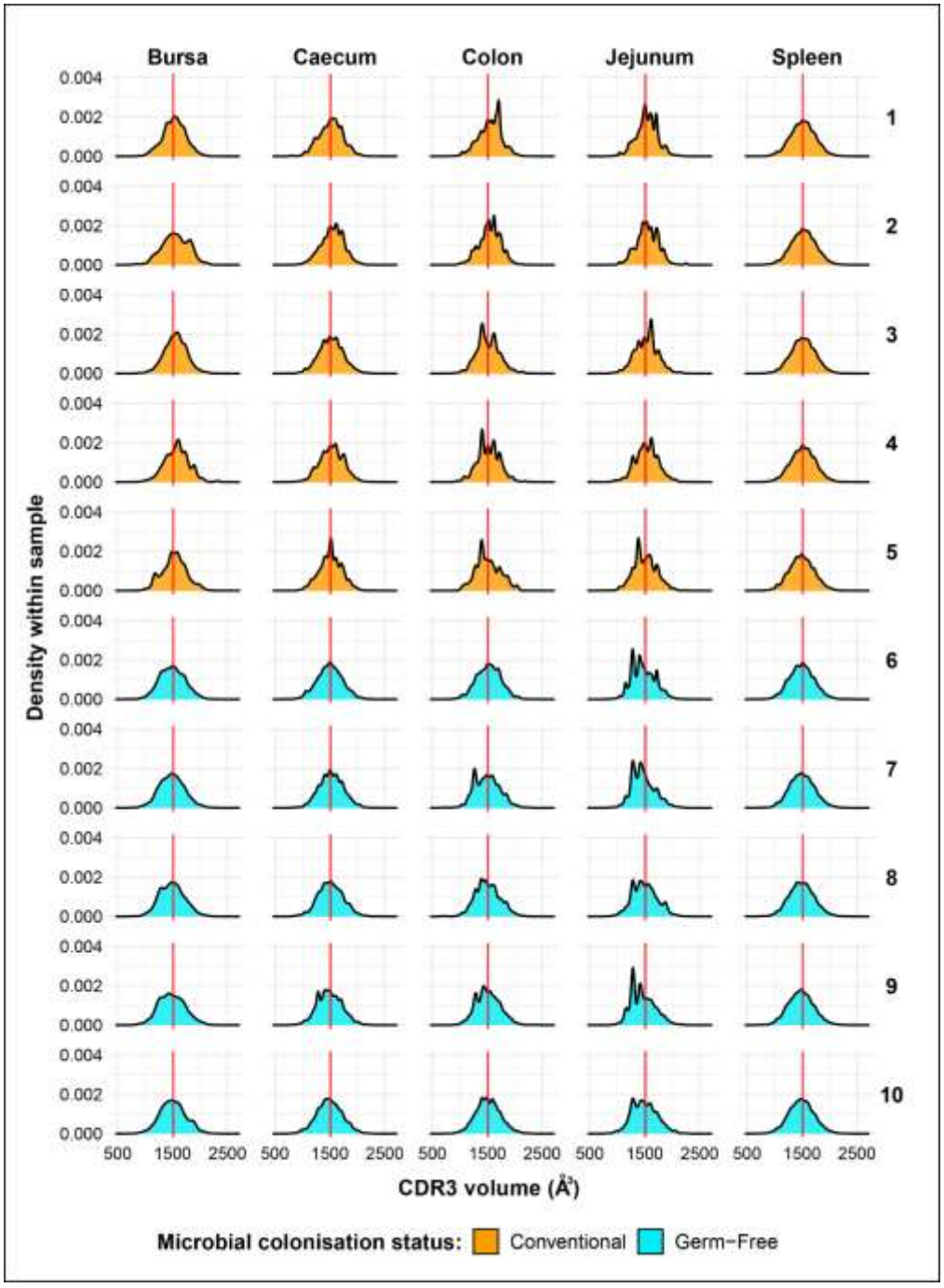

Figure 2. 5: TCRβ CDR3 volume distribution by tissue and bird.

Total CDR3 volume was calculated by summing the individual volumes ($Å^3$) of the comprising amino acid residues. Red lines represent the mean volume recorded across the samples. Each row displays the tissues of an individual bird for which the corresponding number is shown on the right side of the plots. Colours denote the microbial colonisation status of chickens for conventional flora (orange) and germ-free (light blue)

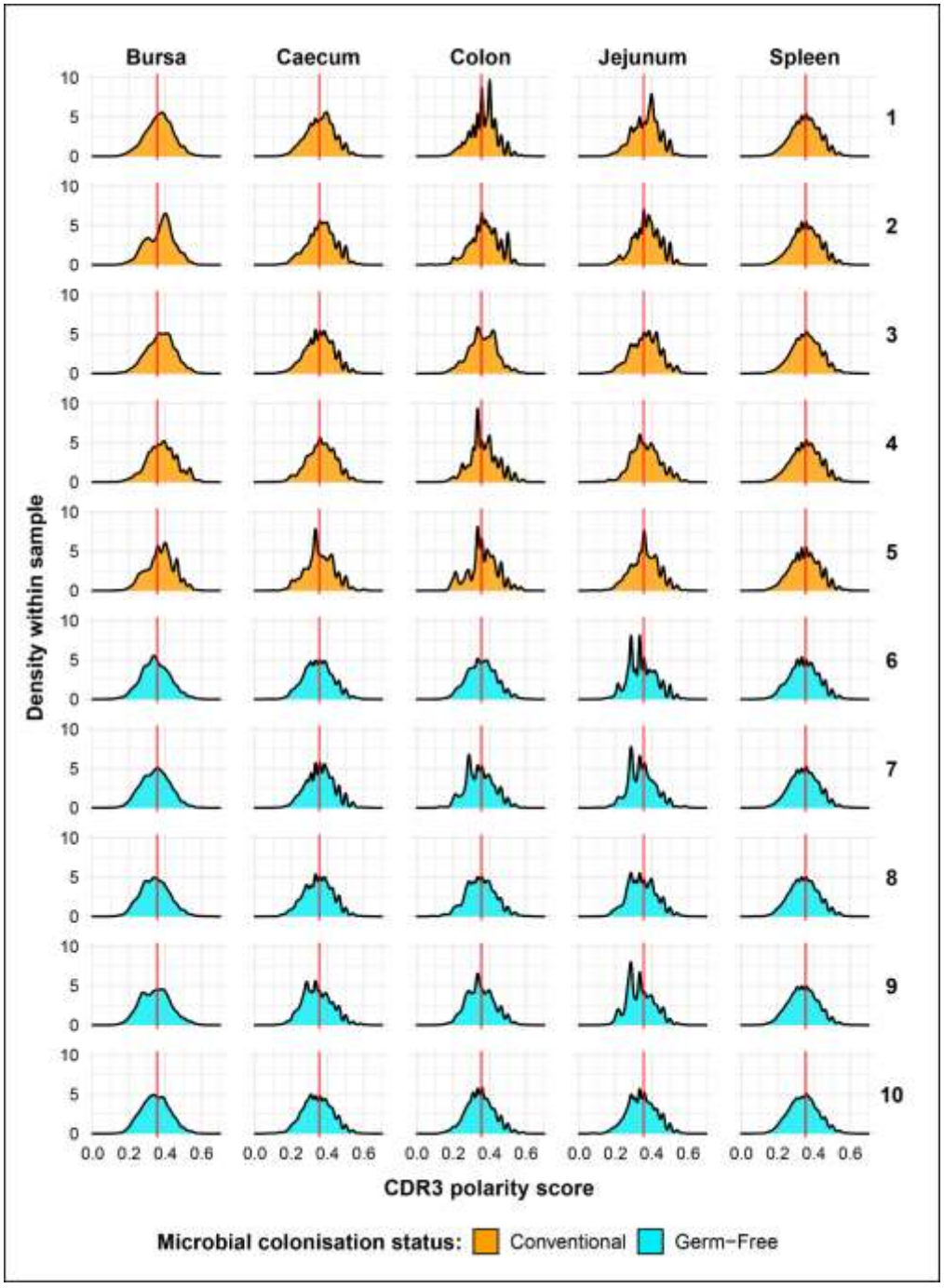

Figure 2. 6: TCRβ CDR3 net polarity score distribution by tissue and bird.

The net CDR3 polarity was calculated by summing the individual polarity values of the comprising amino acids and dividing by the total number of residues. Red lines represent the mean polarity recorded across the samples. Each row displays the tissues of an individual bird for which the corresponding number is shown on the right side of the plots. Colours denote the microbial colonisation status of chickens for conventional flora (orange) and germ-free (light blue)

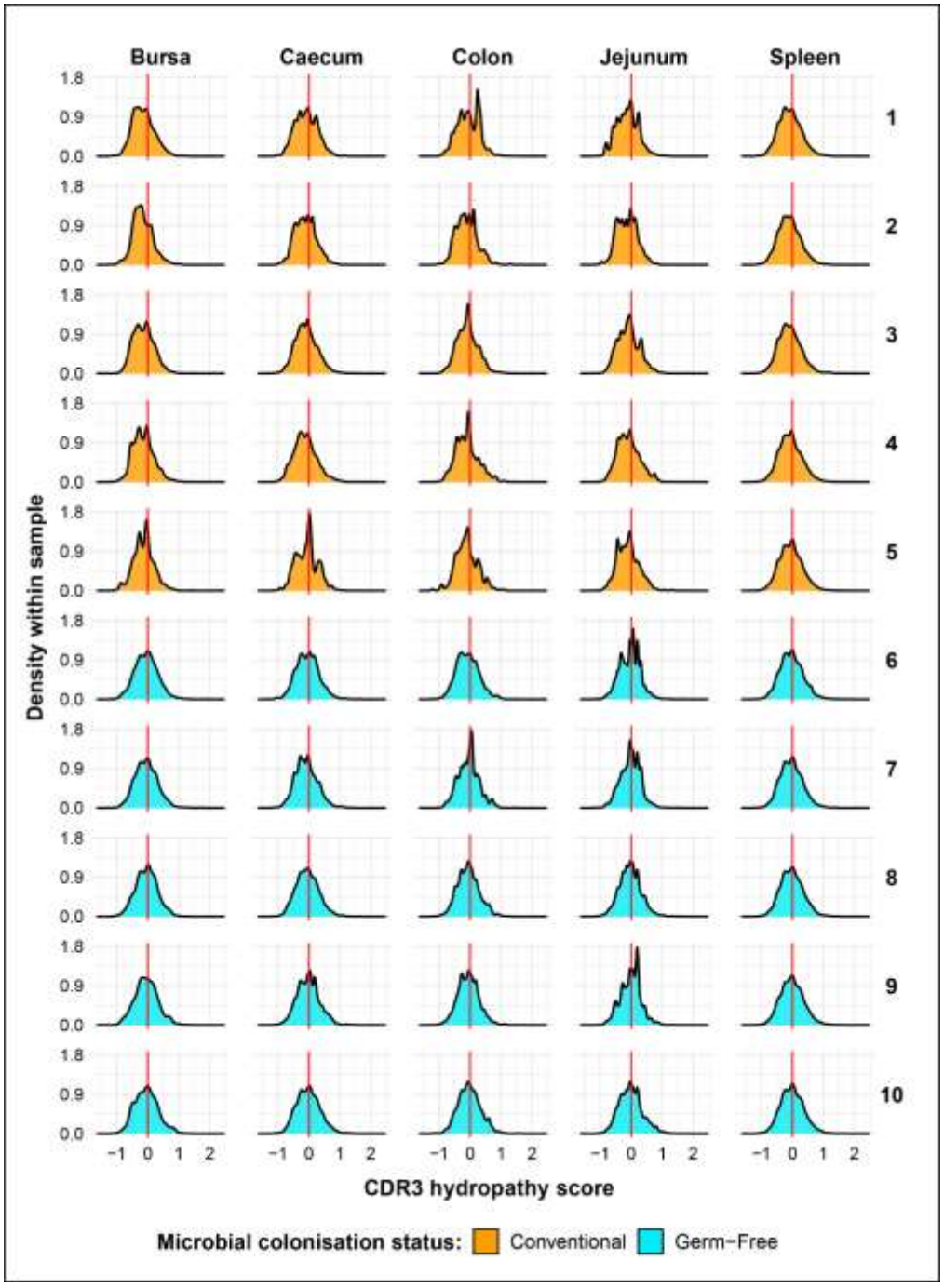

Figure 2. 7: *TCRβ CDR3 net hydropathy score distribution by tissue and bird.*

The net CDR3 hydropathy was calculated by summing the individual hydropathy values of the comprising amino acids and dividing by the total number of residues. Red lines are present at the value of 0. Each row displays the tissues of an individual bird for which the corresponding number is shown on the right side of the plots. Colours denote the microbial colonisation status of chickens for conventional flora (orange) and germ-free (light blue)

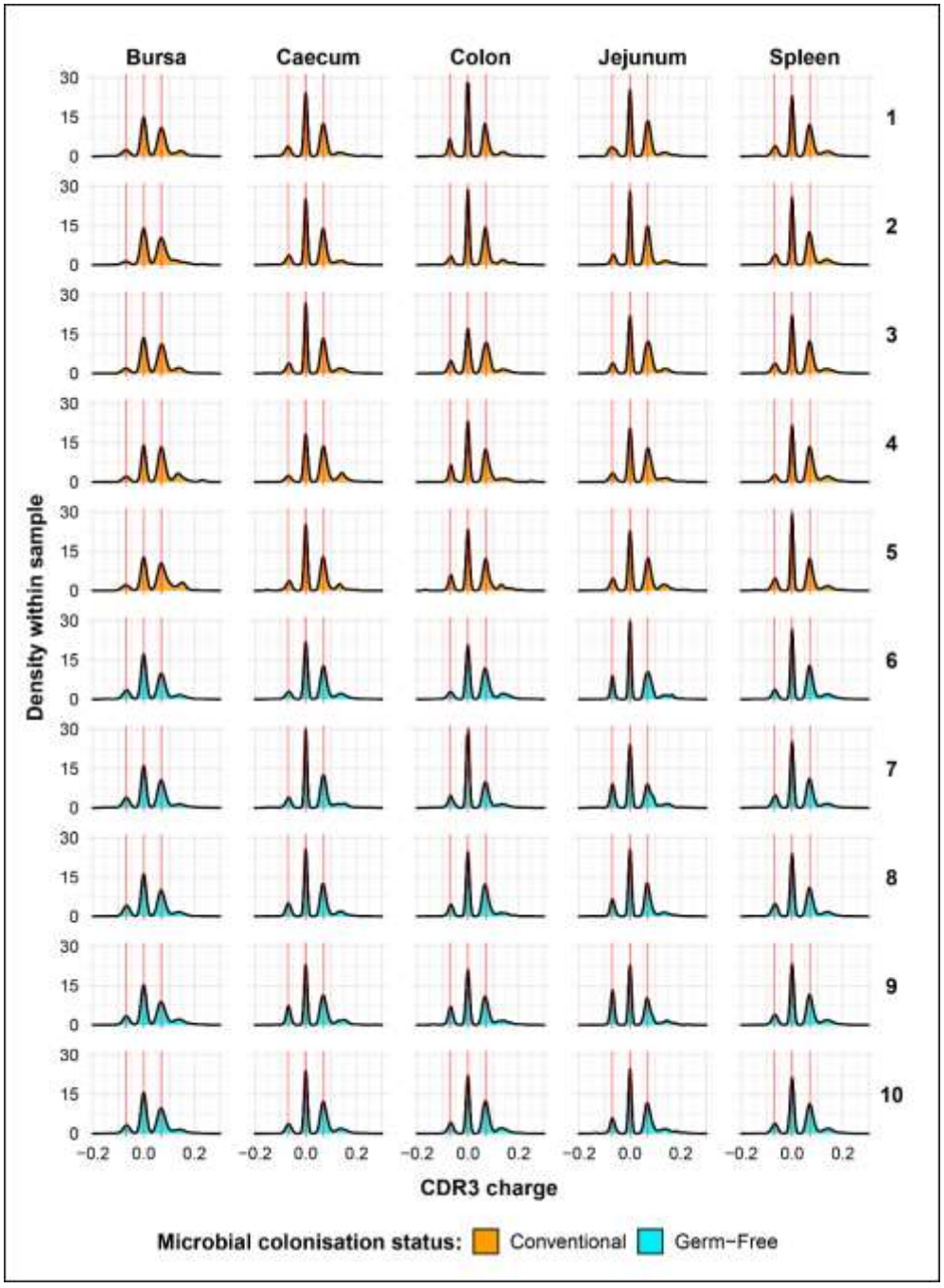

Figure 2. 8: *TCRβ CDR3 net charge distribution by tissue and bird.*

The net CDR3 charge was calculated by summing the individual charges of the comprising amino acids and dividing by the total number of residues. Red lines represent the first 3 most abundant densities (approximately –0.06, 0, and 0.07) recorded across the samples. Each row displays the tissues of an individual bird for which the corresponding number is shown on the right side of the plots. Colours denote the microbial colonisation status of chickens for conventional flora (orange) and germ-free (light blue)

The net hydropathy score distribution of the CDR3 sequences (**Figure 2.7**) show no pronounced difference between the groups, although tissue-specific effects are more apparent in the intestinal samples, where the distributions are noisier. Regarding the net charge of the CDR3 amino acids (**Figure 2.8**), 3 major peaks are present across all samples, with the largest one being concentrated around 0. The other two distribution peaks are present almost symmetrically at -0.06 and 0.07, with positively charged clones being more abundant. Interestingly, the variability is quite pronounced across individuals, with the 3 peaks exhibiting different magnitudes depending on bird and tissue sample, seemingly irrespective of colonisation status.

The patterns revealed by the distributions of CDR3 sequences with respect to their amino acid physicochemical properties indicate that there might be tissue-specific effects on the TCRβ repertoire, and that these patterns might also be influenced by exposure to the microbial flora. However, a more in-depth analysis which employs statistical methods was required to draw conclusions on both the presence and magnitude of such effects.

II.3.3.5. Tissue-specific repertoire diversity

The analysis of clonal diversity offers valuable insights into the TCRβ repertoire of each tissue type between the two treatment groups (**Figure 2.9**). In terms of clonal richness (D_0), the repertoire of germ-free chickens is significantly more diverse in the bursa and caecum, whilst there is no difference compared to the conventional birds in the other tissues. However, when "typical clones" are considered (D_1), the difference between the colon samples also becomes significant, with the germ-free being more diverse than the conventional birds. Although the effective number of species is lower, these patterns are also maintained for the "dominant clones" (D_2).

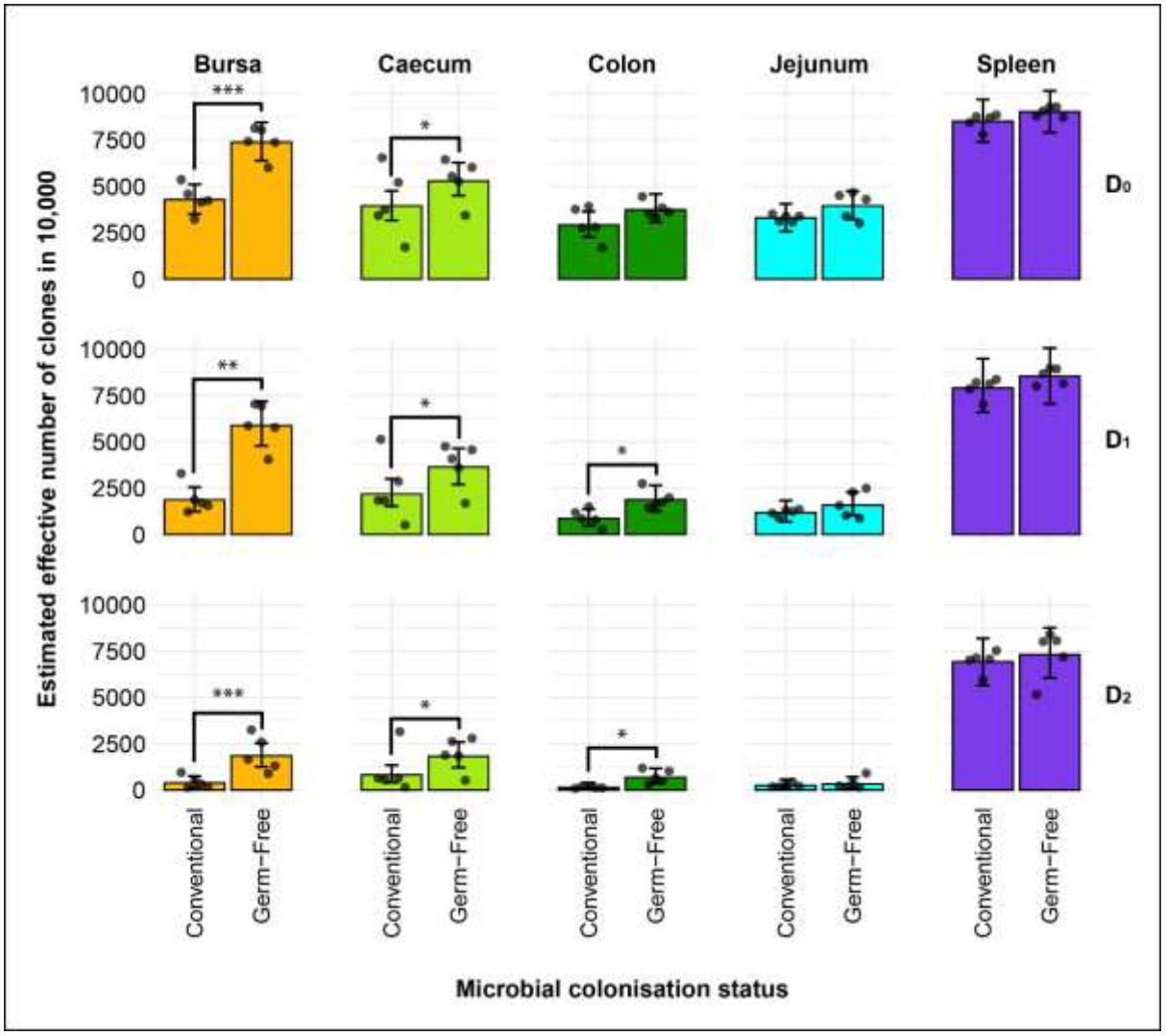

Figure 2. 9: *Effective diversity within conventional and germ-free samples.*

Different rows show the effective number of clones corresponding to clonal richness (D0), the typical clones (D1), and dominant clones (D2). Tissues are colour coded for the bursa (orange), caecum (green), colon (dark green), jejunum (light blue), and spleen (purple). Dots represent individual bird observations of the effective number of species calculated in each tissue for the corresponding Hill number values. Error bars show the 95% bootstrap confidence intervals for the point estimates generated from 1000 simulations of the model. Statistically significant differences between the model estimates are depicted above the plots based on their corresponding p-values: * = $p < 0.05$; ** = $p < 0.01$, *** = $p < 0.001$.

The large intestines (caecum and colon) and bursa of conventional birds were less diverse in terms of both the number of clones present (caecum and bursa) and the typical and dominant clones in the tissues (colon, caecum, and bursa), as suggested by the D_1 and D_2 measurements, respectively. By contrast, the spleen and jejunum samples exhibit no such pronounced differences, suggesting that microbial colonisation does not influence the repertoire diversity in those tissues. These results strongly indicate that microbial colonisation is a driver of clonal expansions within the resident TCRβ repertoire, particularly in the intestinal tissues where the highest microbial loads are present. Comparable patterns of diversity with the same significant differences (between tissues and/or treatment groups) were observed when considering the repertoires at the amino acid level (**Figure A.1**).

II.3.3.6. Public and private clonal compartments

Clonal sharing across individuals is a key aspect of the T cell repertoire that could be used to predict the possibility of shared responses based upon repertoire. The public clonal compartment constitutes a dominant component of the repertoire in all tissues, with the exception of the spleen where it was found at a lower but still pronounced level (**Figure 2.10**). In the intestinal segments, the proportion of public clones generally exceeded 45% of the total identified TCRβ clones, sometimes reaching almost 75% in the jejunum and colon. Interestingly, there were no obvious differences between the germ-free and conventional chickens (**Figure A.2**). The private clonal compartment in the spleen is at significantly higher levels than the public clones, amounting close to 90% of sequences. By contrast, in the caecum and bursa, the two compartments were not significantly different to one another, with the exception of the germ-free caecal samples which had a higher proportion of private clones. In the colon and jejunum, however, the public clones were significantly more abundant, encompassing more than half of the total clonal compartment.

At the amino acid level (**Figure A.3**), the patterns were comparable with a slightly higher proportion of public clones being identified. This resulted in significantly higher proportions of public rather than private clones in the bursal compartments of both treatment groups. Additionally, in the caecum, the previously identified significant

difference between the public and private clones in the germ-free was no longer observed due to the higher proportion of public clones at the amino acid level. Furthermore, the conventional birds exhibited significantly higher proportions of public rather than private clones in the caecum when the CDR3 amino acid rather than nucleotide sequences were considered. No differences were observed between the groups when individual tissues were considered (**Figure A.4**).

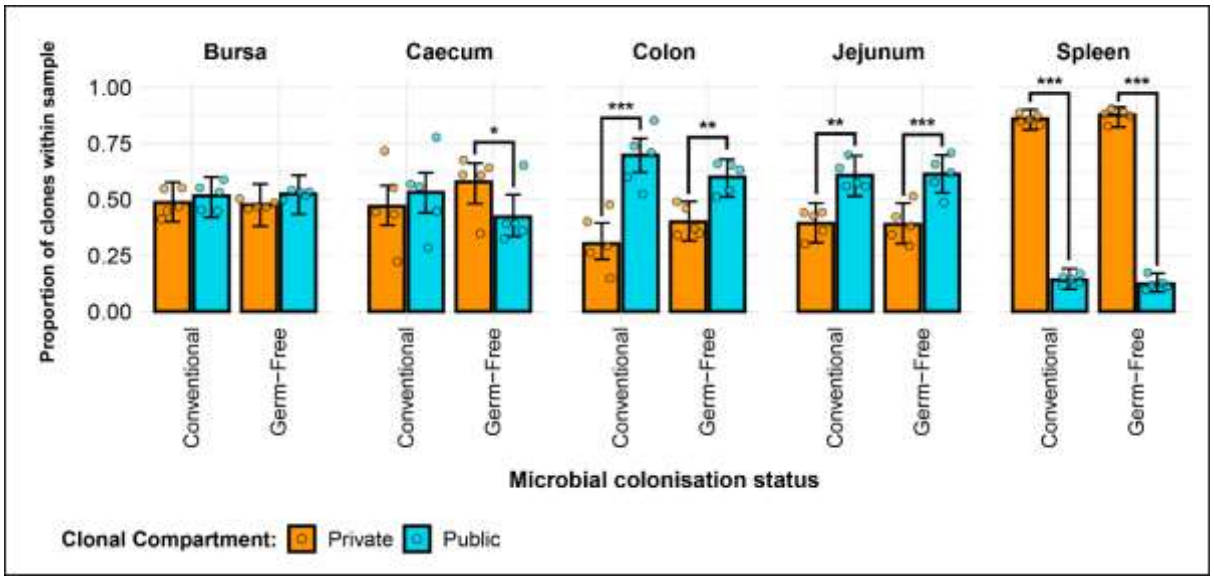

Figure 2. 10: *TCRβ clone CDR3 nucleotide public and private compartments.*
Private (individual-restricted) clones are shown in orange. Public clones (shared between more than two individuals) and are shown in light blue. Dots represent individual bird observations of public and private clonal compartments. Error bars represent 95% bootstrap confidence intervals for the point estimates generated from 1000 simulations of the model. Statistically significant differences between the model estimates are depicted above the plots based on their corresponding p-values: * = $p < 0.05$; ** = $p < 0.01$, *** = $p < 0.001$.

As the publicness of clones, in the context of the TCR repertoire, is a relative term, it is important to discriminate between different degrees of clonal sharing (i.e. how many individuals share a particular clone of TCRβ). When incorporating the different categories of public clones into the model, differences become apparent between the two microbial treatment groups when specific public classes are considered (**Figure 2.11**). The clones with higher degrees of publicness occupy less of the total clonal compartments within tissues.

Public clones which are found in fewer than five birds seem to dominate the total clonal composition with no significant differences between the two microbial groups. However, when considering the 'common publics' (i.e. found in more than five birds but not in all birds of the analysis), all tissues aside from the spleen showed a significantly higher proportion in the conventional microbiota birds. Interestingly, ubiquitous clones which are present in all birds can be identified, albeit at a low overall proportion of the total population. The highest proportions of ubiquitous clones were recorded in the jejunum and caecum, where the germ-free samples have significantly higher levels than their conventional counterparts. Similar patterns were observed when considering the level of CDR3 amino acids (**Figure A.5**), with the notable exception of the caecum, where the germ-free birds exhibited significantly higher proportions of private clones than the conventional birds.

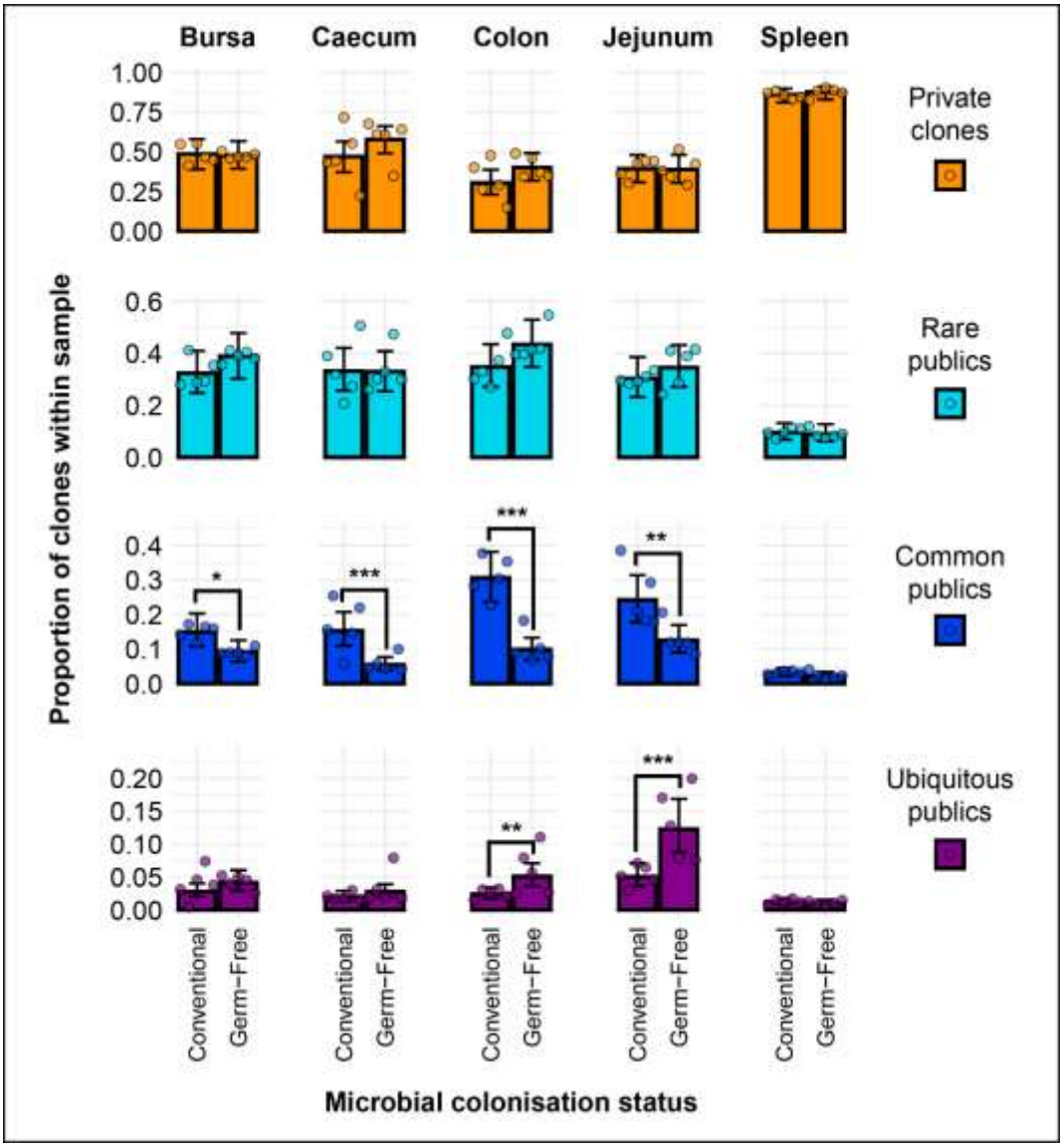

Figure 2. 11: *TCRβ clone CDR3 nucleotide private and public compartments based on different levels of clonal sharing between birds.*

Private (individual-restricted) clones are shown in orange. Rare publics (shared between ≥2 individuals and up to 5) and are shown in light blue. Common publics (shared between ≥5 and up to 9 birds) are shown in dark blue. Ubiquitous publics (found in all birds which were incorporated in the analysis) are shown in purple. Dots represent individual bird observations of private and distinct public clonal compartments. Error bars represent 95% bootstrap confidence intervals for the point estimates generated from 1000 simulations of the model. Statistically significant differences between the model estimates are depicted above the plots based on their corresponding p-values: * = $p < 0.05$; ** = $p < 0.01$, *** = $p < 0.001$.

The high proportion of public clones in the samples warranted further investigation. Cross-contamination due to experimental error was unlikely as a possibility given that the samples from the two treatment groups were processed and sequenced separately, and precautions were taken to prevent cross-contamination between individual tissue samples. Moreover, TCRβ CDR3 sequences reported in other published works (also using different lines of chicken) were compared at the amino acid and, where available, nucleotide levels with the sequencing results of the current analysis. As such, several amino acid sequences from previously published works of lower sequencing depth were identified in the current dataset (**Figure 2.12**). As such, 24/97 (~25%) CDR3 amino acid sequences from Mwangi *et al.* 2010 [144], 20/96 (~21%) from Mwangi *et al.* 2011 [154], 14/275 (~5%) from Ren *et al.* 2014 [155], and 8/119 (~7%) from Zhang *et al.* 2020 [111] were found to be shared with the current dataset. Interestingly, not all cross-study shared CDR3 sequences were from the public clonal compartment of the current microbial colonisation experiment. This suggests that the 'true public compartment' may be larger than the present analysis was able to identify.

As single amino acids may be coded for by distinct codons, , fewer CDR3 nucleotide sequences from this analysis are present in other reported datasets (**Table 2.2**), the majority of which are found in Mwangi *et al.* 2010. Out of the shared sequences, none were identified which are shared between all birds of the current analysis. However, whilst most shared CDR3s belong to rare public or common public compartments (see above), there are five TCRβ sequences which are considered private in the current analysis.

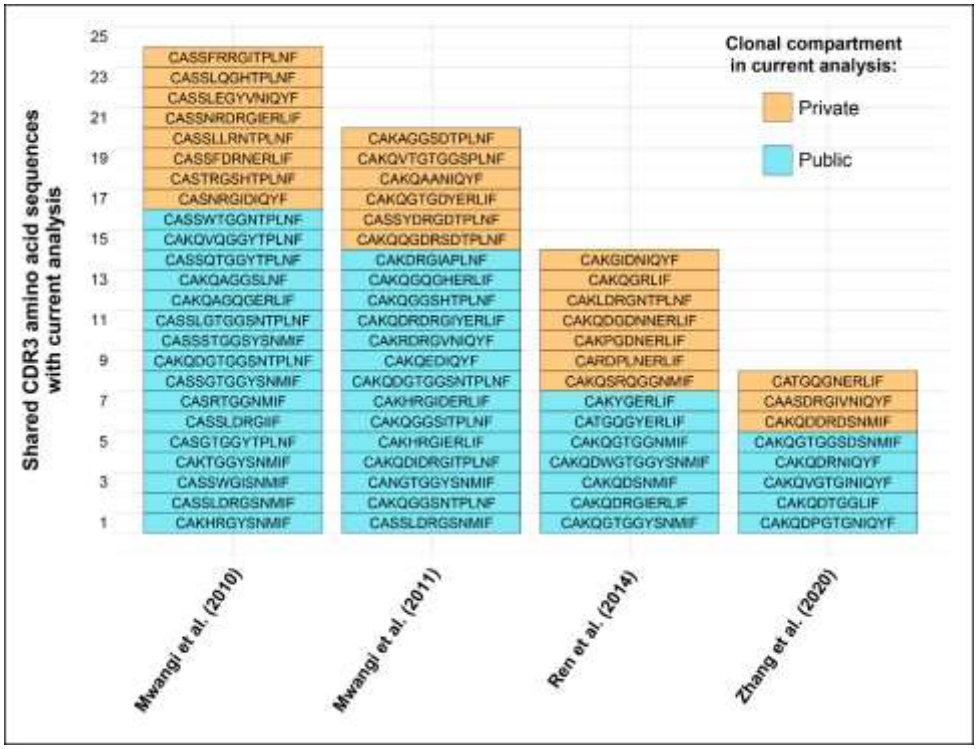

Figure 2. 12: *TCRβ shared CDR3 amino acid sequences with other published works.*
Sequence identity based on clonal compartments within current analysis is colour coded for the private (individual-restricted) and public (shared between two or more birds) repertoires in orange and light blue, respectively.

II.3.3.7. TCRβ V family usage and contributions to public compartments

The results of the analysis on individual V family usage reveal several patterns across the different tissue samples from the microbial colonisation groups (**Figure 2.13**). First, there was a higher Vβ1 contribution in all tissues of conventional birds when compared to their germ-free counterparts. Second, when considering the recently described Vβ3 family [111], all germ-free samples exhibited significantly higher contributions of Vβ3 clones to the TCRβ compartment, and these T cells are almost absent altogether from the tissues of the conventional birds, aside from the jejunum. Moreover, in the jejunal samples of germ-free birds, the Vβ3 clones were also found at the highest levels across all samples. Finally, only the bursal and splenic tissues show significant differences in the contribution of Vβ2 family

to the overall TCRβ repertoire, with conventional birds exhibiting lower proportions than the germ-free counterparts.

Publication	CDR3 nucleotide sequence	Clonal compartment in current analysis
Mwangi et al. (2010)	TGTGCCAGCAGTTTGGACAGGGGGATCATTTTC	Private
	TGTGCCAGCAGTGGGACAGGGGGATACAGTAACATGATTTTC	Private
	TGTGCCAGCAACAGGGGGATCGATATCCAGTATTTT	Private
	TGTGCCAGCAGTTTACAGGGACACACACCACTGAACTTT	Private
	TGTGCCAGCGGGACAGGGGGATACACACCACTGAACTTT	Rare publics
	TGCGCTAAGCAAGCGGGACAGGGCGAAAGACTGATCTTT	Rare publics
	TGTGCCAGCAGTCAGACAGGGGGATACACACCACTGAACTTT	Rare publics
	TGTGCCAGCAGTTCGACAGGGGGATCGTACAGTAACATGATTT	Rare publics
	TGTGCCAGCAGTTGGACAGGGGGAAACACACCACTGAACTTT	Rare publics
	TGTGCCAGCAGTAACCGGGACAGGGGGATCGAAAGACTGATCT	Rare publics
	TGTGCCAGCAGTTTGGACAGGGGGAGTAACATGATTTTC	Common publics
	TGTGCCAGCAGTTGGGGGATCAGTAACATGATTTTC	Common publics
	TGCGCTAAGACAGGGGGATACAGTAACATGATTTTC	Common publics
	TGTGCCAGCAGGACAGGGGGTAACATGATTTTC	Common publics
Mwangi et al. (2011)	TGTGCCAGCAGTTTGGACAGGGGGAGTAACATGATTTTC	Common publics
Zhang et al. (2020)	TGCGCTAAGCAAGTCGGGACAGGGATTAATATCCAGTATTTT	Private
	TGCGCTAAGCAAGATCGTAATATCCAGTATTTT	Rare publics

Table 2. 2: *TCRβ CDR3 nucleotide sequences shared with other published works.*
Sequence identity based on clonal compartments within current analysis is specified based on the specific private or public compartments. One sequence was found to be shared between the datasets and is highlighted in red.

By incorporating the distribution of V family clones in the private and public compartments, a more detailed pattern of the tissue-specific differences between the two gut microbiota colonisation groups is revealed (**Figure 2.14**). The overall higher Vβ1 presence in the conventional chickens was predominantly attributed to Vβ1 public clones. As such, this clonal compartment has a higher Vβ1 presence in all tissues aside for the spleen where the difference between the model estimates was not deemed statistically significant. Although the overall Vβ1 proportion of the repertoire was higher in the spleen, there were no significant differences in terms of either the public or private clonal compartments between the treatment groups. At the same time, concerning the private

compartments, there were no significant differences in Vβ1 family distribution between the two groups.

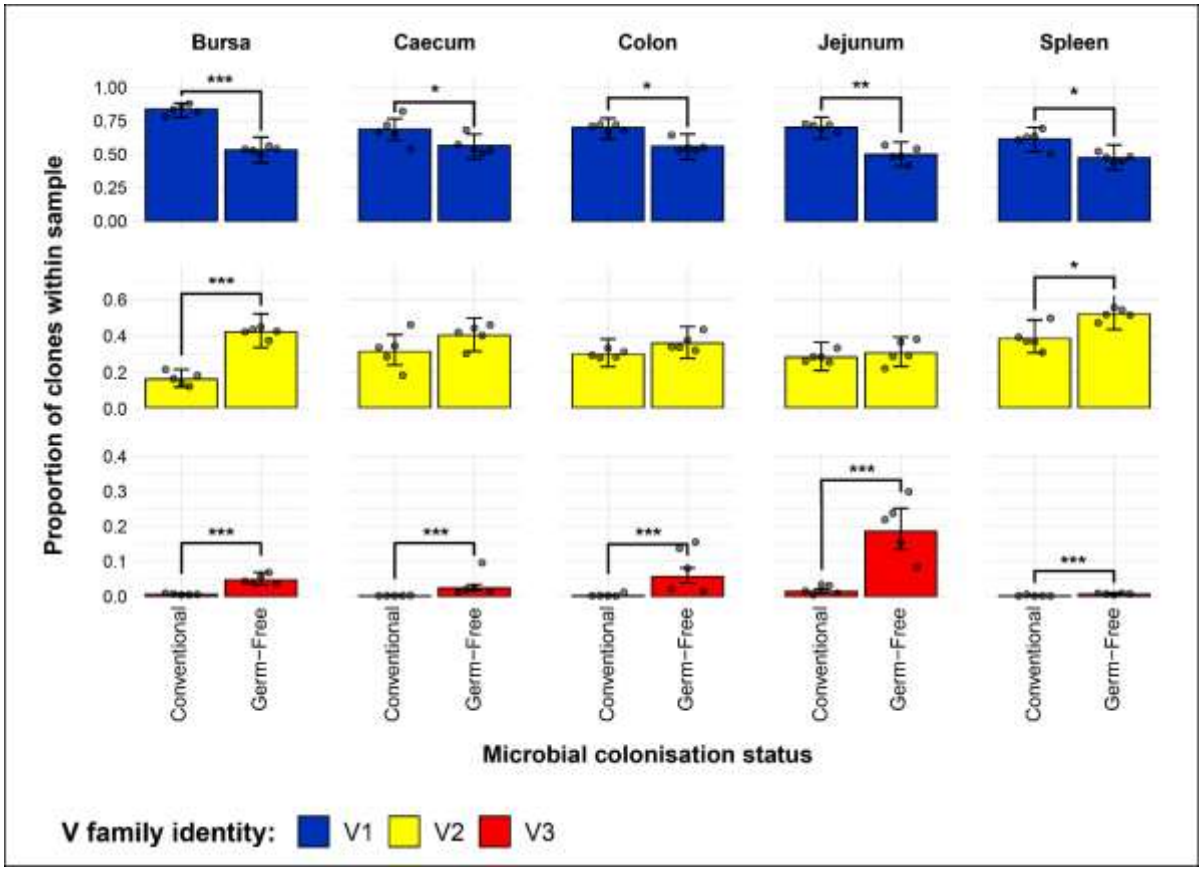

Figure 2. 13: *TCRβ V family usage in individual tissue samples across treatment groups.*
V family identities are shown in blue (Vβ1), yellow (Vβ2), and red (Vβ3). Grey dots represent individual bird observations for each V family. Error bars represent 95% bootstrap confidence intervals for the point estimates generated from 1000 simulations of the model. Statistically significant differences between the model estimates are depicted above the plots based on their corresponding p-values: * = $p < 0.05$; ** = $p < 0.01$, *** = $p < 0.001$.

With the Vβ2 family, the only significant differences that related to microbial status were in the bursa, where both the public and private compartments of germ-free birds showed higher proportions of Vβ2 clones. This is consistent with the previous estimates of the simpler model and reveals that the higher levels of Vβ2 in the germ-free bursa are similarly distributed between the public and private clonal compartments. For the spleen, the higher

levels of Vβ2 clones in the germ-free which were observed with the initial model seem to be attributable to the private clonal compartment, although the estimates for the private and public clonal compartments of the two groups are not significantly different from one another.

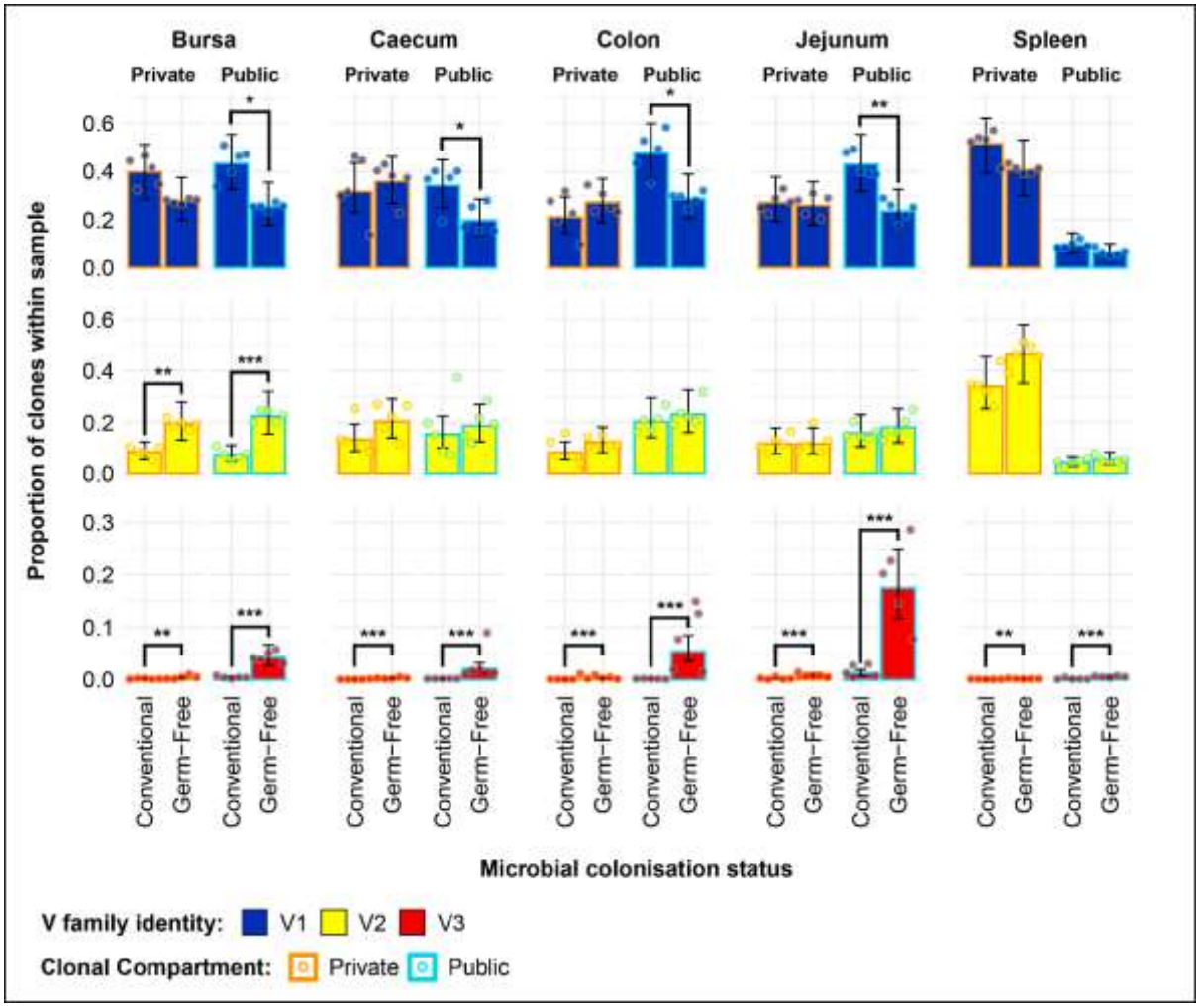

Figure 2. 14: *TCRβ clone V family publicness in individual tissue samples across treatment groups.*
V family identities are shown in blue (Vβ1), yellow (Vβ2), and red (Vβ3). Private (individual-restricted) clones have an orange outline. Public clones which are shared between more than two individuals have a light blue outline. Dots represent individual bird observations of V family contributions to the public and private clonal compartments. Error bars represent 95% bootstrap confidence intervals for the point estimates generated from 1000 simulations of the model. Statistically significant differences between the model estimates are depicted above the plots based on their corresponding p-values: * = $p < 0.05$; ** = $p < 0.01$, *** = $p < 0.001$.

The incorporation of the public and private clonal compartments showed several interesting patterns for the Vβ3 family. First, Vβ3 clones are at very low levels in all birds, except for the germ-free jejunum where they are most abundant. Second, the germ-free birds have a significantly higher presence of Vβ3 clones in both the private and public compartments for all tissues. Third, the much higher relative levels of Vβ3 clones revealed by the initial model in the germ-free birds are predominantly public.

The distribution of V family clones in the private and public compartments warranted further investigation by considering the degrees of clonal sharing. As such, the model was expanded to incorporate the different categories of public clones as described above. This revealed several differences at the levels of clonal compartment, tissue, and microbial status. In the spleen, there were no microbial status-driven differences between any of the clonal compartments within Vβ families, with the notable exception of the Vβ3 family of the germ-free, which exhibited higher levels in the private, rare public, common public, and ubiquitous clones (**Figure 2.15**). In the bursa, the previously identified higher level of Vβ1 public clones in the conventional chickens was mainly attributable to the common publics, as no significant differences were present between rare public or the ubiquitous clones of the two groups. By contrast, the greater total Vβ2 public compartment of the germ-free group is attributable to both rare and common publics, both of these compartments exhibiting higher levels than in the conventional birds. At the same time, as observed in the spleen, the Vβ3 bursal clones were relatively more abundant in the germ-free group in all public compartments, albeit at very low levels.

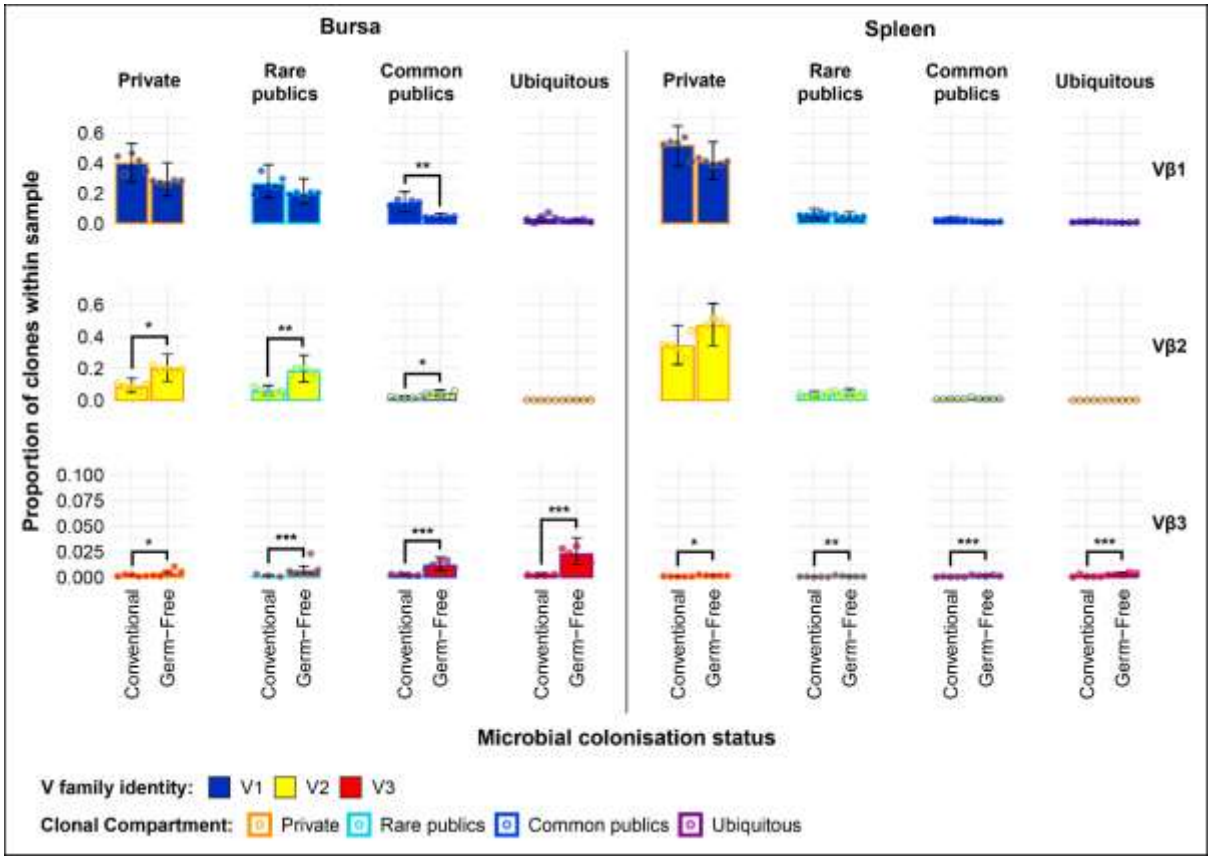

Figure 2. 15: *TCRβ clone V family private and public compartments in the bursa and spleen based on different levels of clonal sharing between birds.*

Private (individual-restricted) clones are outlined in orange. Rare publics (shared between ≥2 and up to 5 birds) and are outlined in light blue. Common publics (shared between ≥5 and up to 9 birds) are outlined in dark blue. Ubiquitous publics (found in all birds which were incorporated in the analysis) are outlined in purple. V family identities are shown in blue (Vβ1), yellow (Vβ2), and red (Vβ3). Dots represent individual bird observations of V family contributions to the public and private clonal compartments. Error bars show the 95% bootstrap confidence intervals for the point estimates generated from 1000 simulations of the model. Statistically significant differences between the model estimates are depicted above the plots based on their corresponding p-values: * = $p < 0.05$; ** = $p < 0.01$, *** = $p < 0.001$.

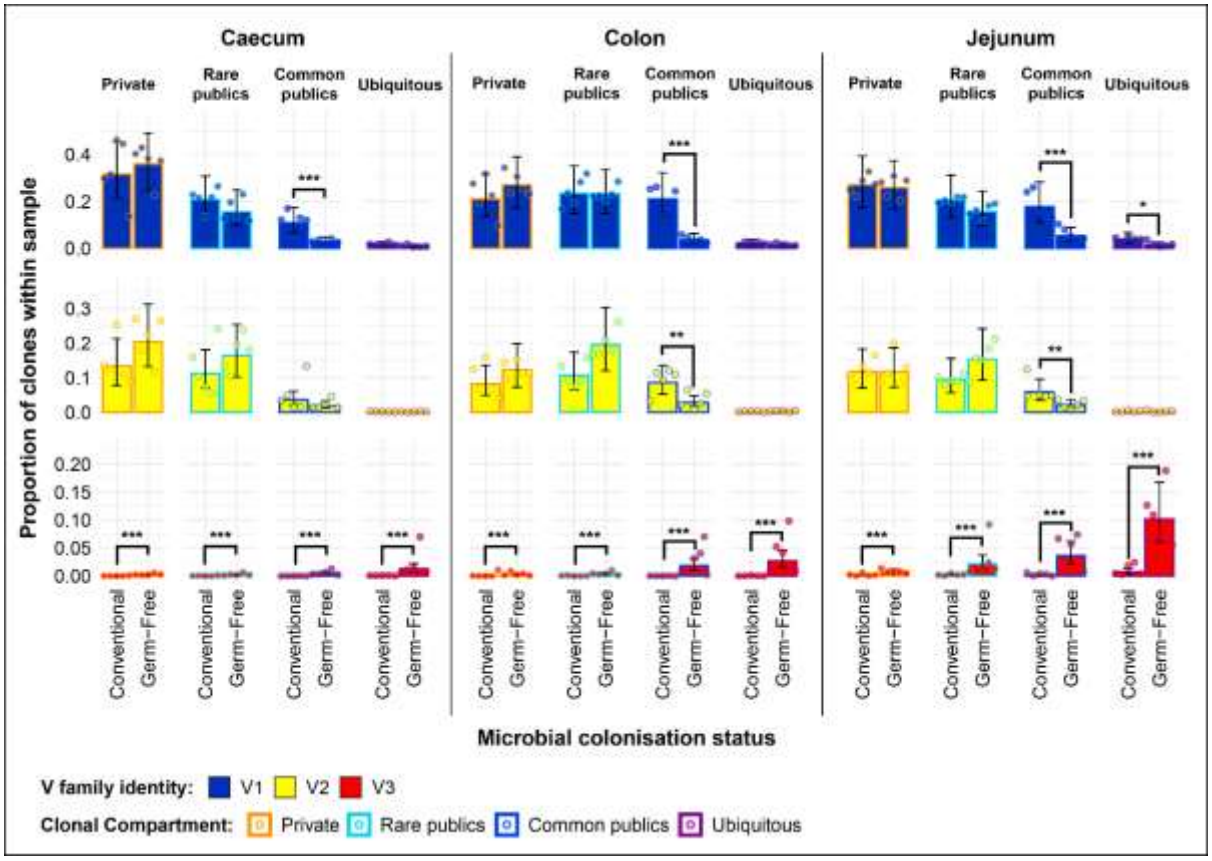

Figure 2. 16: *TCRβ clone V family private and public compartments in the intestinal tissues based on different levels of clonal sharing between birds.*

Private (individual-restricted) clones are outlined in orange. Rare publics (shared between >2 individuals up to 5) and are outlined in light blue. Common publics (shared between >5 and up to 9 birds) are outlined in dark blue. Ubiquitous publics (found in all birds which were incorporated in the analysis) are outlined in purple. V family identities are shown in blue (Vβ1), yellow (Vβ2), and red (Vβ3). Dots represent individual bird observations of V family contributions to the public and private clonal compartments. Error bars show the 95% bootstrap confidence intervals for the point estimates generated from 1000 simulations of the model. Statistically significant differences between the model estimates are depicted above the plots based on their corresponding p-values: * = $p < 0.05$; ** = $p < 0.01$, *** = $p < 0.001$.

The expanded model also reveals important patterns in the intestinal samples (**Figure 2.16**). The higher presence of Vβ1 public clones in the conventional birds suggested by the simpler model can be mainly attributed to the common public compartment. At the same time, there was a small but significantly higher ubiquitous Vβ1 clone presence in the jejunal

samples of conventional SPF birds. When considering at the Vβ2 family, although the simpler model did not reveal marked differences between the total public compartment of intestinal tissues, conventional birds exhibit significantly higher levels of Vβ2 common publics in the colon and jejunum. Notably, as seen in the bursa and spleen, the levels of Vβ2 ubiquitous clones were very low or absent altogether in all intestinal samples. The germ-free birds also exhibited higher levels of Vβ3 clones in all public clonal compartments, with the ubiquitous clones reaching the highest levels in all intestinal tissue samples.

Together, the results of the Vβ family models, including the incorporation of clonal compartments based on the degree of sharing between birds reveal patterns which were obscured in the global repertoire analyses. Importantly, the Vβ3 family is predominantly public and much more abundant in the small and large intestines of germ-free chickens as opposed to their conventional microbiota counterparts.

II.3.3.8. TCRβ J gene usage and contributions to public compartments

When considering the distributions of Jβ clones in the total repertoire of the samples, no consistent patterns were observed in terms of the differences related to microbial status (**Figure 2.17**). Significant differences were only observed in the bursa and jejunum, where the conventional birds differ from the germ-free. In the former tissue, the conventional birds contained a higher proportion of the Jβ1 and lower levels of Jβ3, whilst in the jejunum the conventional birds contained higher proportions of Jβ4 and less Jβ2 than in the germ-free.

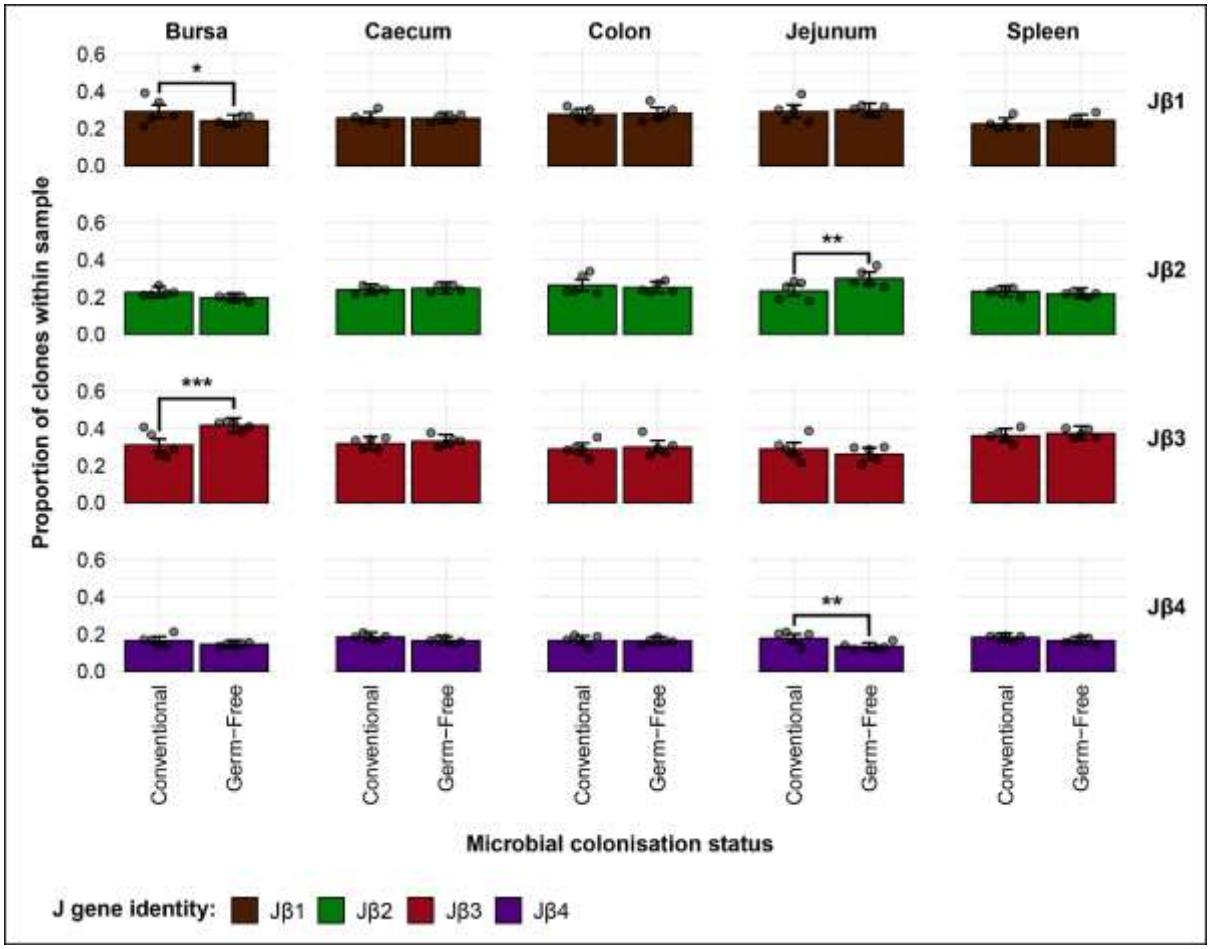

Figure 2. 17: *TCRβ J gene usage in individual tissue samples across treatment groups.*
V family identities are shown in brown (Jβ1), green (Jβ2), dark red (Jβ3), and purple (Jβ4). Grey dots represent individual bird observations for specific Jβ clones. Error bars represent 95% bootstrap confidence intervals for the point estimates generated from 1000 simulations of the model. Statistically significant differences between the model estimates are depicted above the plots based on their corresponding p-values: * = $p < 0.05$; ** = $p < 0.01$, *** = $p < 0.001$.

Similar observations can be made regarding the distribution of Jβ rearranged clones in the public and private compartments (**Figure 2.18**). Few significant differences were present between the two microbial colonisation groups, without any consistent pattern. The colon of conventional birds exhibits higher levels of Jβ1 public clones and lower levels of Jβ2 private clones than the germ-free. In the jejunum, the conventional chickens have higher Jβ4 and fewer Jβ2 public clones than the germ-free. No other significant differences were detected, and the model was not further expanded to include the different categories of Jβ publics segregated on the of clonal sharing between birds.

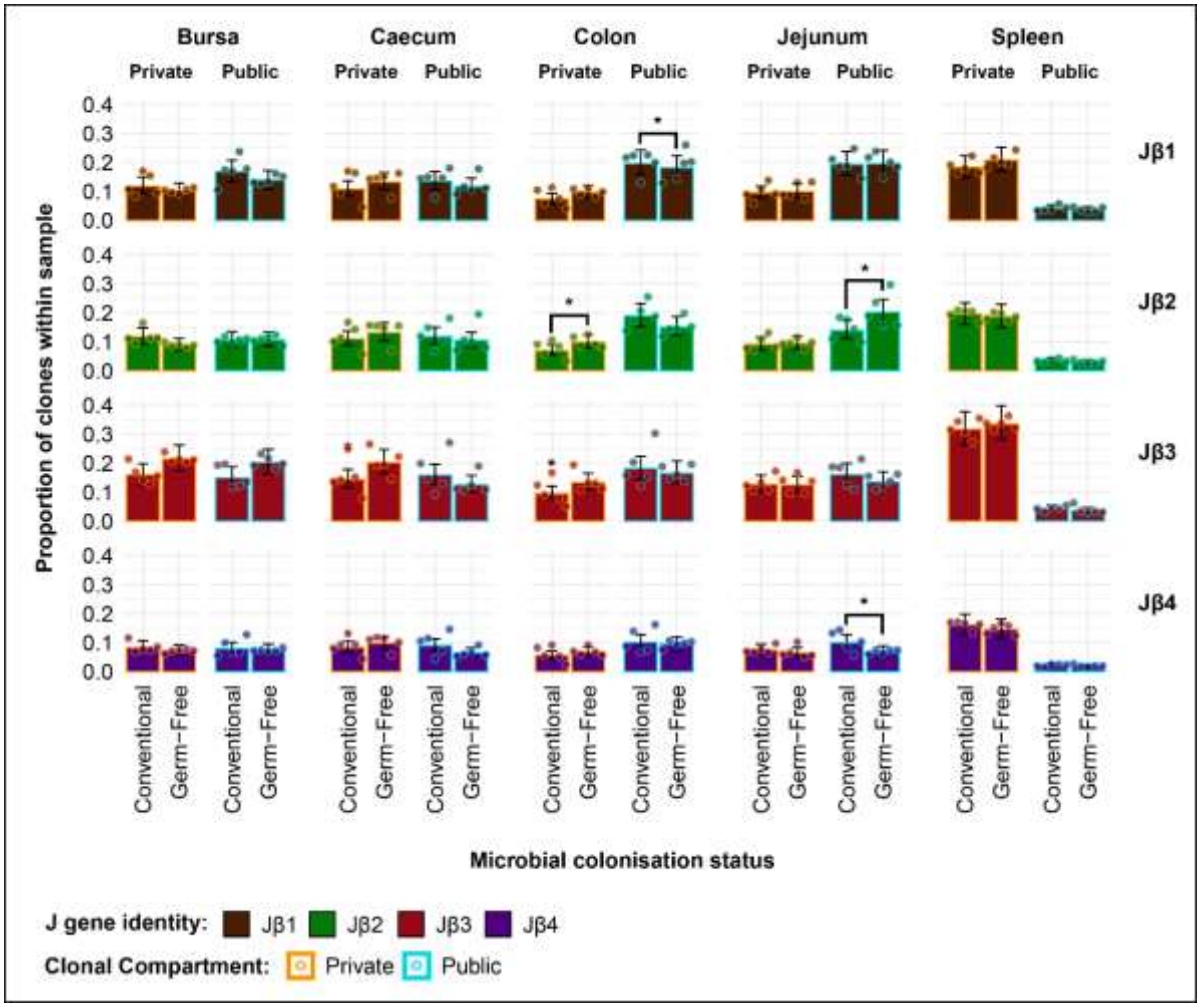

Figure 2. 18: *TCRβ J gene publicness in individual tissue samples across treatment groups.*
J family identities are shown in brown (Jβ1), green (Jβ2), dark red (Jβ3), and purple (Jβ4). Private (individual-restricted) clones have an orange outline. Public clones which are shared between more than two individuals have a light blue outline. Dots represent individual bird observations for specific Jβ clone contributions to the public and private clonal compartments. Error bars represent 95% bootstrap confidence intervals for the point estimates generated from 1000 simulations of the model. Statistically significant differences between the model estimates are depicted above the plots based on their corresponding p-values: * = $p < 0.05$; ** = $p < 0.01$, *** = $p < 0.001$.

II.3.3.9. Microbial status-restricted repertoires and clonal expansions

As significant effects of both tissue type and microbial treatment were observed in the V family contributions to the private and public clonal compartments, specific clonal expansions in the two groups were examined further. Clones which were found at or above

0.5% of the total repertoire in at least one sample were considered to be expanded. Focus was put on clones which were expanded in at least two birds (i.e. public clones) of a microbial treatment group and absent or below the expansion threshold in all individuals of the other.

Several group-restricted expanded public clones were found in the conventional microbiota chicken samples with 16 belonging to the Vβ1 family and 7 to the Vβ2 (**Figure 2.19**). Interestingly, although the identified clones show a pronounced expansion in at least one sample, only 3 TCRβ clones were expanded across multiple birds, and none showed pronounced expansion in the spleen, where (if present) they were at low levels. Of these, two belong to the Vβ1 family and exhibit expansions in the bursa of several birds, one of which also showing patterns of expansions in the jejunum. The remaining Vβ2 clone which was expanded in multiple conventional microbiota birds shows marked levels (>5%) in 3 colon samples and is also present above 1% in 4 jejunal samples.

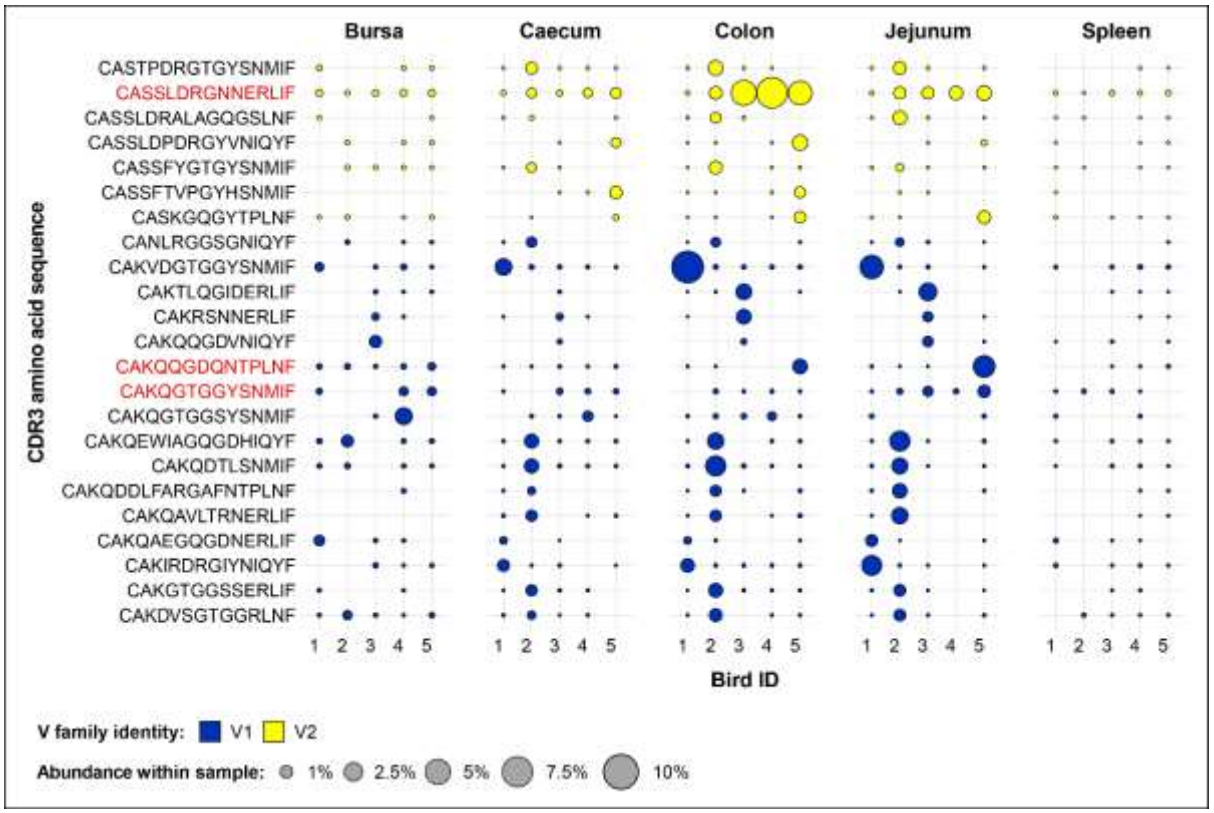

Figure 2. 19: Clonal expansions in the restricted repertoire of conventional birds.
Circles indicate the presence of clones with a specific CDR3 amino acid sequence and are proportional to the abundance within each bird's tissue clonal compartment. The plot shows only

the clones which are preferentially expanded in the conventional birds (at or above 0.5% and at less than 0.5% in the germ-free). Colours indicate V family identity: blue – V1 and yellow – V2. CDR3 amino acid sequences which are expanded in multiple birds are shown in red.

A different pattern was observed when examining the germ-free restricted clones (**Figure 2.20**). Here, all but one of the 12 clones have a Vβ2 gene, whereas the remaining belongs to the Vβ1 family. Furthermore, out of the identified germ-free restricted and expanded TCRβ sequences, more than half show consistent patterns of expansion across multiple tissues from different birds. Importantly, the CDR3 amino acid sequences CAASDRDRGINMIF and CAASDRDRGNERLIF show convergence of 3 and 2 distinct clonotypes by nucleotide sequence, respectively. All these clones belong to the Vβ2 family, and exhibit marked levels of expansion, especially in the jejunum.

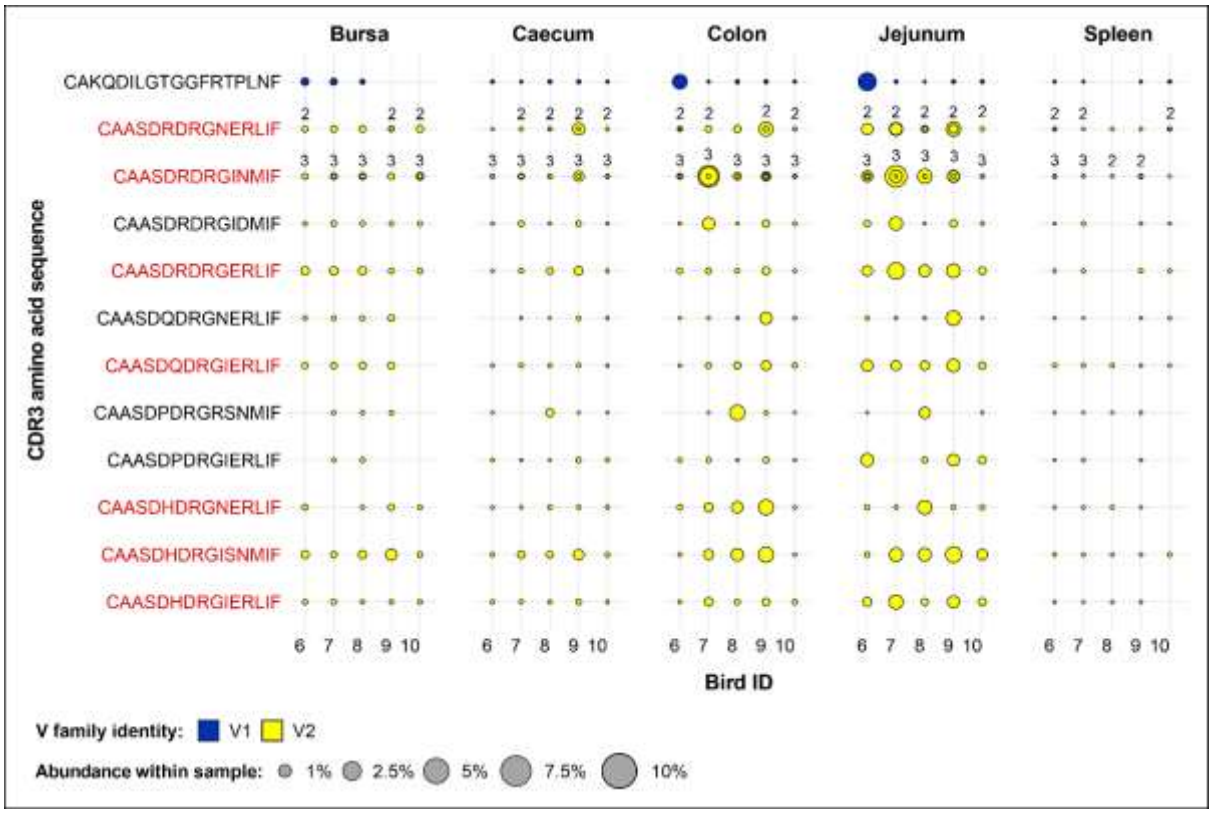

Figure 2. 20: *Clonal expansions in the restricted repertoire of germ-free birds.*

Circles indicate the presence of clones with a specific CDR3 amino acid sequence and are proportional to the abundance within each bird's tissue clonal compartment. Overlapping circles display different clones based on nucleotide sequence which share the same CDR3 amino acid

sequence. The number of convergent CDR3 nucleotide sequences recovered from the samples is displayed on top of the circles, if two or more are present. The plot shows only the clones which are preferentially expanded in the germ-free birds (at or above 0.5% and at less than 0.5% in the conventional). Colours indicate V family identity: blue – V1 and yellow – V2. CDR3 amino acid sequences which are expanded in multiple birds are shown in red.

Interestingly, for the TCRVβ3 clones, no clonal expansions were either restricted to germ-free or conventional groups with many clones present in a range of tissues in all or almost all birds (**Figure 2.21**). In a number of cases, the overall proportion of the expanded TCRVβ3 clones were greater in germ-free compared with conventional birds (e.g. with the CDR3: CASSDRDRGERLIF). The level of representation of this CDR3 (comprising two expanded clones at nucleotide sequence) in the jejunum was between 3 and 6% of the total TCRVβ repertoire in all germ-free birds. Although the CDR3 were variable in length we noted that in a central portion of the CDR3 a DRG motif was present in 18/20 expanded TCRVβ3 clones. The DRG motif is derived from one of the three D segment open reading frames. Interestingly the DRG motif was also overrepresented in TCRVβ2 germ-free specific expanded clones (**Figure 2.20**) but not in the expanded clones seen in TCRVβ1 or TCRVβ2 in conventional birds. Therefore, the proportions of CDR3 amino acid clones that encode the DRG motif in germ-free or conventional birds for each TCRVβ family and each tissue were considered (**Figure A.5**). The DRG motif is overrepresented in TCRVβ3 and is particularly prominent in the jejunum and other intestinal tissues. When all unique clones of each Vβ family are considered (i.e. not including clonal expansions), for TCRVβ1 and TCRVβ2 CDR3 those containing the DRG motif was represented in ~10% of the CDR3 whereas for TCRVβ3 this sequence was identified in ~50% of the CDR3 (**Figure A.6**).

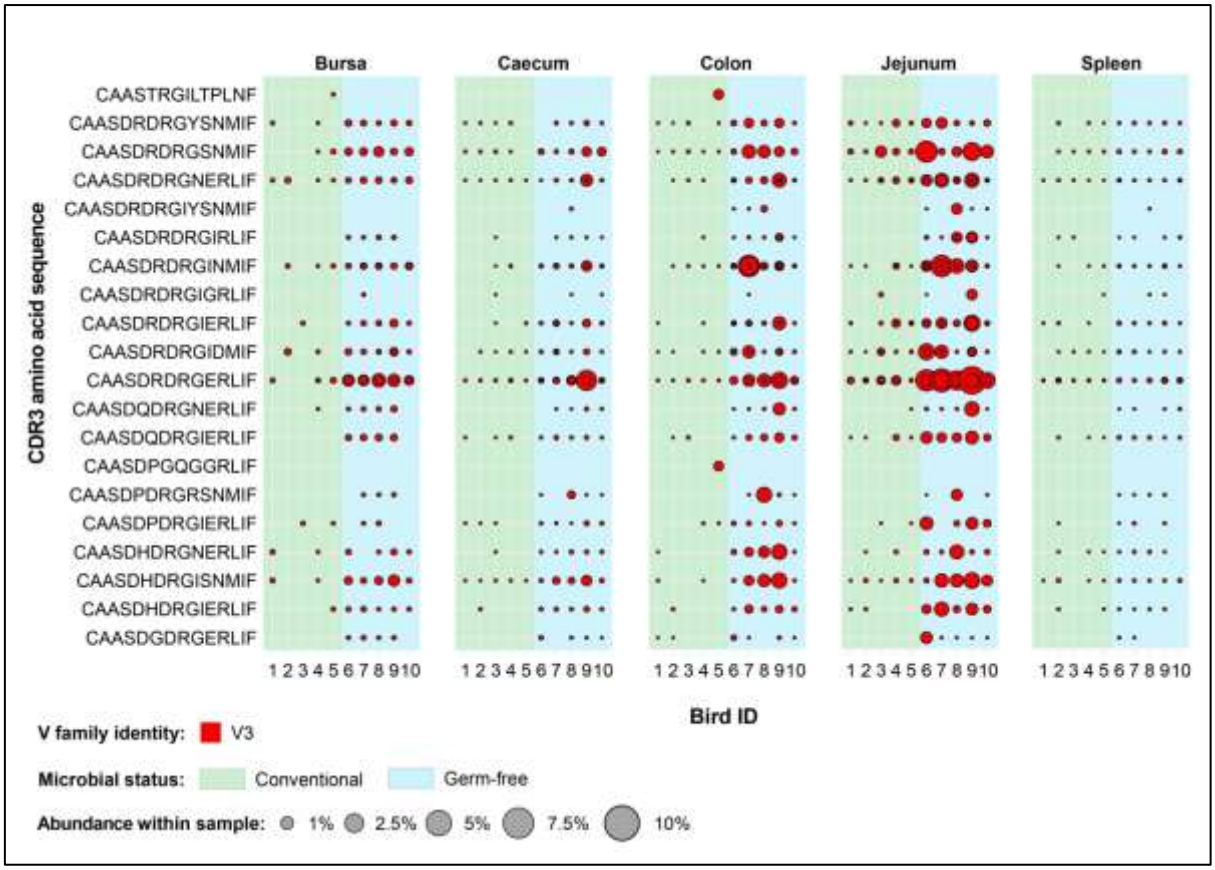

Figure 2. 21: Tissue-specific clonal expansions in Vβ3 clones of germ-free and conventional birds.

Red circles indicate the presence of clones with a specific CDR3 amino acid sequence and are proportional to the abundance within each bird's (total) tissue clonal compartment. Overlapping circles display different clones based on nucleotide sequence which share the same CDR3 amino acid sequence. The plot shows all the Vβ3 clones which are found at expanded (at or above 0.5%) in any of the birds included in this analysis (both germ-free and conventional). Background colours indicate microbial status group identity: green – conventional, light blue – germ-free.

II.3.4. Discussion

The microbiota is an important driver of the innate and adaptive immune systems, particularly in the gut and other mucosal tissues [141]. Most studies have been focussed on mammalian systems and to consider the phylogenetic breadth of such interactions we chose to study the chicken. While relatively few studies have attempted to evaluate the effects of the gut microbiota on gut-associated lymphocytes in chickens, these do suggest important roles of the commensal microbiota in the development and normal functioning of the

immune system [136,138,156,157]. The function of the adaptive immune system is dependent upon the structure of the repertoire of those receptors that recognise antigens. As with other species, TCRαβ+ T cells are a key part of the chicken immune system having both direct and indirect effects on immunity against pathogens [76]. TCRβ-based repertoire analysis provides a key tool to determine the structure of the TCRαβ+ T cell populations including the basal available diversity as well as clonal bias/expansions according to circumstance. To consider the impact of microbial status on the repertoire of TCRαβ+ T cells a high-throughput sequencing (HTS) approach was adopted to interrogate multiple tissues of chickens reared under conventional or germ-free conditions. This HTS-based analysis provided fundamental insights into the core chicken TCRβ receptor repertoire at an unprecedented level and revealed that the microbiota shapes the diversity and composition of tissue-specific T cell compartments.

The observed diversity patterns are broadly consistent with previous results which have illustrated that the presence of microbiota drives clonal expansions that are otherwise not present under germ-free conditions [144]. The current HTS analysis revealed a range of novel features of the chicken TCRβ population. For example, we were able to determine differences in TCRβ repertoire between tissues at the level of CDR3 sequence identity. The highest levels of clonal expansions were found in the gut segments, in particular those that relate to the large intestine (caecum and colon), and the highest diversity was detected in the spleen. As the large intestine contains the highest levels of microbial colonisation (and associated antigenic stimulus), this can be postulated as the factor that drives local clonal expansions in conventional birds. Indeed, the caecum is known to harbour the highest microbial densities of all intestinal segments [136] and the TCRβ repertoire in this tissue was the least diverse in birds reared with conventional microbiota. A very high proportion of rare clones was seen in the spleen of all birds irrespective of microbial status. As chickens lack conventional lymph nodes [76], our TCRβ repertoire data is consistent with the presence of a large population of naïve T cells in this tissue. The spleen may be an important organ for the generation of primary immune responses in the chicken. Indeed, even in mammals, primary immune responses can develop in the absence of lymph nodes (albeit with delayed dynamics) as evident in lymphotoxin alpha deficient mice [75].

Although the bursa has very few T cells (<4% of bursal lymphocytes [104,148]), this organ is physically linked to the intestine (via the bursal duct) and the TCRβ diversity was influenced by microbial status. As the main site of B cell development, the function of the bursal T cells remains unknown. Previous studies indicated that the T cell infiltration and expansion occurs in response to challenge with Infectious Bursal Disease Virus (IBDV) [148,158,159]. We hypothesise that the resident T cells might play other roles in relation to microbial antigens derived from the commensal microbiota of the gut. The presentation of microbially derived antigens by bursal antigen presenting cells, including B cells, might also promote the selected expansion of TCRαβ+ T cells which in turn might sustain and promote B cell expansions in relation to the microbiota within the gut. This topic deserves further investigation, and future studies might provide insight into the functional importance of bursal T cells under both physiological and pathological conditions.

The high degree of clonal sharing between birds (publicness) was a striking feature of the TCRβ repertoires as were the tissue specific differences in the levels of publicness. More than half of the total clones in the intestinal tissues and the bursa were shared between different individuals. Given the high theoretical diversity which can be generated during TCR rearrangement and the fact that the realised repertoire in any individual is restricted by the total number of T cells, a high degree of clonal sharing between different individuals is unlikely by chance [160]. However, previous studies in rodents and humans have also revealed that the degree of TCRβ sharing between individuals can amount to a significant percentage of the total repertoire. In one study, close to 4% of human TCRβ CDR3 nucleotide sequences are shared between two individuals, and up to 40% when considering the amino acid level [161]. In chickens, the current analysis indicates that almost 50% of TCRβ CDR3 nucleotide sequences were public in the gut tissues and in excess of 10% were public in the spleen. The differences in levels of publicness between tissues (spleen versus gut) has not been reported previously and may reflect the intrinsic biology of gut resident T cells. Some of these clones were present across a wide range of tissues and expanded in gut tissues of conventional birds (e.g. the TCRβ CDR3 with the amino acid sequence CASSLDRGNNERLIF) which may represent a common public clone reactive against antigens delivered by the microbiota. It is noteworthy that there were also some, although fewer, expanded public clones in germ-free individuals. These public clones may represent

TCRαβ+ cells reactive against food antigens or unconventional T cells that are clonally pre-expanded (as seen with CD1-restricted iNKT cells in humans [162]). The birds used for the current analysis were from the PA12 line, which represent a closed flock "outbred" line of White Leghorn chicken. Hence the levels of publicness seen in the current analysis are not likely a consequence of high levels of inbreeding. Indeed, some of the clones identified in the present study were also found in the few other studies that analysed TCRβ sequences from different lines of chicken (although the studies were at a much lower depth than the present study) [111,144,154,155]. This suggests that the observed patterns of clonal sharing might relate to the intrinsic biology of the chicken TCRβ repertoire and could therefore apply more widely. Hence, there is a strong suggestion that the TCRβ repertoires of chickens are biased towards specific rearrangements, potentially through the VDJ recombination process itself, thymic selection or post-thymic clonal expansion in the peripheral tissues.

The chicken TCRβ locus contains only 16 Vβ segments across 3 families (11 Vβ1, 4 Vβ2, and 1 Vβ3). By contrast, humans have at least 57 functional Vβ segments and mice have up to 30 Vβ segments which can contribute to generating the repertoire diversity [163]. The chicken TCRβ locus also contains only 4 Jβ segments as opposed to mice (12) or humans (13), and only 1 Dβ gene (mice and humans have 2) [87]. Together, these features of the chicken genome result in less intrinsic potential for generating TCRβ CDR3 diversity which may partially explain the higher degree of clonal sharing between individuals. The high levels of clonal sharing may mean that the available pre-expanded (anticipatory) repertoire of chickens is less diverse than seen in mammals. This has potential to impact on the ability of chickens to combat pathogens and respond to vaccines. Where multiple individuals utilise a TCR with the same sequence, a pathogen that is selected as a TCR escape variant in one individual may have continued advantage once transferred to other individuals. This has important implications for both pathogen resistance and vaccination in chickens. At the same time, this may indirectly affect the evolution of pathogens, including those that may be zoonotically transferred from chickens to humans.

Other intrinsic biological features may contribute to the high levels of public clones which were observed in this study. Chickens are one of the species with a high number of circulating γδ T cells, and the abundance of these cells increases with age [76,78,79]. By

contrast, in mice and humans, the proportion of circulating of γδ T cells is much lower and the relative importance (and full spectrum of roles) for γδ T cells in different species remains to be determined (for reviews, see [80] and [81]). Nonetheless, it may be that the αβ and γδ T cells work together in many circumstances and the magnitude of particular γδ populations may influence the level of publicness of αβ T cells. Indeed, there are well documented public αβ T cells which perform non-classical functions, and the relative importance of these unconventional cells may differ according to the vertebrate species in question [164]. It is worth noting that within the γδ T cell populations in humans, mice and chickens there are a mixture of subsets with public (or hyper public) TCR [79]. It might therefore be worth considering the repertoire structure of both αβ and γδ T cells as an important defining feature of cells with unconventional functional capability.

There is, however, another explanation for the observed patterns of TCRβ public clones and this relates to the chicken MHC [86,88]. Briefly, the chicken MHC is more compact than in mammals and a less diverse set of MHC genes is expressed per haplotype (often one dominant MHC class I and one dominant MHC class II gene). This restricted or "Minimal Essential MHC" [165] has functional consequences presenting a less diverse set of self-peptides in the thymus which could then restrict the repertoire of developing TCR αβ T cells. This may lead to a higher likelihood of similar TCRVβ CDR3 being selected in different individuals. There may be intrinsic differences in the publicness and repertoire of T cells restricted to MHC class I (CD8+) and MHC class II (CD4+), but these cell populations were not separated in our current analysis. It is also worth mentioning that different MHC molecules in the chicken have been classified as fastidious or promiscuous based upon the breadth of peptides that they present (for a review, see [88]) which may influence the breadth and level of publicness seen in the chicken TCRβ repertoire.

Although public TCRβ sequences were identified in all samples, the highest levels were in the intestinal and bursal samples which suggests that tissue-specific factors play an important part in shaping the resident T cell compartment. Importantly, high levels of clonal sharing were identified in both germ free and conventional birds, indicating that the gut microbiota is not the sole driver of the patterns of publicness in these tissues. When incorporating the different degrees of clonal sharing, however, the common publics are more pronounced in the conventionally-reared birds, whereas the ubiquitous clones are

more prominent in the germ-free individuals. The higher presence of ubiquitous clones in the germ-free may represent expanded T cells in response to food-derived antigens or unconventional T cell populations that respond to intrinsic stimuli. By contrast, the higher level of common publics (with less degree of sharing) in the conventional chickens may reflect the broad spectrum of antigen-specific expansions which can occur under the influence of the gastrointestinal microbiota.

Non-classical T cells with invariant or very limited repertoires are known to occur in mice or humans and their CDR3s were often shared between individuals [166,167]. Although these cells have yet to be described in chickens, they are known to be more abundant in specific tissues, especially in mucosal tissues such as the gut (e.g. iNKT cells or MAIT cells). There, these invariant T cells are often considered to exhibit innate-like functions and some have been demonstrated to interact with non-polymorphic presentation molecules such as CD1 and can respond to microbial derived antigens [162]. Interestingly, CD1 genes can be identified in the chicken genome which supports the proposal that nonclassical T cell subsets are likely to be present in birds [168,169]. With this in mind, the high percentage of public clones in the chicken intestinal tissues could be explained by the increased presence of unconventional invariant T cells in these sites.

Although the genetic and physiological mechanisms that result in the high degree of clonal sharing between birds are outside the scope of the current study, the patterns of clonal sharing deserve further investigation. Furthermore, some of the private sequences in this study were also detected in other datasets despite most being based upon much lower sequence depth than the current study. Hence the degree of publicness or clonal sharing is likely to be higher than reported here although for many of these we expect that these will represent lower level public TCR rather than those found at higher frequency in a greater proportion of birds. The issues and contributing factors surrounding TCR publicness are ill-defined in all vertebrates, and this is a topic that deserves more attention.

Microbial colonisation was found to markedly influence the distribution of tissue specific Vβ family clones and their patterns of clonal sharing but less so when grouped according to Jβ gene usage. The Vβ domain of the TCR contains the CDR1 and CDR2 loops required for interacting with the MHC during antigen presentation [160]. By contrast, the retained

parts of the J gene encode regions in the TCR involved in chain heterodimerisation and are not modified during rearrangement [160]. As such, these functional attributes may be the main driver of the observed differences. The differential contributions to CDR3 diversity and the functional domains that the V and J segments encode may bias clonal selection and antigen-specific expansions towards particular Vβ rather than Jβ TCR rearrangements.

The Vβ1 clones were more prominent in the conventional microbiota birds, irrespective of tissue type, suggesting that T cells with Vβ1 rearrangements may preferentially respond to microbially-derived antigens. This is supported by the fact that the clonal expansions restricted to the conventional birds were predominantly identified within Vβ1. By contrast, the lower proportions of Vβ1 in the intestines of germ-free birds are balanced by a higher proportion of Vβ3 clones, almost exclusively public. This suggests that the Vβ3 rearranged TCR sequences may have a tissue-specific function, perhaps relating to mucosal homeostasis. Another interesting aspect is that the only differences in Vβ2 clones according to microbial status were in the bursa and spleen, with germ-free chickens exhibiting higher relative proportions than their conventional counterparts. Collectively, these results indicate that the different Vβ families in the chicken may be utilised in cells that may perform different (but overlapping) functions, at least according to the publicness and clonal structure of the TCRβ associated with each family. Whether these families contribute differentially to pools of conventional and unconventional TCRαβ+ T cells could be a profitable avenue for future exploration.

In conclusion, our deep sequencing approaches of the TCRβ repertoire in conventional and germ-free chickens identified some novel and important aspects of avian T cell biology. These included the high proportion of public clones and the tissue bias of such clones. The work also defined the impact of microbial status on the developing gut TCRβ repertoire and how microbes shape its diversity and features. Moreover, the results provide a basis for future studies on the chicken TCR repertoire and in developing comparative biological frameworks on the evolution and structure of the TCR repertoire.

Statement of Authorship for joint/multi-authored papers for PGR thesis

To appear at the end of each thesis chapter submitted as an article/paper

The statement shall describe the candidate's and co-authors' independent research contributions in the thesis publications. For each publication there should exist a complete statement that is to be filled out and signed by the candidate and supervisor **(only required where there isn't already a statement of contribution within the paper itself).**

Title of Paper	The influences of microbial colonisation and germ-free status on the chicken TCRβ repertoire
Publication Status	X Published □ Accepted for Publication □Submitted for Publication □Unpublished and unsubmitted work written in a manuscript style
Publication Details	Dascalu S, Preston SG, Dixon RJ, Flammer PG, Fiddaman S, Boyd A, Sealy JE, Sadeyen J-R, Kaspers B, Velge P, Iqbal M, Bonsall MB and Smith AL (2023) The influences of microbial colonisation and germ-free status on the chicken TCRb repertoire. Front. Immunol. 13:1052297. doi: 10.3389/fimmu.2022.1052297

Student Confirmation

Student Name:	Stefan Dascalu		
Contribution to the Paper	- Carried out the sample preparation and computational analysis and wrote the first draft of the manuscript. - Major contributions to conceptualization and designed all the analyses and refined the computational methods for interpreting the results.		
Signature		Date	04/01/2023

Supervisor Confirmation

By signing the Statement of Authorship, you are certifying that the candidate made a substantial contribution to the publication, and that the description described above is accurate.

Supervisor name and title: Dr Adrian Lee Smith (Associate Professor)		
Supervisor comments: Stefan performed most of the work presented in the paper and played a major role in designing the approaches.		
Signature 	Date	12/01/2023

This completed form should be included in the thesis, at the end of the relevant chapter.

II.4. Protocol development - Multicolour staining methodology for identifying chicken lymphocyte subsets

One of the main difficulties in characterising the immune response in species other than human or mouse is the availability of reagents and the existence of high-throughput and robust protocols which consider host-specific factors [170]. These issues imply that even the most fundamental tools of modern-day immunology are hindered in terms of their ability to produce research output. For example, albeit flow cytometry and fluorescence-assisted cell sorting (FACS) being instrumental in most immunological studies, this technique's potential is limited by the availability and diversity of anti-avian fluorescently-labelled antibodies [87,170,171]. As such, overcoming some of these difficulties by generating more efficient and higher throughput methods might result in a better understanding of the avian immune system in the context of health and disease. The following section describes a high-throughput flow cytometry protocol which has been developed to characterise avian lymphocyte populations.

II.4.1. Animal tissue samples

Specific pathogen-free chickens aged 2-3 weeks were obtained from the Pirbright Institute (UK) animal facility for testing and optimising the staining method. For evaluating the applicability of the technique in the context of sterile immunity, samples were obtained from an animal experiment in which Dekalb White chickens (Henry Stewart & Co.) were immunised with two types of vaccines via subcutaneous injections. One group (n=8) was immunised with 0.2 ml of 1024 HA units/ml recombinant H7HA-expressing herpes virus of turkey (rHVT) vaccine and another group (n=8) was vaccinated with 0.2 ml of 4.5×105 PFU/ml inactivated Newcastle Disease Virus (iNDV) vaccine. The inoculations were administered 3 days after hatching and were followed by subsequent boosters of the same dosage at day 7 and 13. The birds were then monitored daily and culled at day 38 post-vaccination when their tissues were processed and analysed. All birds were hatched and

reared in the poultry facility according to national and institute-specific regulations (licence number P68D44CF4).

II.4.2. Lymphocyte sample preparations

Cell suspensions in RPMI were generated from freshly harvested chicken spleens. Subsequently, lymphocytes were isolated using Histopaque1083™ gradient centrifugation, and the cell viability was assessed using Trypan Blue exclusion. Following this step, the samples were resuspended in freezing medium (80% foetal calf serum, 20% dimethyl sulfoxide) and transferred into cryovials. The tubes were then placed into passive isopropanol cryogenic storage containers to be frozen to -80°C. When used for the staining experiments, individual tubes were thawed using a 37°C water bath for 1-2 minutes and resuspended in FACS buffer (1X PBS, 2% foetal calf serum, 1 mM EDTA, 0.1% sodium azide).

II.4.3. Panel Design and Gating Strategy

A panel of commercially available fluorescently labelled antibodies and other cytometry reagents (**Table 2.3**) were chosen with regards to the characteristics of the cell analyser (BD LSRFortessa™) which was used on the samples (**Figure 2.22**). Because the lymphocyte samples were preserved at -80°C and thawing may have led to a considerable loss in cell viability, a distinction between live and dead cells was made using a commercially available marker. The mouse anti-chicken antibodies were chosen to discriminate between cell types based on specific surface marker expression. As such, lymphocyte populations such as B cells (Bu-1+) and T cells (CD3+) could be identified. This latter population was further divided based on the structure of the T cell receptor (TCR) into γδ T cells (CD3+TCRγδ+) and αβ T cells (CD3+TCRγδ–). Moreover, among these T cell subsets, an additional functional differentiation could be made regarding the co-receptors which are expressed on their surface (TCRαβ+CD4+, TCRαβ+CD8αα+, TCRγδ+CD8αβ+, TCRγδ+CD8αα+, and TCRγδ+CD8–) [76,78].

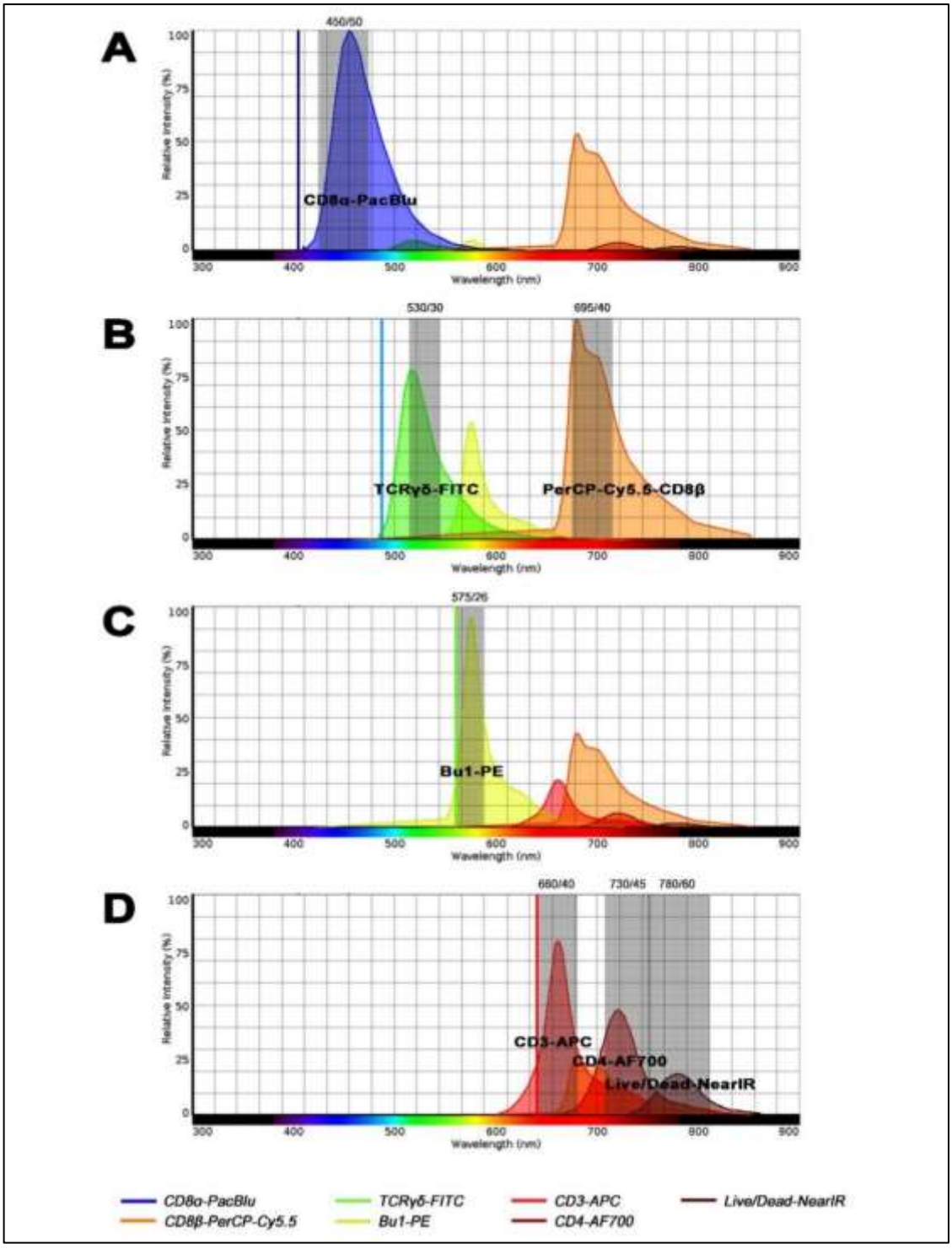

Figure 2. 22: *Fluorescence spectra of the reagents used for lymphocyte staining.*

Fluorophores are shown with their respective antibody specificities. (**A**) Violet laser (405nm): detection of Pacific Blue (450/50 nm filter). (**B**) Blue laser (488nm): FITC (530/30 nm filter) and PerCP-Cy5.5 (695/40 nm filter). (**C**) Yellow laser (561 nm): detection of PE (575/26 nm filter). (**D**) Red laser (640nm): detection of APC (660/40 nm filter), AF700 (730/45 nm filter), and LiveDead-NearIR (780/60 nm filter). Figure based on images generated with Spectra Viewer (Thermo Fisher Scientific), using the BD LSRFortessaTM cell analyser configurations.

II.4.4. Staining Optimisation

To ensure that the stain behaved optimally, the flow cytometry reagents (see **Table 2.3**) were titrated based on the quantities which were recommended by the manufacturers. With regards to the calculated staining indices and individual inspection of the resulting cytometry plots (data not shown), several concentrations of antibodies were selected to be used in combination. In the end, 10 possible mixes were tested, and the one that yielded the highest resolution of the desired cell populations was selected. To confirm the staining procedure worked, the observed frequencies of the lymphocyte subsets was also compared with expected values from published data and from the antibody manufacturers.

Reagent	Specificity	Fluorophore	Manufacturer	Catalogue Number
Mouse anti-chicken CD8α	CD8α+ T cells	Pacific Blue	Southern Biotech	8220-26
Mouse anti-chicken TCRγδ	γδ T cells	Fluorescein (FITC)	Southern Biotech	8230-02
Mouse anti-chicken CD8β	CD8β+ T cells	N/A	Southern Biotech	8280-08
Mouse anti-chicken Bu-1	B cells	r-Phycoerythrin (PE)	Southern Biotech	8395-09
Mouse anti-chicken CD3	T cells	Allophycocyanin (APC)	Southern Biotech	8200-11
Mouse anti-chicken CD4	CD4+ T cells	AlexaFluor700 (AF700)	Southern Biotech	8210-27
Live/Dead Near-Infrared	Dead Cells	Near-infrared	Thermo Fisher Scientific	L34976
Streptavidin	Biotin	Peridinin-chlorophyll-cyanine 5.5 (PerCP-Cy5.5)	BD Biosciences	551419

Table 2. 3: *Cytometry reagents used for labelling chicken lymphocyte preparations.*

II.4.5. Data analysis

The raw reads from the flow cytometer were examined using FlowJo™, and the resulting lymphocyte population frequency data were evaluated using the R Studio software [29]. The differences between the vaccine treatments were evaluated by constructing a mixed effects linear model in which the *response* was the estimated percentage of each lymphocyte population, by using the following formula:

$$RESPONSE \sim cell\ population \times treatment + (1 \mid bird)$$

Here, *cell population* and *treatment* are the explanatory variables which denote the lymphocyte population of interest and the vaccination treatment, respectively. The variable *bird* was included as a random intercept to capture the individual-specific variance. The models were then implemented using the lme4 package in R, with p values and 95% confidence intervals for the model estimates being computed using the lmerTest package [130,131]. To achieve the normality of residuals and homoscedasticity, a logit transformation was applied given the proportional nature of the data [129]. The fit of the model and the validity of its assumptions were then evaluated and deemed satisfactory (data not shown).

II.4.6. Results

II.4.6.1. Multicolour Staining Protocol for Chicken Lymphocyte Subsets

The staining procedure yielded good resolutions B cell and T cell subsets of interest (**Figure 2.23**). Furthermore, the observed population frequencies resembled the expected values from the scientific literature and the cytometry reagent manufacturers (**Table 2.4**). The results show that the lymphocytes from chicken splenocyte samples could efficiently be separated into various functionally important cell subsets, based on the differential expression of surface markers.

II.4.6.2. Lymphocyte populations under different vaccination treatments

When applied in the context of vaccination, some chicken lymphocyte populations were markedly distinct between the tested groups of birds (**Figure 2.24**). The overall frequency of αβ T cells was found to be higher in the iNDV-vaccinated birds than in the rHVT-HA immunised chickens. More specifically, the CD8+ αβ T cells were at higher frequencies in the iNDV-immunised birds than in the rHVT-HA group. At the same time, the rHVT-HA

group also had significantly lower CD8αβ+ γδ T cell levels than iNDV treatment group. These results suggest that the different vaccine treatments elicit different immune responses with regards to the specific lymphocyte populations which they activate.

Population of Interest	Observed	Expected	References
B cells	10.7 – 11.5%	15%	[172]
T cells	64.6 – 67.2%	>60%	[173–176]
αβ T cells	48.4 – 51.1%	50%	[173,174]
αβ T cells CD8+	23.4 – 25.6%	25%	[173,174,177,178]
αβ T cells CD4+	11.3 – 13%	10%	[173,174,179]
γδ T cells	11.6 – 12.4%	15%	[78,175]
γδ T cells CD8αα+	0.61 – 1%	6%	[78,175,177]
γδ T cells CD8αβ+	2.72 – 4.3%	3%	[78,175,177,178]
γδ T cells CD8–	3.8 – 4.98%	6%	[78]

Table 2. 4: *Expected and observed values for the stained populations of interest.*

Percentages are of total viable spleen cells in samples and are approximations taken from 10 separate staining tests of 10 different SPF chickens.

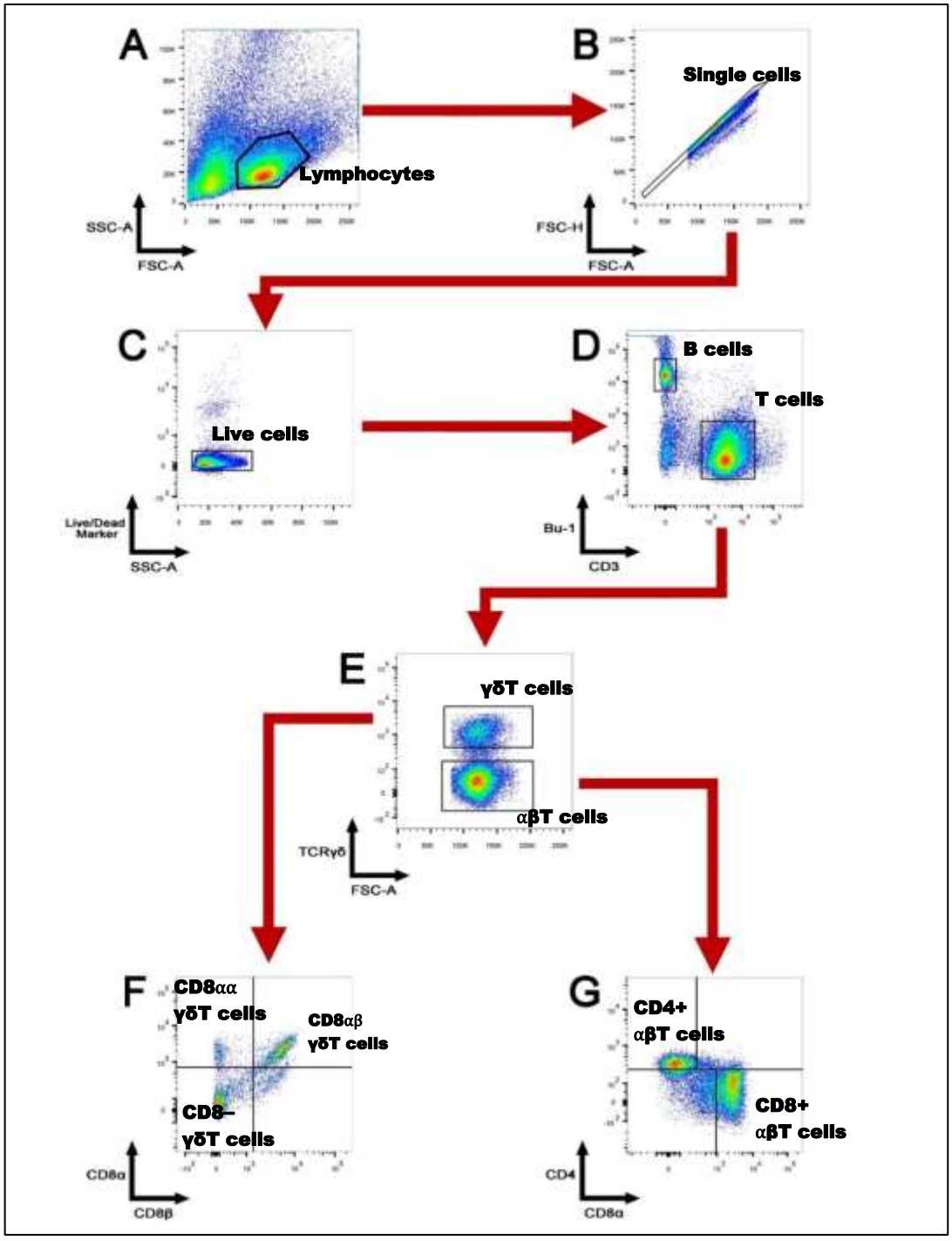

Figure 2. 23: *Flow Cytometry results and gating strategy for the multicolour staining protocol on splenocytes derived from a specific pathogen-free chicken.*

(**A**) Main cell gate. (**B**) Single cell gate. (**C**) Live cell gate (Live/Dead–). (**D**) Lymphocyte subset gates: B cells (top left, Bu1+CD3–) and T cells (bottom right, Bu1–CD3+). (**E**) T cell gates: γδ T cells (top, TCRγδ+) and αβ T cells (bottom, TCRγδ–). (**F**) γδ T cell subsets: CD8α+CD8β+ (top right), CD8α+CD8β– (top left), CD8α–CD8β– (bottom left). (**G**) αβ T cell subsets: CD4+ CD8α– (top left), CD4–CD8α+ (bottom right).

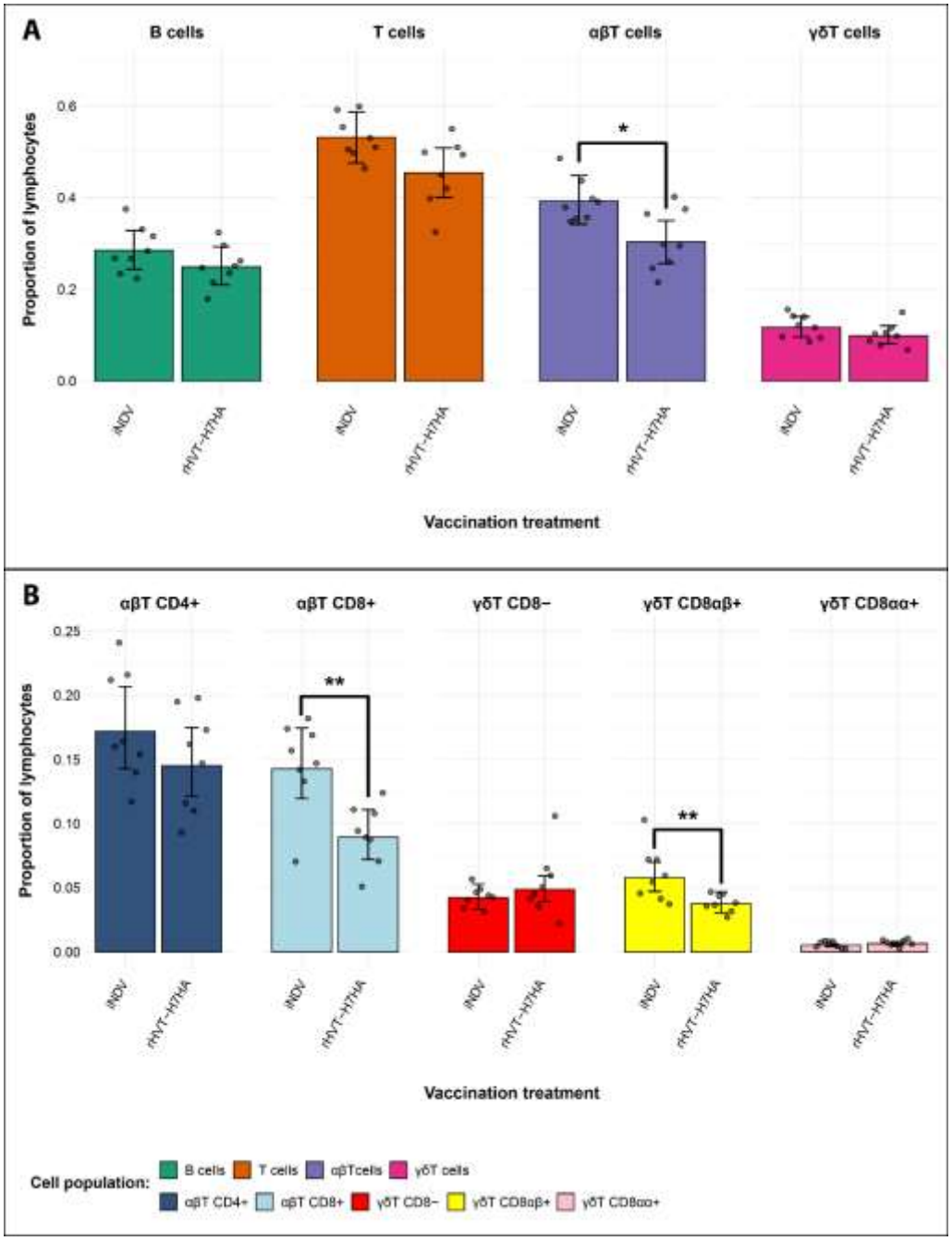

Figure 2. 24: *Splenic lymphocyte populations model estimates for the iNDV and rHVT-H7HA vaccinated chickens.*

(**A**) B and T cell compartments, and main T cell lineages. (**B**) T cell populations based on differential expression of CD8 and/or CD4 surface markers. Grey dots represent individual bird observations for lymphocyte population. Error bars represent 95% bootstrap confidence intervals for the point estimates generated from 1000 simulations of the model. Statistically significant differences between the model estimates are depicted above the plots based on their corresponding

p-values: * = $p < 0.05$; ** = $p < 0.01$. The frequencies of CD3–Bu1– lymphocytes (~25%) are not shown.

II.4.7. Discussion

The insufficient number of high-throughput methods and/or the availability of reagents for veterinary science represent major impediments towards addressing important problems including global food security and the control of infectious agents such as influenza viruses. Therefore, adapting existing technologies from related fields (e.g. medical sciences), optimising existing procedures, and even elaborating novel methods altogether constitute means through which many such issues could be resolved. With this in mind, very powerful tools such as flow cytometry have enormous potential if applied to veterinary studies, especially in the context of infectious diseases and responses to vaccination.

The efficacy of the multicolour staining procedure detailed in the above has been confirmed by comparing the observed frequencies of the lymphocyte populations of interest with expected values from published data and the instructions from the manufacturers of the cytometry reagents [78,172–179]. The method represents a higher-throughput version of common cytometric assays which are carried out in veterinary studies. Indeed, this technique allows for a high-resolution separation of chicken lymphocyte populations of interest, with only one sample serving as input. This represents a major advantage, as it not only requires less starting material, but also controls for variation between different samples, including experimental error.

The applicability of the method is reflected by the results obtained in the context of vaccination, as significant differences were found between the inactivated NDV and the rHVT-H7HA vaccination treatments. Interestingly, the αβ T cell responses were found to be lower in the rHVT-HA vaccinated group, with higher CD8+ αβ T cells being present in the iNDV-immunised birds. Furthermore, there are higher levels of CD8αβ+ γδ T cells in this latter group, a cell population which has been previously shown to exhibit cytotoxic activity in the context of infection [85]. Together, the results are indicative of a drive towards a stronger cell-mediated immune response in the iNDV-vaccinated group. However, the actively-replicating viral-vectored vaccine would be expected to elicit a

stronger cell-mediated immune response than immunisations with an inactivated virus [7,87,106]. As no specific assessments of the actual immune responses were performed, claims about why this phenomenon is observed remain purely speculative. Potential effects might include the immunogenicity of the antigens, the age of the birds, and even the particular breed of chicken that was used in the study [78]. Evaluating the individual contribution of these factors was outside the scope of this current work, and the samples from the vaccine experiments were used solely to demonstrate its applicability in the context of vaccination.

II.4.8. Conclusion

Flow cytometry and fluorescence-assisted cell sorting represent very powerful tools of modern-day immunology [87,170,171]. Unfortunately, their use in veterinary immunology is limited by the availability of specific fluorescently labelled antibodies and the existence of robust and high-throughput methods for the surface labelling of cells. The multicolour staining protocol described herein can be successfully used to characterise functionally important chicken lymphocyte populations. Furthermore, subject to further optimisation, this staining procedure can also be used to sort the chicken lymphocyte subsets of interest via FACS, thus allowing more specific assessments to be performed such as cytokine expression profiles and immune receptor repertoire analyses.

II.5. Viruses and vaccine preparation

A stock of recombinant reverse-genetics (RG) virus was generated by the AIV group at the Pirbright Institute prior to the DPhil research, using a well-established protocol involving eight influenza gene plasmids in HEK 293T/MDCK cell co-culture [180]. This RG virus comprised all eight genes from A/chicken/Pakistan/UDL-01/08 (UDL-01/08). The subsequent steps for vaccine preparation were carried out by the DPhil candidate. RG viruses from cell culture were propagated in 10 day-old embryonated hen's eggs and the allantoic fluid was harvested, clarified by centrifugation at 3000 rpm for 20 minutes at 4°C and transferred to fresh containers prior to chemical inactivation. Virus inactivation was achieved by adding β-propiolactone 0.1% (v/v) to clarified infectious allantoic fluid, mixing well before incubating at room temperature for eight hours then incubating at 4°C for 24 hours [181]. Inactivation of virus was confirmed by sequentially passaging virus in 10 day-old embryonated hen's eggs three times. Once chemical inactivation was confirmed, allantoic fluid was concentrated by ultracentrifugation at 135,000 x g for two hours and pelleted virus was resuspended in PBS. The resulting solutions were titrated by performing haemagglutination assays (see below).

II.6. Haemagglutination and haemagglutination inhibition assays

The haemagglutination titre of the virus and the haemagglutination inhibition (HI) titre of the chicken antisera were determined using established protocols [182]. Briefly, to determine the haemagglutination titre, a two-fold dilution series of virus in PBS was prepared in V-bottom 96-well plates (Thermo Fisher Scientific) and incubated 1:1 with 1% chicken red blood cells (RBCs) in PBS for one hour at 4°C. The haemagglutination titre was recorded as the reciprocal of the highest dilution that virus caused complete haemagglutination of RBCs.

To determine the HI titre, a two-fold dilution series of post-infection chicken polyclonal antisera was incubated with 4 haemagglutinating units (HAU) per 25 μl of virus for one hour at room temperature then incubated 1:1 with chicken 1% RBCs in PBS for one hour

at 4°C. The HI titre was recorded as the reciprocal of the highest dilution of chicken antiserum that completely inhibited haemagglutination of RBCs.

II.7. H9N2-specific ELISAs using whole inactivated purified virus

To assess the levels of H9N2-reactive IgM and IgY in vaccinated and/or challenged birds, enzyme-linked immunosorbent assays (ELISAs) were developed using whole purified and inactivated H9N2 influenza virus. For this, Nunc MaxiSorp (Thermo Fisher Scientific) flat-bottom 96-well plates were coated with 50 µl per well of 0.25 µg/ml inactivated purified H9N2 and left overnight at 4°C. The following day, the plates were washed 4 times using 0.1% Tween 20 (Sigma-Aldrich) in PBS (all further washing steps were performed in the same way). Subsequently, the plates were then incubated for 30 minutes at room temperature using 100 µl of blocking buffer (0.25% BSA in 0.1% Tween-20 in PBS) in each well. Following another wash step, 50 µl of 1:800 serum dilution was added to duplicate wells and incubated for 1h at room temperature. The plates were then washed again and incubated for 30 minutes with 50 µl of either a 1:7000 dilution of goat IgG conjugated with horseradish peroxidase (HRP) having anti-chicken IgY specificity (Biorad, cat. AAI29), or 1:3000 dilution of goat IgG conjugated with horseradish peroxidase (HRP) having anti-chicken IgM specificity (Invitrogen, cat. PA1-84676). After another wash step, 50 µl of OptEIA TMB Substrate (BD Biosciences) was added to each well of the plate and left at room temperature. The reaction was stopped using 50 µl of 2M H2SO4 after exactly 20 minutes of incubation. The optical density of the wells was then read using a 450/630 nm setting of a ELx808 plate reader (BioTek). The raw optical density (OD) values were then standardised using the sample to positive ratio. For this, a sample of pooled sera from three 24-day-old naïve birds from a separate experiment was also added as a negative control to the ELISA plates. Similarly, a sample of pooled sera from three 24-day-old birds that were vaccinated at day 1 and 14 post-hatching during a separate experiment was used as a positive control. Because of the high number of serum samples, multiple 96-well plates were used for the ELISA procedure. Standardisation was performed by calculating the sample-to-positive ratio, using the following formula:

$$\frac{[Sample\ OD] - [Negative\ control\ OD]}{[Positive\ control\ OD] - [Negative\ control\ OD]}$$

Therefore, the formula above allowed for OD values to be standardised across the ELISA plates and thus minimized potential noise differences through the use of negative and positive controls that were added to the plates.

II.8. H9N2 matrix gene qRT-PCR assessment of chicken swab samples

Total RNA from buccal and cloacal swab samples from H9N2 infected birds was extracted using the QIAamp Virus BioRobot MDx Kit (Qiagen) on a Biorobot Universal (Qiagen). Total RNA concentration was then measured using the NanoPhotometer NP80 (IMPLEN GmbH) in order to standardise across samples. A quantitative real-time PCR (qRT-PCR) using H9N2 matrix (M) gene primers was performed on samples using an M gene of known concentration (8.5 x 10^7 copies/µl) as a standard, which was previously generated within the AIV group at the Pirbright Institute. For the qRT-PCR reactions, the Superscript III Platinum One-Step qRT-PCR Kit (Invitrogen) was used following the manufacturer's instructions on a Quantstudio 5 Real-Time PCR System (Thermo Fisher Scientific). The results were then analysed using the Quantstudio 5 software (Thermo Fisher Scientific).

II.9. H9N2 vaccination and infection animal experiment

The animal experiment was carried out at the Pirbright Institute (Pirbright, UK) as part of the DPhil project. Both the staff at the Pirbright animal facility and the AIV research group contributed to the work required for the animal experiment. The DPhil Candidate designed and oversaw the experiment whilst also participating in and assisting with (without performing procedures) vaccination, infection, culling, and sample collection. White leghorn chicken (Valo breed, n=70) were hatched and reared in the poultry facility according to national and institute-specific regulations (licence number P68D44CF4). The

birds were divided into 6 treatment groups (G1-6) and maintained together until the infection birds were transferred to isolators at day 21 post-hatching (see below). All uninfected birds remained together for the duration of the experiment. Chickens from G1 (n=10), G2 (n=10), G4 (n=10), and G5 (n=10) received a single subcutaneous injection of 0.2ml of 1024 HAU/dose inactivated H9N2 vaccine immediately upon hatching (**Figure 2.25**). Individuals from G2 and G5 received an additional dose of the vaccine at 14 days after hatching. Birds from G3 (n=15) and G6 (n=15) did not receive the vaccine. Weekly blood samples were collected from all birds immediately after the first intervention (i.e. infection or vaccination). At day 21 post-hatching, birds from G1-3 received a single intranasal inoculation of 0.1ml of 10^6 pfu/ml H9N2 low pathogenic avian influenza virus (50 μl in each nostril). Following infection, birds (G1-3) were weighed daily and buccal and cloacal swabs were collected each day for 10 consecutive days. At day 3 and at day 14 post-infection, 5 birds from each group (G1-G6) were culled and tissue samples (trachea, lung, spleen, bursa, caecum, colon, and jejunum) were harvested and stored in *RNAlater* (Thermo Fisher Scientific). Additionally, at day 7 post-infection, 5 birds from G3 and G6 were culled and their tissues were harvested as for the rest of the time points. Lymphocyte suspensions were also prepared from splenic tissues using the gradient-based method described in **section II.4** and viably frozen for later analyses.

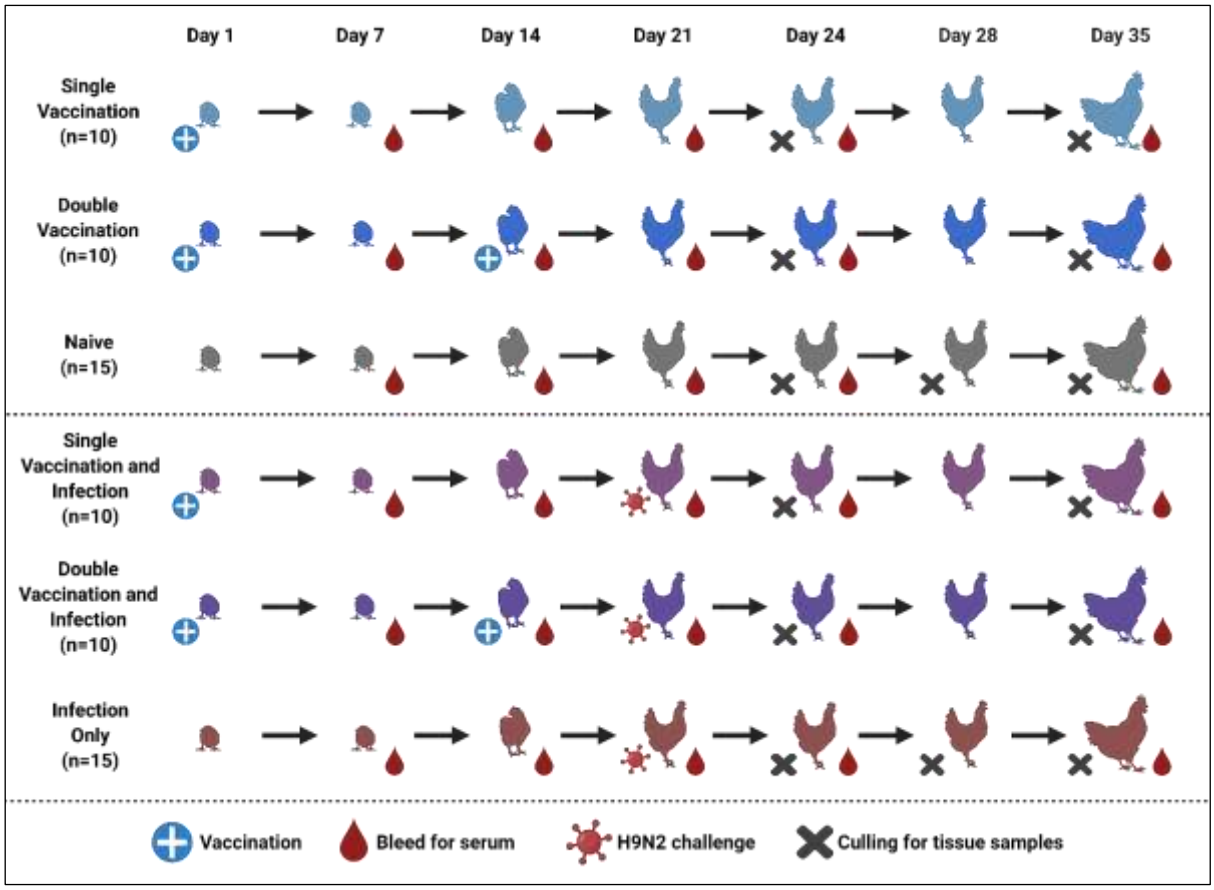

Figure 2. 25: *Design of the H9N2 vaccination and infection animal experiment.*

Birds were split into 6 groups which received either an inactivated H9N2 vaccine at day 1, or both at days 1 and 14, or no vaccination. At day 21, half of the birds (belonging to all vaccination regime treatments) were infected with H9N2 avian influenza virus. Birds were then culled at days 24 (n=5 from all groups), day 28 (n=5 from the unvaccinated treatments), and at day 35 (n=5 from all groups). Blood and tissue samples were harvested and processed for subsequent analyses. Buccal and cloacal swab samples were collected from the infected birds with one pre-infection sampling and 10 other daily swabs after infection.

Chapter III: Antibody and Cellular Dynamics Following H9N2 Vaccination and Challenge

III.1. Abstract

The avian adaptive immune system is stimulated by influenza A viruses and develops humoral and cell-mediated responses in order to control and resolve the infection. Systemic stimulation through infection and/or vaccination results in antigen-specific B cells becoming activated and producing virus-specific IgM antibodies, which later class-switch to the higher affinity IgY antibodies. At the same time T cell immunity develops both through CD8+ cytotoxic T lymphocytes and through CD4+ T helper cells which contribute to cell-mediated and humoral responses, respectively. Furthermore, other cells of the adaptive immune system such as the γδ T cells may contribute to adaptive immunity and respond specifically to H9N2 infection or vaccination-derived stimuli. In this chapter, I assess some of the fundamental adaptive immune responses in chickens that were infected with and/or vaccinated against avian influenza H9N2. These measurements include the evaluation of the systemic antibody responses following vaccination(s) and infection via ELISAs and HI assays, viral qPCR results for swab samples during the course of infection, and frequency changes in major splenic lymphocyte subsets by using a custom flow cytometry staining protocol. As such, the results provide important insights into the dynamics of the chicken antibody responses to infection and vaccination whilst also describing the impacts of infection and vaccination on functionally relevant lymphocyte populations in the spleens of immunised birds.

III.2. Introduction

Influenza A viruses are single-stranded, negative-sense, segmented RNA viruses (fam. *Orthomyxoviridae*) that have their primary reservoir in wild aquatic birds [1,5,6,8]. as a group, they exhibit a broad host specificity, which includes poultry, swine, horses, bats, and

humans [4]. As such, influenza A viruses have the capacity to cause severe economic losses due to infection of domestic animal hosts, but also pose a significant zoonotic risk when they cross the species barrier from domestic animal to humans [1,6–8]. Indeed, these pathogens represent major medical and social burdens with regards to both seasonal epidemics and the more dramatic pandemics which they can cause.

Influenza A viruses are broadly classified with respect to their haemagglutinin (HA) and neuraminidase (NA) surface glycoproteins [5,6]. To date, at least 18 HA (H1-H18) and 11 NA (N1-N11) subtypes have been described across a wide range of different species [6]. The HA and NA glycoproteins represent major antigenic targets against which the adaptive immune response is mounted. However, the inherent ability of these pathogens to evade host immunity via antigenic drift or antigenic shift poses considerable challenges to controlling their spread, in both human and non-human animal hosts [5–7,11]. These features of influenza viruses also have profound implications for traditional prevention methods such as vaccination. In a manner similar to the seasonal influenza vaccination in humans (reviewed in 7), the effectiveness of vaccine-induced immune memory decreases rapidly in non-human hosts due to the emergence of escape variants [11,49–51]. Moreover, veterinary influenza A vaccination is poorly regulated, with reduced coordination within and between different countries and frequent use of sub-optimal vaccines in terms of homologous seed strains [52]. With this in mind, domestic birds are of particular importance as these animals represent a virus reservoir where avian influenza viruses (AIVs) are hyper enzootic. Furthermore, AIVs readily evolve and diversify within poultry which often serve as intermediates from which the viruses can spread to other domestic animals, wild birds and humans [5,6,18,19]. Indeed, not only are poultry readily infected by AIVs, but these events are associated with significant economic losses each year [8,20–23]. Cumulatively, these factors render the understanding of the avian immune responses to AIVs essential for the efficient control of these pathogens [32,53].

Out of the AIVs, focus has been predominantly placed on subtypes H5 and H7 due to their propensity to evolve into high pathogenicity avian influenza (HPAI) viruses and cause outbreaks in poultry with significant bird mortality [28–30]. However, AIV subtype H9N2 is a prominent low pathogenicity avian influenza (LPAI) virus subtype which has become enzootic in many countries across Asia, the Middle East, northern and western Africa, and

some parts of Europe [33–36]. Furthermore, H9N2 AIVs have been commonly causing zoonotic infections, with increased H9N2 seropositivity among agricultural workers in recent years [33,37–41]. As such, several countries across the world have implemented poultry vaccination strategies in order to contain viral spread and prevent possible human outbreaks. However, these efforts involve the use of inactivated H9N2 vaccines, and there is still a limited understanding about both the infectious process itself and the immunological effects of vaccination within avian hosts.

The most frequently used method of vaccinating poultry involves the use of inactivated virus, which mostly triggers an antibody-mediated immune response [44,183,184]. In a commercial setting, poultry are vaccinated as young as 1-day post-hatch, against multiple pathogens using a variety of modalities and as these birds mature, they get additional vaccinations and even booster immunisations [44]. The impact that these immunisations have on young and developing birds is largely unknown. A more comprehensive understanding of the immune dynamics of both infection and vaccination is paramount to maximise the efficacy of current practices and inform on the development of future strategies. In this chapter, I provide a detailed analysis of the antibody-mediated immune response against AIV subtype H9N2 using virus-specific IgM and IgY ELISAs and HI assays. Furthermore, using an in-house custom-made flow-cytometry protocol (see **section II.4**), I examine the splenic lymphocyte compositions of birds that were subjected to H9N2 vaccination(s) with inactivated vaccines and/or infection. The results presented herein offer important information about the dynamics of the chicken systemic antibody responses, the utility of vaccination timing, and the protection offered against AIV infection by an inactivated H9N2 virus vaccine. These data also provide some core immunological measurements for later studies on the T and B cell repertoire (Chapters 4 and 5).

III.3. Specific Materials and Methods

III.3.1. Models of H9N2 antibody dynamics

The IgM and IgY ELISAs and HI assay methodologies are described in detail in **Chapter II** (see **sections II.6** and **II.7**). Based on preliminary exploratory analyses, the data for each

of the antibody responses can be characterised using a log-normal distribution. With this in mind, the log-transformed data was modelled using maximum likelihood approaches. Several models were chosen considering biological phenomena such as initial antigen-dependent increase in antibody production by B cells, sustained antibody production by plasma cells, and cellular senescence and antibody decay [87]. Therefore, four equations were selected to describe the major trends which are expected to govern antibody dynamics upon antigenic stimulation.

$$A = c + aT - bT^2 \qquad \textbf{(E 3.1)}$$

$$A = c + aT^2 e^{-bT} \qquad \textbf{(E 3.2)}$$

$$A = c + a(1 - e^{-bT}) \qquad \textbf{(E 3.3)}$$

$$A = c + a\frac{T}{b+T} \qquad \textbf{(E 3.4)}$$

In the models above, A is the log-transformed measured antibody response (IgM, IgY, or HI) T represents the log-transformed number of days post initial immunisation, and parameter c is a constant describing the intercept. A quadratic model (**E 3.1**) was chosen to depict the initial expansion of antibody-secreting cells in the presence of antigen, followed by a decline caused by cellular senescence and clearance of antibodies. Here, parameters a and b describe the rate of antibody production and clearance, respectively. The second choice of equation (**E 3.2**) represents an increase-decrease model which also captures these processes, with an initial (quadratic) increase characterised by a, followed by an exponential decline characterised by b.

Two additional choices of model were included to depict the plateauing phase observable in the IgY response (see **III.4.Results**), as the length of the animal study was not sufficient to capture the declining phase in antigen-specific IgY after initial immunisation. As such, an exponential plateau equation (**E 3.3**) and a Monod-type equation (**E 3.4**) model the observed behaviour in IgY, where parameter a represents the maximum value of the system

(i.e. the asymptote), while parameter b relates to the deceleration in the production of antibodies.

For all of the chosen model equations specified above (**E 3.1 – 3.4**), the likelihood value (*L*) of the antibody response given each model was computed using the following formula:

$$L(A|model) = \prod_{i=1}^{N} \frac{1}{A_i \sigma \sqrt{2\pi}} e^{-\frac{(\ln A_i - \mu_i)^2}{2\sigma^2}} \quad \text{(E 3.5)}$$

In this likelihood function (**E 3.5**), μ is the estimate of the model for the natural antibody response A at each i observation taken at T days post initial immunisation (the values of A and T being log-transformed – see above).

III.3.2. Flow cytometry staining and analysis

Splenocytes from the vaccination and infection experiment (described in **section II.9**) were isolated, viably frozen, and subsequently stained using the multicolour flow cytometry methodology developed and optimised in **section II.4**. The mixed-effects linear models used previously were adapted to analyse the differences between the immunisation regimes of the current experiment.

III.3.3. Analyses of antibody responses

For the non-parametric analysis of antibody responses, Kruskal-Wallis tests were performed at each time point in order to assess if the effect of treatment group is significant at each timepoint [185]. Following this stage, post-hoc Conover tests were performed using the Benjamini-Hochberg correction for multiple comparisons [186,187].

To evaluate the antibody temporal dynamics models, the Akaike information criterion (AIC) was computed, and the AIC weights were used for selecting the best fit given the

data [188]. Furthermore, the R^2 value was calculated to reveal how much of the variance within each treatment group is explained by the models.

III.4. Results

III.4.1. H9N2-specific antibody responses following vaccination and challenge

Distinct patterns were observed for the humoral responses of chickens based on the immunisation regime to which they were subjected (**Figure 3.1** and **Tables 3.1 – 3.3**), as indicated by the IgM and IgY ELISAs (whole virus antigen preparation) and the HI assays which were performed on the sera of birds. There were no detectable IgM, IgY, or HI responses at day 7 in the vaccinated treatment groups (post-hoc Kruskal-Conover test, corrected p values >0.05). At day 14 these measurements became significantly different to the unvaccinated birds (post-hoc Kruskal-Conover test, corrected p values <0.01). There were no differences at day 7 or day 14 in terms of IgM, IgY, or HI titres between the immunised groups themselves (post-hoc Kruskal-Conover test, corrected p values >0.05).

By day 21 of age, after the secondary immunisation was administered to the corresponding groups at day 14, differences became apparent between the single vs. double vaccination regimes. When looking at the IgM responses, the double vaccination treatments exhibited higher levels of IgM than the single vaccination group (post-hoc Kruskal-Conover test, corrected p values <0.05), but not higher than the single vaccination treatment which was subsequently infected after the blood samples were taken (post-hoc Kruskal-Conover test, corrected p values >0.05), potentially due to the high within-group variability of IgM responses in this treatment. Lastly, the double vaccination treatments also exhibited similar levels of IgM responses between them (post-hoc Kruskal-Conover test, corrected p values >0.05).

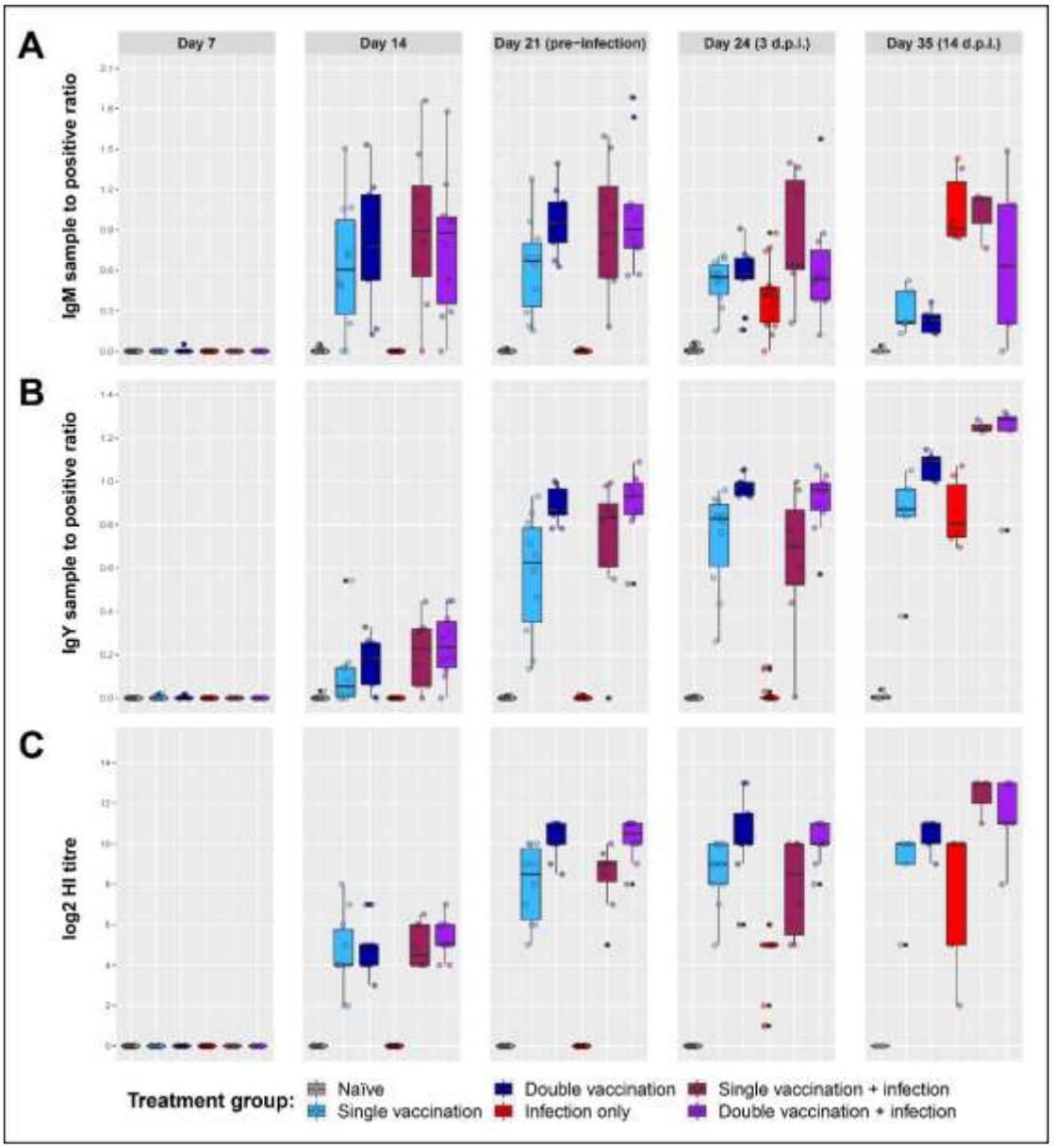

Figure 3. 1: *H9N2-specific antibody levels and haemagglutination inhibition (HI) potential of sera in chickens following vaccination and infectious challenge.*

(**A**) IgM ELISA sample-to-positive ratios. (**B**) IgY ELISA sample-to-positive ratios. (**C**) HI titres of serum samples. Sample-to-positive ratios for the ELISAs were calculated for each sample's OD value using a known positive and a known negative in order to standardise across plates.

The IgY responses at day 21 also began to reflect the effects of multiple immunisations. As such, the double-vaccinated treatments exhibited higher levels of IgY and HI titres than the single immunisation groups (post-hoc Kruskal-Conover test, corrected p values <0.05). There were no significant differences between the groups that received an equal number of vaccinations (post-hoc Kruskal-Conover test, corrected p values >0.05).

		IgM				
Day	**Treatment**	Naïve	Single vaccination	Double vaccination	Infection only	Single vacc. + inf.
14	Single vaccination	*** 0.000				
	Double vaccination	*** 0.000	0.258			
	Infection only	0.295	*** 0.000	*** 0.000		
	Single vaccination + inf.	*** 0.000	0.295	0.923	*** 0.000	
	Double vaccination + inf.	*** 0.000	0.351	0.812	*** 0.000	0.330
21 (pre-inf)	Single vaccination	*** 0.000				
	Double vaccination	*** 0.000	* 0.015			
	Infection only	0.689	*** 0.000	*** 0.000		
	Single vaccination + inf.	*** 0.000	0.116	0.508	*** 0.000	
	Double vaccination + inf.	*** 0.000	* 0.016	0.904	*** 0.000	0.844
24 (3 d.p.i)	Single vaccination	*** 0.000				
	Double vaccination	*** 0.000	0.776			
	Infection only	*** 0.000	0.128	0.065		
	Single vaccination + inf.	*** 0.000	0.147	0.268	** 0.002	
	Double vaccination + inf.	*** 0.000	0.934	0.785	0.117	0.535
35 (14 d.p.i)	Single vaccination	* 0.021				
	Double vaccination	* 0.040	0.772			
	Infection only	*** 0.000	** 0.008	** 0.004		
	Single vaccination + inf.	*** 0.000	** 0.021	* 0.014	0.964	
	Double vaccination + inf.	** 0.003	0.276	0.162	0.068	0.155

Table 3. 1: *Kruskal-Conover test results for IgM responses in the infection study.*
Benjamini-Hochberg corrections were used for multiple-sample comparisons. Significance levels are denoted alongside the p values with one (p<0.05), two (p<0.01), or three (p<0.001) asterisks. Calculated p values are rounded to 3 digits.

After blood samples were collected on day 21, the birds were challenged with H9N2 avian influenza, and subsequent measurements were taken at 3 days post infection (dpi), which is known to correspond to peak viraemia [189]. At this stage, in terms of IgM responses, there were no significant differences between the vaccination groups (post-hoc Kruskal-Conover test, corrected p values >0.05). At the same time, the infection only birds began to exhibit detectable IgM responses which were not significantly different to the other vaccination

treatments (post-hoc Kruskal-Conover test, corrected p values >0.05), with the exception of the group that received a single vaccination and was infected (post-hoc Kruskal-Conover test, corrected p values <0.01). However, as observed at earlier timepoints, this group exhibited a high between-bird variability, which likely resulted in the significance of this difference but not the others.

		IgY				
Day	Treatment	Naïve	Single vaccination	Double vaccination	Infection only	Single vacc. + inf.
14	Single vaccination	*** 0.000				
	Double vaccination	*** 0.000	0.093			
	Infection only	0.755	*** 0.000	*** 0.000		
	Single vaccination + inf.	*** 0.000	0.064	0.792	*** 0.000	
	Double vaccination + inf.	*** 0.000	0.092	0.444	*** 0.000	0.612
21 (pre-inf)	Single vaccination	*** 0.000				
	Double vaccination	*** 0.000	** 0.004			
	Infection only	0.577	*** 0.000	*** 0.000		
	Single vaccination + inf.	*** 0.000	0.337	* 0.046	*** 0.000	
	Double vaccination + inf.	*** 0.000	** 0.001	0.587	*** 0.000	* 0.020
24 (3 d.p.i)	Single vaccination	*** 0.000				
	Double vaccination	*** 0.000	*** 0.000			
	Infection only	0.075	*** 0.000	*** 0.000		
	Single vaccination + inf.	*** 0.000	0.994	*** 0.000	*** 0.000	
	Double vaccination + inf.	*** 0.000	** 0.006	0.201	*** 0.000	* 0.012
35 (14 d.p.i)	Single vaccination	** 0.007				
	Double vaccination	*** 0.000	0.055			
	Infection only	** 0.007	0.888	* 0.037		
	Single vaccination + inf.	*** 0.000	** 0.003	0.123	** 0.002	
	Double vaccination + inf.	*** 0.000	** 0.002	0.135	** 0.002	0.811

Table 3. 2: *Kruskal Conover test results for IgY responses in the infection study.*
Benjamini-Hochberg corrections were used for multiple-sample comparisons. Significance levels are denoted with one (p<0.05), two (p<0.01), or three (p<0.001) asterisks. Calculated p values are rounded to 3 digits.

Important differences based on the number of immunisations were present when considering the IgY levels and HI titres at 3 dpi. Low levels of IgY were detected in the infection-only group, although not deemed significant when compared to the naïve controls (post-hoc Kruskal-Conover tests, corrected p values >0.05). However, the detectable HI titres in those birds resulted in a significant difference from the naïve treatment (post-hoc Kruskal-Conover test, corrected p value <0.001). At the same time, the HI titres of the

uninfected birds were significantly lower than the vaccinated groups, irrespective of infection (post-hoc Kruskal-Conover test, corrected p values <0.001).

The immunised birds had comparable levels of IgY and HI between the groups that received the same number of vaccinations prior to challenge, and infection did not markedly influence this pattern in terms of either of those measurements (post-hoc Kruskal-Conover tests, corrected p values >0.05). At the same time, the double vaccinated treatments exhibited higher levels of IgY and HI titres when compared to the single vaccination treatments, irrespective of infection status (post-hoc Kruskal-Conover tests, corrected p values <0.05).

		HI				
Day	**Treatment**	Naïve	Single vaccination	Double vaccination	Infection only	Single vacc. + inf.
14	Single vaccination	*** 0.000				
	Double vaccination	*** 0.000	0.662			
	Infection only	1.000	*** 0.000	*** 0.000		
	Single vaccination + inf.	*** 0.000	0.635	0.973	*** 0.000	
	Double vaccination + inf.	*** 0.000	0.126	0.358	*** 0.000	0.416
21 (pre-inf)	Single vaccination	*** 0.000				
	Double vaccination	*** 0.000	*** 0.000			
	Infection only	1.000	*** 0.000	*** 0.000		
	Single vaccination + inf.	*** 0.000	0.923	*** 0.000	*** 0.000	
	Double vaccination + inf.	*** 0.000	*** 0.000	0.792	*** 0.000	*** 0.000
24 (3 d.p.i)	Single vaccination	*** 0.000				
	Double vaccination	*** 0.000	** 0.003			
	Infection only	*** 0.000	*** 0.000	*** 0.000		
	Single vaccination + inf.	*** 0.000	0.527	*** 0.001	*** 0.000	
	Double vaccination + inf.	*** 0.000	** 0.009	0.620	*** 0.000	** 0.004
35 (14 d.p.i)	Single vaccination	** 0.007				
	Double vaccination	*** 0.000	0.092			
	Infection only	* 0.012	0.757	0.059		
	Single vaccination + inf.	*** 0.000	** 0.004	0.070	** 0.003	
	Double vaccination + inf.	*** 0.000	* 0.013	0.330	** 0.008	0.300

Table 3. 3: *Kruskal Conover test results for HI responses in the infection study.*
Benjamini-Hochberg corrections were used for multiple-sample comparisons. Significance levels are denoted with one (p<0.05), two (p<0.01), or three (p<0.001) asterisks. Calculated p values are rounded to 3 digits.

At day 35, corresponding to 14 dpi, the effects of infection on the antibody responses became much more pronounced. When analysing the IgM responses, the groups which were challenged with H9N2 virus had comparable levels (post-hoc Kruskal-Conover test, corrected p values >0.05). Likewise, the non-infected vaccinated groups had similar antigen-specific IgM responses (post-hoc Kruskal-Conover test, corrected p values >0.05). However, the infected birds generally exhibited higher levels of IgM than their uninfected counterparts (post-hoc Kruskal-Conover test, corrected p values <0.05), with the notable exception of the double vaccinated and infected group. These birds exhibited a large within-group variability, which coupled with the small sample size at this timepoint, rendered the differences with all other immunisation treatments not statistically significant (post-hoc Kruskal-Conover test, corrected p values >0.05).

The day 35 IgY and HI measurements also exhibited profound differences based on the immunisation regimes of the groups. The IgY antibody levels and the HI titres of the infection-only birds showed similar levels to the single vaccination group (post-hoc Kruskal-Conover tests, corrected p value >0.05). The uninfected and vaccinated birds were also not significantly different from one another in terms of their IgY and HI titres (post-hoc Kruskal-Conover tests, corrected p values >0.05). However, slightly higher levels of IgY in the double vaccination treatment were suggested by the significant difference between this group and the infection-only birds (post-hoc Kruskal-Conover test, corrected p value <0.05). The double vaccination group also showed no statistically significant difference in IgY levels or HI titres when compared to the vaccinated and infected treatments (post-hoc Kruskal-Conover tests, corrected p values >0.05). However, although the values of IgY and HI in these latter groups were not significantly different between them (post-hoc Kruskal-Conover tests, corrected p values >0.05), their higher levels were suggested by the significant differences to the single vaccination group and the infection-only birds (post-hoc Kruskal-Conover tests, corrected p values <0.05).

III.4.2. Altered dynamics of infection based on prior anti-H9N2 immunisations

The H9N2 matrix gene-specific qRT-PCR of the infected birds' buccal swab samples revealed important differences between the amount of viral shedding that occurs at various time points (**Figure 3.2 A** and **Table 3.4**). There was no detectable viral genetic material in the cloacal swab samples (data not shown), indicating that the birds did not shed detectable levels of H9N2 from the gastro-intestinal tract. As such, this suggests that the line of chicken used for the experiment is not permissive for gastrointestinal infection with H9N2 and subsequent viral shedding [190].

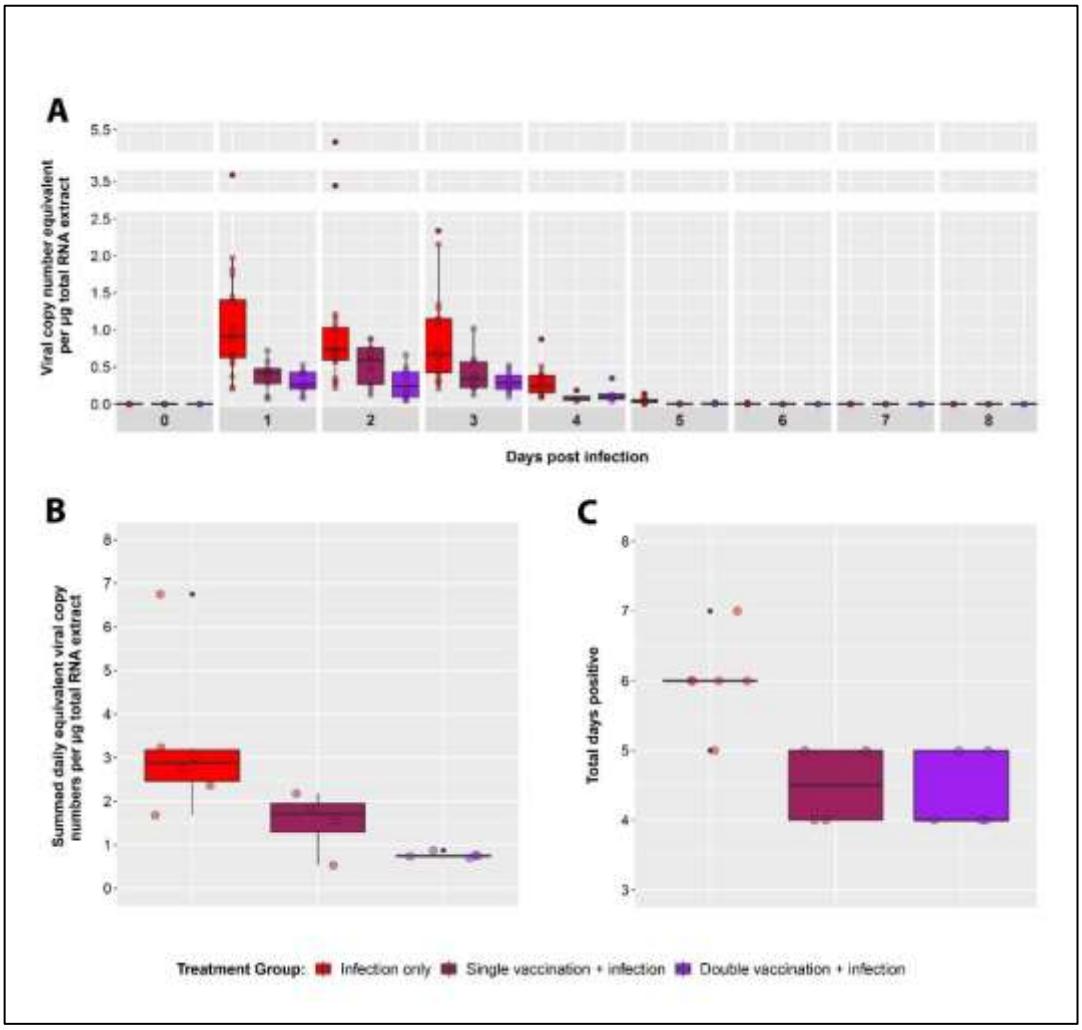

Figure 3. 2: *H9N2 matrix gene qRT-PCR results of buccal swab samples.*

(**A**) Viral copy number equivalent per µg total RNA extract in the infected bird groups from day 0 (pre-infection) to day 8 post-infection. (**B**) Total daily number of equivalent viral copies per ug

total RNA extract in the remaining birds at the end of the experiment. (**C**) The total number of days the surviving birds at the end of the experiment were positive for H9N2 infection.

At day 1 post-infection, all the infected birds had detectable levels of H9N2 genetic material in buccal swab samples. Furthermore, although there was no difference between the two vaccinated groups (post-hoc Kruskal-Conover test, corrected p value >0.05), the unvaccinated birds had significantly higher equivalent viral copies than the vaccinated groups (post-hoc Kruskal-Conover tests, corrected p values <0.01). At day 2, the only significant difference was between the double-vaccinated and the unvaccinated, with lower amounts of viral genetic material detected in the former (post-hoc Kruskal-Conover test, corrected p value <0.001). Of note is that at day 2, following the multiple sample comparison correction, the differences between the single vaccination group and the others were not deemed statistically significant (post-hoc Kruskal-Conover tests, corrected p value ~0.06), although they exhibit intermediate levels as opposed to the other treatments.

		Viral copy number equivalent	
dpi	Treatment	Infection only	Single vacc. + inf.
1	Single vaccination + inf.	** 0.001	
	Double vaccination + inf.	*** 0.000	0.397
2	Single vaccination + inf.	0.066	
	Double vaccination + inf.	*** 0.000	0.066
3	Single vaccination + inf.	* 0.010	
	Double vaccination + inf.	*** 0.001	0.398
4	Single vaccination + inf.	* 0.016	
	Double vaccination + inf.	* 0.030	0.508
5	Single vaccination + inf.	** 0.004	
	Double vaccination + inf.	** 0.004	0.647
6	Single vaccination + inf.	0.170	
	Double vaccination + inf.	0.390	0.390

Table 3. 4: Kruskal Conover test results for daily viral copy number equivalent detected by qRT-PCR in the infection study.

Benjamini-Hochberg corrections were used for multiple-sample comparisons. Significance levels are denoted with one (p<0.05), two (p<0.01), or three (p<0.001) asterisks. Calculated p values are rounded to 3 digits.

From day 3 to day 5, the unvaccinated chickens had significantly higher levels of equivalent viral copies than the birds in the vaccinated groups (post-hoc Kruskal-Conover tests, corrected p values <0.05) and there was no significant difference between the vaccinated treatments. At day 6, only the qRT-PCR results for the swabs originating from unvaccinated birds were positive, albeit at low levels. Only one bird from the unvaccinated group tested positive at day 7 and became negative the following day.

	Treatment	Infection only	Single vacc. + inf.
Total viral shedding	Single vaccination + inf.	* 0.015	
	Double vaccination + inf.	*** 0.001	0.159
Total days positive	Single vaccination + inf.	** 0.003	
	Double vaccination + inf.	** 0.002	0.779

Table 3. 5: *Kruskal Conover test results on qRT-PCR data for total viral shedding and total days positive in the birds that were culled at the end of the infection study.*

Benjamini-Hochberg corrections were used for multiple-sample comparisons. Significance levels are denoted with one (p<0.05), two (p<0.01), or three (p<0.001) asterisks. Calculated p values are rounded to 3 digits.

Overall, the qRT-PCR data indicated that the amount of viral shedding was dependent on prior vaccination, with double-vaccinated birds having on lower values than the single-vaccinated, followed by the unvaccinated birds which display the highest amounts. Furthermore, when considering the total equivalent viral copies present in all daily swab samples of the birds at the end of the experiment (**Figure 3.2 B** and **Table 3.5**), the unvaccinated birds had a significantly higher amount than both vaccine treatments (post-hoc Kruskal-Conover tests, corrected p values <0.05), although the difference between the single-vaccinated and double-vaccinated birds was nonsignificant (post-hoc Kruskal-Conover test, corrected p value >0.05). Similarly, when considering the total duration of infection (**Figure 3.2 C** and **Table 3.5**), the infection lasted on average longer in the

unvaccinated birds than in either of the vaccine treatments (post-hoc Kruskal-Conover tests, corrected p values <0.05), which displayed similar levels between them (post-hoc Kruskal-Conover tests, corrected p value >0.05). Therefore, both the amount of viral shedding and the time during which shedding occurs were influenced not only by prior vaccination against H9N2, but also by the number of immunisations.

III.4.3. Temporal trends following vaccination and infectious challenge

Mathematical models of the human and mouse immune systems in the context of antigenic challenge have provided important insights into the within-host dynamics of pathogens, including avian influenza viruses [191,192]. However, this work has not yet been mirrored in poultry in spite of the fruitful results of within-host models in humans and mice. Therefore, in order characterise the temporal trends of antibody responses, several mathematical models were chosen based on the observed results and with respect to the inherent biology of antibody responses upon stimulation with antigen (see section III.3.). As such, in order to account for the 7-day time lag observable in birds that received a vaccination on day 1, the timepoint of day 7 was used as the first day of immunisation. Subsequently, the fit of each model to the observed ELISA measurements was evaluated using the calculated AIC values and the model predictions were overlapped with the experimental observations (**Figure 3.3**).

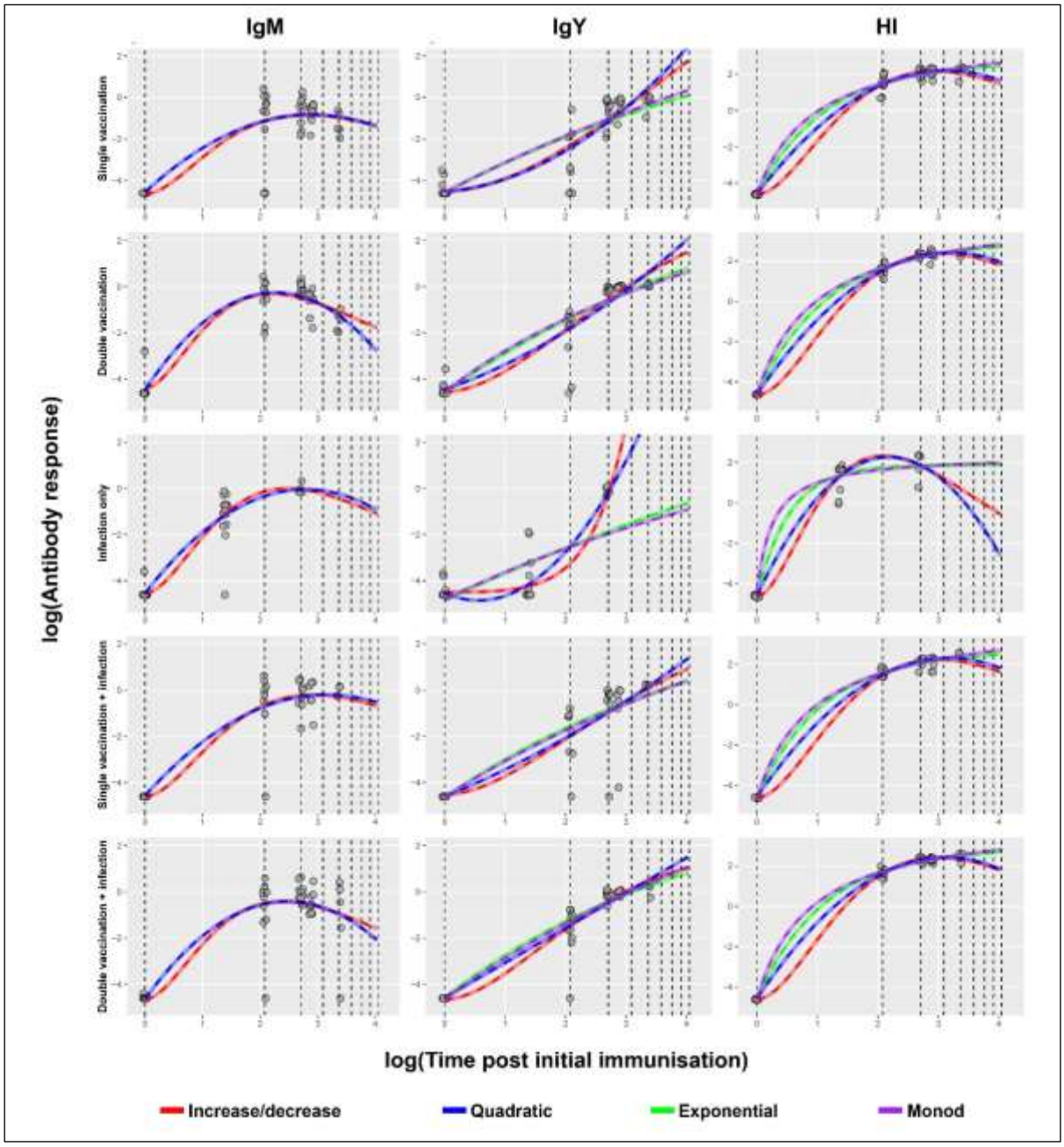

Figure 3. 3: *Model fits to the measured antibody responses in the vaccination and challenge experiment.* IgM, IgY, and HI model fits are shown on the left, middle, and right columns, respectively. Responses of each vaccination regime are shown on different rows. Black dotted lines are placed at (log transformed) 7-day time intervals post initial immunisation. The increase/decrease and quadratic model fits are shown in red and blue, respectively. The two additional model fits for the IgY and HI responses (see Methods), are shown in green (exponential plateau model) and purple (Monod-type model). The groups that received vaccination upon hatching were modelled using 7 days of age as the initial timepoint of vaccination to account for the 7-day time lag present in the responses of the birds in those treatments.

All IgM models showed comparable explanatory power based on the AIC score alone (**Table 3.6**). When considering the AIC weights, the quadratic model was slightly favoured for all treatment groups, with the exception of the single vaccination treatment, where the increase/decrease model was preferred.

Treatment Group	IgM Model	Optimised values for parameters				AIC	AIC weight	R^2
		σ	a	b	c			
Single Vaccination	Increase/Decrease	0.92	3.6	-0.71	-4.65	-64.36	0.51	0.22
	Quadratic	0.91	2.57	-0.44	-4.57	-64.24	0.49	0.22
Double vaccination	Increase/Decrease	0.6	6.19	-0.91	-4.38	-31.99	0.22	0.13
	Quadratic	0.59	3.72	-0.82	-4.47	-34.5	0.78	0.12
Infection only	Increase/Decrease	0.66	5.41	-0.8	-4.53	-129.65	0.48	0.11
	Quadratic	0.64	3.24	-0.58	-4.55	-129.79	0.52	0.11
Single vaccination and infection	Increase/Decrease	0.86	3.8	-0.69	-4.59	3.33	0.48	0.19
	Quadratic	0.89	2.77	-0.44	-4.58	3.16	0.52	0.19
Double vaccination and infection	Increase/Decrease	1	5.46	-0.84	-4.64	3.56	0.45	0.26
	Quadratic	1	3.42	-0.69	-4.64	3.18	0.55	0.26

Table 3. 6: *Optimised model parameters and evaluation of fit for IgM responses in each immunisation treatment of the vaccination and infectious challenge experiment.*

The parameter σ is the optimised standard deviation of the log-normal distribution for each fit. The values for a, b, and c correspond to the parameters of each model described in the Methods section. AIC, AIC weights, and R^2 values were used to evaluate the models.

The IgY models also exhibited comparable explanatory powers for the recorded measurements of each group (**Table 3.7**). Although the increase/decrease and quadratic models generally had lower AIC scores, they did not accurately depict the dynamics of the infection only treatment group, given their actual fit to the observed data.

Treatment Group	IgY Model	Optimised values for parameters				AIC	AIC weight	R^2
		σ	a	b	c			
Single Vaccination	Increase/Decrease	0.82	0.7	-0.15	-4.52	-84.78	0.39	0.19
	Quadratic	0.86	0.23	0.37	-4.53	-83.93	0.6	0.19
	Monod	0.94	25.05	16.5	-4.57	-73.22	0	0.24
	Exponential	0.9	10.1	-0.15	-4.6	-71.62	0	0.24
Double vaccination	Increase/Decrease	0.72	1.19	-0.29	-4.55	-23.17	0.2	0.15
	Quadratic	0.75	0.9	0.18	-4.45	-20.48	0.77	0.16
	Monod	0.78	14.28	7.03	-4.56	-13.71	0.01	0.18
	Exponential	0.79	11.35	-0.16	-4.57	-15.65	0.02	0.18
Infection only	Increase/Decrease	0.6	0.03	1.11	-4.49	-245.4	0.54	0.14
	Quadratic	0.57	-1.15	1.02	-4.53	-245.69	0.46	0.14
	Monod	1.06	16.1	12.59	-4.81	-191.01	0	0.49
	Exponential	1.07	15.53	-0.08	-4.86	-193.22	0	0.47
Single vaccination and infection	Increase/Decrease	1.13	1.05	-0.28	-4.52	-16.36	0.33	0.33
	Quadratic	1.13	1.06	0.11	-4.61	-16.41	0.32	0.32
	Monod	1.15	19.54	11.56	-4.63	-15.4	0.2	0.33
	Exponential	1.18	9.26	-0.2	-4.67	-14.89	0.15	0.34
Double vaccination and infection	Increase/Decrease	0.57	1.62	-0.38	-4.65	-44.71	0.16	0.09
	Quadratic	0.58	1.51	0	-4.58	-41.73	0.72	0.09
	Monod	0.59	21.85	11.3	-4.67	-40.43	0.08	0.1
	Exponential	0.61	9.06	-0.23	-4.6	-38.7	0.04	0.1

Table 3. 7: *Optimised model parameters and evaluation of fit for IgY responses in each immunisation treatment of the vaccination and infectious challenge experiment.*

The parameter σ is the optimised standard deviation of the log-normal distribution for each fit. The values for a, b, and c correspond to the parameters of each model described in the Methods section. AIC, AIC weights, and R^2 values were used to evaluate the models.

The within-group explanatory power of the HI models was also relatively similar based on the AIC scores, and different models were favoured based on the treatment group which is considered (**Table 3.8**). As such, the AIC weights favoured the increase/decrease models for the single vaccination and the double vaccination plus infection treatments, the quadratic model for the uninfected and double vaccinated birds, and the Monod-type model for the single vaccinated and infected birds. All models had equal explanatory power for the infection only treatment group. However, when looking at the variance explained by the models in all groups, they failed to explain the behaviour of the recorded HI observations ($R^2 \leq 0.02$). Although less pronounced, the explanatory power of the models was also low when considering both the IgM ($R^2 \leq 0.26$) and IgY ($R^2 \leq 0.49$) data.

Treatment Group	HI Model	Optimised values for parameters				AIC	AIC weight	R^2
		σ	a	b	c			
Single Vaccination	Increase/Decrease	0.25	5.75	-0.68	-4.61	11.56	0.53	0.01
	Quadratic	0.26	4.36	-0.7	-4.61	10.1	0.26	0.01
	Monod	0.26	8.94	0.97	-4.6	14.08	0.07	0.01
	Exponential	0.26	7.26	-0.88	-4.61	12.83	0.14	0.01
Double vaccination	Increase/Decrease	0.18	5.58	-0.66	-4.63	31.1	0.38	0
	Quadratic	0.19	4.39	-0.69	-4.62	32.02	0.61	0
	Monod	0.2	9.27	1	-4.62	44.21	0	0.01
	Exponential	0.2	7.52	-0.84	-4.58	41.14	0	0
Infection only	Increase/Decrease	0.41	11.69	-0.96	-4.61	-73.6	0.25	0.02
	Quadratic	0.41	6.28	-1.44	-4.59	-73.6	0.25	0.02
	Monod	0.42	6.98	0.25	-4.59	-73.6	0.25	0.02
	Exponential	0.41	6.5	-1.84	-4.61	-73.6	0.25	0.02
Single vaccination and infection	Increase/Decrease	0.27	5.58	-0.67	-4.59	35.45	0.01	0.01
	Quadratic	0.23	4.35	-0.69	-4.58	31.55	0	0.01
	Monod	0.21	9.04	0.96	-4.63	23.66	0.58	0.01
	Exponential	0.22	7.25	-0.91	-4.6	24.4	0.4	0.01
Double vaccination and infection	Increase/Decrease	0.13	5.7	-0.66	-4.59	8.84	0.84	0
	Quadratic	0.14	4.49	-0.72	-4.58	5.15	0.13	0
	Monod	0.15	9.04	0.89	-4.61	16.41	0	0
	Exponential	0.13	7.47	-0.91	-4.61	11.97	0.03	0

Table 3. 8: *Optimised model parameters and evaluation of fit for HI responses in each immunisation treatment of the vaccination and infectious challenge experiment.*

The parameter σ is the optimised standard deviation of the log-normal distribution for each fit. The values for a, b, and c correspond to the parameters of each model described in the Methods section. AIC, AIC weights, and R^2 values were used to evaluate the models.

III.4.4. Immunisation regime effects on splenic lymphocyte composition

Significant differences were observed between the immunisation regimes in terms of the proportions of specific lymphocyte subsets (**Figure 3.4**). The B cell compartments of the all the immunised groups were significantly higher than the naïve birds. By contrast, no significant differences between the groups were observed when considering the total T cell compartment, or the total αβ and γδ T cells. However, differences between the immunisation treatment groups were observed within these T cell lineages.

Within the αβ T lymphocytes, the CD4+ cells were at significantly higher levels in all immunised (either through infection or vaccination) birds than in the naïve group. By contrast, there are no significant differences between the CD8+ αβT cell compartments of the treatment groups. The CD8αα+ γδ T cell subpopulations of the two groups of double

vaccinated birds are at significantly lower levels than the naïve, irrespective of infection status. At the same time, the CD8αβ+ γδ T cells of the groups that received one or two vaccinations and were subsequently infected are at significantly higher levels than in the naïve birds. Lastly, the CD8 negative γδ T cells are at higher levels in the single vaccination and the double vaccination treatment groups, but not in any of the infected groups.

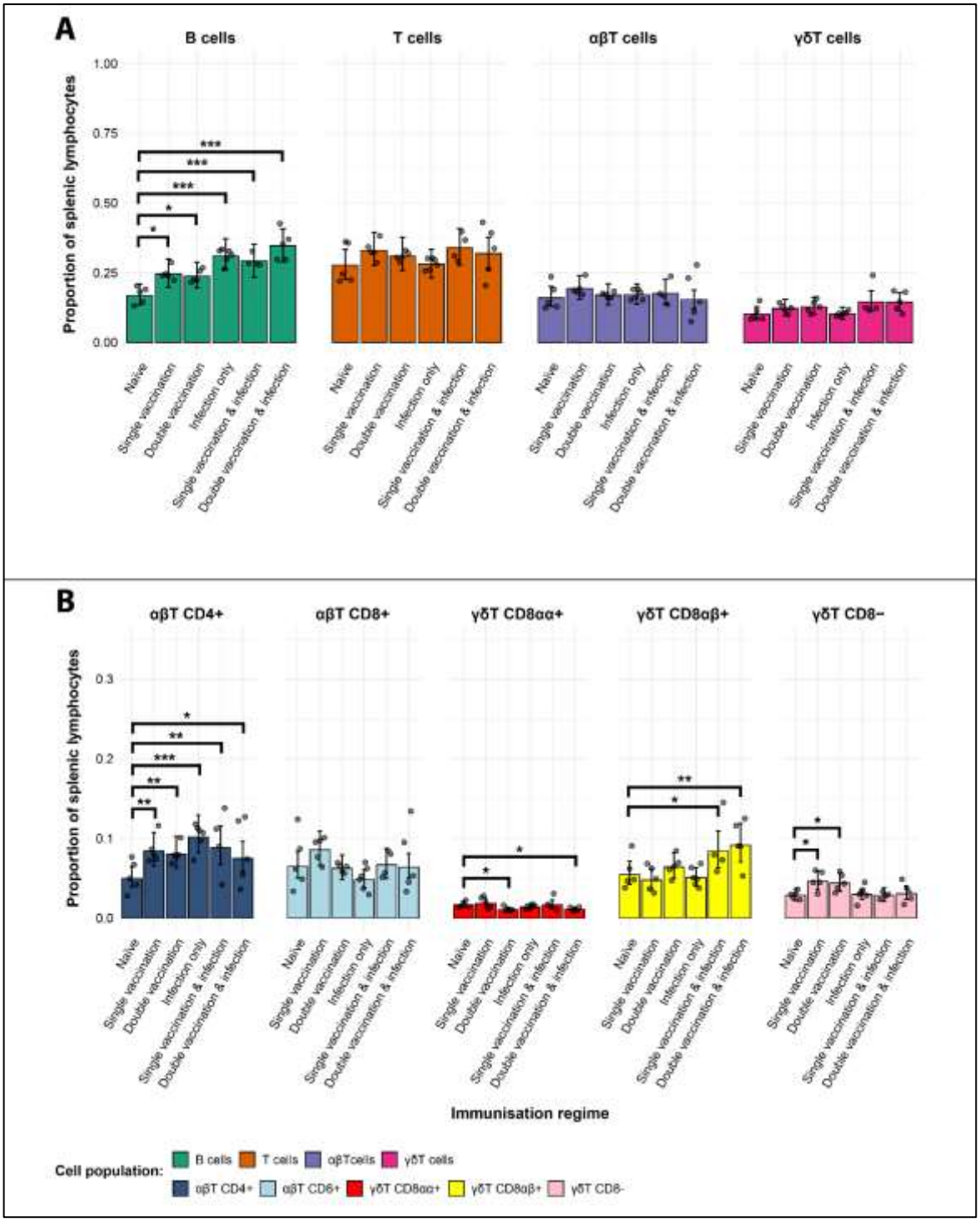

Figure 3. 4: *Splenic lymphocyte populations model estimates for the different H9N2 immunisation regimes.* (**A**) B and T cell compartments, and main T cell lineages. (**B**) T cell populations based on differential expression of CD8 and/or CD4 surface markers. Grey dots represent individual bird observations for lymphocyte population. Error bars represent 95% bootstrap confidence intervals for the point estimates generated from 1000 simulations of the model. Statistically significant differences between the model estimates are depicted above the plots based on their corresponding

p-values: * = $p < 0.05$; ** = $p < 0.01$. The frequencies of CD3–Bu1– lymphocytes (~30%) are not shown.

III.5. Discussion

Previous studies have shown that AIV infection and/or vaccination are important drivers for antibody-mediated immunity [105,193]. Naïve B cells respond to AIV-specific antigens, leading to measurable responses via standard laboratory procedures such as ELISAs or HI assays [105,193,194]. The analysis presented herein quantifies the H9N2-specific antibody responses of chickens that were subjected to immunisations through vaccination(s), infection, or combinations of the two, whilst also revealing the effects of these specific immunisation regimes on the frequencies of lymphocyte subsets in the spleen.

The dynamics of the H9N2-specifc antibody responses following vaccination of one-day-old chickens exhibited a delayed production of IgM and IgY, beginning at least 8 days post-immunisation, with measurable responses being recorded on day 14. At this time point, the HI titres of most birds were not above the correlated protective thresholds against mortality or severe disease. The absence of measurable responses at day 7 is consistent with previous findings which showed that AIV-specific antibody responses are detected at least 8 days following the vaccination of older chickens, time during which the humoral immune response develops [195]. In addition, a further delay in responses has previously been recorded when vaccination was administered upon hatching due to the immature immune response of very young birds [196,197]. Of note is that the presence of maternal antibodies was also shown to hinder the development of virus-specific antibody responses in newly hatched chicks, but this phenomenon was not relevant in the current experiment given that the eggs from which the chicks hatched were derived from specific pathogen-free (SPF) hens [198]. This is further supported by the results of the day 7 IgM and IgY ELISAs which were unable to detect H9N2-specific antibodies in the sera of birds.

A stark difference in the development of antibody responses was evident in the infection only group as opposed to the groups that received a vaccine at day 1 post-hatching, with IgM responses being detected in almost all birds as early as 3 days after infectious challenge.

Although very little IgY was detected and this was only in a few birds, HI titres correlated with protection against mortality were present in all but two birds of the infection only group. This more rapid induction of H9N2-specific antibody responses in the infection only group could be due to a higher antigenic stimulation via infection and viral replication, but also because the immune system of these birds is more mature [106,196].

The effects of multiple immunisations were evident on the H9N2-specific antibody responses of the chickens. At day 14, before the second vaccination was administered to the specific groups, the variability between the IgM and IgY responses of all the (at the time single) vaccinated birds was high, and this pattern was also maintained for the single vaccination groups at day 21. By contrast, the groups that received a second vaccine on day 14 had much less variable and overall higher H9N2-specific antibody responses at day 21, suggesting that multiple immunisations are able to focus the humoral immune responses and develop a better protection. This phenomenon was particularly evident at day 35, when the two vaccinated and infected groups exhibited the highest levels of H9N2-specific antibody responses, further providing evidence of the increased protection conferred by multiple immunisations.

Vaccinations with inactivated influenza viruses predominantly trigger antibody-mediated systemic responses, which are known to offer protection against infectious challenge [42,58]. The M gene qPCR results of the infected groups demonstrate that less viral shedding occurs in vaccinated birds as opposed to their unvaccinated counterparts, and this effect is dependent on the number of vaccinations previously received. Indeed, the double vaccination and infection birds exhibit both the lowest levels of daily viral shedding, and lowest overall shedding. At the same time, both single and double vaccinated birds had a lower overall duration of infection, further suggesting that vaccination with an inactivated H9N2 virus is able to offer protection against disease and decrease the time window for infectious spread.

The antibody dynamics models revealed that simple equations can be used to capture the temporal trends in the IgM, IgY and HI responses of H9N2-immunised birds. The results indicate that although the simple models considered for the analysis generally have acceptable fits to the data, they do not fully explain the behaviours of the IgM and IgY

antibody responses and the corresponding HI titres of the immunisation groups. Indeed, the high individual variability between birds is not captured by the equations, as only the mean responses are modelled. As naïve antigen-specific B cells undergo class-switching upon stimulation, these responses are also intimately connected and inherently depend on the genetic makeup of each individual bird [58,77]. Therefore, the inability of these simple models to capture the heterogeneity between the immune system responses of different individuals hinders their use in predicting the dynamics of H9N2-specific antibody responses in chickens. Furthermore, as the number of post initial immunisation timepoints is small, the sequential annealing optimisation method resulted in inadequate estimation for the parameters, especially as the declining phase was not captured by the observations. Future modelling work that incorporates the variability between individuals and connects the IgM and IgY responses to the protective abilities of these antibodies through HI are required in order to fully capture and predict the dynamics of antibody responses against avian influenza infections. Such studies have the potential to minimise the use of animal experiments required in assessing vaccine-induced responses, as only simple immunological data might be sufficient to predict the protective antibody responses triggered by AIV vaccination or challenge.

The protective responses suggested by IgM and IgY ELISAs and the HI assays on the sera collected from the birds are correlated to the increased frequency of B cells in the spleens of vaccinated and/or infected birds, when compared to their naïve counterparts. Inactivated vaccines are known to be an important driver of B cell-mediated immunity [92,105,193], and vaccinated birds could have thus been expected to have increased B cell frequencies as a consequence. However, H9N2 infection with or without vaccination(s) also increases splenic B cell frequencies significantly, indicating that viral replication is also a strong inducer of humoral immunity. For all of the vaccinated and/or infected groups, the drive towards antibody responses is also suggested by the significantly higher CD4+ αβ T cells, as this population of lymphocytes is known to be involved in humoral immunity through the contribution of helper T cells [199,200].

Antibody-mediated responses alone are not sufficient in the protection against AIV, as previous studies revealed that high antibody titres were unable to completely block H9N2 transmission [91–93]. Cellular immunity via effector CD8+ T cells is known to contribute

to the control and clearance of AIV infections [90,201]. Interestingly, there were no significant changes in the overall percentage between the groups in terms of CD8+ αβ T cells, suggesting that, at least in the spleen, the frequency of this population does not change markedly under vaccination (with killed antigen) and/or infection scenarios. For the vaccinated groups, it is plausible that the MHC class I pathway is poorly activated through immunisation with an inactivated vaccine, which would lead to inefficient CD8+ αβ T cell stimulation. Indeed, inactivated vaccines against AIVs (and other pathogens) are known to generally induce poor CD8+ responses in birds and mammals [42,58]. However, infectious challenge, either alone or in combination with vaccination, also did not significantly alter the CD8+ αβ T cell frequencies in the spleen. As chickens lack lymph nodes, this might be a consequence of the distant location of the spleen to the site of infection and the insufficient MHC class I antigenic stimulation required for CD8+ T cell expansion. Relatedly, the homing of CD8+ T cells to the infected tissues from the spleen might mask changes in lymphocyte proportions. As the spleens were harvested two weeks after the infectious challenge, it is also plausible that AIV-specific CD8+T cell responses in the infected groups might have concentrated in the sites of infection and the spleens not exhibiting significant differences to the naïve birds at the time when the tissues were collected for the flow cytometric analysis. In support of this explanation is that previous AIV infection studies have shown that CD8+ αβ T cell frequencies remain unchanged in the spleen but increase in other tissues such as the lung, thus suggesting recruitment to the infected tissues following infectious challenge [199]. Lastly, another possible explanation for the absence of any differences in the splenic CD8+ αβ T cell proportions in the groups is that clonal competition within the spleen limits the expansions of CD8+ αβ T cells under H9N2 immunisation scenarios, potentially in favour of CD4+ responses [202]. In the absence of lymph nodes, the spleen might be expected to concentrate more germinal centres involved in antigen-specific B cell maturation which occurs with the involvement of CD4+ T cells [203,204].

Chicken γδ T cells are found at much higher frequencies in the spleen and in the circulation than in mice or humans [80,205] and have previously been shown to exhibit important functions during viral and bacterial infections [78,83,84]. Importantly, both the CD8− γδ subpopulation and especially the CD8+ γδ T cells have been previously shown to exhibit

cytotoxic activities, in an MHC-independent manner [85]. When compared to the naïve birds, the vaccination only groups exhibited higher levels of CD8− γδ T cells, suggesting that this subpopulation may be involved in vaccination-specific responses and less so during infection. Interestingly, both groups that received a double vaccination had lower frequencies of CD8αα+ γδ T cells than the naïve, a pattern which may be attributable to the multiple vaccine-derived antigens to which these birds were subjected to. Lastly, the groups that were previously vaccinated before infection have higher levels of CD8αβ+ γδ T cells, suggesting that the previously vaccinated birds have enhanced responses following infectious challenge in this T cell subset which has been previously demonstrated to exhibit important cytotoxic abilities [85]. Together, the observed differences in frequency between the immunisation groups are strong indicators that vaccination, infection, and the number of immunisations can induce significant changes in the splenic lymphocyte cell composition in chickens.

Taken together, the analyses of the immunological changes triggered in chickens by vaccination and/or infection with AIV subtype H9N2 indicate that an important antibody-mediated response towards both vaccine- and infection-derived antigens develops following immunisation(s). The group-specific differences in terms of the bird immune responses and their ability to control infection constitute a solid basis for a more detailed examination of their adaptive immune repertoires. Indeed, although strong antibody responses were recorded in all of the vaccinated and/or infected groups, both T and B cell populations in the spleen exhibited differences when compared to the naïve birds, suggesting that both lymphocyte lineages participate in the avian H9N2 antigen-specific responses.

Chapter IV: IgM and IgY Antibody Repertoires Following H9N2 Immunisation

IV.1. Abstract

Avian influenza viruses (AIVs) cause significant losses to the poultry sector each year and can also infect a wide variety of hosts, including humans. To date, the vaccination of birds remains the most important method for the prevention and control of AIV outbreaks. Most of the national vaccination strategies against AIV infection use whole-virus inactivated vaccines, which predominantly trigger a systemic antibody-mediated immune response, which remains poorly understood. Indeed, no studies to date have examined the antibody repertoire of birds that were infected with and/or vaccinated against AIV. In this chapter, I evaluate the changes in the H9N2-specific systemic antibody repertoires by analysing both IgM and IgY responses in chickens that were subjected to vaccination(s) and/or infectious challenge. The results show that a large proportion of the IgM and IgY clones are shared across multiple individuals, and that these public clonal responses are dependent on both the immunisation status of the birds and the specific tissue that was examined. Furthermore, the analysis reveals specific clonal expansions which are restricted to particular H9N2 immunisation regimes. These results indicate that both the nature and number of immunisations are important drivers of the antibody responses in chickens following H9N2 antigenic stimulation. Together, the results of this analysis reveal important information about the avian IgM and IgY antibody repertoires and their responses to H9N2 infection and/or vaccination, whilst also providing information on the fundamental biology of the antibody responses in birds.

IV.2. Introduction

Avian influenza viruses (AIVs) are responsible for major losses to the poultry sector each year at a global level [8]. These pathogens also pose major reasons for concern due to their potential to jump the species barrier and infect other domestic animals and even humans

[4]. Furthermore, efficient control of outbreaks and prevention through practices such as vaccination is hindered by their high mutation rate and the ability of subtypes to reassort and generate novel strains.

Influenza viruses are classified based on the haemagglutinin (HA) and neuraminidase (NA) surface proteins, which mediate cellular attachment and release, respectively [4]. These proteins also serve as major antigenic targets for the adaptive immune systems of avian and mammalian hosts. Indeed, the majority of the antibody responses are directed towards the HA and NA proteins, with protective titres being able to block the infection of cells [42].

The ability of influenza-specific antibodies to recognise and bind to viral epitopes stems from the diversity of the B cell receptors (BCRs / immunoglobulins) which is generated during B cell development [77]. This process involves the somatic rearrangement of variable (V) and joining (J) genes for the light chains of antibodies and V, diversity (D) and J genes for the heavy chains [77]. However, most avian species only possess one functional V and J genes for both the antibody light and heavy chains, and very limited diversity is present between the D genes if there are more than one present [77]. Instead, avian species use gene conversion to diversify their antibody repertoires, a process during which fragments of variable length are inserted into the functional V segment from the pseudo-V genes which are located upstream the immunoglobulin gene clusters [77,114]. This process, coupled with the heavy and light chain pairing and the somatic hypermutation which increases the affinity to antigens is able to generate vast amounts of diversity in the antibody repertoires of avian hosts.

To date, very limited information is available regarding the antibody repertoires of avian hosts, especially in the context of infection. As antibody responses are known to contribute significantly to protection against AIVs, and veterinary vaccination generally involves the use of inactivated vaccines which predominantly stimulate humoral immunity [42], the current chapter explores the effects of vaccination and/or infection on the IgM and IgY repertoires of chickens. The methods and design of the animal experiment are detailed in Chapter II, with the repertoire analysis being adapted for the analysis of antibodies.

IV.3. IgM repertoire analysis results

IV.3.1. Recovered sequences and productively rearranged IgM chains

The sequencing of the 5'RACE PCRs yielded a total of 2,295,729 sequences, out of which ~97.3% were productively rearranged. There was substantial heterogeneity in terms of total reads obtained across individual samples (**Figure 4.1**), with no consistent patterns being observed between immunisation regimes or tissue types. Almost all samples had more than 1000 productive reads, with the notable exception of the trachea of one bird from which 5 sequences were recovered, with only 3 being productively rearranged. Due to the low number of reads recovered, this sample was disregarded from the analysis, but the splenic and bursal sequences from the same bird were included, as the read numbers were sufficient.

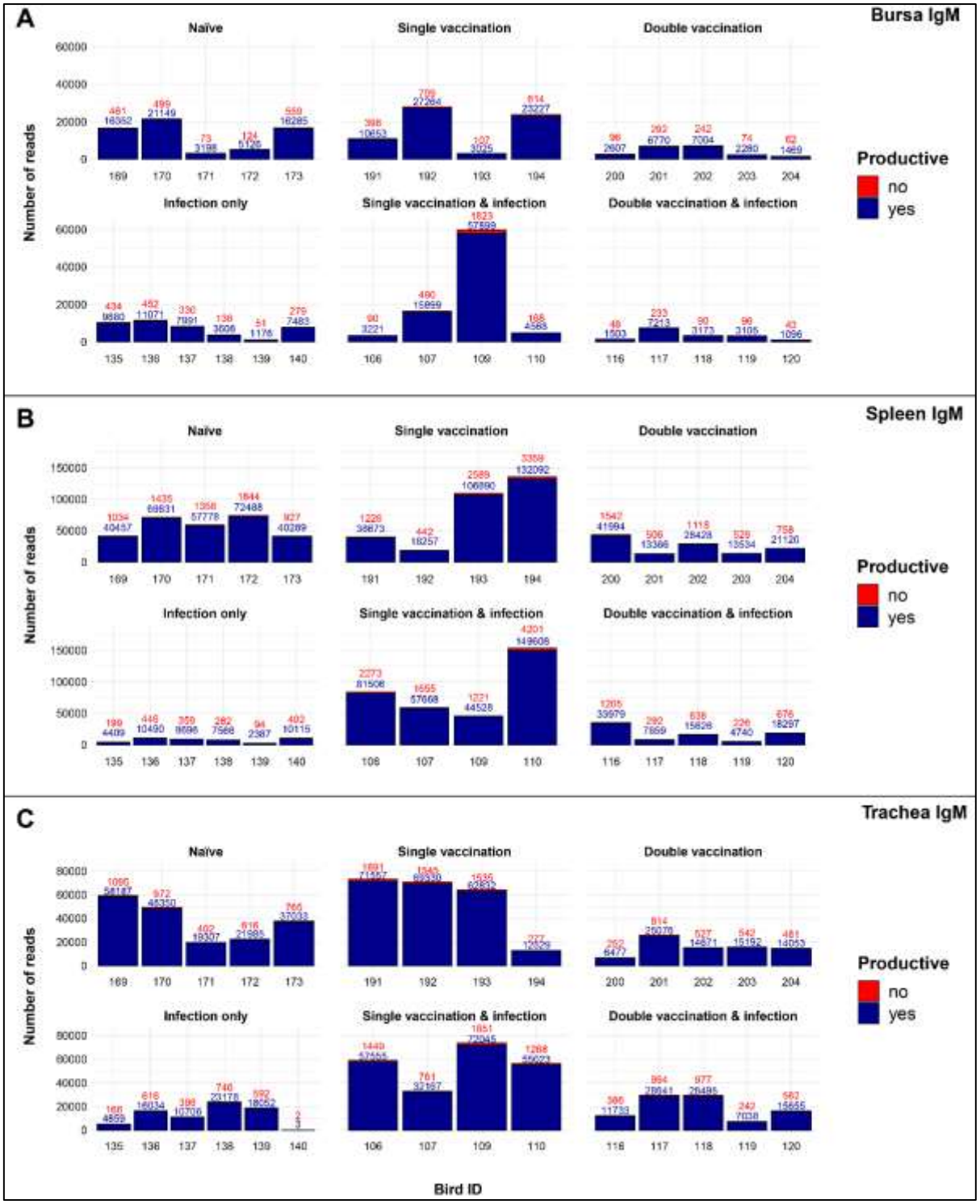

Figure 4. 1: *Total number of IgM sequence reads identified in tissues of chickens that were subjected to different immunisation regimes.*

(**A**) Splenic samples, (**B**) bursal samples, (**C**) tracheal samples. Bird numbers displayed on the x axis and individuals are grouped based on the corresponding immunisation status which is illustrated above each panel. Productive and unproductive reads are shown in blue and red, respectively.

IV.3.2. IgM clonal homeostasis within samples

By observing the IgM clonal homeostasis plots of the samples, several remarks can be made regarding the influences of immunisation regime and tissue type (**Figure 4.2**). First, there is no apparent influence of the H9N2 treatment across tissues, except the double vaccinated groups in the spleen, which exhibit less pronounced proportions of expanded clones, compared to the other immunisation regimes. Second, there are observable differences between the tissues, with the trachea generally displaying the highest proportion of expanded clones across the groups, and the bursa the lowest. However, due to the high heterogeneity in total sequence reads obtained from the samples, it is difficult to determine the extent to which tissue type and immunisation regime contribute to the observed patterns, in the absence of formal statistical analyses.

IV.3.3. IgM repertoire diversity

The IgM clonal diversity was found to be influenced by both tissue type and H9N2 immunisation regime (**Figure 4.3**). In the bursa, no differences in diversity were observed between the groups regarding clonal richness (D_0), typical clones (D_1), or dominant clones (D_2) at the nucleotide level. In the spleen, the only significant difference to the naïve birds was in double vaccinated and the double vaccinated and infected groups, both exhibiting significantly higher levels of diversity in terms of dominant clones. Lastly, in the trachea, significantly higher levels of diversity were observed in all the immunised groups in both clonal richness (D0) and typical clones (D1), when compared to the naïve group. However, only the double vaccinated and infected group showed significantly higher diversity to the naïve birds when looking at the dominant clones (D2). Of note is that similar patterns with the same significant differences to the naïve birds were observed when the amino acid clonal diversity was considered (**Figure A.7**).

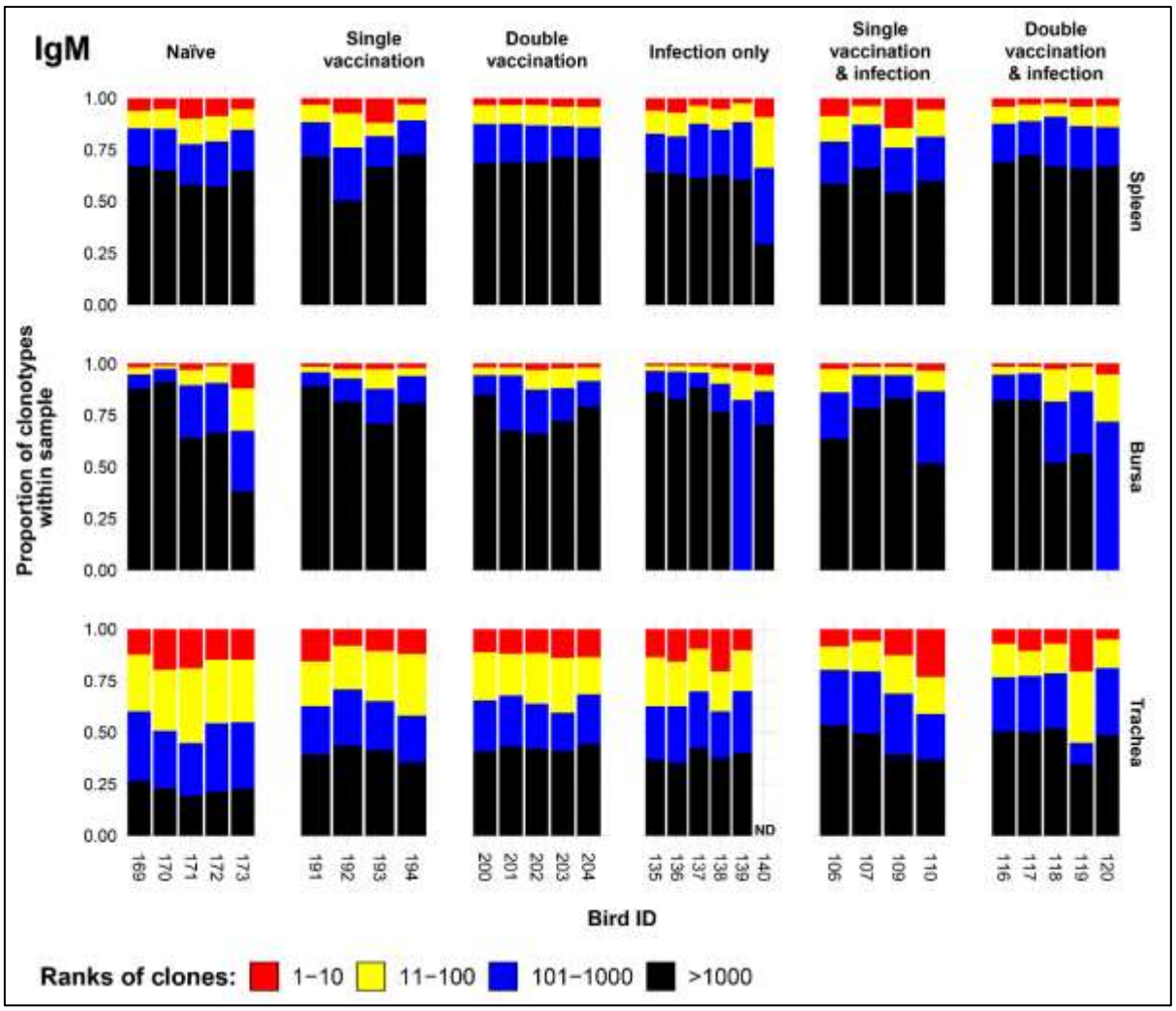

Figure 4. 2: *IgM clonal homeostasis plots of individual tissue samples.*

Bird numbers displayed on the x axis and individuals are grouped based on the corresponding immunisation status which is illustrated above each panel. Clones were ranked based on their abundance into four categories: first 10 most abundant (red), from 11-100 (yellow), 101-1000 (blue), and above 1000 (black) in terms of total abundance within each sample. The proportions of clonotypes are displayed on the y axis.

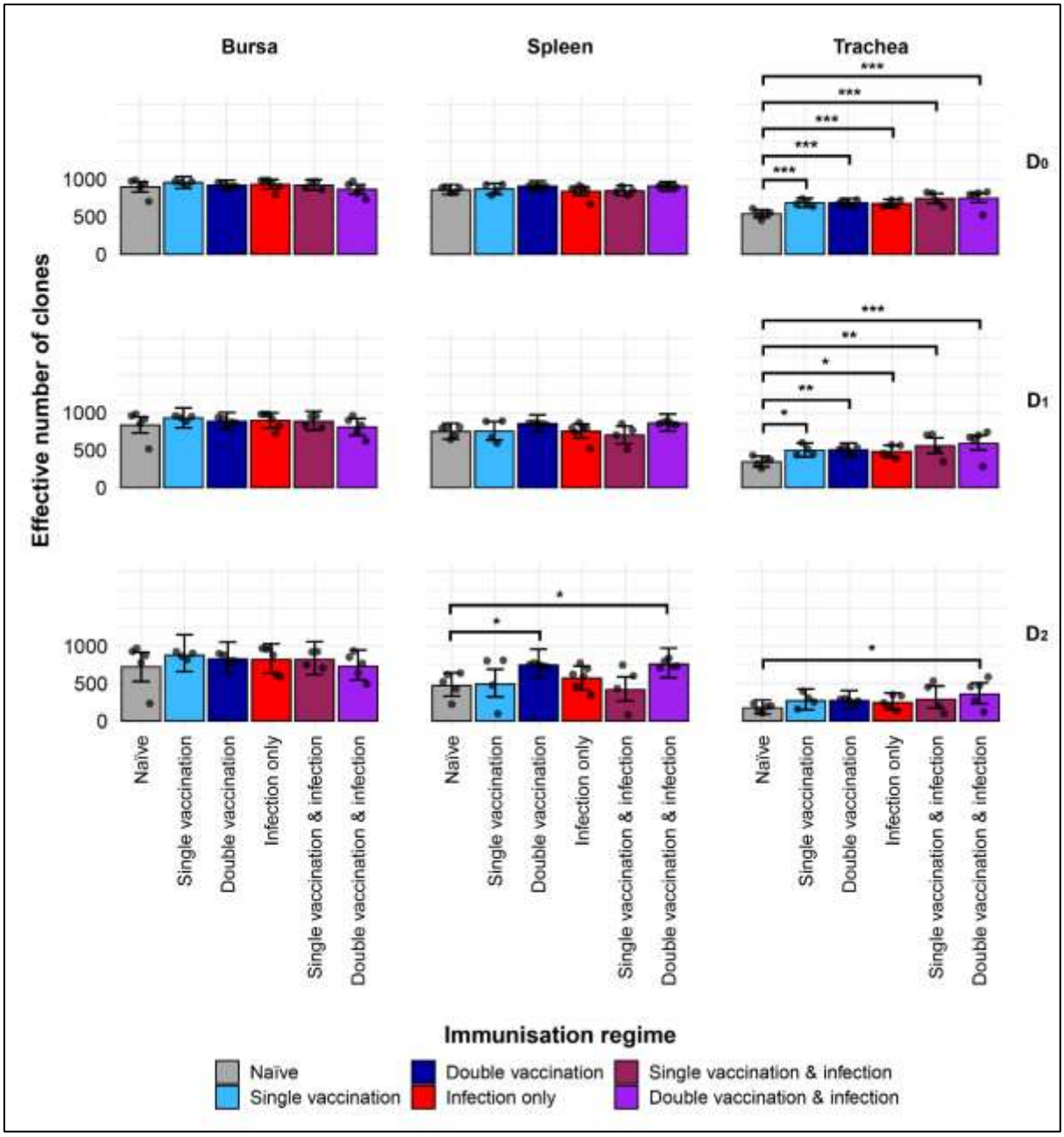

Figure 4. 3: *IgM clonal diversity within samples.*

Different rows show the Hill numbers corresponding to clonal richness (D0), the "typical" clones (D1) and the "dominant" clones (D2) in a theoretical sample of 1000 sequences. Immunisation regimes are colour coded and displayed on the x axes. Dots represent individual bird observations of the effective number of species calculated in each tissue for the corresponding H values. Error bars show the 95% bootstrap confidence intervals for the point estimates generated from 1000 simulations of the model. Statistically significant differences between the model estimates are depicted above the plots based on their corresponding p-values: * = $p < 0.05$; ** = $p < 0.01$; *** = $p < 0.001$.

IV.3.4. Public and private IgM clonal compartments

The partitioning of IgM sequences into private and public clones (at the level of nucleotides) reveals effects of both tissue type and immunisation regime on the composition of the repertoire both within and between the samples (**Figure 4.4**). The bursal tissue samples of all groups exhibited significantly more private than public clones, with the notable exception of the double vaccination and infection group, which had comparable proportions of public and private clones. By contrast, the tracheal samples of all groups exhibited significantly higher proportions of public clones than private, with the former reaching more than 75% of the total clones in some individuals. In the spleen, the infection only group had significantly more private clones than public. At the same time, the single vaccination and infection exhibited more public than private clones in the spleen. The other groups had comparable levels of private and public clones in repertoires of splenic samples. When considering the public and private compartments at the amino acid level (**Figure A.8**), the differences remained the same with the exception of the splenic clonal compartment of the double vaccinated and infected chickens, which exhibited significantly higher public clones.

Differences between the groups were also evident regarding the contribution of private and public clones to the repertoire (**Figure 4.5**). In the bursa, the double vaccination regimes exhibited lower proportions of private clones and higher proportions of public clones than the naïve group in the bursa, irrespective of infection. In the spleen, there were no significant differences to the naïve birds in the sizes of either public or private repertoires of any of the immunised treatment groups. Lastly, in the trachea, the only immunisation regime that exhibited a difference to the naïve birds was the infection only group, showing significantly higher proportions of private clones and lower proportions of public clones. At the amino acid level (**Figure A.9**) the significant differences to the naïve were also observable as for the nucleotide level, with the notable addition of the splenic compartments of the single vaccinated and infected birds, which exhibited significantly lower levels of private clones and higher proportions of public clones than the naïve group.

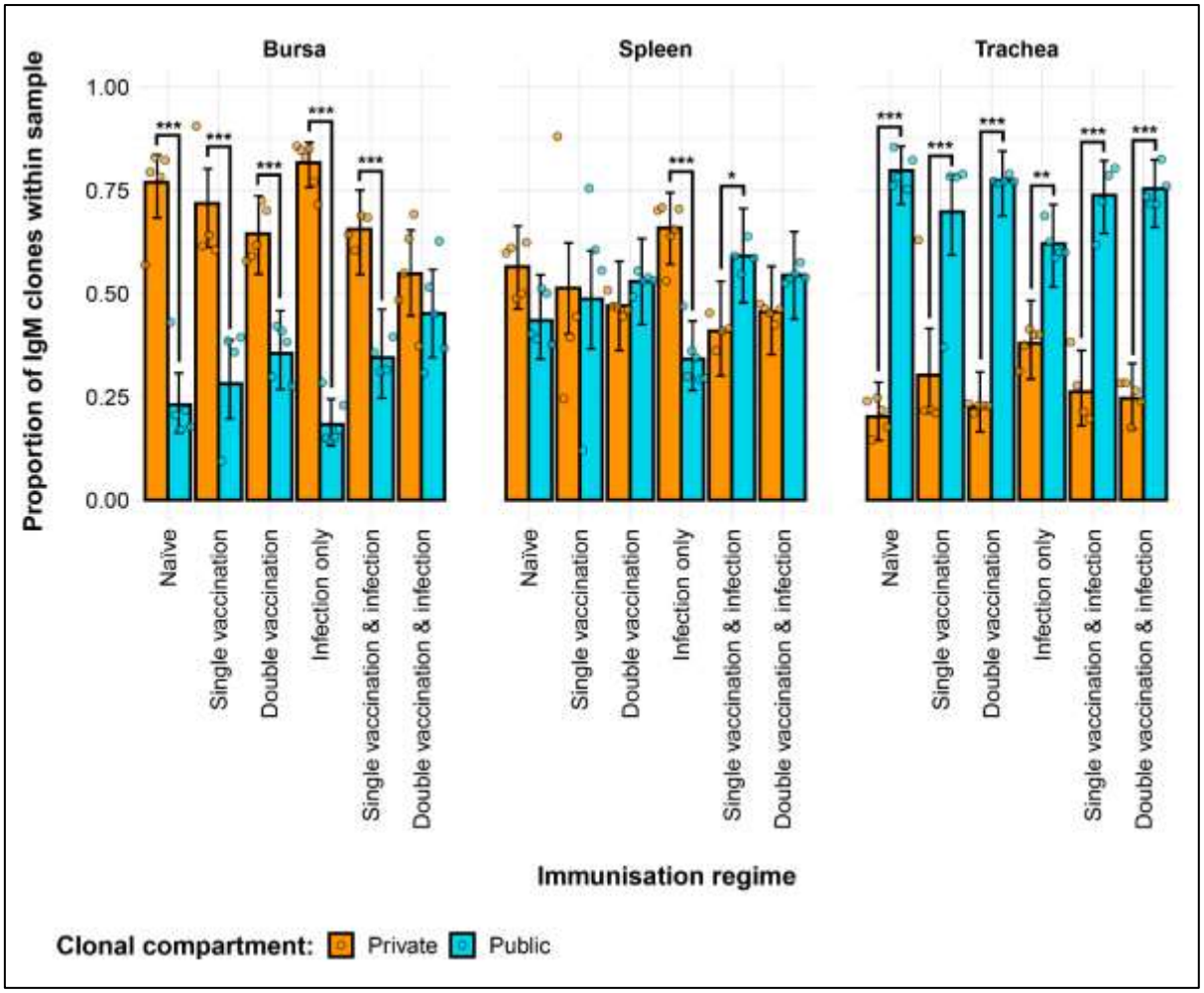

Figure 4. 4: *Differences between the IgM public and private compartments under different H9N2 immunisation regimes based on clone CDR3 nucleotide structure.*

Private (individual-restricted) clones are shown in orange. Public clones (shared between more than two individuals) and are shown in light blue. Dots represent individual bird observations of public and private clonal compartments. Error bars represent 95% bootstrap confidence intervals for the point estimates generated from 1000 simulations of the model. Statistically significant differences between the model estimates are depicted above the plots based on their corresponding p-values: * = $p < 0.05$; ** = $p < 0.01$; *** = $p < 0.001$.

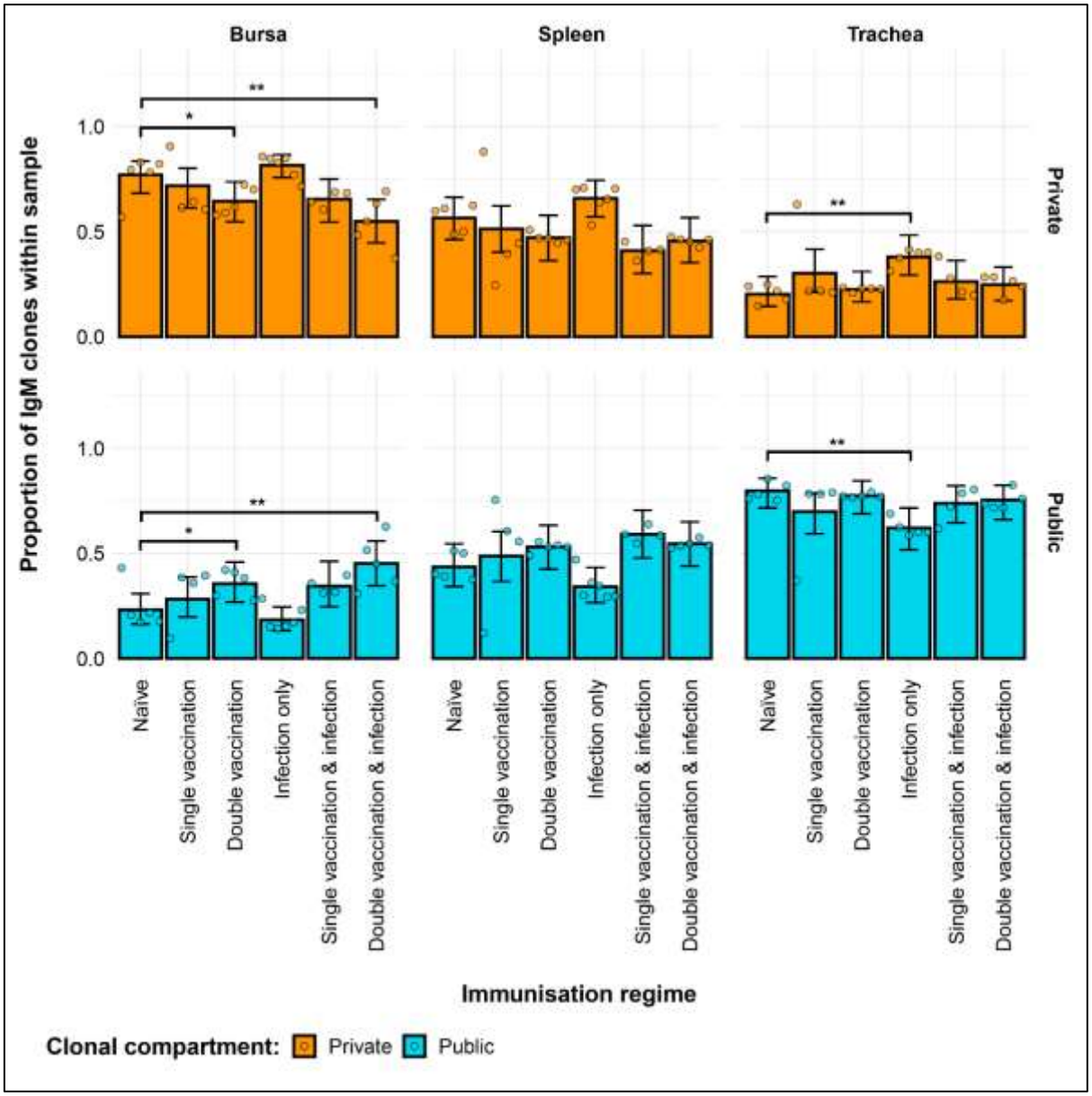

Figure 4. 5: *Differences within the IgM public and private compartments under different H9N2 immunisation regimes based on clone CDR3 nucleotide structure.*

Private (individual-restricted) clones are shown in orange. Public clones (shared between more than two individuals) and are shown in light blue. Dots represent individual bird observations of public and private clonal compartments. Error bars represent 95% bootstrap confidence intervals for the point estimates generated from 1000 simulations of the model. Statistically significant differences between the model estimates are depicted above the plots based on their corresponding p-values: * = $p < 0.05$; ** = $p < 0.01$; *** = $p < 0.001$.

The partitioning of public IgM clones based on their degree of clonal sharing reveals additional effects between the samples (**Figure 4.6**). Notably, the most substantial component of the total public repertoire is comprised of rare public clones. As such, the differences to the naïve birds regarding the proportion of total public clones were also displayed by the rare public compartment of the immunisation regimes across tissues. When looking at the private clones, the differences to the naïve group in the trachea and bursa were also consistent with the ones revealed by the model without the partitioning of the public compartment. However, in the spleen, the single vaccination and infection group now exhibited significantly lower proportions of public clones to the naïve.

Regarding the more frequently shared IgM clones, both the common public and the ubiquitous clonal compartments were at relatively low levels, each generally amounting to less than 5% of the repertoire of individual birds. There were no significant differences between the IgM repertoires of the immunisation regimes regarding the common clones, but some were evident in the ubiquitous clonal compartments. In the bursa, the single vaccination and the single vaccination and infection groups showed significantly higher levels than the naïve birds. There were no observable differences to the naïve birds in the splenic ubiquitous clones of any immunised group. Lastly, in the trachea, the double vaccinated group had significantly higher proportions of ubiquitous clones than the naïve chickens.

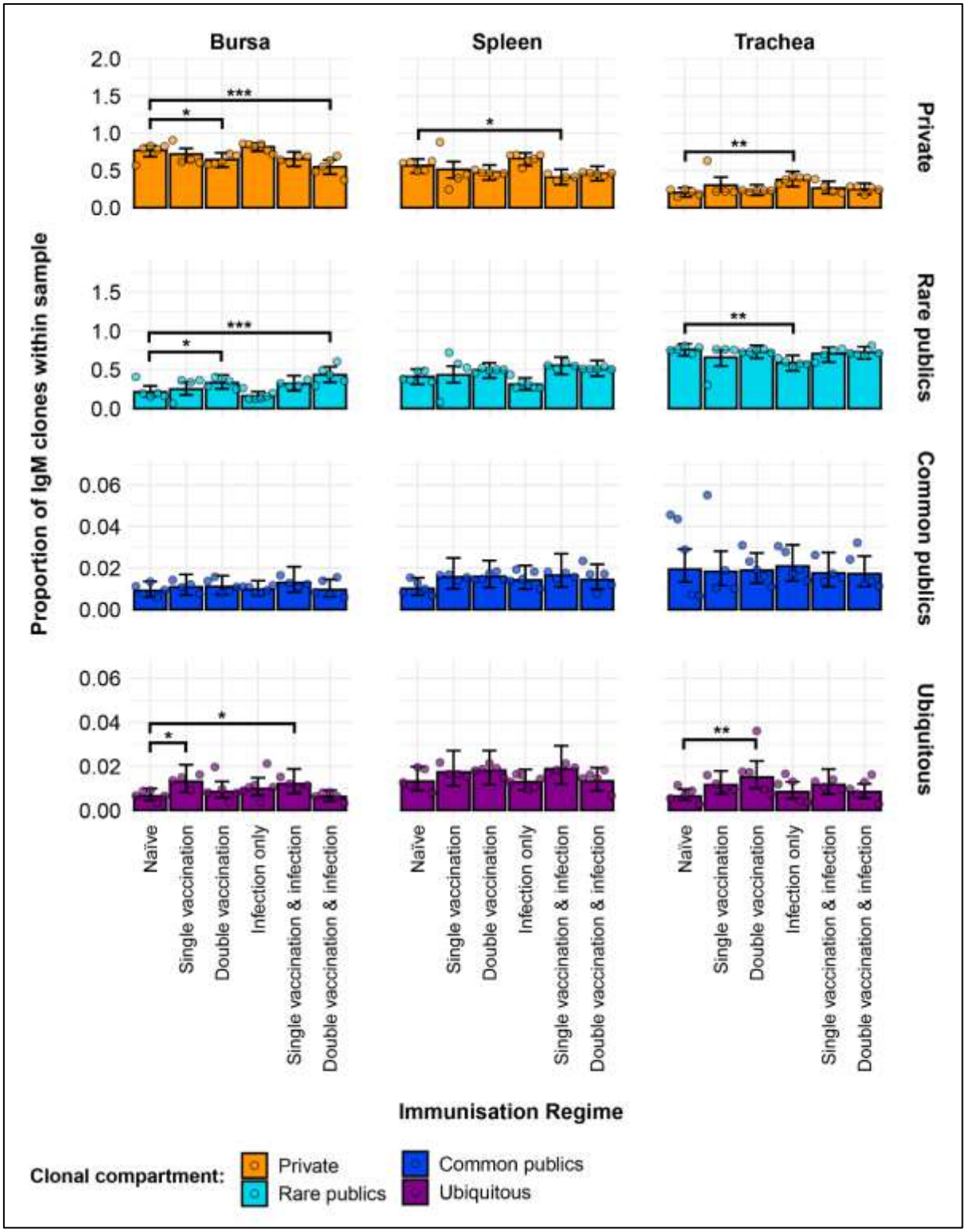

Figure 4. 6: *Model estimates of IgM clone CDR3 nucleotide private and public compartments based on different levels of clonal sharing.*

Private (individual-restricted) clones are shown in orange. Rare publics (shared between 2 or more than 2 individuals up to 50%) and are shown in light blue. Common publics (shared between more than 50% and up to 90% birds) are shown in dark blue. Ubiquitous publics (found in 90% or more

of the birds which were incorporated in the analysis) are shown in purple. Dots represent individual bird observations of private and distinct public clonal compartments. Error bars represent 95% bootstrap confidence intervals for the point estimates generated from 1000 simulations of the model. Statistically significant differences between the model estimates are depicted above the plots based on their corresponding p-values: * = $p < 0.05$; ** = $p < 0.01$; *** = $p < 0.001$.

The patterns of publicness remained very similar at the amino acid level (**Figure A.10**), with the notable increase in all of the public compartments. Other differences to the naïve birds also became apparent for the single vaccination and infected group, which now exhibited significantly lower proportions of private clones in the bursa, and higher proportions of rare public clones in the bursa and in the spleen.

IV.3.5. IgM public repertoires restricted to immunisation regimes

Only 3 IgM clones which are present and expanded across multiple individuals were found restricted to the infected birds, and unexpanded or absent in the uninfected groups (**Figure 4.7**). Of these, one clone (CDR3: CAKSTAGTCWYDDAGSID) is present only in birds from the vaccination and infection treatments. This clone is expanded in the spleen and tracheas of two single vaccinated and infected birds. Additionally, one of the single vaccination and infection birds also shows an expansion in the bursa, whereas the clone was not detected in the other bird. At the same time, this clone is also identified in the bursa of a bird from the double vaccinated and infected group, but it is not expanded.

The remaining two public IgM clones restricted to the infected groups were identified in both infection-only birds and single vaccinated and infected individuals, although expansions were present only in the former. One clone (CDR3: CAKESDGAGSID) was present in almost all the analysed tissues of the individuals belonging to the infection-only group, and in one splenic sample of a single vaccinated bird. The expansions of this IgM clone were identified in the trachea of one bird, and bursa of another. Interestingly, the clone was not identified in the trachea of the bird that exhibited an expansion in the bursa. The other clone (CDR3: CAKNADAGGCCDDID) was found in both the infection only

and single vaccination and infection groups but only showed expansions in 3 tracheal samples of the infection-only birds.

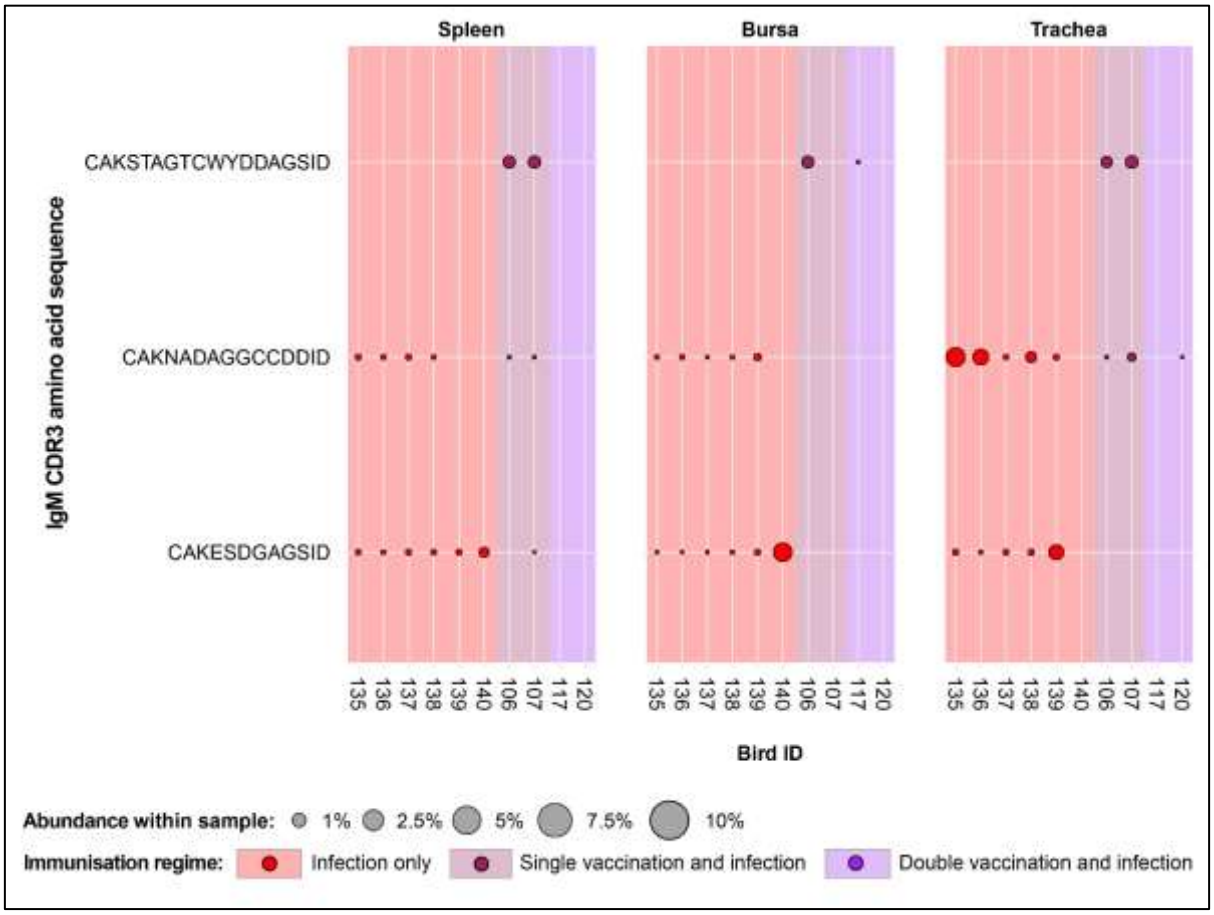

Figure 4. 7: *IgM Clonal expansions in the restricted repertoire of infected birds.*
Circles indicate the presence of clones with a specific CDR3 amino acid sequence and are proportional to the abundance within each bird's tissue clonal compartment. The plot shows only the clones which are expanded in the infected treatment groups (at or above 0.5% and at less than 0.5% in any of the uninfected). Background and circle colours indicate the immunisation regime identity: red – infection only; dark red – single vaccination and infection; purple – double vaccination and infection.

Expansion patterns were found when observing IgM clones in the uninfected treatment groups (**Figure 4.8**). Expansions were only observed in the vaccinated groups and not in the naïve birds. Of these, three clones were found expanded in the single vaccination

treatment, and one clone in the double vaccination treatment. In the former group, all 3 clones are present in all analysed tissues of 3 birds, although their patterns of expansion differ. One clone (CDR3: CAKGSGCCGSRGRTAGTID) was found at comparable proportions (~1%) in the tissues of the 3 birds. Another clone (CDR3: CAKSSYECAYDCWGYAGSID) also displayed expansions across all tissues of the three single vaccinated chickens, particularly in the spleen of one bird, where it reached close to 10% of the repertoire. The remaining one (CDR3: CAKSSYECAYDCWGYAGSID) was only expanded in the spleen and trachea of one single vaccinated bird, but still present in the bursa and in all the tissues of the remaining two birds. The clone that was expanded in the double vaccinated birds (CDR3: CAKESSSAVSID) was present in the five individuals of the group in all tissues, except for one bursal sample. The identified expansions were in the tracheas of two birds, reaching ~0.5% and ~2% of the repertoire, respectively.

When considering the public IgM expansions restricted to the vaccination groups (including under infection settings), only one clone (CDR3: CAKESSYADSID) is expanded in both infected and uninfected vaccinated groups (**Figure 4.9**). In the double vaccinated treatment group, this IgM clone was expanded in all splenic and tracheal samples. Furthermore, this clone was present in all bursal tissues of the double vaccinated birds, but only expanded in one. This clone was also identified in the bursa and trachea of one single vaccinated bird, although it was unexpanded. However, in the double vaccination and infection group, the clone is present at unexpanded levels in the spleen, and in 3 bursal samples. In the trachea, all birds of the double vaccinated and infected possess this clone, with one expansion being present.

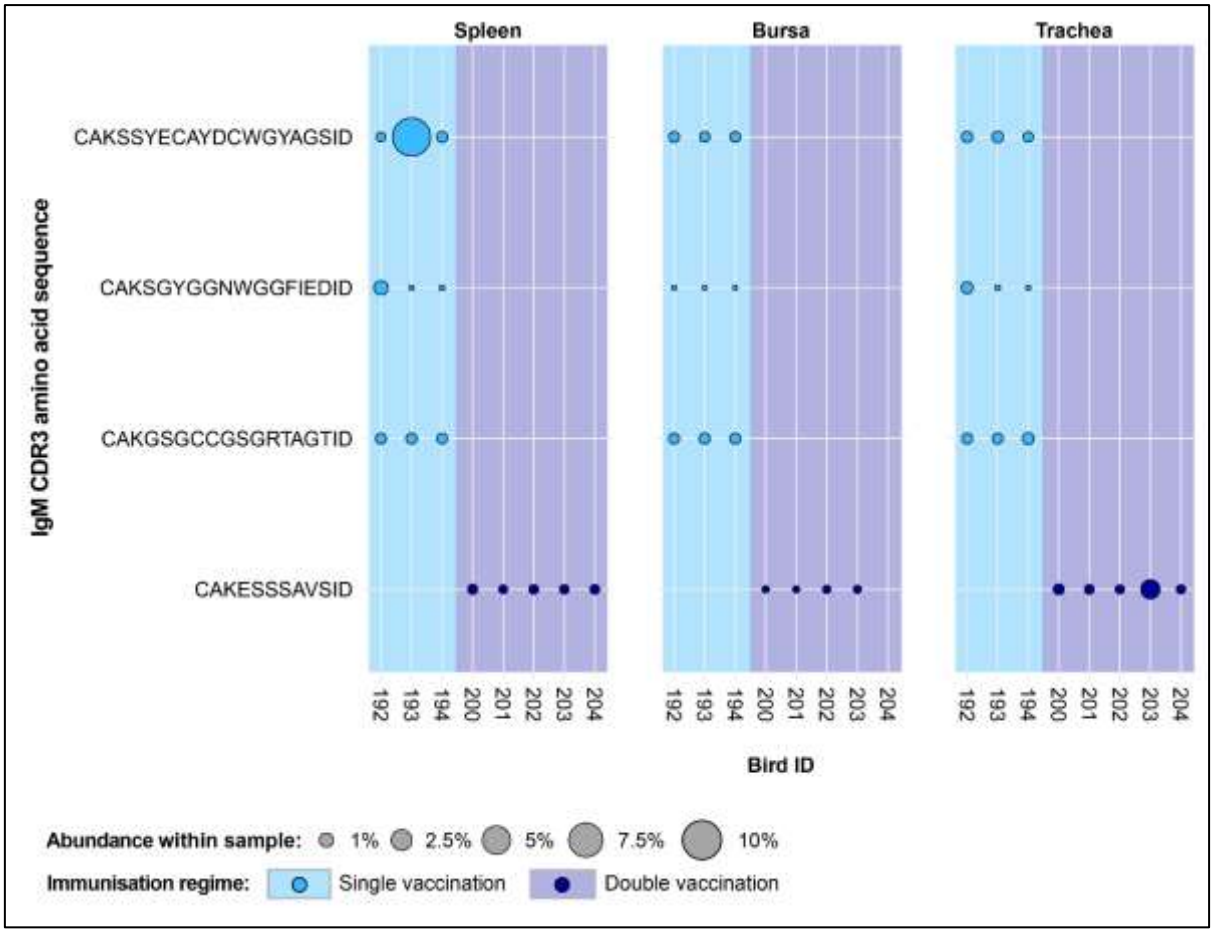

Figure 4. 8: *IgM Clonal expansions in the restricted repertoire of uninfected birds.*

Circles indicate the presence of clones with a specific CDR3 amino acid sequence and are proportional to the abundance within each bird's tissue clonal compartment. The plot shows only the clones which are expanded in the uninfected treatment groups (at or above 0.5% and at less than 0.5% in any of the infected). Background and circle colours indicate the immunisation regime identity: light blue – single vaccination; dark blue – double vaccination.

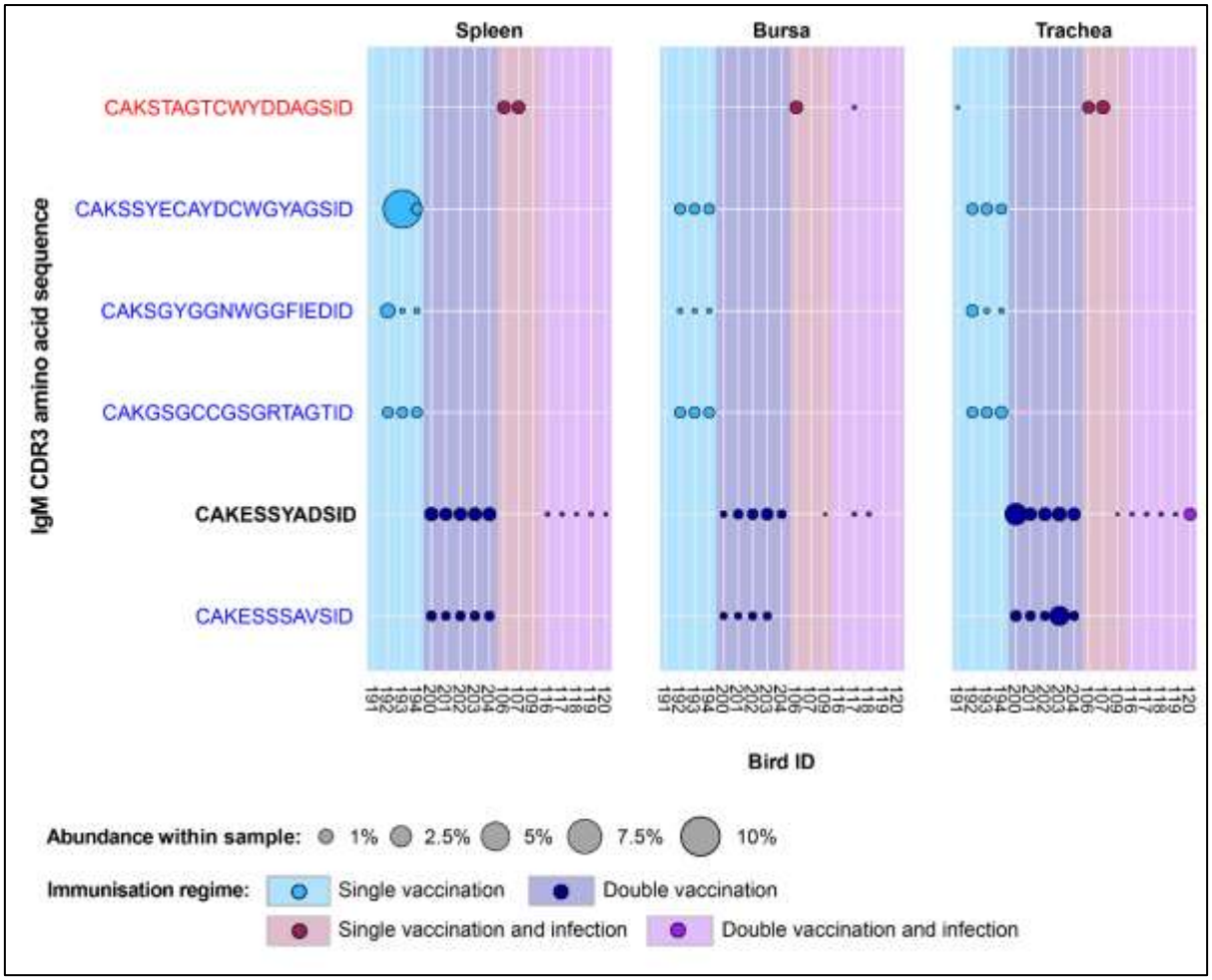

Figure 4. 9: *IgM Clonal expansions in the restricted repertoire of vaccinated birds.*

Circles indicate the presence of clones with a specific CDR3 amino acid sequence and are proportional to the abundance within each bird's tissue clonal compartment. Overlapping circles display different clones based on nucleotide sequence which share the same CDR3 amino acid sequence. The plot shows only the clones which are expanded in the vaccinated treatment groups (at or above 0.5% and at less than 0.5% in any of the naïve or infection only groups). CDR3 amino acid sequences which coincide with clones restricted to infected and uninfected birds are shown in red and blue, respectively. Background and circle colours indicate the immunisation regime identity: light blue – single vaccination; dark blue – double vaccination, dark red – single vaccination and infection; purple – double vaccination and infection.

IV.4. IgY repertoire analysis results

IV.4.1. Recovered sequences and productively rearranged IgY chains

A total of 2,165,701 IgY reads were recovered after sequencing, of which 2,081,899 (~96.1%) were productively rearranged (**Figure 4.10**). A high heterogeneity in terms of read numbers was observed both across and within tissue types. Four samples were excluded from the proportion-based analyses as they had ≤500 productively rearranged reads. This was done to minimise the influence of potentially dominant clones on the repertoire composition of the samples in question. Of note is that the immunisation regime groups affected by the removal of these samples remained at least at n=4 samples per tissue, which is comparable to the samples of the groups with the lowest number of birds (i.e. the single vaccination and single vaccination and infection).

IV.4.2. IgY clonal homeostasis within samples

The patterns of clonal homeostasis illustrated the influence of tissue type and treatment group on the IgY repertoire (**Figure 4.11**). The tracheal samples generally exhibit the highest levels of expansion followed by the spleen and then the bursa, irrespective of the immunisation regime in question. Heterogeneity between samples is pronounced, indicating that the influence of the individual is important. In the bursa and spleen, the clonal homeostasis patterns between the groups are generally comparable to one another. The trachea exhibits the highest levels of IgY clonal expansions, most notably in the uninfected groups.

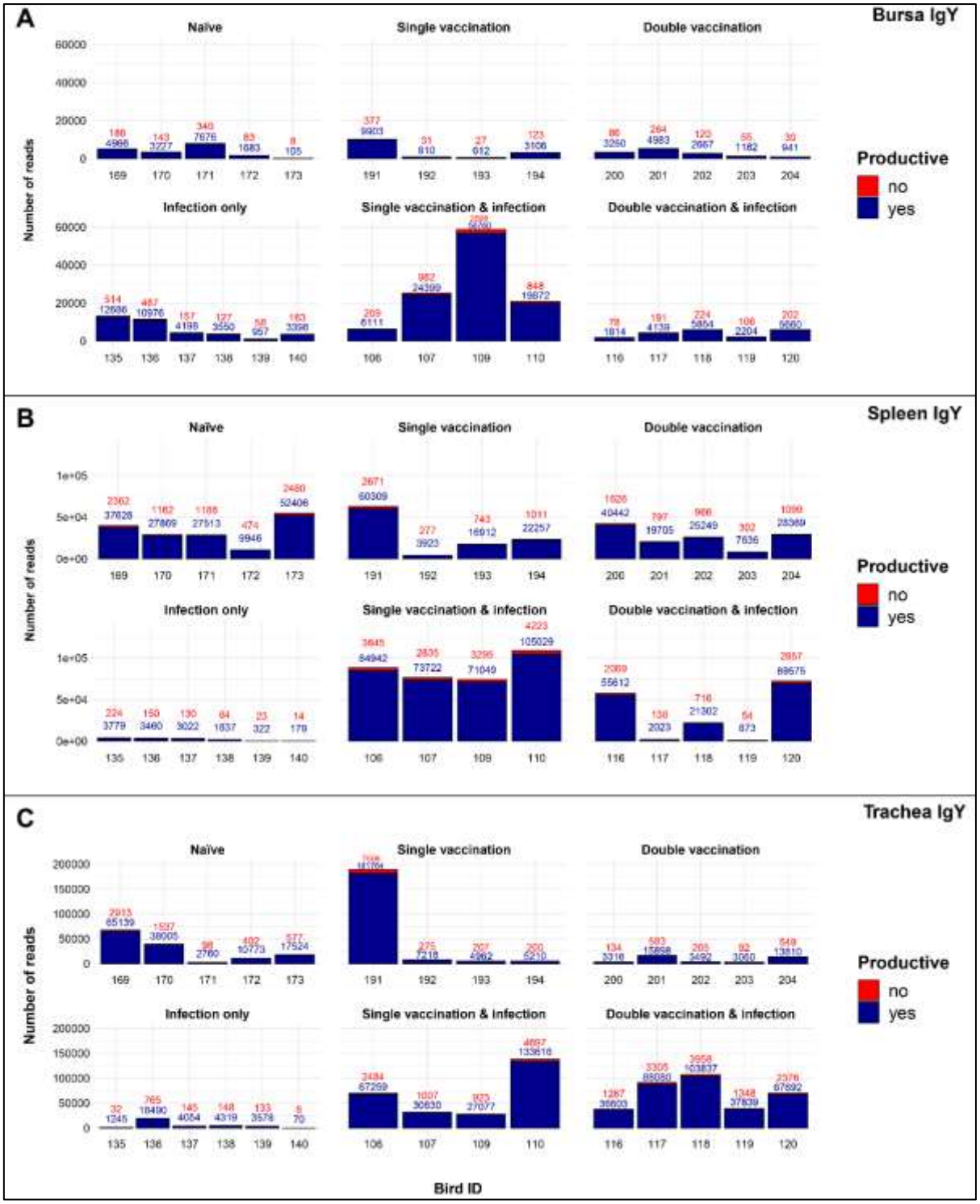

Figure 4. 10: *Total number of IgY sequence reads identified in tissues of chickens that were subjected to different immunisation regimes.*

(**A**) Splenic samples, (**B**) bursal samples, (**C**) tracheal samples. Bird numbers displayed on the x axis and individuals are grouped based on the corresponding immunisation status which is illustrated above each panel. Productive and unproductive reads are shown in blue and red, respectively.

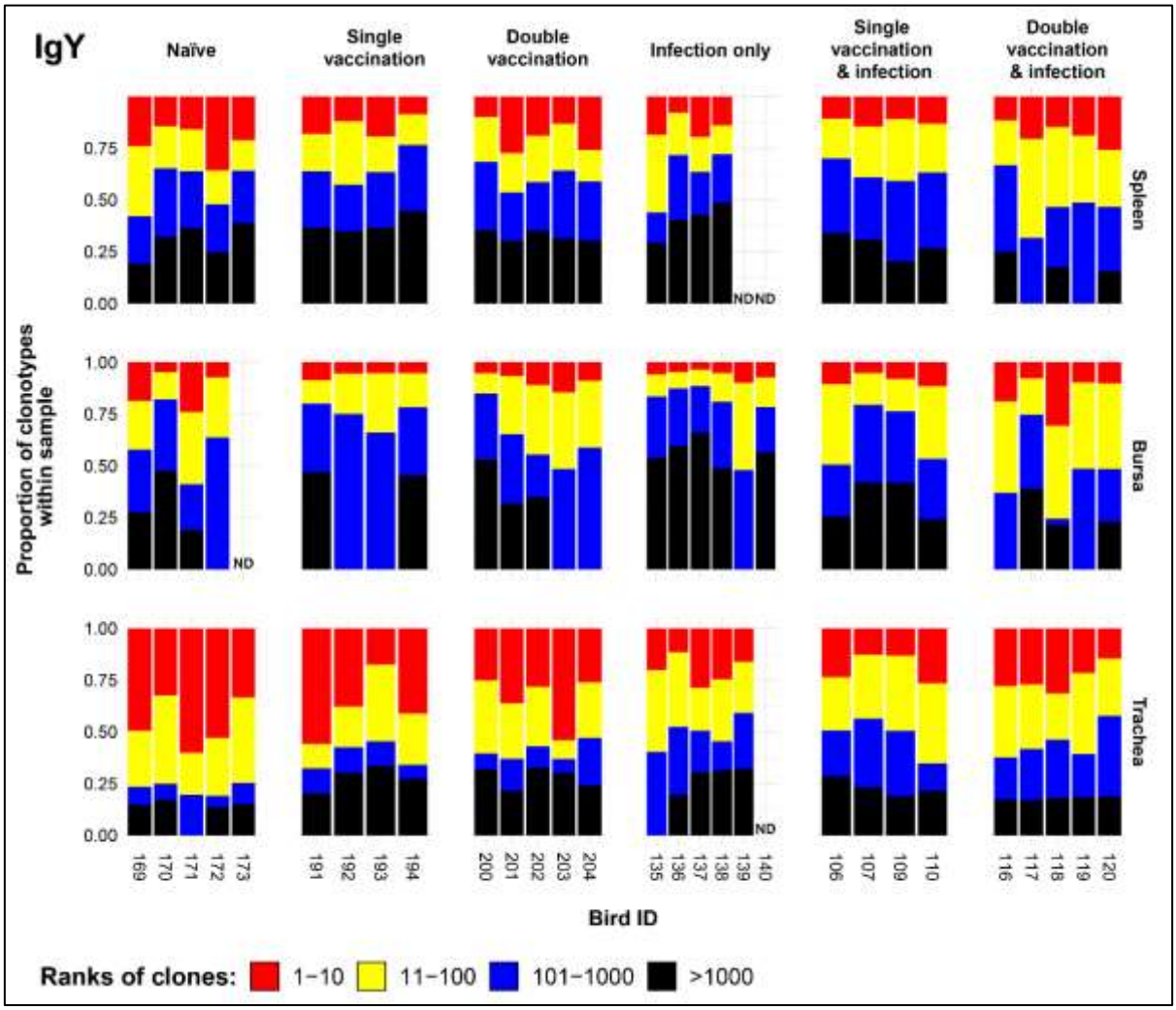

Figure 4. 11: *IgY clonal homeostasis plots of individual tissue samples.*

Bird numbers displayed on the x axis and individuals are grouped based on the corresponding immunisation status which is illustrated above each panel. Clones were ranked based on their abundance into four categories: first 10 most abundant (red), from 11-100 (yellow), 101-1000 (blue), and above 1000 (black) in terms of total abundance within each sample. The proportions of clonotypes are displayed on the y axis. Samples which were removed due to a low read number are displayed as having no data (ND) at the corresponding locations.

IV.4.3. IgY repertoire diversity

The IgY diversity patterns provide interesting features of the clonal landscape in the H9N2 immunisation regimes, consistent with the clonal homeostasis observations (**Figure 4.12**). In the bursa, the groups that received one immunisation, through either vaccination or

infection are significantly more diverse in terms of clonal richness (D_0) than the naïve treatment. These differences are maintained when considering both only the typical clones (D_1) or the dominant clones (D_2). The diversity of the splenic samples is similar between the immunisation regimes and the naïve birds, with no significant difference being present when either clonal richness or typical clones are considered. However, when looking at the dominant clones, the single vaccination and infection group has significantly more diverse repertoires than the naïve group. The single vaccination treatment also seems to be more diverse than the naive, although this difference was not statistically significant. In the trachea, all immunised groups are statistically more diverse in terms of both IgY clonal richness and typical IgY clones than the naïve group. When considering the dominant clones, however, only the infection only and the single vaccination and infection groups have significantly higher levels of diversity than the naïve birds in the trachea.

When considering the diversity at the level of CDR3 amino acids (**Figure A.11**), no significant differences between the groups were observable in the bursa at any of the diversity levels (D0, D1, and D2). In the spleen, similar patterns to the nucleotide clonal diversities were observable in terms of clonal richness and typical clones (i.e. no significant differences), but differences were present at the level of dominant clones. As such, as opposed to the nucleotide clonal diversity, the single vaccination and infection group was not significantly different to the naïve birds, and both of the double vaccinated groups (with and without infection) exhibited significantly higher levels of diversity than the naïve group. Lastly, all the immunised groups showed significantly higher diversities than the naïve birds in terms of clonal richness and typical clones, and only the double vaccinated and infected group exhibited higher clonal diversity when compared to the naïve group.

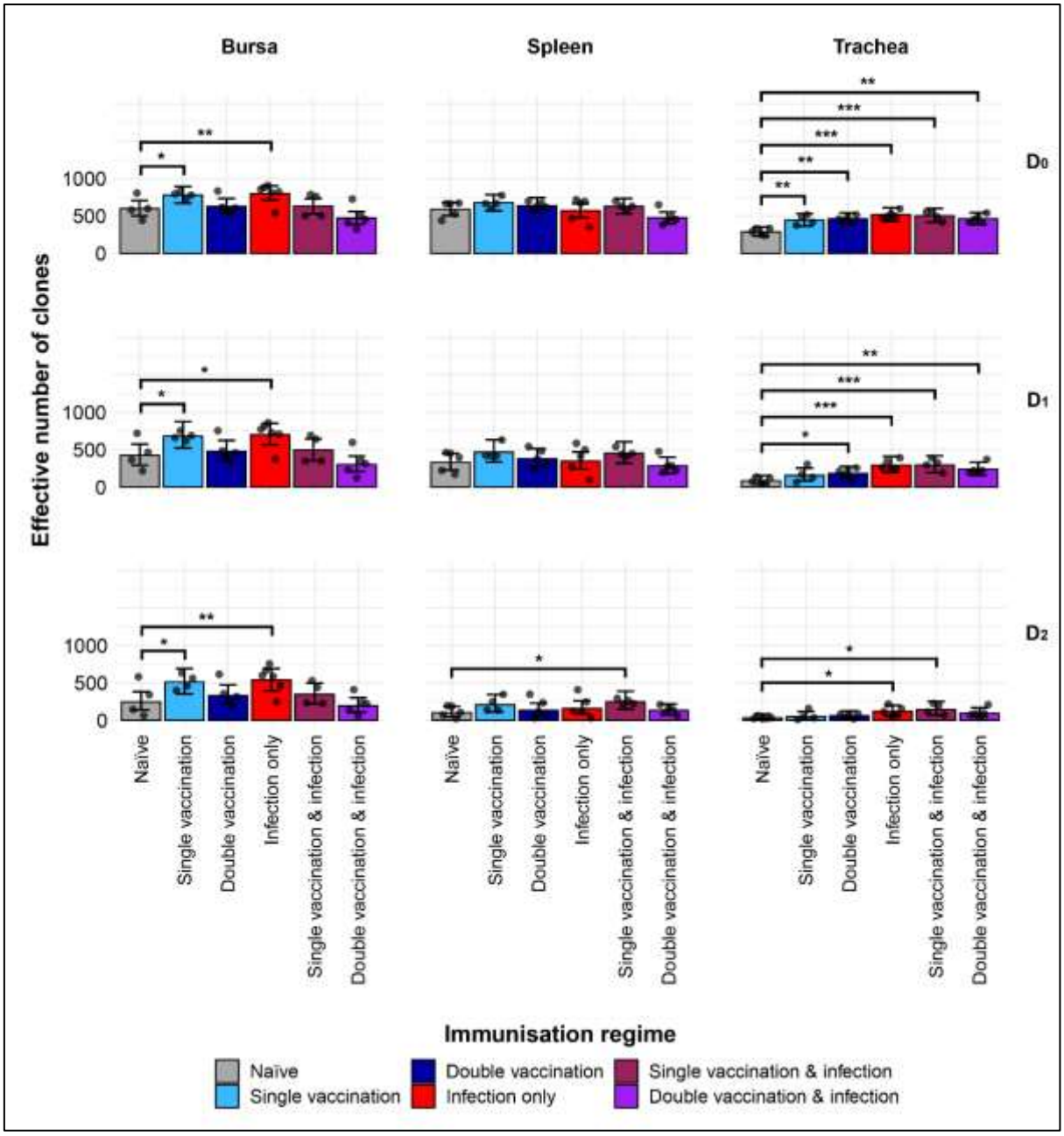

Figure 4. 12: *IgY clonal diversity within samples.*

Different rows show the Hill numbers corresponding to clonal richness (D0), the "typical" clones (D1) and the "dominant" clones (D2) in a theoretical sample of 1000 sequences. Immunisation regimes are colour coded and displayed on the x axes. Dots represent individual bird observations of the effective number of species calculated in each tissue for the corresponding H values. Error bars show the 95% bootstrap confidence intervals for the point estimates generated from 1000 simulations of the model. Statistically significant differences between the model estimates are depicted above the plots based on their corresponding p-values: * = $p < 0.05$; ** = $p < 0.01$; *** = $p < 0.001$.

IV.4.4. Public and private IgY clonal compartments

The IgY repertoires of the H9N2 immunisation regimes exhibited significant differences in terms of their private and public clones (**Figure 4.13**). In the bursa, the naïve, single vaccination, and infection only groups showed significantly higher contributions of private clones than public clones to the repertoire. The opposite pattern was observed for the double vaccination treatment which exhibited significantly higher contributions of public clones as opposed to private clones. The vaccinated and infected groups showed similar contributions in terms of public and private clones to the repertoire. In the spleen, the double vaccinated group and the single vaccination and infected group exhibited significantly higher proportions of public rather than private clones. Lastly, all tracheal samples of the immunisation regimes had significantly higher proportions of public clones as opposed to private, which reached more than 50% of the repertoire on most occasions, with public clones exceeding 80% of the total clones. At the amino acid level, the patterns are similar with slightly higher proportions of public as opposed to private clones (**Figure A.12**).

The private and public clonal compartments of the immunised groups also differed in terms of their relative sizes in the repertoire when compared to the naïve birds (**Figure 4.14**), and these patterns were also generally shared at the level of amino acids (**Figure A.13**). In the bursa, the double vaccination regime and the single vaccination and infection birds had significantly higher proportions of public clones and lower levels of private clones than the naïve group. In the spleen, only the double vaccinated birds exhibited a significant difference to the naïve, having higher levels of public clones and lower levels of private clones. Lastly, the tracheal samples of the singly immunised birds, either through vaccination or infection, exhibited higher proportions of private clones and lower proportions of public clones than the naïve birds.

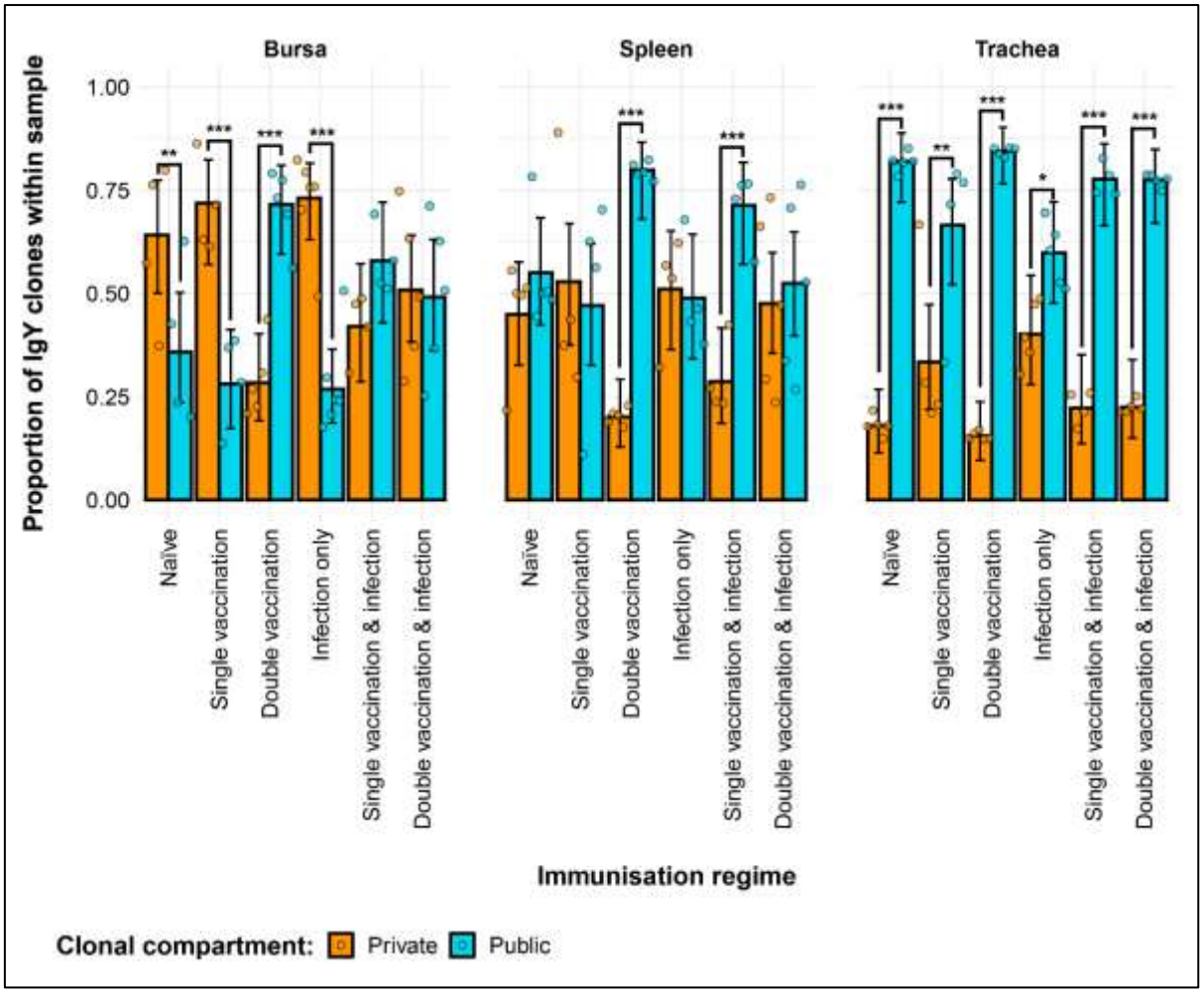

Figure 4. 13: *Differences between the IgY public and private compartments under different H9N2 immunisation regimes based on clone CDR3 nucleotide structure.*

Private (individual-restricted) clones are shown in orange. Public clones (shared between more than two individuals) and are shown in light blue. Dots represent individual bird observations of public and private clonal compartments. Error bars represent 95% bootstrap confidence intervals for the point estimates generated from 1000 simulations of the model. Statistically significant differences between the model estimates are depicted above the plots based on their corresponding p-values: * = $p < 0.05$; ** = $p < 0.01$; *** = $p < 0.001$.

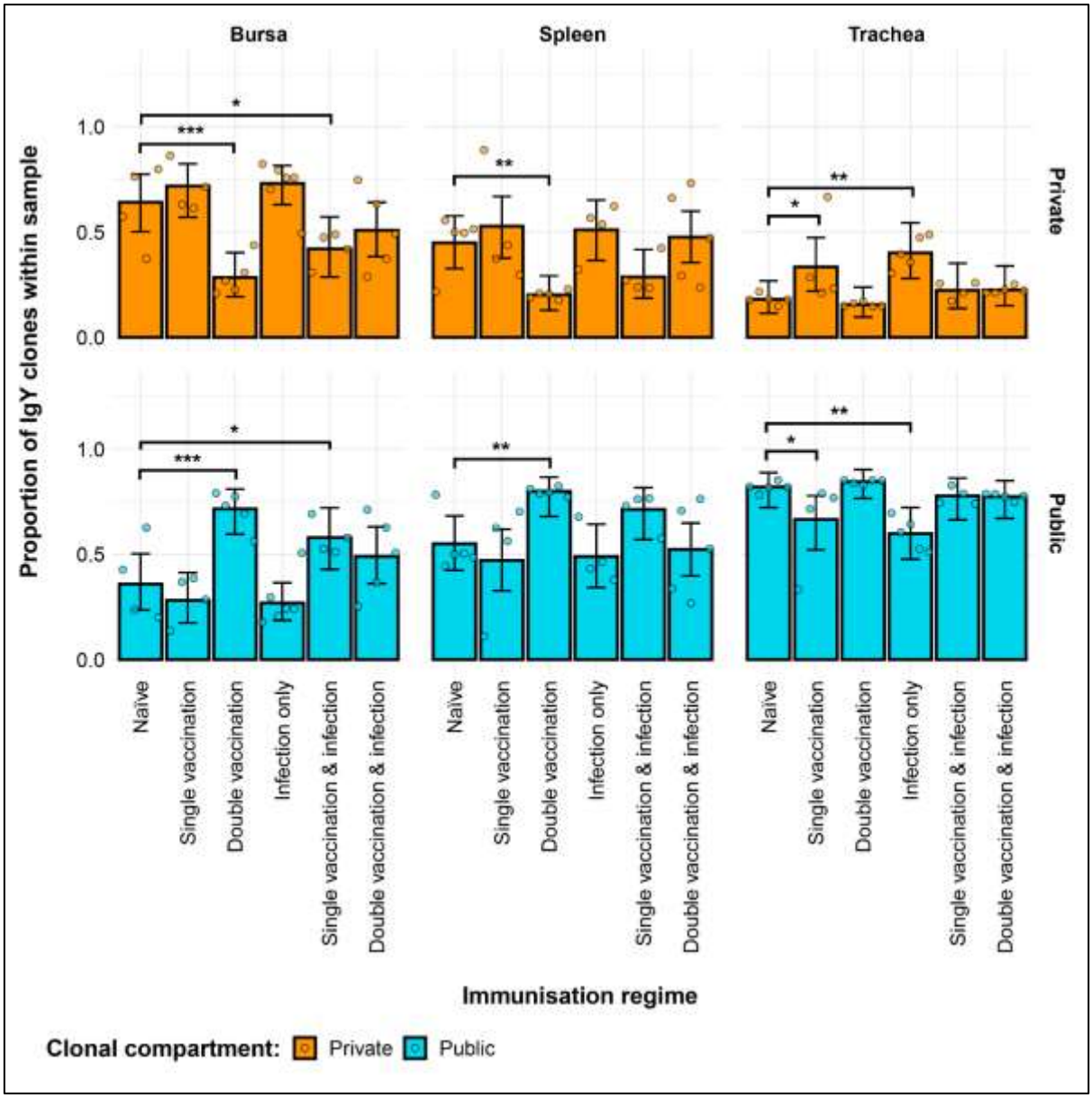

Figure 4. 14: *Differences within the IgY public and private compartments under different H9N2 immunisation regimes based on clone CDR3 nucleotide structure.*

Private (individual-restricted) clones are shown in orange. Public clones (shared between more than two individuals) and are shown in light blue. Dots represent individual bird observations of public and private clonal compartments. Error bars represent 95% bootstrap confidence intervals for the point estimates generated from 1000 simulations of the model. Statistically significant differences between the model estimates are depicted above the plots based on their corresponding p-values: * = $p < 0.05$; ** = $p < 0.01$; *** = $p < 0.001$.

Further partitioning of the public clones into categories based on the degree of clonal sharing between individuals revealed several patterns in terms of tissue and group-specific differences **(Figure 4.15**). The majority of public clones are rare publics (shared between 2 and up to 50% of individuals), irrespective of tissue type or immunisation regime. However, some of the previously observed differences between the groups were masked by using this model. As such, in the bursa and spleen, the single vaccinated treatments were not deemed to be significantly different anymore in terms of private clones to the naïve. The other previously described differences in terms of private clones remained significant, and were also mirrored in the rare public compartment, with the exception of the aforementioned samples of the single vaccination groups.

Other significant differences between the immunised groups and the naïve birds were revealed when considering the common public clones (shared by ≥50% and <90% of birds) and the ubiquitous clones (found in ≥90% of individuals). In the bursa, the double vaccination and infection birds had significantly lower common public clones than the naïve, whilst the other groups do not exhibit any differences. In the trachea, all three infected groups, irrespective of vaccination status showed significantly higher proportions of common publics than the naïve group. No differences between the groups were observed in the spleen. By contrast, when looking at the ubiquitous clones, there were no differences between the groups in either the trachea or the bursa, but one difference was apparent in the spleen. There, the ubiquitous clones of the double vaccination treatment were at statistically higher levels than the naïve group. Taken together, these results reveal interesting effects of both tissue type and H9N2 immunisation regime on the private and public clonal compartments of the birds, especially as the patterns were again very similar when the amino acid clones were considered (**Figure A.14**).

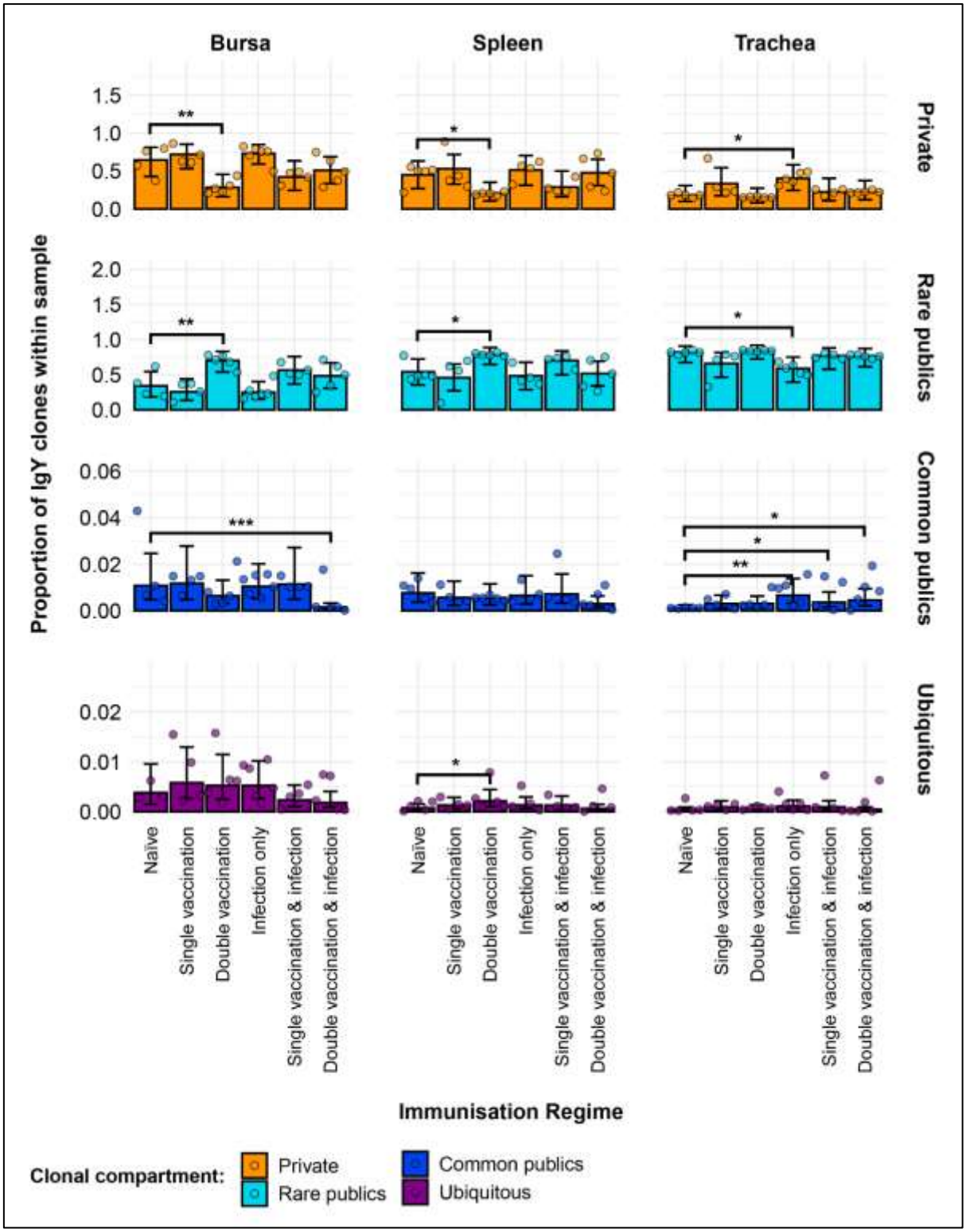

Figure 4. 15: *Model estimates of IgY clone CDR3 nucleotide private and public compartments based on different levels of clonal sharing.*

Private (individual-restricted) clones are shown in orange. Rare publics (shared between 2 or more than 2 individuals up to 50%) and are shown in light blue. Common publics (shared between more than 50% and up to 90% birds) are shown in dark blue. Ubiquitous publics (found in 90% or more

of the birds which were incorporated in the analysis) are shown in purple. Dots represent individual bird observations of private and distinct public clonal compartments. Error bars represent 95% bootstrap confidence intervals for the point estimates generated from 1000 simulations of the model. Statistically significant differences between the model estimates are depicted above the plots based on their corresponding p-values: * = $p < 0.05$; ** = $p < 0.01$; *** = $p < 0.001$.

IV.4.5. IgY public repertoires restricted to immunisation regimes

A total of 28 IgY public CDR3 amino acid clones were expanded in birds belonging to the infected groups and found absent or unexpanded in the uninfected groups (**Figure 4.16**). Of these, one CDR3 amino acid clone (CTKCAYSWCAAGSID) was comprised of two unique clonal lineages with different CDR3 nucleotide sequences. Although only showing expansions in the trachea and bursa of one double vaccinated and infected bird, it was found present at unexpanded levels in all the individuals of the group across multiple tissues and in the bursa of a single vaccination and infection bird. The majority of the other infection-restricted public clones are also only expanded in one individual and generally only in one tissue, in spite of them being shared across multiple birds. Only one clone (CDR3: CAKAAGSID) was found at expanded levels in the tracheas of one infection only individual and one single vaccination and infection individual.

In the uninfected bird groups, 25 IgY public clones were present at expanded levels but absent or unexpanded in the infected groups (**Figure 4.17**). Interestingly, the identified public clones only show one or more expansions within the members of a single group, whilst generally not being detected outside of the particular immunisation regime where it was found. The only exception to this pattern is a clone (CDR3: CAKSAYGGYFGWGTYAGSID) which was found expanded in the spleen and bursa of a single vaccinated bird, whilst also being present at unexpanded levels in a double vaccinated bird. Additionally, clones identified in 6/11 of the double vaccinated group and 3/8 of the single vaccinated group were expanded across multiple individuals and tissues. By contrast, no clone that was identified in the naïve exhibited expansions across multiple individuals.

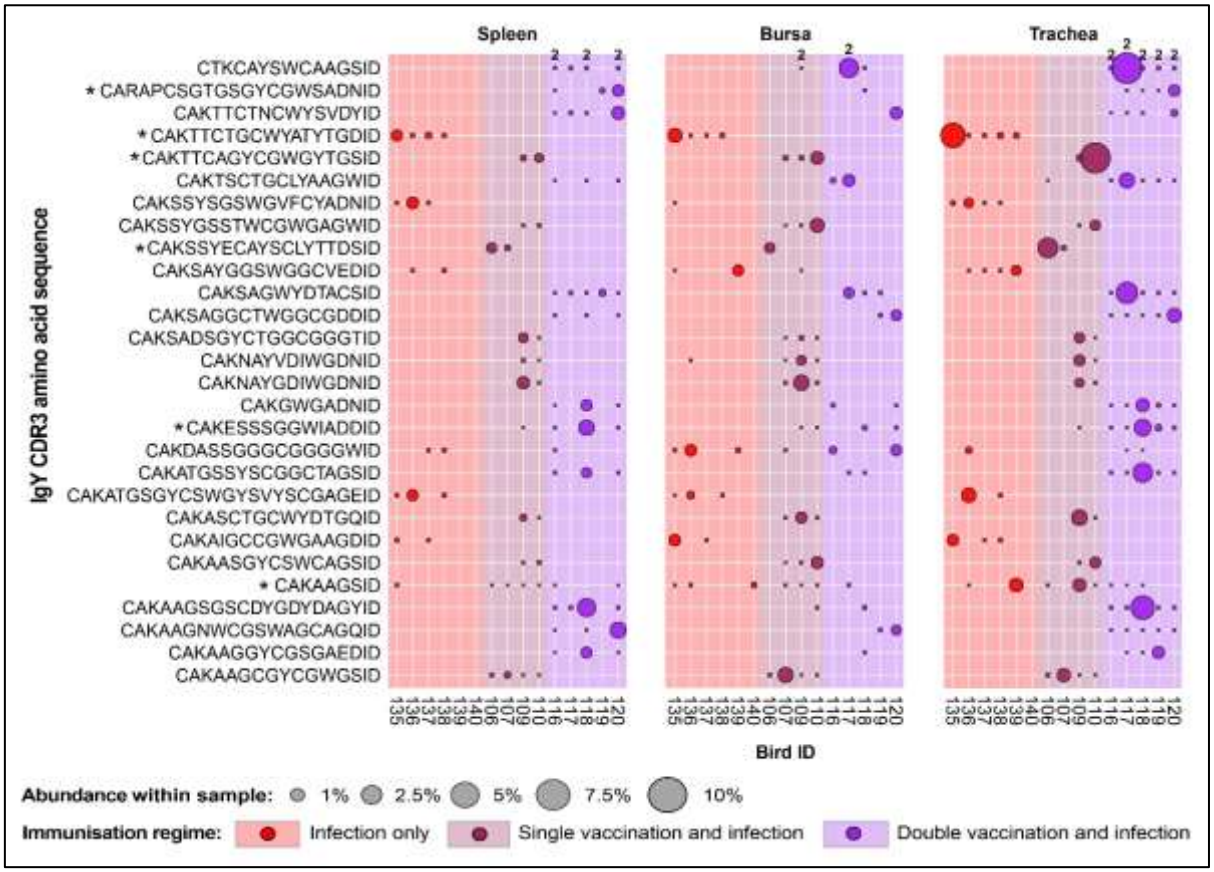

Figure 4. 16: *IgY clonal expansions in the restricted repertoire of infected birds.*

Circles indicate the presence of clones with a specific CDR3 amino acid sequence and are proportional to the abundance within each bird's tissue clonal compartment. Overlapping circles display different clones based on nucleotide sequence which share the same CDR3 amino acid sequence. The plot shows only the clones which are expanded in the infected treatment groups (at or above 0.5% and at less than 0.5% in any of the uninfected). Clones which are expanded in multiple birds are identified with an asterisk next to the CDR3 amino acid sequence. Background and circle colours indicate the immunisation regime identity: red – infection only; dark red – single vaccination and infection; purple – double vaccination and infection.

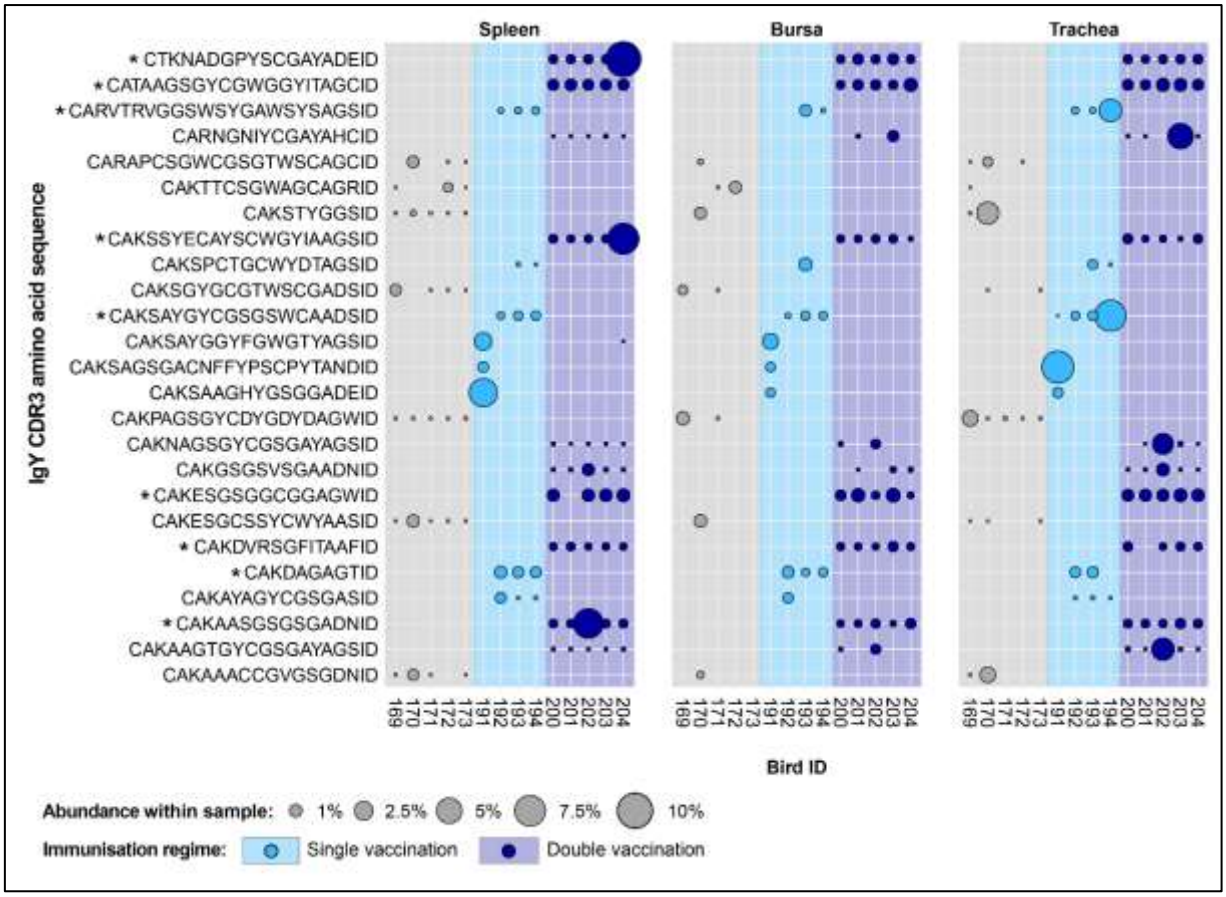

Figure 4. 17: *IgY clonal expansions in the restricted repertoire of uninfected birds.*
Circles indicate the presence of clones with a specific CDR3 amino acid sequence and are proportional to the abundance within each bird's tissue clonal compartment. The plot shows only the clones which are expanded in the uninfected treatment groups (at or above 0.5% and at less than 0.5% in any of the infected). Clones which are expanded in multiple birds are identified with an asterisk next to the CDR3 amino acid sequence. Background and circle colours indicate the immunisation regime identity: light blue – single vaccination; dark blue – double vaccination.

The majority of the 43 public IgY clones which were expanded in any of the vaccinated groups but below the expansion threshold or absent altogether from the unvaccinated groups (**Figure 4.18**), were either found previously as restricted to the infection immunisation regimes (19/43 – shown in red) or the uninfected treatment groups (20/43 – shown in blue). The remaining 4 clones were expanded across both the infected and uninfected groups (shown in black). Only one of these clones (CDR3: CAKSAYGGSWGGFIEDID) was present across birds from all the vaccinated groups and

exhibited expansions in individuals belonging to different immunisation regimes. The other 3 sequences were present either only in the single vaccinated groups (CDR3: CARAPCSTTWSCWYAAGSID) or only in the double vaccinated groups (CDR3s: CAKAARTAGYGVDDID and CAKAALTAGYGVDDID). Interestingly, the clones were present in the double vaccinated immunisation regimes only differ by a single amino acid and were found in all the birds of these groups. These clones were absent from some samples and only expanded in the tissues of a double vaccinated bird and a double vaccinated and infected individual.

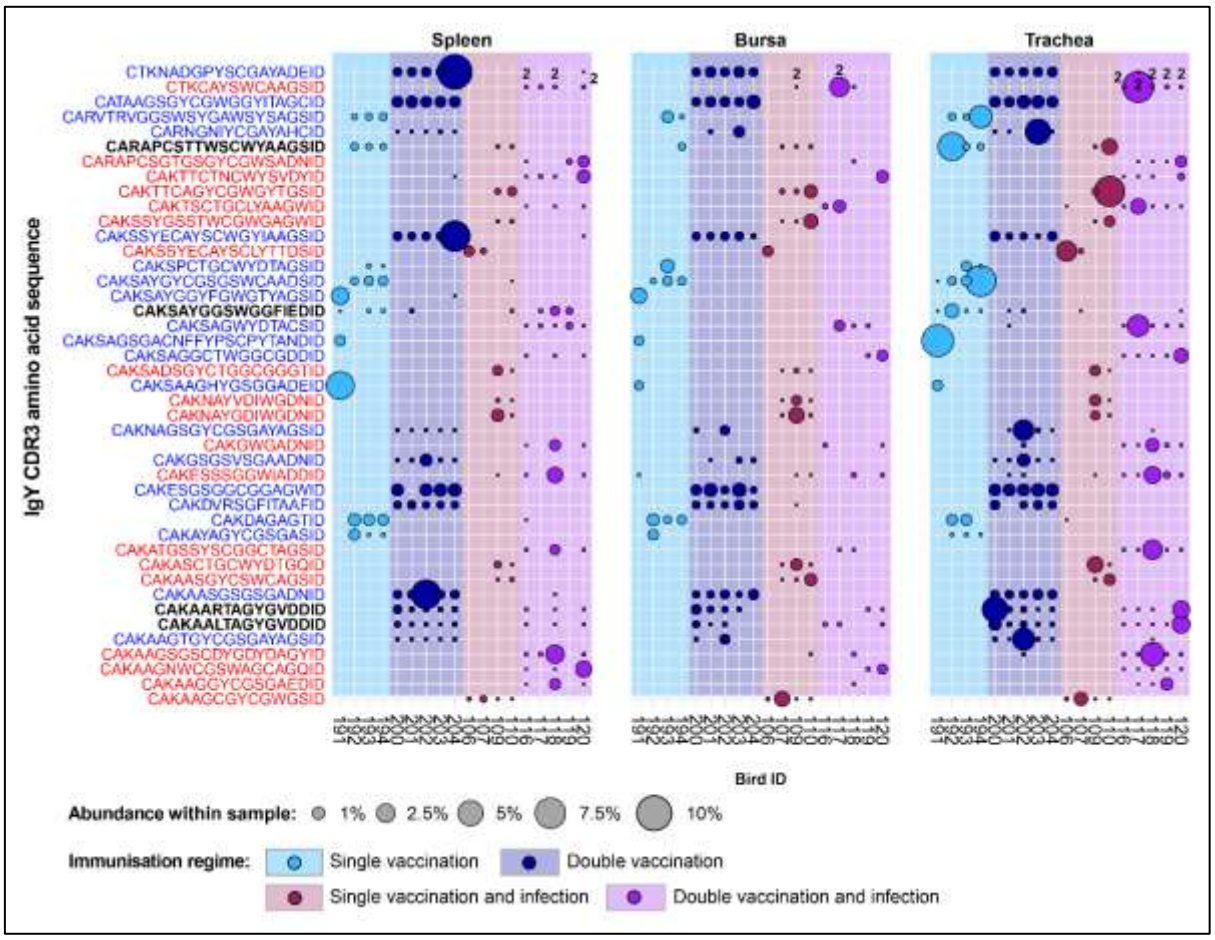

Figure 4. 18: *IgY clonal expansions in the restricted repertoire of vaccinated birds.*

Circles indicate the presence of clones with a specific CDR3 amino acid sequence and are proportional to the abundance within each bird's tissue clonal compartment. Overlapping circles display different clones based on nucleotide sequence which share the same CDR3 amino acid sequence. The plot shows only the clones which are expanded in the vaccinated treatment groups (at or above 0.5% and at less than 0.5% in any of the naïve or infection only groups). CDR3 amino

acid sequences which coincide with clones restricted to infected and uninfected birds are shown in red and blue, respectively. Background and circle colours indicate the immunisation regime identity: light blue – single vaccination; dark blue – double vaccination, dark red – single vaccination and infection; purple – double vaccination and infection.

IV.5. Shared CDR3 sequences between the IgM and IgY repertoires

A comparison between the IgM and IgY revealed that 24,705 unique CDR3 amino acid sequences and 21,950 nucleotide sequences are found in both databases. Out of the identified CDR3s, 15,363 (~62.2%) amino acid sequences and 13,518 (~61.6%) nucleotide sequences were present in both IgM and IgY forms in at least one individual. When looking at the proportion of the repertoire that these shared CDR3 sequences occupied in individual tissue samples, several patterns became apparent (**Figure 4.19**). First, for all the immunisation regimes, the shared CDR3 sequences occupied a significantly larger proportion of the IgY repertoire rather than the IgM repertoire in the bursa and spleen but not in the trachea. In this latter tissue, the shared CDR3 sequences were at comparable levels in the IgM and IgY repertoires, with the exception of the single vaccination group, where the shared CDR3s were at higher proportions in the IgY than in the IgM repertoires. Furthermore, the shared CDR3 sequences in the IgM repertoire were at much higher levels in the trachea than in the spleen and bursa.

When the differences between the groups were considered, the three tissues exhibited distinct patterns in terms of the shared CDR3 sequences in both IgM and IgY repertoires (**Figure 4.20**). In the bursa, the single vaccination, double vaccination, and single vaccination and infection groups exhibited significantly higher proportions of shared IgM sequences than the naïve birds. In the spleen, the shared IgM sequences were at significantly higher proportions in the single vaccination and double vaccination groups, but not in the single vaccination and infection group, which although exhibited slightly higher proportions, they were not deemed statistically significant. No significant differences in the proportions of shared CDR3 sequences within the IgM repertoire were observed between any of the immunised groups and the naïve treatment in the trachea. These

differences are not mirrored by the IgY repertoire, as the naïve group generally exhibits higher proportions of shared CDR3 sequences when compared to the other groups. In the bursa, the proportion of shared CDR3 sequences is significantly lower than in the naïve birds in the double vaccination, infection only, and double vaccination and infection groups. In the spleen, only the infection only and the double vaccination and infection have significantly lower proportions of shared CDR3 sequences of the total IgY repertoire than the naïve group. Lastly, in the trachea, only the double vaccination group exhibits significantly lower proportions than the naïve, when considering the IgY repertoire.

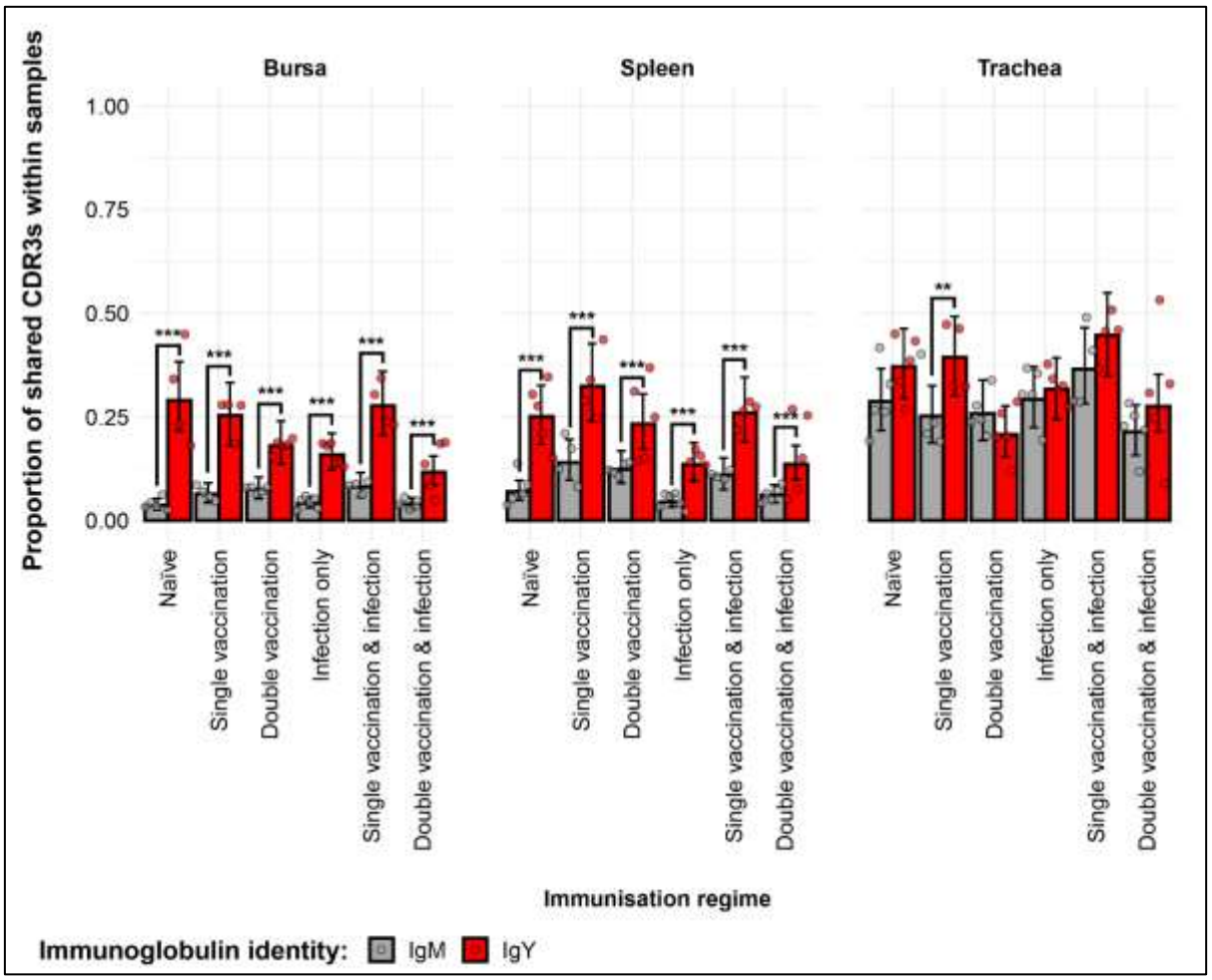

Figure 4. 19: *Differences between the proportions of the repertoire occupied by shared IgM and IgY CDR3 sequences under different H9N2 immunisation regimes.*

IgM and IgY clones are shown in grey and red, respectively. Dots represent individual bird observations. Error bars represent 95% bootstrap confidence intervals for the point estimates generated from 1000 simulations of the model. Statistically significant differences between the

model estimates are depicted above the plots based on their corresponding p-values: * = p < 0.05; ** = p < 0.01; *** = p < 0.001.

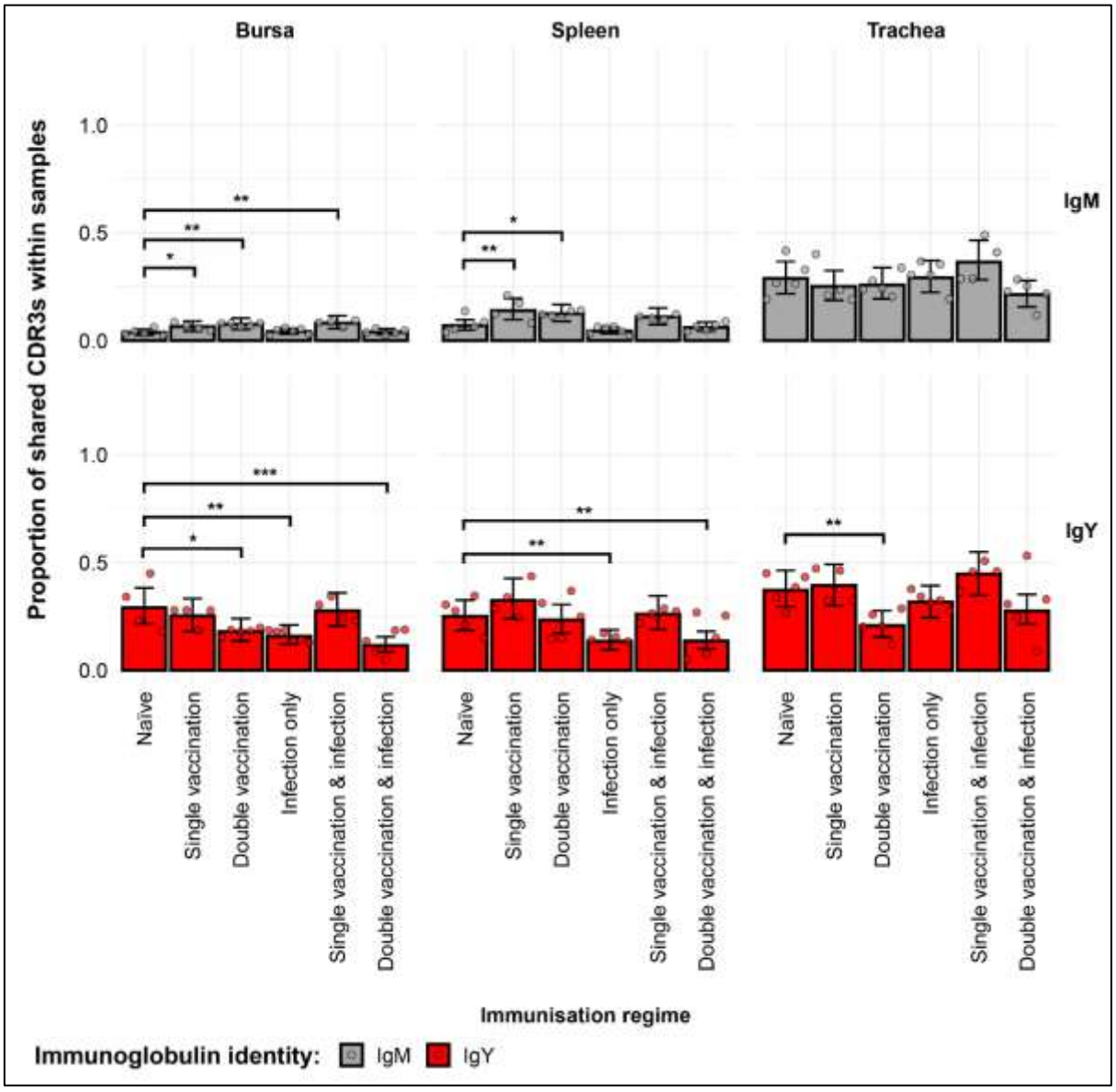

Figure 4. 20: *Group differences in the proportions of the repertoire occupied by IgM or IgY CDR3 sequences under different H9N2 immunisation regimes.*

IgM and IgY clones are shown in grey and red, respectively. Dots represent individual bird observations. Error bars represent 95% bootstrap confidence intervals for the point estimates generated from 1000 simulations of the model. Statistically significant differences between the model estimates are depicted above the plots based on their corresponding p-values: * = p < 0.05; ** = p < 0.01; *** = p < 0.001.

IV.6. Discussion

The antibody responses to avian influenza are an important mechanism for viral clearance. However, the influences of viral infection on the humoral immune system of birds are poorly understood, and the changes on the immune repertoire of H9N2-immunised chickens have not been previously explored. As the features of the avian immunoglobulin repertoire underpin the antigen specificity of the humoral response, information about the changes caused by antigenic exposure is key to both the understanding of the systemic antibody responses to infection and the protection offered by vaccination.

The patterns of expansion revealed by the clonal homeostasis plots reveal marked differences in the IgY and IgM repertoires of the birds which are dependent both on immunisation regime and tissue type considered. Overall, the IgY repertoire exhibited higher clonal dominance than the IgM in the spleen and bursa, a pattern which is consistent with the antigen-specific expansion and class-switching, characteristic of IgY. Interestingly, the IgM repertoire in the trachea across all groups also exhibited higher dominance than in the bursa or spleen, showing levels that were slightly lower yet comparable to IgY. Moreover, the infected groups exhibited lower levels of IgY dominance in the trachea, which may indicate multiple clonal expansions in response to H9N2 infection in the upper respiratory tract. This pattern, although not as pronounced, could also be observed in the IgM repertoires of the infected groups. Together, these differences suggest the resident IgM+ and IgY+ B cells are not as diverse in the trachea, but as class switching, expansion, and recruitment to the site of infection occur, the diversity of the IgY repertoire decreases with antigen-specific cells responding to infection. These observations are also supported by the diversity analyses, which revealed that at the level of dominant clones, the infected groups exhibited significantly higher levels of diversity in both IgM (double vaccination and infection) and IgY (infection only and single vaccination and infection). A possible explanation for the heterogeneity between the infection groups in terms of dominant clone diversity in the IgM and IgY repertoires is that the double vaccinations followed by infectious challenge in the specific group have led to an activation of antigen-specific IgM+ B cells (including memory cells) with lower antigen-dependent proliferation ability, the

effect thus not being mirrored in the class-switched IgY+ cells present in the trachea, where the high-affinity clones dominate the repertoire.

The observable differences in diversity in the bursa and spleen may be attributable to the number and nature of the immunisations to which the groups were subjected to. In the bursa, no differences in diversity between the groups were present in the IgM repertoires. However, the IgY repertoires of the single vaccinated and the infection only groups exhibited significantly higher diversity levels than the naïve birds in clonal richness (D_0), typical clones (D_1), and dominant clones (D_2). As the bursa is an organ not traditionally associated with germinal centre development and class-switching to IgY, this pattern constitutes an interesting topic for future investigations. In the spleen, the observable differences between the groups in both IgM and IgY diversities were only deemed statistically significant at the dominant clone (D_2) level. As such, the groups that received two or more immunisations, exhibited higher dominant clone diversity in either the IgY (double vaccination and double vaccination and infection) or IgM (single vaccination and infection) repertoires. Only the double vaccinated groups, irrespective of infection, exhibited higher dominant clone diversities in their IgM repertoires, whereas the single vaccination and infection group showed higher levels of IgY diversity. Lastly, all immunised groups exhibited higher diversity levels for IgM and IgY in the trachea when compared to the naïve, in terms of both clonal richness and typical clones. When tracheal dominant clones (D_2) were considered, only the infected groups showed higher levels of diversity in IgM (double vaccinated and infected) or IgY (infection only and single vaccinated and infected). It is therefore plausible that the nature of the immunisation(s) plays an important effect on the diversity of the repertoire, and further inquiries into the mechanisms which underpin these differences may provide important information about the humoral immune responses to avian influenza vaccination and infection.

A high degree of clonal sharing between individuals was observed in both IgM and IgY repertoires, with the latter generally exhibiting higher proportions of public clones. The IgM and IgY public clones occupied significantly higher proportions of the repertoire than the private clones in the trachea, irrespective of immunisation regime. By contrast, the other tissues did not display such consistent differences between the public and private repertoires, with the exception of the IgM repertoires in the bursal samples, where all the

groups, with the exception of the double vaccination and infection, had significantly higher proportions of private clones. No clear rule that can be attributable to the immunisation regimes seems to govern the public vs. private clonal composition in the tissues of birds, and it is likely that both the nature and the number of immunisations contribute to the observed patterns differences. The differences between the immunised treatment groups and the naïve birds further support that both nature and number of immunisations dictate the observable patterns in the relative proportions of public and private clones contributing to the total IgM and IgY repertoires. Regardless, the very high contribution of public clones to the IgM and IgY repertoires is an important finding, which may have profound implications for our understanding of the avian immune system.

The degree of clonal sharing among individuals revealed that the majority of the public compartment is comprised of rare publics, which were shared between two and up to 50% of the birds included in this analysis. Indeed, most of the previously identified differences in terms of (total) public clones were mirrored by the rare publics. Although the clonal compartments with higher degrees of clonal sharing, the common and the ubiquitous publics, occupied a much smaller proportion of the IgM and IgY repertoires, their proportional contribution indicates that a baseline of clonal sharing is present across individual birds. Furthermore, it is very likely that a higher sequencing depth would have resulted in clones which were deemed private by the current analysis to be found at low levels in multiple individuals and would thus be public. Together, the findings about clonal sharing have important implications, as they indicate that the diversity of immunoglobulin CDR3 specificities may be much more limited between multiple individuals than previously believed. This, in turn, might imply a constrain on an individual bird's ability to respond to antigenic challenge, which has profound consequences in the defence against pathogens and efficient responses to vaccination.

A possible explanation for the high degree of publicness observable in the IgM and IgY repertoires relates to the mechanism of immunoglobulin rearrangement during B cell development. As opposed to mammals that use a RAG-dependent V(D)J rearrangement process, birds rely on the process of gene conversion. Although, in theory, gene conversion can yield comparable or even higher magnitudes of CDR3 diversity, the genetic and physiological processes which underpin it may in fact be constrained or exhibit biases

towards specific gene segments which are used and/or towards specific CDR3 arrangements. This is an interesting hypothesis to explore, and future molecular studies are required for examining the gene conversion during immunoglobulin diversification in avian species.

Profound differences in the clonal expansion profiles restricted to specific treatments were evident between the IgM and IgY repertoires. Considerably fewer treatment-restricted expansions were present in the IgM repertoires as opposed to the IgY, a result which supports that antigen-stimulated IgM+ B cells undergo expansion and class-switch to IgY. Interestingly, for both IgM and IgY uninfected-restricted or infected-restricted expansions, the identified clones were generally only found in birds belonging to the same immunisation group, with very few exceptions present. One explanation for this pattern is that environmental effects have impacted the bird groups differently and this has influenced their IgM and IgY repertoires. This may be true for the infected groups, as they were moved to isolators just prior to infection on day 21, and environment, although expected to resemble the initial conditions, was different enough to exert this influence on their repertoires. However, the single vaccinated group and the double vaccinated group was housed in the same isolator, unlike the infection only group which was housed in a separate isolator. Similarly, all three of the uninfected groups were housed together throughout the experiment, including after the infection groups were moved to the isolators. Therefore, environmental differences alone could not account for the observed differences as groups that were housed together still exhibit expansions of the same clones which are not identified in other groups. Another explanation relates to experimental cross-contamination of the samples, but this again is unlikely as 5' RACE PCRs were performed in 96-well plates that contained samples from multiple groups. Therefore, as environmental factors and cross-contamination were not able to account for the observed patterns, the interesting possibility remains that the specific combination of immunisation conditions through infection and/or vaccination(s) may lead to convergent expansions within individuals of the same group.

The few IgY and IgM clones that were expanded across individuals belonging to multiple groups were restricted to infection, with none being shared across the uninfected groups. When the vaccination-restricted clones were considered, only one IgM clone and four IgY

clones were found expanded in birds from the infected and uninfected groups. These identified CDR3 sequences restricted to the vaccinated groups and expanded in birds belonging to infected and uninfected groups may represent lineages of B cells that respond to H9N2 under both immunisation scenarios. These clones, stimulated through vaccination(s), may thus possess a higher affinity for the virus, and may offer increased protection during infection. Furthermore, if a comparable number of restricted clonal expansions were to be detected in the IgL repertoires, screening for antigen specific (paired) light and heavy chain sequences (e.g. for the production of H9N2-specific monoclonal antibodies) might be narrowed down to a few (IgH and IgL) CDR3 sequences based solely on repertoire data. As this was outside the scope of the current research, such endeavours could substantially increase the throughput in generating antigen-specific antibodies not just for avian influenza viruses, but for other infectious agents as well.

The comparison between the two immunoglobulin sequence databases revealed that proportions of CDR3 nucleotide sequences which were shared between them were significantly higher in the IgY form in the spleen and bursa, but not in the trachea. In this latter tissue, both IgM and IgY had comparable proportions of CDR3 sequences which were shared between them. A higher presence of shared CDR3 sequences would be expected in the IgY, as B cells undergo class-switching upon antigenic stimulation, and all IgY sequences would ultimately be derived from IgM. Although somatic hypermutation is expected to occur, this process is difficult to unravel based on bulk sequence data alone. The comparable presence of shared IgM and IgY CDR3 sequences in the trachea suggests that the B cell composition of this tissue is fundamentally different to the bursa and spleen, a pattern which would indeed be expected given the roles in lymphocyte development and homeostasis which these two organs fulfil, respectively. The differences between the immunised groups and the naïve birds in terms of the CDR3 sequences in the analysed tissues were not generally consistent between the IgM and IgY repertoires and cannot clearly be attributed to either number or nature of immunisations, suggesting that the interplay between these two may dictate the shared CDR3 repertoire between the two classes of immunoglobulins. The relationship between the IgM and IgY repertoires therefore requires further investigation, and network analyses and genetic similarity analyses

which were outside the scope of the current analysis would be required to better understand their profiles, including the phenomena of class-switching and somatic hypermutation.

Together, the analyses of the IgM and IgY repertoires of chickens subjected to different H9N2 immunisation regimes revealed important findings which constitute a solid foundation for future research aimed at increasing our understanding of the avian humoral responses to avian influenza, and the adaptive immune system more broadly. The findings presented herein strongly suggest that not only does the nature of the immunisation (i.e. vaccination or infection) influence the immunoglobulin repertoires of the individuals, but also the number of immunisations received and the particular combination of immunisations to which the birds were subjected to. Unravelling the complexities of the avian immunoglobulin repertoires thus serves as a fruitful area for future research, whilst also having the potential to inform on practices such as vaccination, which remains paramount for efficient infectious control at a global level.

Chapter V: Changes in Chicken TCRβ Repertoires under H9N2 Vaccination and Infection Scenarios

V.1. Abstract

Avian influenza viruses (AIVs) stimulate both the innate and adaptive immune systems of their avian hosts. However, little is known about the influences of AIV antigenic stimulation on the adaptive immune repertoire of birds. As T cell-mediated immunity is recognised as an important mechanism of protection against AIVs, this chapter explores the TCRβ repertoire of chickens following vaccination and/or infection with H9N2 AIV. Major differences were found between immunised groups and naïve birds in terms of repertoire diversity and clonal composition in terms of V and J gene usage in the bursa, spleen, and trachea. Furthermore, a large proportion of public clones, which are shared across multiple individuals, was found to contribute to the repertoires of the analysed birds, in both tissue and immunisation-specific manners. The results presented in this chapter provide important insights into the chicken TCRβ repertoire upon H9N2 infection and/or vaccination, whilst also revealing general information about the biology of the avian adaptive immune receptor repertoire and the changes elicited by antigenic stimuli.

V.2. Introduction

Influenza A viruses are versatile pathogens that can evade host immunity through the phenomena of antigenic drift and antigenic shift [5,6]. Although these viruses can infect a wide variety of species, their natural reservoir is in wild aquatic birds, being widely prevalent in both wild and domestic avian species. These avian influenza viruses (AIVs) are a major cause of concern at a global level, not only because of the major economic costs which they incur to the agricultural sector, but also because of their potential to jump across the species barrier and infect humans [8]. To date, vaccination remains the primary method of

preventing AIV infections and outbreaks, but the current understanding of both AIV infection and vaccination of avian hosts is incomplete [42].

Upon infection, AIVs stimulate both the humoral and cell-mediated components of the avian adaptive immune system, with their interplay being essential for viral clearance [42,55]. The ability of the adaptive immune system to respond specifically to pathogens stems from the unique antigen specificities of T and B cell receptors (TCRs and BCRs) [76,77]. The total of unique TCRs and BCRs constitutes the adaptive immune repertoire which exhibits an enormous theoretical potential of diversity. This is achieved at the genetic level during T and B cell development, when variable (V), joining (D) and, in the case of heavy chains diversity (D) genes are rearranged to form a functional chain of the B and T cell receptors [76,77]. Although birds diversify their BCRs differently than mice and humans through the process of gene conversion, TCR diversification occurs in a similar manner [76]. For instance, the TCRβ genetic organisation includes 16 Vβ genes across 3 families (11 Vβ1, 4 Vβ2, and 1 Vβ3). One Vβ gene somatically rearranges with one of the 4 Jβ genes, and the Dβ and Cβ genes (chickens have single genes for the Dβ and Cβ), to yield the functional TCRβ chain. In addition, modifications at the V-D-J junctions through nucleotide additions and/or deletions further increase the resulting diversity of the TCRβ repertoire. Lastly, the combinatorial pairing of light and heavy chains (α and β for αβ T cells; γ and δ for γδ T cells) supplements the aforementioned processes, thus resulting in very high levels of diversity. Upon antigenic stimulation, T and B lymphocytes are able to recognise a plethora of unique antigens to which they are able to mount efficient immune responses.

Although both T and B cell responses are important during AIV infection, T cell specificities against influenza-derived antigens have been receiving more attention recently, as they are able to generate responses against conserved viral epitopes, thus also being able to offer protection against heterologous strains [90,204]. Furthermore, previous studies have suggested that T cell responses during AIVs are required for efficient protection, as high titres of H9N2-specific antibodies were insufficient block H9N2 from being transmitted [91–93]. Although many questions regarding T cell-mediated immunity against influenza A viruses have been answered in human and non-human mammalian hosts (reviewed in [53]), little of this work has been mirrored in poultry, in spite of their

importance in AIV infections [53,206]. Furthermore, no studies to date have assessed the avian T cell repertoire responses to AIVs. Indeed, while many functions of immunity are conserved across species, the unique features of the avian immune system (minimal essential MHC, absence of lymph nodes in species such as chickens etc.) are likely to play a significant role on the T cell response during infectious challenge and/or vaccination [54,207–209].

The current chapter illustrates the results of the tissue-specific TCRβ repertoire in the spleen, bursa, and trachea of chickens that were culled on day 35, following specific H9N2 immunisation regimes. The laboratory methodology, computational techniques, and design of the animal experiment are described in detail in **Chapter II** of the thesis.

V.3. TCRβ Repertoire analysis results

V.3.1. Recovered sequences and productively rearranged TCRβ chains

The sequencing of the 5'RACE PCRs yielded a total of 2,152,750 chicken TCRβ reads, out of which 1,999,167 (~92.86%) were productively rearranged (i.e. within frame). Although the sequence yield is high, the samples are heterogeneous both within and across tissue type, with the most reads generally being obtained from the spleen samples, and the lowest from the bursa (**Figure 5.1**).

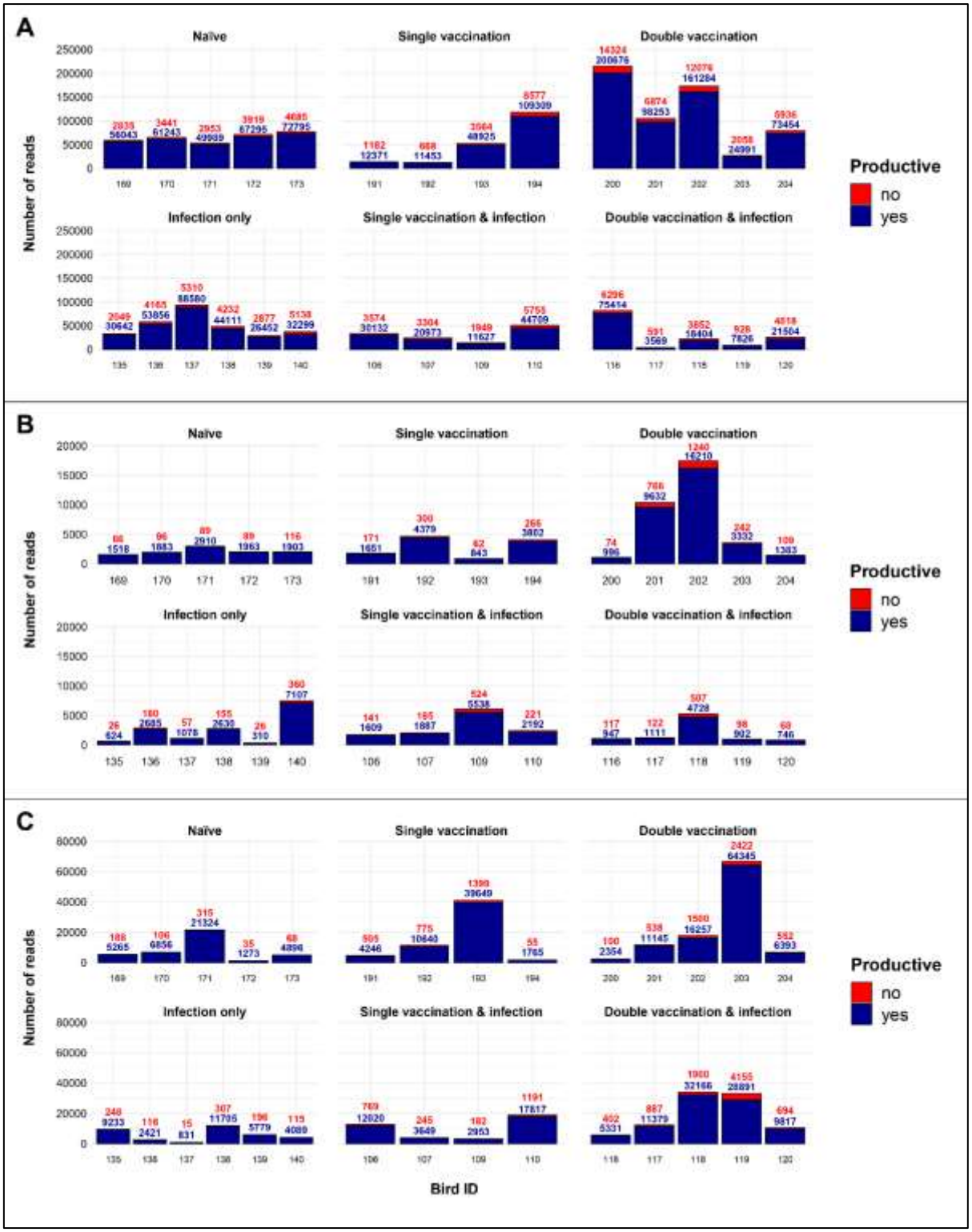

Figure 5. 1: *Total number of TCRβ sequence reads identified in tissues of chickens that were subjected to different immunisation regimes.*

(**A**) Splenic samples, (**B**) bursal samples, (**C**) tracheal samples. Bird numbers displayed on the x axis and individuals are grouped based on the corresponding immunisation status which is illustrated above each panel. Productive and unproductive reads are shown in blue and red, respectively.

V.3.2. TCRβ Clonal homeostasis within samples

The patterns of clonal homeostasis (**Figure 5.2**) revealed that both the tissue and the immunisation group influence the composition of the TCRβ repertoire in the samples. Overall, the splenic samples exhibited the lowest patterns of expansion (greatest clonal diversity as suggested by the lower proportion of total sequences in the largest groups of clones), whilst the tracheal samples showed the highest. Within the spleen and trachea, the immunisation treatment seems to have a greater effect than observed in the bursa. For the bursa, individual heterogeneity made any statements difficult to assert by observation alone, although there was an indication that individual birds from the three infected groups may have larger clonal expansions.

In the spleen, all the infected groups exhibit larger expansions than their uninfected counterparts. Moreover, this effect may have been enhanced by the number of immunisations received, with the *single vaccinated and infected* and *double vaccinated and infected* groups presenting more clonal expansions based on the number of prior vaccinations.

The opposite pattern to the splenic tissues was apparent when considering the tracheal samples. As such, the highest patterns of expansion were present in the naïve birds, followed by the two uninfected and vaccinated groups. Conversely, the infection only treatment birds exhibited the smallest expansions of all the infected groups, whilst the infected and vaccinated groups seemed to have more pronounced patterns of clonal expansion. For both the uninfected treatments and their infected counterparts, the effect of the number of vaccinations was difficult to assess by observation, especially because of the heterogeneity between individuals and the small sample sizes.

Indeed, although useful as an exploratory analysis, more complex methods which employ quantitative statistics were required to correctly assess the patterns of clonal expansion and the effects of tissue type and immunisation regime.

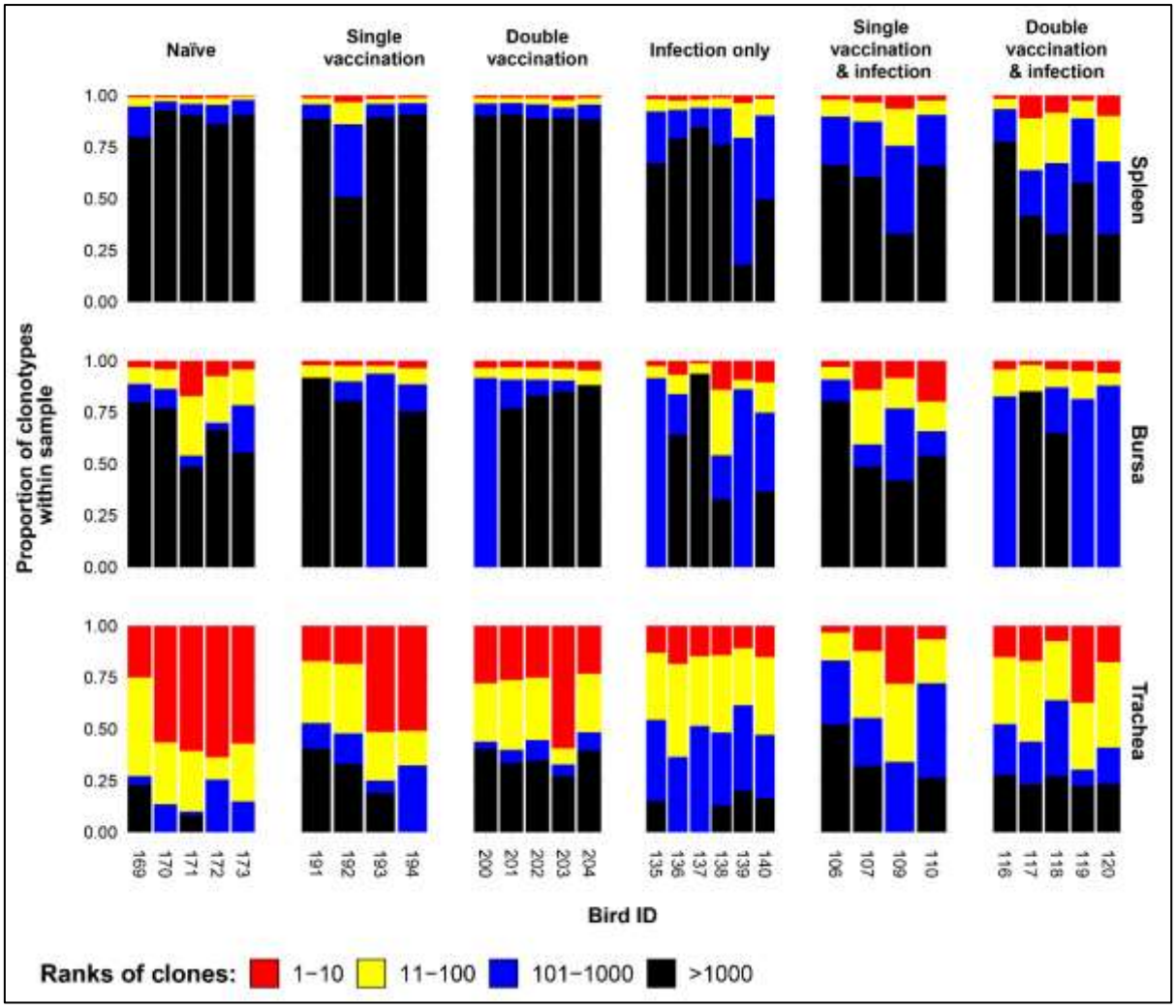

Figure 5. 2: *TCRβ clonal homeostasis plots of individual tissue samples.*

Bird numbers displayed on the x axis and individuals are grouped based on the corresponding immunisation status which is illustrated above each panel. Clones were ranked based on their abundance into four categories: first 10 most abundant (red), from 11-100 (yellow), 101-1000 (blue), and above 1000 (black) in terms of total abundance within each sample. The proportions of clonotypes are displayed on the y axis.

V.3.3. TCRβ repertoire diversity

After computing the sample-specific effective number of clones corresponding to different diversity settings (i.e. clonal richness – D_0, the species richness equivalent; typical clones – D_1, Shannon diversity equivalent; dominant clones – D_2, Gini-Simpson equivalent) where the abundance of each clonotype is weighted differently, the values were used in constructing a linear mixed-effects model (described in **section II.2.1**) using the sample

standardisation value of 1000 sequences. Significant differences were observed in all tissues when evaluating the hill number estimates of the immunised groups and the naïve birds (**Figure 5.3**). Relatedly, all these differences were mirrored at the level of amino acid clones (**Figure A.15**).

In the bursa the diversity estimates were higher in the vaccinated and uninfected groups than in the naïve birds, irrespective of the computed diversity measure. In the spleen, the double vaccinated and infected group exhibited significantly lower diversity than the naïve birds at all measures of diversity. No other significant differences were revealed in the spleen between the other groups and the naïve birds at the clonal richness and typical clone measures. However, at the level of dominant clones, the single vaccinated and infected group also had significantly lower diversity than the naïve birds.

In the spleen, the double vaccinated and infected group exhibits significantly less diversity than the naïve birds in terms of clonal richness, typical clones, and dominant clones. The single vaccinated and infected group is also significantly less diverse than the naïve, but only at the level of dominant clones. No other significant differences to the naïve birds were found in the spleen, although the infected only birds exhibited slightly less diverse repertoires at all the analysed levels of diversity.

In the trachea, all immunised groups exhibited significantly higher levels of diversity than the naïve treatment, and this pattern was consistent both in terms of clonal richness and the typical clones. By contrast, when considering the dominant clones, only the infected immunisation regimes remained significantly higher than the naïve group.

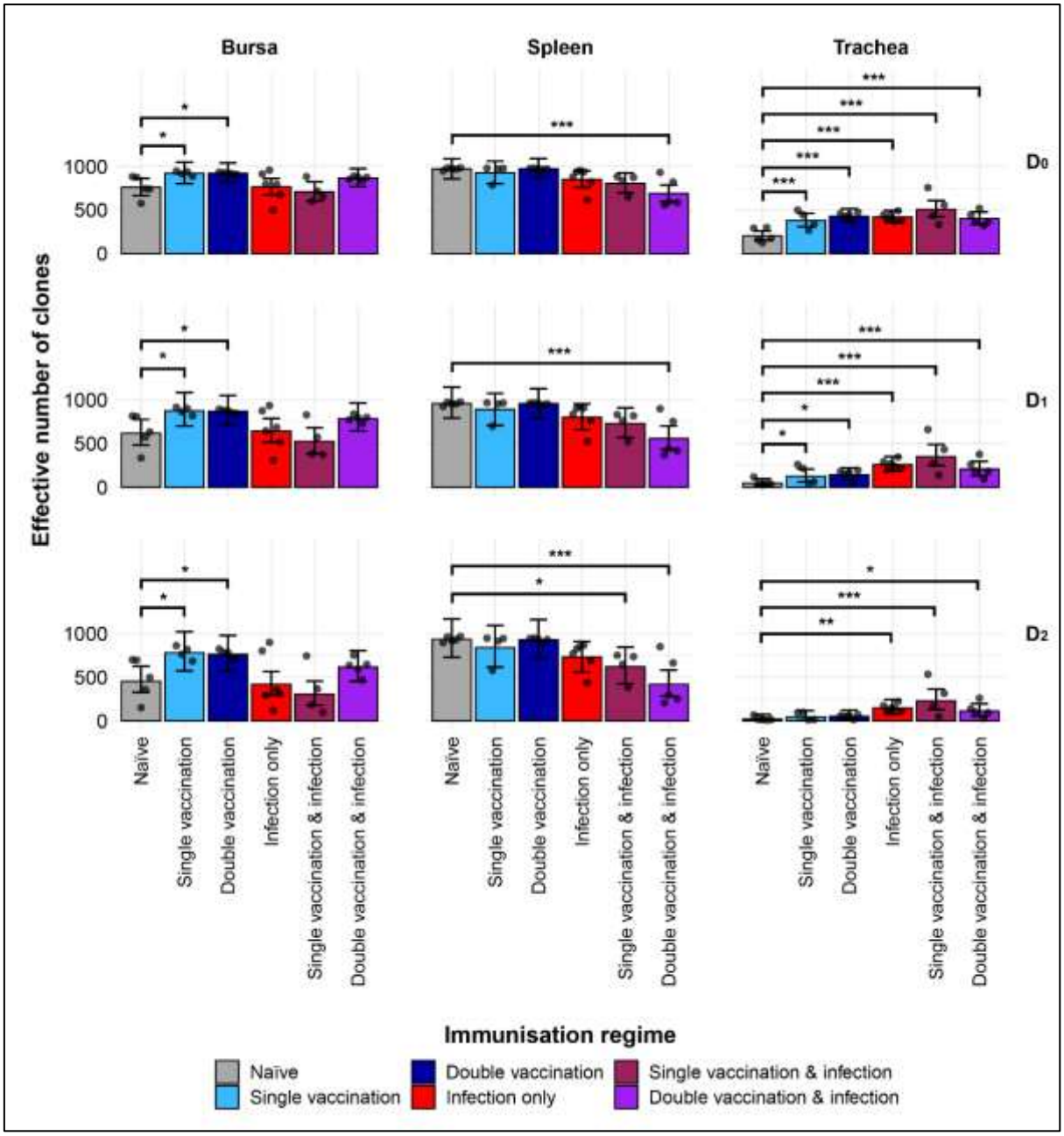

Figure 5. 3: *TCRβ clonal diversity within samples.*

Different rows show the Hill numbers corresponding to clonal richness (D_0), the "typical" clones (D_1) and the "dominant" clones (D_2) in a theoretical sample of 1000 sequences. Immunisation regimes are colour coded and displayed on the x axes. Dots represent individual bird observations of the effective number of species calculated in each tissue for the corresponding H values. Error bars show the 95% bootstrap confidence intervals for the point estimates generated from 1000 simulations of the model. Statistically significant differences between the model estimates are depicted above the plots based on their corresponding p-values: * = $p < 0.05$; ** = $p < 0.01$; *** = $p < 0.001$.

V.3.4. Public and private TCRβ clonal compartments

Overall, the degree of TCRβ clonal sharing between different individuals is high, but this effect is dependent on tissue type and the immunisation regime (**Figure 5.4**), and again, these differences were mirrored at the level of amino acid clones (**Figure A.16**). In general, based on the tissues, the largest public compartments (clones shared between two or more birds included in the analysis) are observable in the tracheal samples and the lowest in the spleen. However, the treatment group has an important influence on the size of the public and private clonal compartments in all tissue types.

In the bursa, the public compartment was significantly higher in the treatment groups that received two or more immunisations, either through vaccination alone or through vaccination and infection. There were no significant differences between the public and private clonal compartments of the naïve, single vaccinated only, or infected only birds.

In the spleen, the private TCRβ clonal compartment was significantly larger in the naïve, single-vaccinated, and infection only treatments. By contrast, the double vaccination and infection group exhibited significantly higher proportions in the public clonal compartment. No significant differences were observed in the double vaccination and the single vaccination and infection groups between the public and private clonal compartments, although the latter seemed to be at slightly higher levels.

In the trachea, all but the infection only immunisation regime exhibited significantly higher levels of clones in the public compartment. In the infection only birds, the levels of clones in the private and public clonal compartments are comparable, as no significant differences were observed.

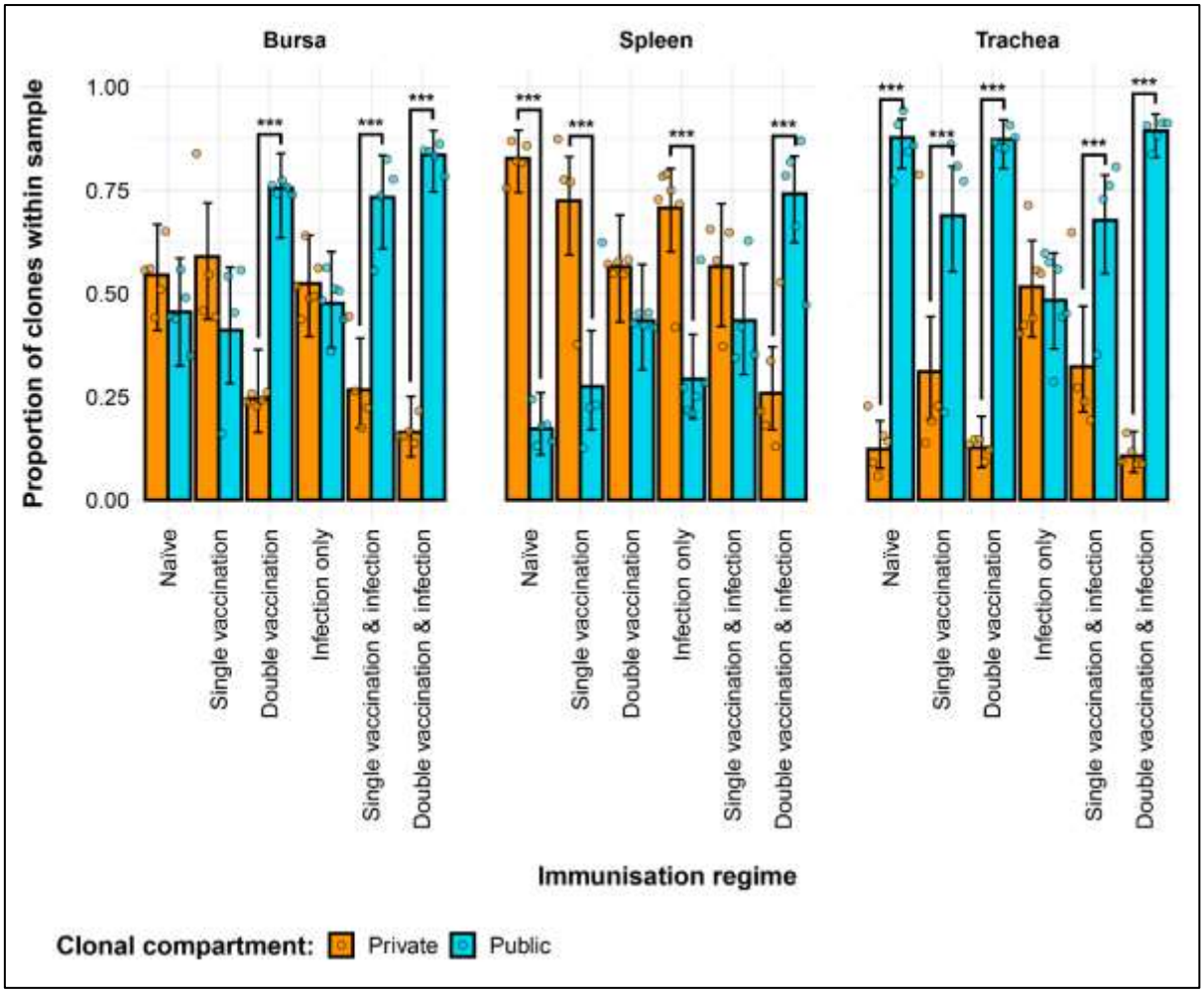

Figure 5. 4: *Differences between the TCRβ public and private compartments under different H9N2 immunisation regimes based on clone CDR3 nucleotide structure.*

Private (individual-restricted) clones are shown in orange. Public clones (shared between more than two individuals) and are shown in light blue. Dots represent individual bird observations of public and private clonal compartments. Error bars represent 95% bootstrap confidence intervals for the point estimates generated from 1000 simulations of the model. Statistically significant differences between the model estimates are depicted above the plots based on their corresponding p-values: * = $p < 0.05$; ** = $p < 0.01$; *** = $p < 0.001$.

When analysing the differences between the groups in the private and public compartments themselves, important effects of the immunisation regimes become apparent (**Figure 5.5**). Furthermore, all the differences to the naïve birds are mirrored when the amino acid clones are considered (**Figure A.17**). In the bursa and spleen, the groups that received two or more immunisations, either through vaccination or infection, have significantly smaller private

clonal compartments than the naïve birds. Indeed, the same groups exhibit significantly larger public clonal compartments than the naïve group in those tissues.

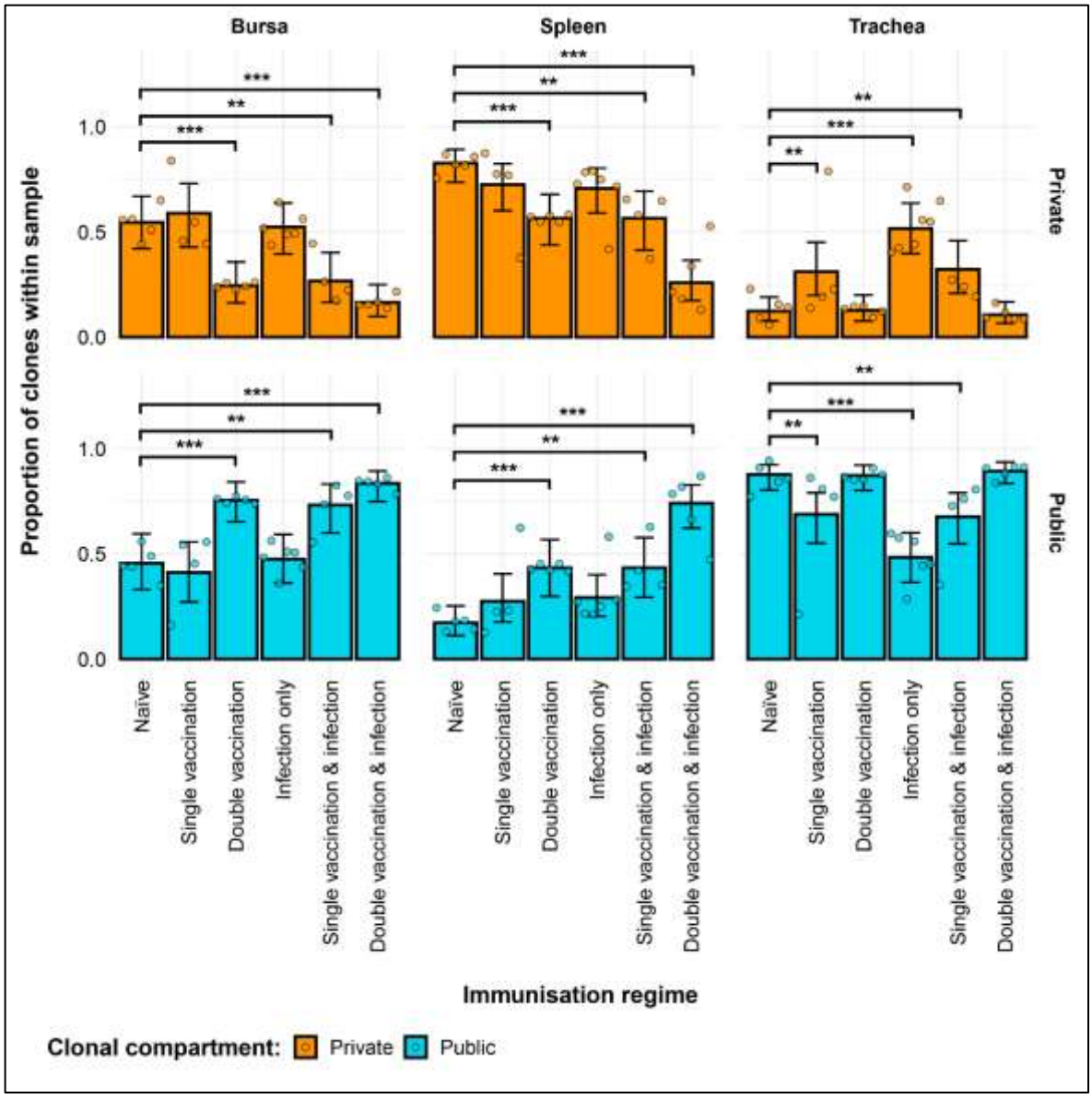

Figure 5. 5: *Differences within the TCRβ public and private compartments under different H9N2 immunisation regimes based on clone CDR3 nucleotide structure.*

Private (individual-restricted) clones are shown in orange. Public clones (shared between more than two individuals) and are shown in light blue. Dots represent individual bird observations of public and private clonal compartments. Error bars represent 95% bootstrap confidence intervals for the point estimates generated from 1000 simulations of the model. Statistically significant differences between the model estimates are depicted above the plots based on their corresponding p-values: * = $p < 0.05$; ** = $p < 0.01$; *** = $p < 0.001$.

In the trachea, both infected and uninfected bird groups that did not receive a double vaccination have a higher proportion of private clones than the naïve. These groups also exhibit a significantly lower percentage of public clones than the naïve birds. By contrast, the chickens that received a double vaccination show comparable levels of private and public clones with the naïve birds, irrespective of their infection status.

When further dividing the public compartment based on the different degrees of clonal sharing, most of the previously observed patterns in the total public compartment can be attributable to the rare public clones (**Figure 5.6**). As such, in the bursa and spleen, the birds that received two or more immunisations have significantly larger rare public compartments than the naïve birds. There are no significant differences between any of the immunisation regimes when considering the common public clone compartment. However, distinct patterns are observable regarding the ubiquitous clones of the immunisation groups. As such, in the bursa, there are significantly higher levels of ubiquitous clones in the double vaccination, infection only, and single vaccination and infection groups than in the naïve treatment. By contrast, in the spleen, the infection only group and the double vaccination and infection treatment have significantly lower levels of ubiquitous clones than the naïve birds. However, all the ubiquitous clonal compartments are at very low levels.

In the trachea, the partitioning of the total public compartment by degrees of clonal sharing masks the significance of the previously observed lower level of publics in the single vaccination treatment as opposed to the naïve group. However, the significantly lower levels of publics in the infection only and the single vaccination and infection groups are attributable to the rare public compartment, which retains this pattern. There are no significant differences between the immunisation regimes in terms of the common publics, and the only significant difference in the ubiquitous clonal compartments with the naïve is in the double vaccination and infection regime, which exhibits lower levels.

The patterns are very similar when the amino acid clones are considered (**Figure A.18**), with the differences between immunised groups and the naïve birds being identical in the

private and rare public clonal compartments. No differences in the amino acid clones are present to the naïve group common public and ubiquitous compartments of the bursa and spleen. In the trachea, the only observable differences to the naïve are in the common public of the infection only, which are at significantly higher proportions, and in the single vaccination ubiquitous clones, which are at significantly lower proportions. Given that the common public and ubiquitous clonal compartments make up smaller portions of the repertoire, the observed differences between the groups are difficult to interpret as the statistical significance of the model estimates may be an artefact of the small group sizes which could disproportionally influence the output.

The sequences from the current experiment were further investigated by comparing them with previously published TCRβ sequences at the nucleotide and/or amino acid levels (where available). As such, multiple sequences from the current experiment were found in previously published datasets. At the nucleotide level (**Figure 5.7A**), 11/97 (~11.3%) sequences from Mwangi *et al.* (2010) [144], 1/9 (~11.1%) sequences from Mwangi *et al.* (2011) [154] and 3/119 (~2.5%) sequences from Zhang *et al.* (2022) [111] were shared with the current dataset. No sequence data was available at the nucleotide level from the study of Ren *et al.* (2014) [155]. Of these identified sequences, the majority (10/15) were identified as rare publics in the current analysis (shared between ≥2 and up to 50% of birds). The remaining clones were identified as private (4 sequences) or common publics (1 sequence). When considering the amino acid level (**Figure 5.7B**), many more CDR3 sequences were identified in the published works, as follows: 23/97 (~23.7%) from Mwangi *et al.* (2010), 26/96 (~27.1%) from Mwangi *et al.* (2011), 26/275 from Ren *et al.* (2014), and 13/119 (~10.9%) from Zhang *et al.* (2022). The degrees of clonal sharing (i.e. rare vs. common vs. ubiquitous publics) were not considered when compared with other published sequences. Clones that were considered public were the ones present in ≥2 birds of the current experiment.

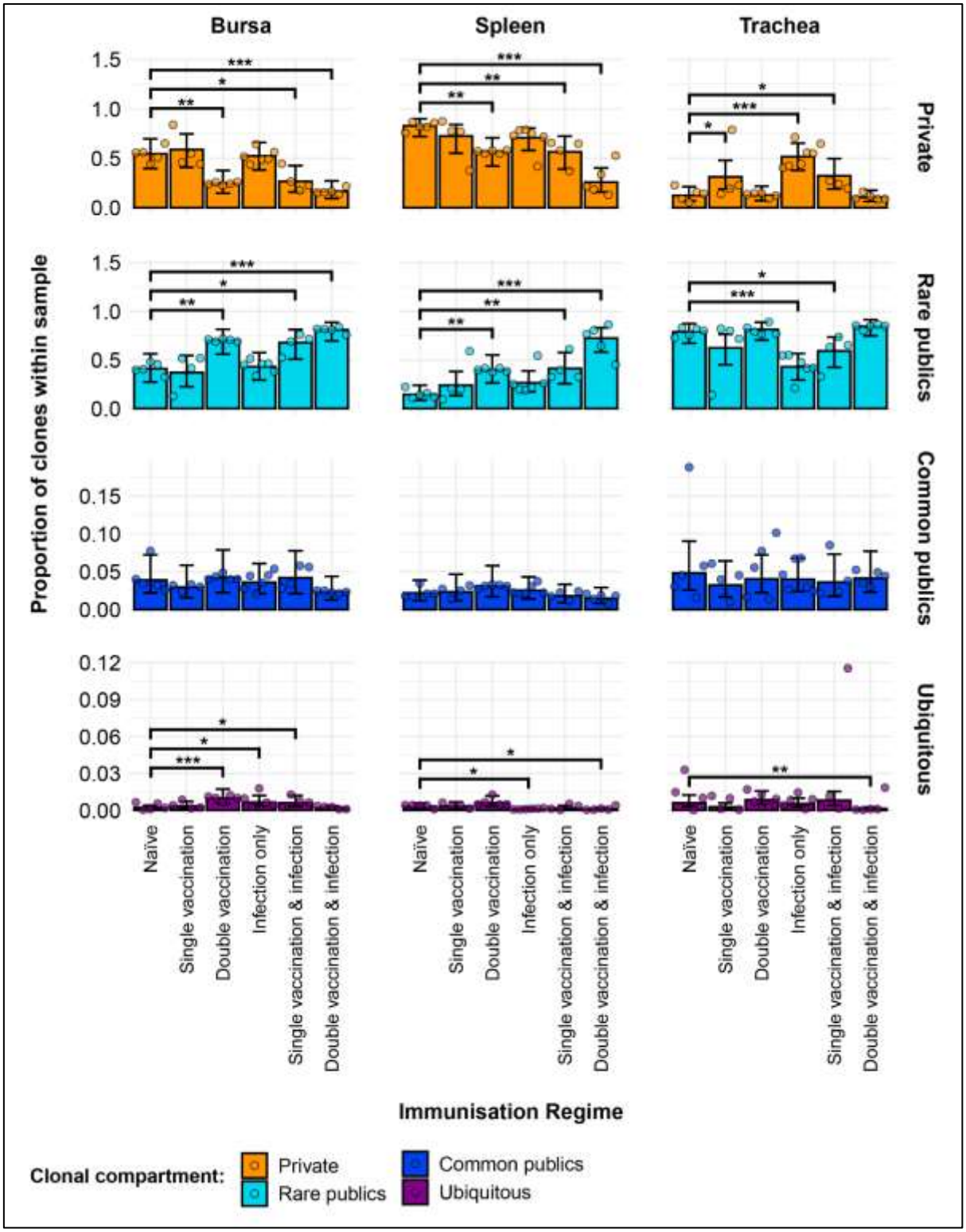

Figure 5. 6: *Model estimates of TCRβ clone CDR3 nucleotide private and public compartments based on different levels of clonal sharing.*

Private (individual-restricted) clones are shown in orange. Rare publics (shared between 2 or more than 2 individuals up to 50%) and are shown in light blue. Common publics (shared between more than 50% and up to 90% birds) are shown in dark blue. Ubiquitous publics (found in 90% or more

of the birds which were incorporated in the analysis) are shown in purple. Dots represent individual bird observations of private and distinct public clonal compartments. Error bars represent 95% bootstrap confidence intervals for the point estimates generated from 1000 simulations of the model. Statistically significant differences between the model estimates are depicted above the plots based on their corresponding p-values: * = $p < 0.05$; ** = $p < 0.01$; *** = $p < 0.001$.

As none of the aforementioned studies used high throughput sequencing, the microbiota repertoire study described in Chapter II was used as a proxy for high sequencing depth (**Figure 5.8**). Out of the 381,564 unique CDR3 nucleotide sequences (302,888 amino acid sequences) in the microbiota experiment, 10,015 (27,111 amino acid sequences) were identified in the current analysis. Moreover, only 5,029 (14,202 amino acid sequences) of these shared sequences were public between the birds of the current experiment, 2,616 (6,979 amino acid sequences) of which also being identified as public in the microbiota study. However, 1,160 nucleotide sequences (2,946 amino acid sequences) identified as public (shared by ≥2 birds) in the microbiota study were also present in the birds of the current analysis but were not shared between individuals (i.e. were private). At the same time, 9,963 private nucleotide sequences (3,826 amino acid sequences) from both datasets were found to be public between individuals belonging to the two experiments.

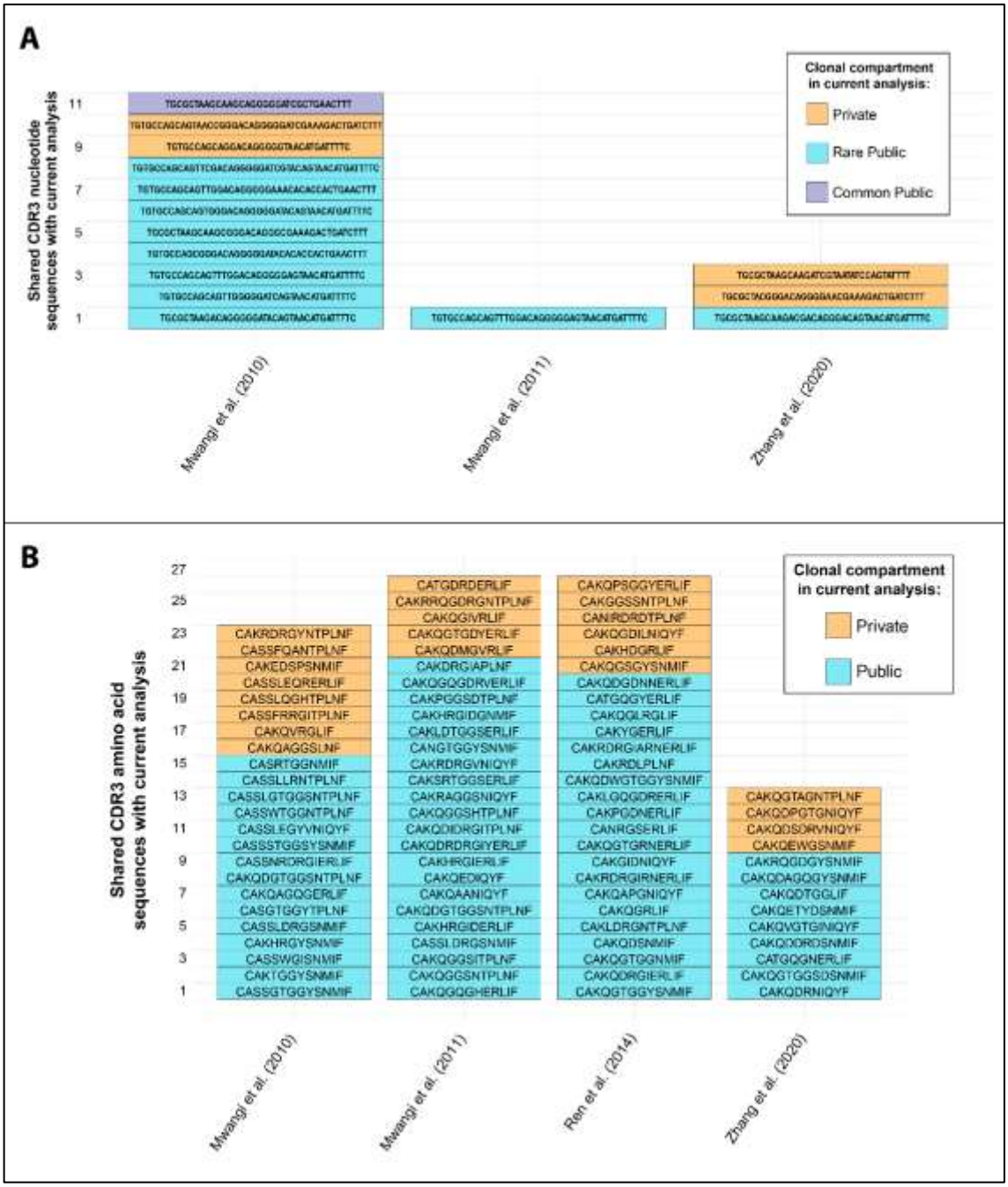

Figure 5. 7: *TCRβ shared CDR3 sequences with other published works.*

(**A**) Shared nucleotide sequences with other published works. Sequence identity based on clonal compartments within current analysis is colour coded for the private (individual-restricted) in orange, rare publics (shared between two and up to 50% of birds) in light blue, and common publics (between 50% and 90% of birds) in dark blue. (**B**) Shared amino acid sequences with other published works. Sequence identity based on clonal compartments within current analysis is colour coded for the private (individual-restricted) and publics (shared by ≥2 birds) in light blue, respectively. Degree of clonal sharing was not carried out at the amino acid level.

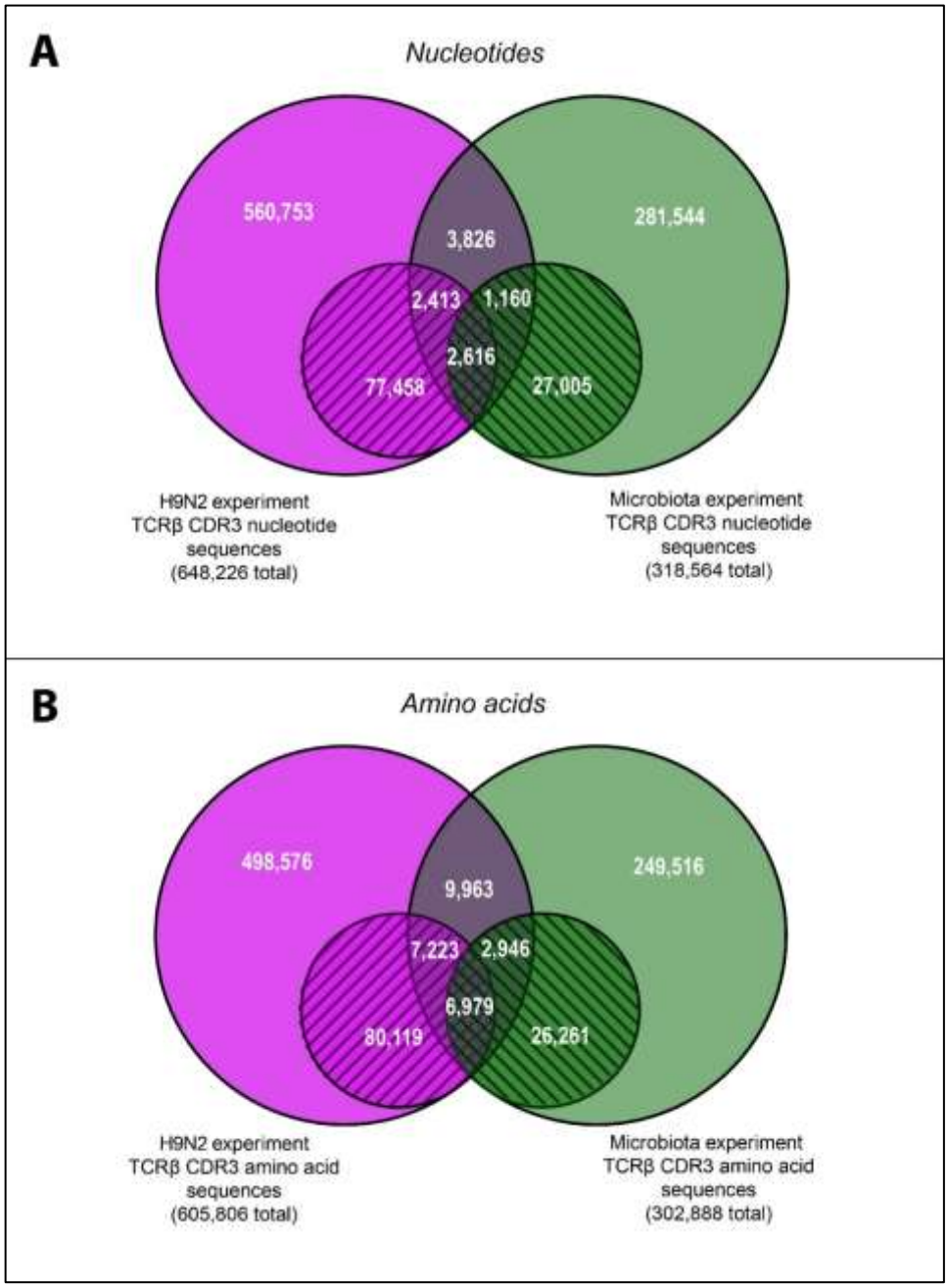

Figure 5. 8: *TCRβ shared CDR3 sequences with previous high throughput repertoire analysis on germfree and microbially colonised chickens (see* ***Chapter II****).*

(**A**) Venn diagram of shared unique TCRβ CDR3 nucleotide sequences. (**B**) Venn diagram of shared unique TCRβ CDR3 amino acid sequences. H9N2 experiment and microbiota sequences are shown in purple and green, respectively. Public sequences (shared by ≥2 birds) within each experiment are displayed crosshatched. The numbers of sequences that are private or public within and between the datasets are shown on the diagram.

V.3.5. TCRβ V family usage and contribution to private and public compartments

The 3 Vβ families are used differently based on tissue type and immunisation regime (**Figure 5.9**). Generally, clones rearranged with Vβ1 family genes make up a larger fraction of the repertoire of tissues, followed by Vβ2 and Vβ3 clones in order of their abundance. The Vβ3 family is at comparatively higher levels in the bursa and trachea than in the spleen, albeit still at low levels relative to the other two Vβ families.

In the bursa, there is a significantly higher Vβ1 family clone contribution to the repertoire in the double vaccinated and infected birds than in the naïve. By contrast, this pattern is reversed in terms of the Vβ2 and Vβ3 families, with significantly lower levels being present in this triple exposure treatment than in the naïve birds.

In the spleen, all of the immunisation regimes with the sole exception of the double vaccinated treatment exhibit significantly higher proportions of Vβ1 clones and lower proportions of Vβ2 clones in their repertoires. Although this pattern seems to also apply to the double vaccination treatment group, the difference is not statistically significant. When considering the Vβ3 family, the only significant difference to the naïve group in the spleen is with the infection only immunisation regime, being at much lower levels. Of note is that all the infected groups have significantly lower proportions of Vβ3 than the single vaccination and double vaccination treatments (p values < 0.05; not displayed in the figure).

In the trachea, there is a significantly higher proportion of Vβ1 clones in the single vaccination and the single vaccination and infection treatments than in the naïve group. At the same time, there is a lower Vβ2 percentage in these groups than in the naïve birds. Interestingly, there is a high heterogeneity amongst individuals in terms of their Vβ3 usage in all groups with the exception of the double vaccination and infection treatment. Concerning this family, significantly lower levels of Vβ3 clones than in the naïve group can also be observed in the single vaccination and infection only groups in the tracheal tissues.

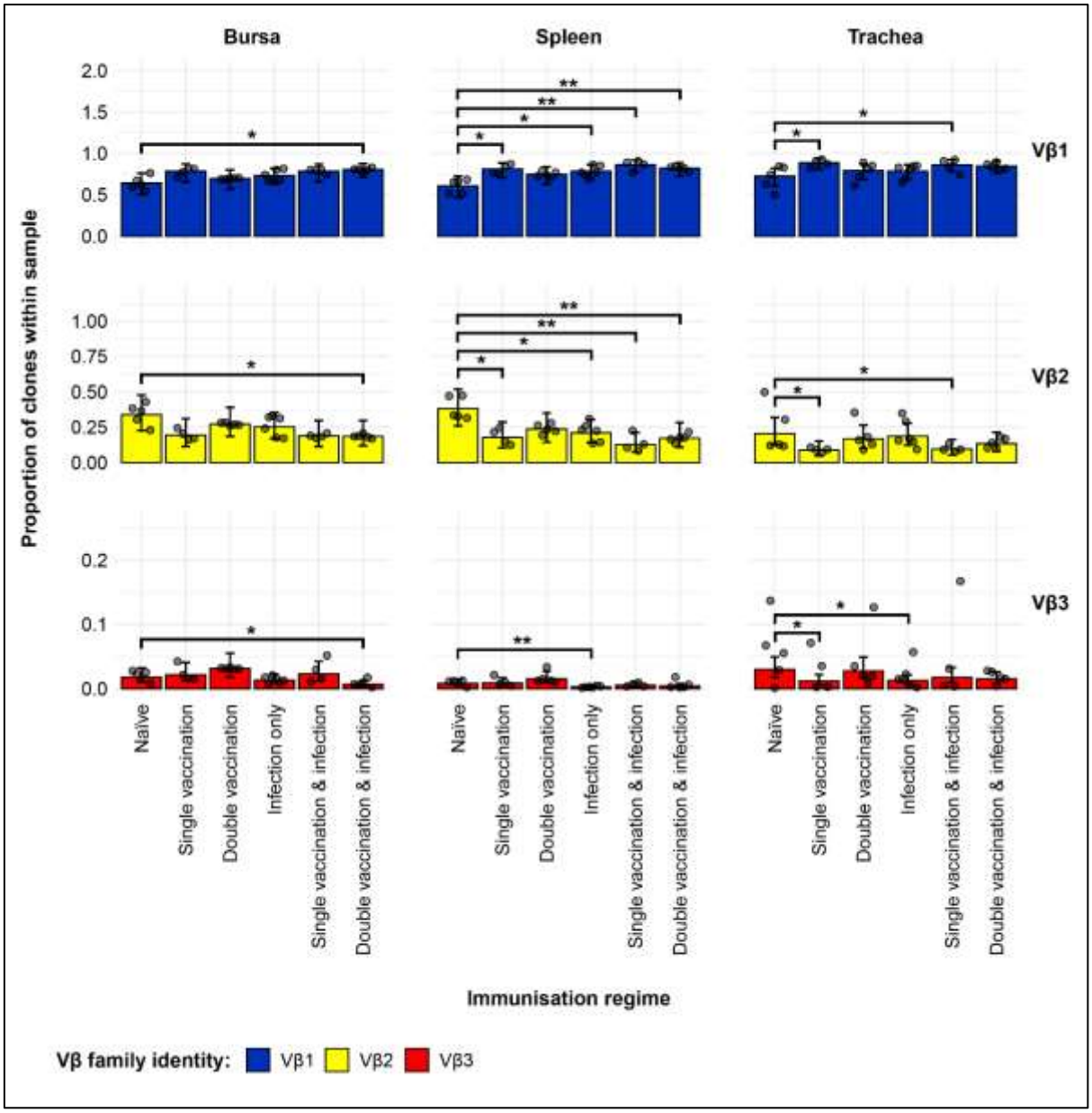

Figure 5. 9: *Model estimates of TCRβ V family usage in individual tissue samples across H9N2 immunisation regimes.*

V family identities are shown in blue (Vβ1), yellow (Vβ2), and red (Vβ3). Grey dots represent individual bird observations for each V family. Error bars represent 95% bootstrap confidence intervals for the point estimates generated from 1000 simulations of the model. Statistically significant differences between the model estimates are depicted above the plots based on their corresponding p-values: * = $p < 0.05$; ** = $p < 0.01$, *** = $p < 0.001$.

The distribution of Vβ family clones across the public and private compartments reveals additional influences of tissue type and immunisation status (**Figure 5.10**). In the bursa, the

private Vβ1 family compartment is significantly lower in the double vaccination groups when compared to the naïve, irrespective of infection status. At the same time, the public Vβ1 compartment is significantly higher than the naïve treatment in all the groups that were subjected to two or more immunisations. These immunisation regimes also exhibit lower levels of Vβ2 private clones than the naïve group. The only significant difference in the Vβ2 public compartment is between the naïve and the single vaccination treatments, the latter group having a smaller contribution of clones to the repertoire. In terms of the Vβ3 family clone distribution in the bursa in relation to the naïve group, the private Vβ3 clonal compartment is significantly higher in the single vaccinated birds, and there are significantly fewer Vβ3 public clones in the infection only group.

In the spleen, the only significant difference in the Vβ1 private clonal compartment with the naïve treatment is for the double vaccinated and infected group. However, all immunisation regimes aside from the single vaccination treatment exhibit significantly higher proportions in the public Vβ1 compartment when compared to the naïve birds. When considering the Vβ2 private clones, all groups show a significantly lower contribution to the repertoire than the naïve birds. No differences between the groups are observed concerning the Vβ2 public compartments. The only difference with the naïve group in the Vβ3 clones is in the public compartment, where the infection only birds have significantly lower proportions of clones contributing to the repertoire.

The tracheal Vβ1 private compartment is significantly higher in the single vaccination, single vaccination and infection, and infection only groups when compared to the naïve. The double vaccinated groups do not exhibit any significant differences when compared to the naïve birds in terms of Vβ1 private compartments. By contrast, the only significant difference when compared to the naïve chickens in terms of the public Vβ1 clonal compartment is for the infection only group, which exhibits lower levels of clones contributing to the repertoire. The Vβ2 private compartment of the infection only immunisation regime is also significantly higher than the naïve group, whilst no other marked differences between the groups are illustrated by the model for this Vβ2 clonal compartment. Conversely, the Vβ2 public compartments of all groups that did not receive a double vaccination exhibit significantly lower levels of clones than the naïve group. Concerning the Vβ3 family, the only significant differences between the model estimates

when compared to the naïve are for the single immunisation groups, either through vaccination or infection, both exhibiting lower levels in the public compartments.

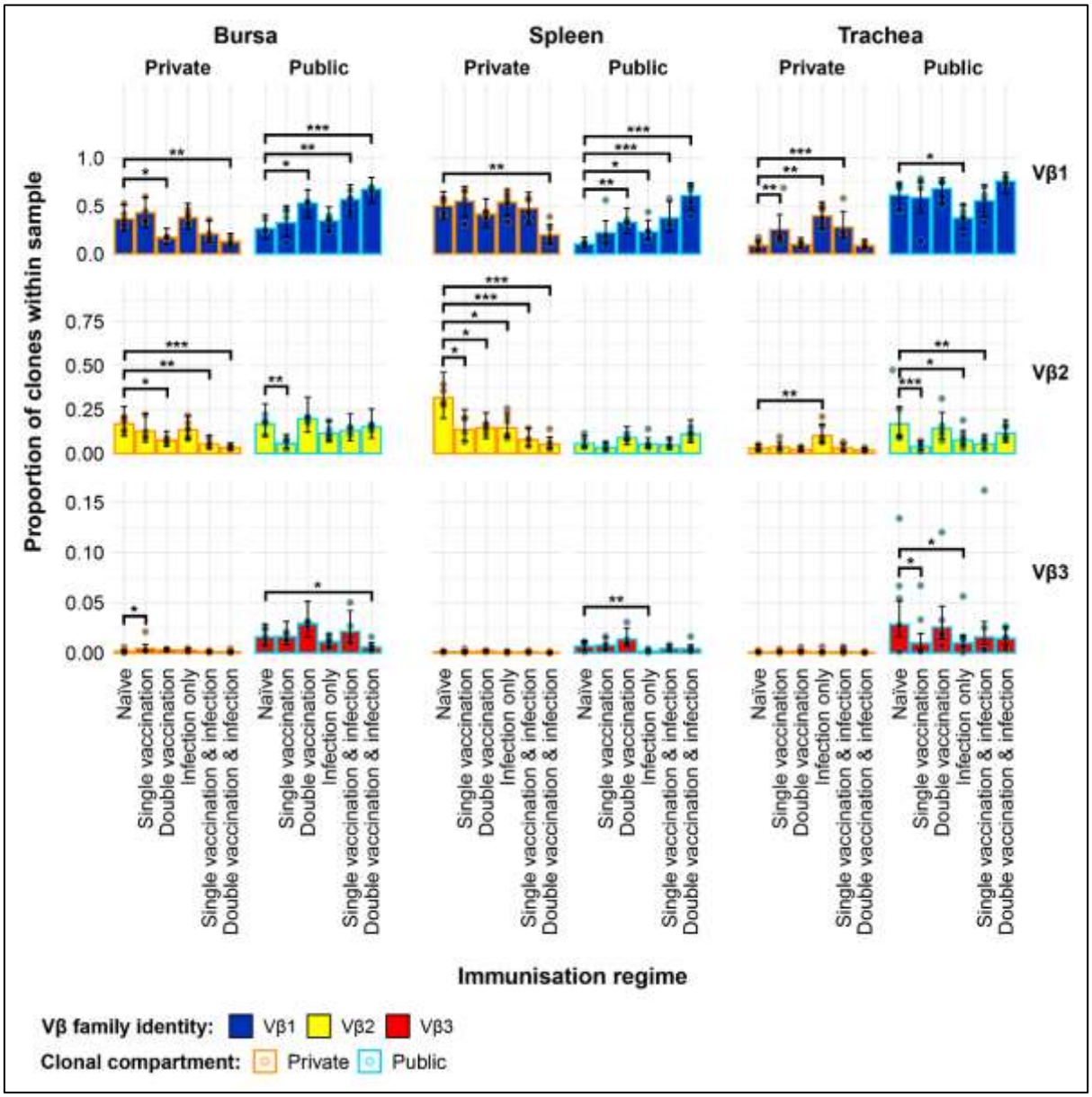

Figure 5. 10: *Model estimates of TCRβ clone V family publicness in individual tissue samples across H9N2 immunisation regimes.*

V family identities are shown in blue (Vβ1), yellow (Vβ2), and red (Vβ3). Private (individual-restricted) clones have an orange outline. Public clones which are shared between more than two individuals have a light blue outline. Dots represent individual bird observations of V family contributions to the public and private clonal compartments. Error bars represent 95% bootstrap confidence intervals for the point estimates generated from 1000 simulations of the model.

Statistically significant differences between the model estimates are depicted above the plots based on their corresponding p-values: * = $p < 0.05$; ** = $p < 0.01$, *** = $p < 0.001$.

V.3.6. TCRβ J gene usage and contribution to public and private compartments

When observing the tissue-specific TCRβ clone distribution in terms of overall J gene usage, the only significant differences between the H9N2 immunisation regimes and the naïve group were observable in the trachea (**Figure 5.11**). As such, the vaccinated groups but not the infection only treatment displayed a significantly higher proportion of Jβ1 clones than the naïve birds. By contrast, all immunisation groups exhibited significantly lower proportions of Jβ2 clones in the trachea than the naïve group. Concerning the Jβ3 clones, all immunised birds showed significantly higher proportions, with the exception of the single vaccination and infection group, as the model estimate was not deemed significantly different to the naïve. The only significant difference in terms of Jβ4 gene usage to the naïve group is for the double vaccinated and infected birds, which show significantly higher proportions of clones.

The incorporation of publicness into the model reveals additional tissue-specific differences in terms of the J gene usage, even in the bursa and spleen, where no differences in terms of total J gene usage were apparent previously.

In the Bursa, all groups that received two or more immunisations exhibited significantly smaller Jβ1 proportions of private clones, and significantly higher proportions of publics than the naïve group (**Figure 5.12**). The same pattern seems to apply concerning the Jβ2 clones, although some differences are not deemed statistically significant by the model output. As such, only the private compartments of the double vaccinated and the double vaccinated and infected birds had significantly lower proportions of clones than the naïve. By contrast, only the public Jβ2 compartments of the double vaccinated and infected and the single vaccinated and infected birds were significantly higher. The pattern of lower proportions in the private compartment for the groups that were subjected to two or more immunisations also applied for the Jβ3 and Jβ4 families. However, the differences in the publics are not all deemed statistically significant for those groups, with only the double

vaccination group and the double vaccination and infection group exhibiting significantly higher levels according to the model output.

In the spleen, significantly lower proportions of clones were observed in the private compartments of the double vaccination and infection group when compared to the naïve, irrespective of Jβ gene identity (**Figure 5.13**). The only other significant difference to the naïve in the private compartment is with the double vaccinated group, which showed lower proportions of Jβ3 private clones. When looking at the splenic public compartment in terms of their Jβ clone distribution, the groups that received two or more immunisations show significantly higher proportions than the naïve treatment in terms of all Jβ clones. At the same time, the public Jβ2 compartment in the spleen of the infection only treatment is significantly larger than the naïve group.

The private compartments in the trachea exhibited significantly higher levels of clones in the infection only and single vaccination and infection groups when compared to the naïve, irrespective of the Jβ gene considered (**Figure 5.14**). However, each Jβ gene showed additional differences, with the exception the Jβ2 clones. As such, there were also significantly higher levels of Jβ1 and Jβ2 clones in the private compartment of the single vaccinated birds, when compared to the naïve treatment. Moreover, the double vaccinated group also exhibited slightly higher Jβ3 clones than the naïve group. In terms of the public compartment, the only significant differences observed between immunisation groups and the naïve birds were for the Jβ1 and Jβ2 clones. There were higher proportions of Jβ1 publics in the double vaccinated, and all groups exhibited significantly lower proportions of Jβ2 publics than the naïve treatment.

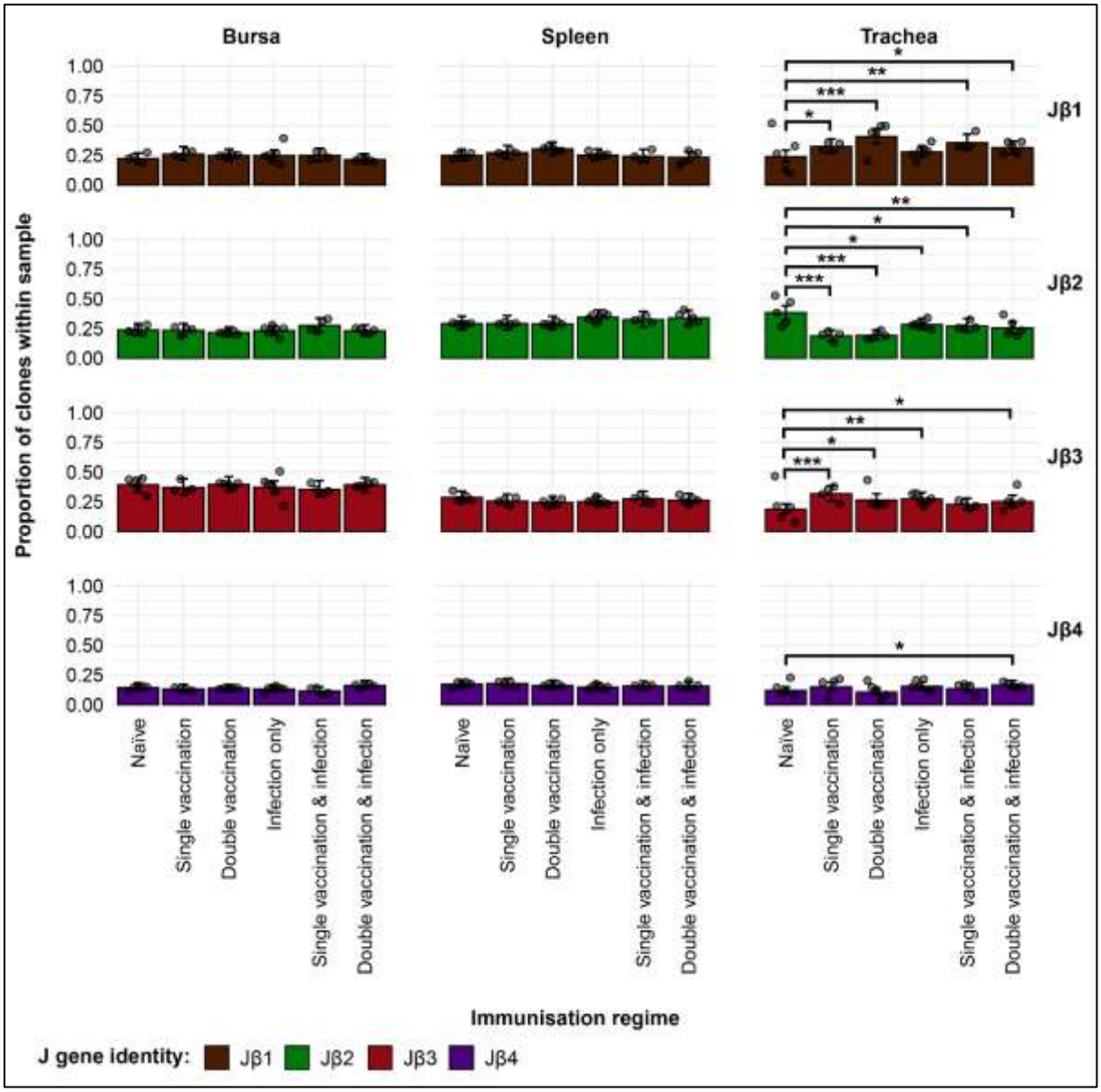

Figure 5. 11: *Model estimates of TCRβ J gene usage in individual tissue samples across H9N2 immunisation regimes.*

V family identities are shown in brown (Jβ1), green (Jβ2), dark red (Jβ3), and purple (Jβ4). Grey dots represent individual bird observations for specific Jβ clones. Error bars represent 95% bootstrap confidence intervals for the point estimates generated from 1000 simulations of the model. Statistically significant differences between the model estimates are depicted above the plots based on their corresponding p-values: * = $p < 0.05$; ** = $p < 0.01$, *** = $p < 0.001$.

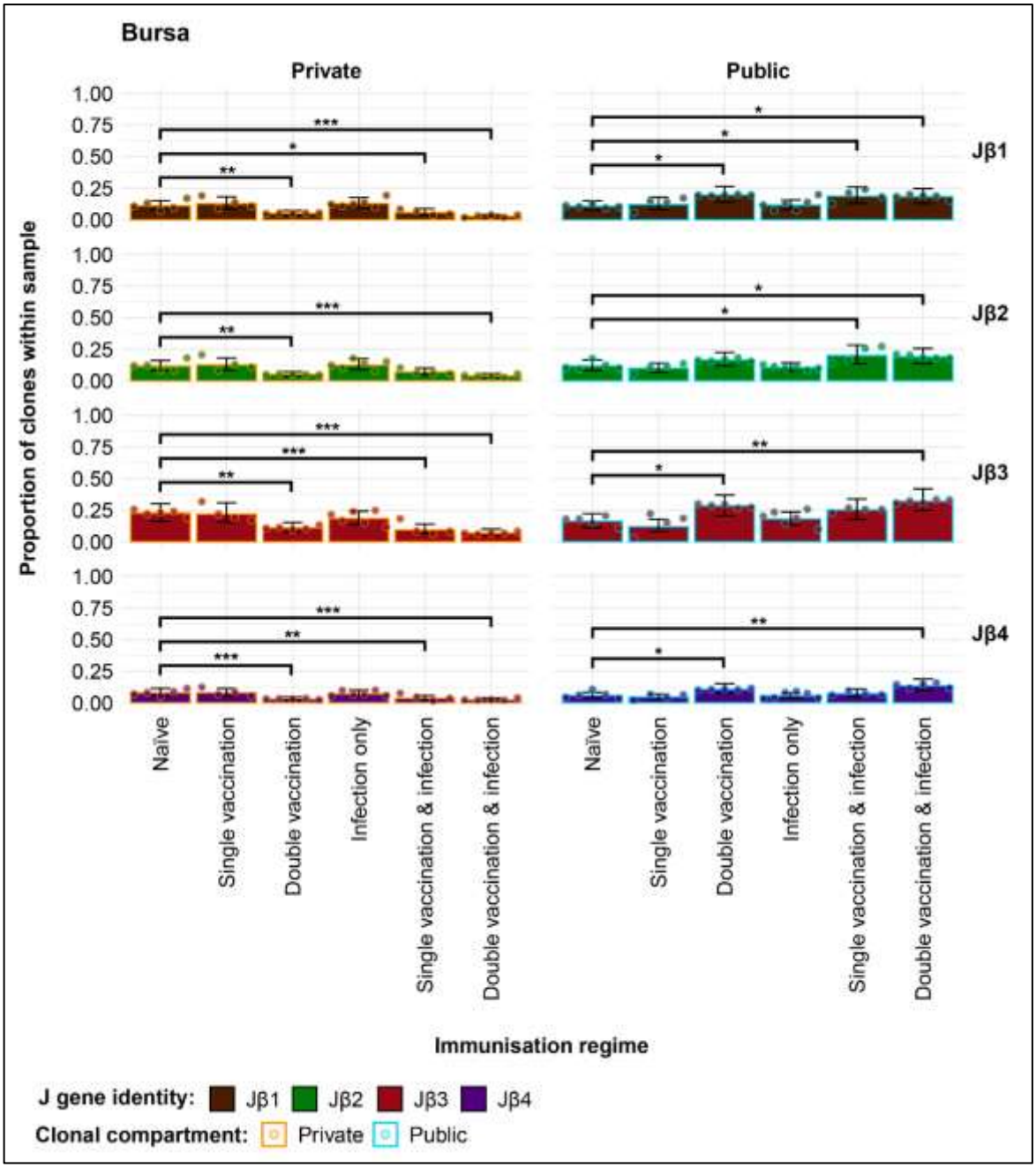

Figure 5. 12: *Model estimates of TCRβ J gene publicness in the bursal samples across H9N2 immunisation regimes.*

V family identities are shown in brown (Jβ1), green (Jβ2), dark red (Jβ3), and purple (Jβ4). Private (individual-restricted) clones have an orange outline. Public clones which are shared between more than two individuals have a light blue outline. Dots represent individual bird observations for specific Jβ clone contributions to the public and private clonal compartments. Error bars represent 95% bootstrap confidence intervals for the point estimates generated from 1000 simulations of the model. Statistically significant differences between the model estimates are depicted above the plots based on their corresponding p-values: * = $p < 0.05$; ** = $p < 0.01$, *** = $p < 0.001$.

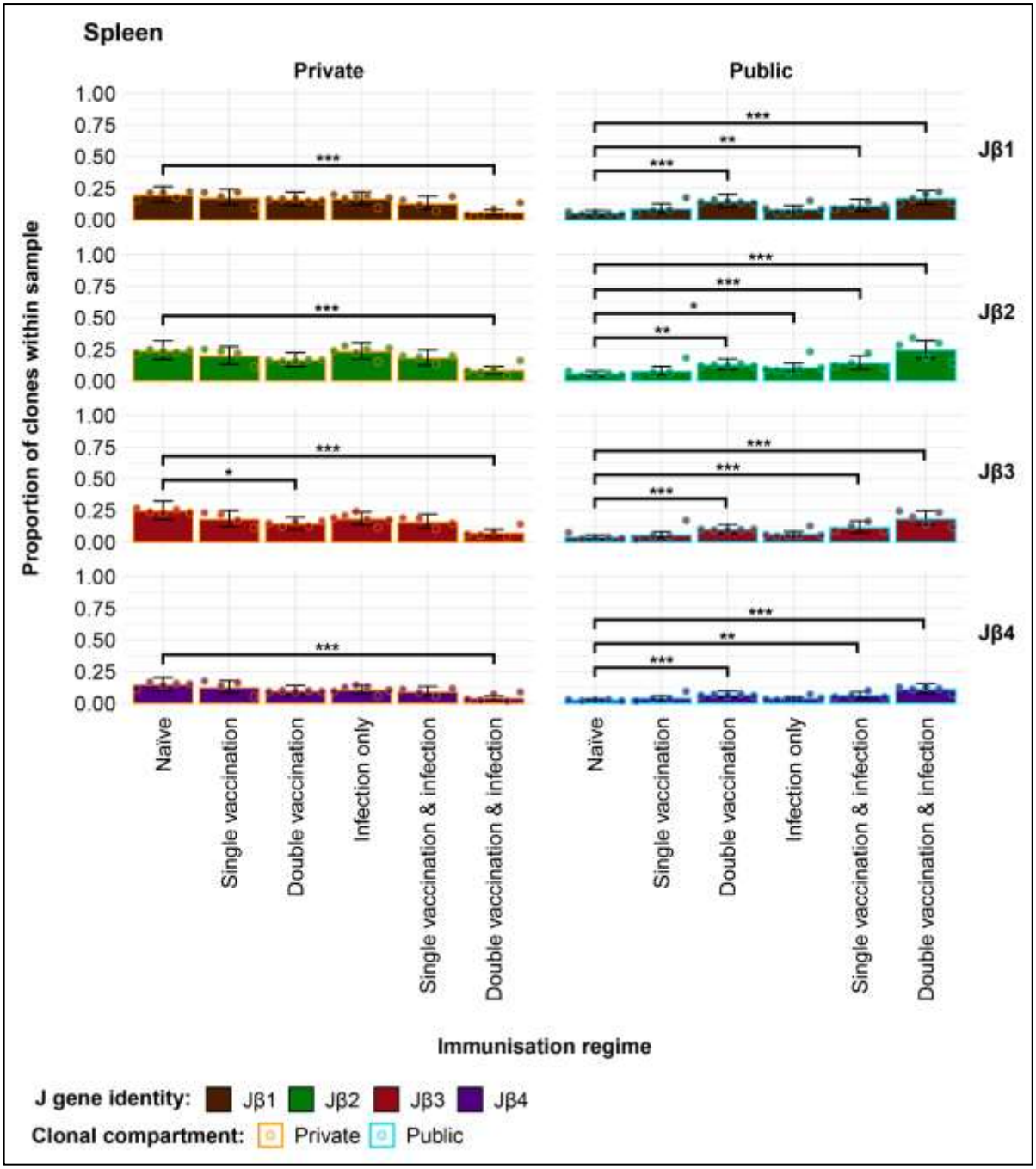

Figure 5. 13: *Model estimates of TCRβ J gene publicness in the spleen samples across H9N2 immunisation regimes.*

V family identities are shown in brown (Jβ1), green (Jβ2), dark red (Jβ3), and purple (Jβ4). Private (individual-restricted) clones have an orange outline. Public clones which are shared between more than two individuals have a light blue outline. Dots represent individual bird observations for specific Jβ clone contributions to the public and private clonal compartments. Error bars represent 95% bootstrap confidence intervals for the point estimates generated from 1000 simulations of the model. Statistically significant differences between the model estimates are depicted above the plots based on their corresponding p-values: * = $p < 0.05$; ** = $p < 0.01$, *** = $p < 0.001$.

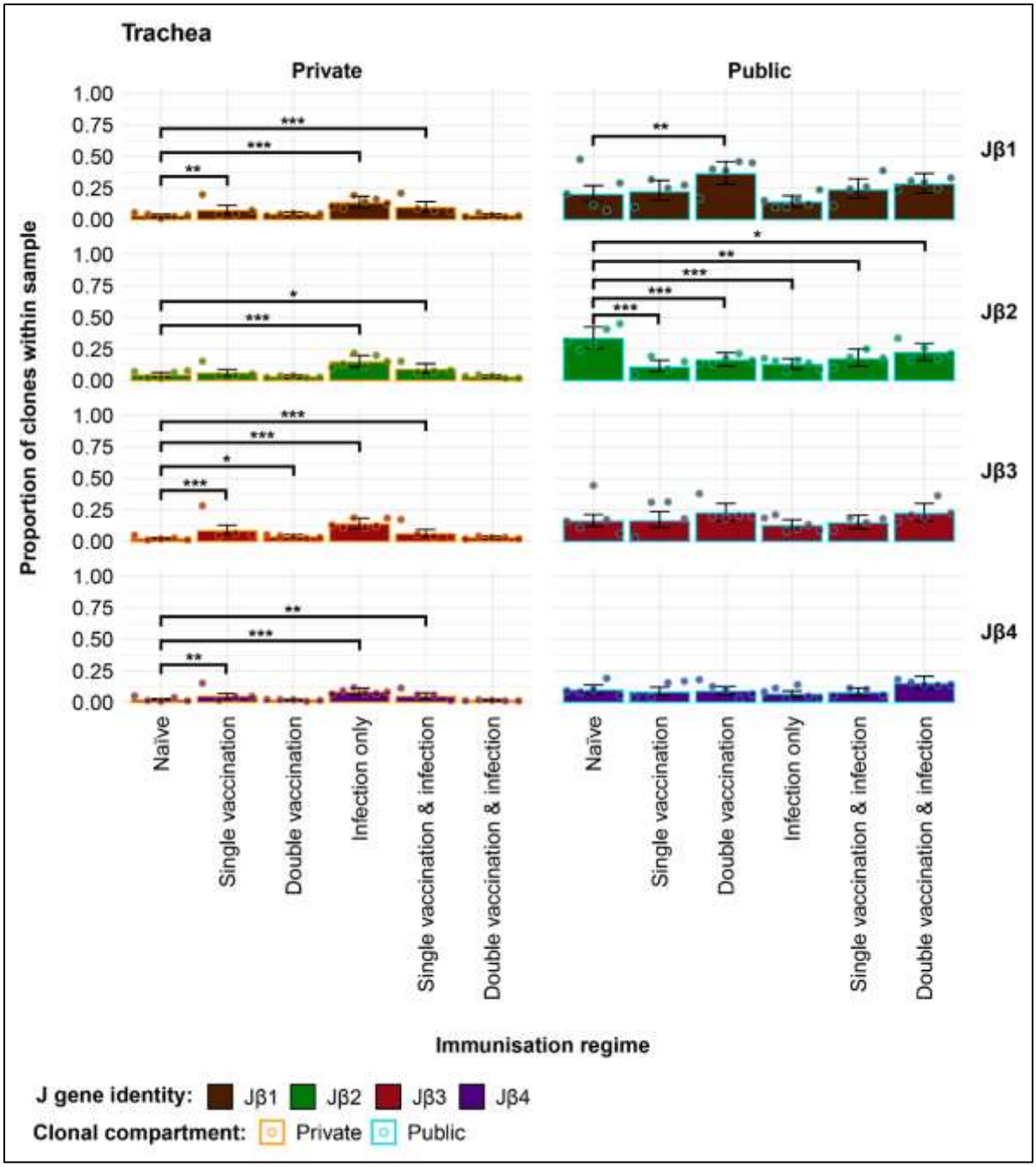

Figure 5. 14: *Model estimates of TCRβ J gene publicness in the tracheal samples across H9N2 immunisation regimes.*

V family identities are shown in brown (Jβ1), green (Jβ2), dark red (Jβ3), and purple (Jβ4). Private (individual-restricted) clones have an orange outline. Public clones which are shared between more than two individuals have a light blue outline. Dots represent individual bird observations for specific Jβ clone contributions to the public and private clonal compartments. Error bars represent 95% bootstrap confidence intervals for the point estimates generated from 1000 simulations of the model. Statistically significant differences between the model estimates are depicted above the plots based on their corresponding p-values: * = $p < 0.05$; ** = $p < 0.01$, *** = $p < 0.001$.

V.3.7. TCRβ repertoires restricted to immunisation regimes

Clones which were only found to be expanded in the infection treatments were examined based on their V family identity, amino acid sequence, and the identity of the tissues and birds in which they were found (**Figure 5.15**). Out of the identified 18 unique CDR3 amino acid sequences, 10 were found to be expanded in more than one bird, and only one sequence (CAKARRDRGPMIF) was private. There was a clear bias towards Vβ1 usage in the identified clones, with 14 sequences having CDR3 sequences rearranged with genes belonging to this family. Two distinct CDR3 sequences are found in each of the Vβ2 and Vβ3 families, all four being expanded across multiple individuals.

When looking at tissue-specific expansions, more sequences are found to be expanded in the bursa and trachea than in the spleen, although many of them are found at very low levels in this latter tissue as well. The effects of the specific infection regime based on the number of vaccinations received prior to infection is also apparent, as clones which are found to be expanded across multiple individuals are generally found at higher levels within birds of the same group.

In contrast to the infection-restricted clones, fewer TCRβ sequences are found to be expanded in the uninfected treatment groups (**Figure 5.16**). Of these, 5 are rearranged with a Vβ1 family gene, whilst the remaining clone is with a Vβ2 gene. As for the infection-restricted clones, the identified clones are at low levels in the splenic samples, with expansions occurring in the bursa and trachea. Moreover, four out of the six clones are expanded across multiple individuals, although they are present at low levels in several birds. One of the identified CDR3 sequences (CAKQDRGINERLIF) is present in 10/14 of the uninfected birds exhibits a consistent expansion in all tissues of a naïve individual, with the nucleotide sequences of two unique clones converging on the same amino acid sequence. Again, clones which are found to be expanded in multiple individuals are generally observed in the repertoires of birds within the same group.

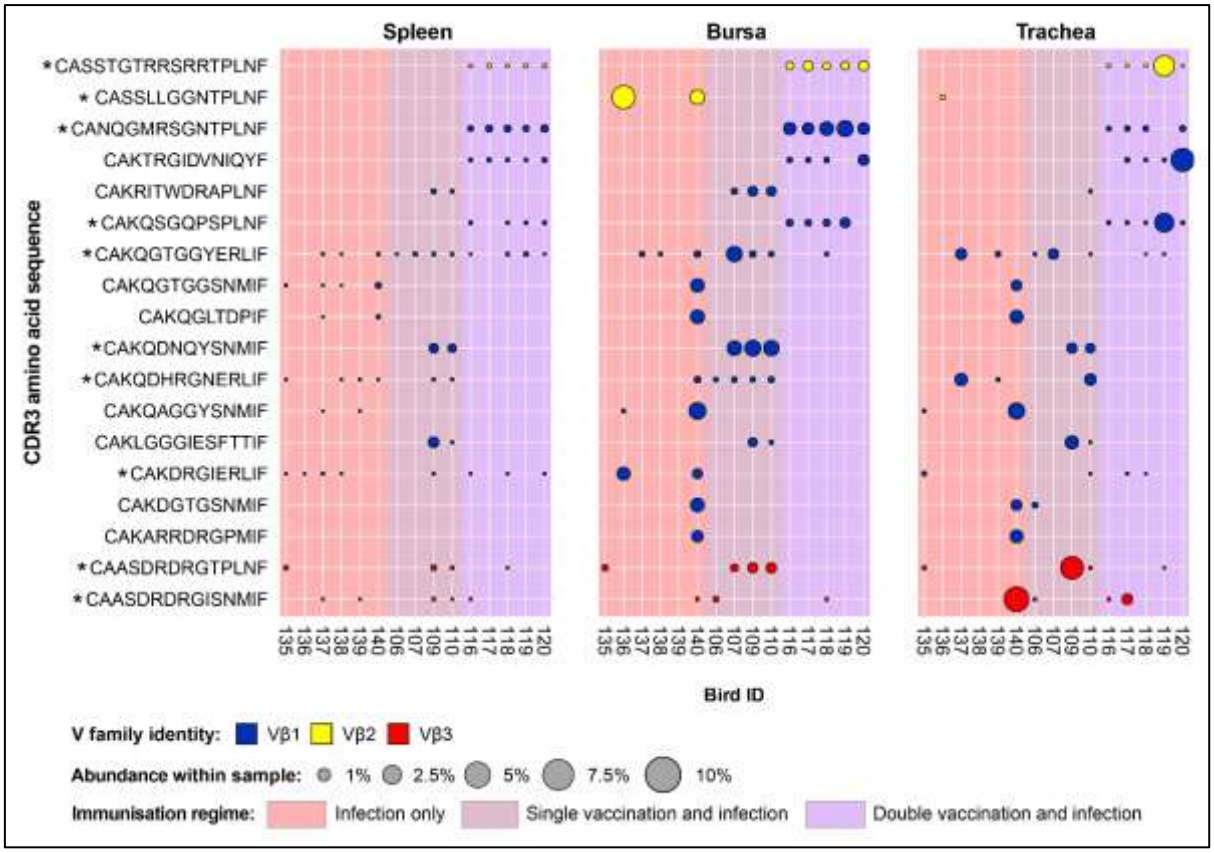

Figure 5. 15: *TCRβ clonal expansions in the restricted repertoire of infected birds.*

Circles indicate the presence of clones with a specific CDR3 amino acid sequence and are proportional to the abundance within each bird's tissue clonal compartment. The plot shows only the clones which are expanded in the infected treatment groups (at or above 0.5% and at less than 0.5% in any of the uninfected). The colour of the circles indicates V family identity: blue – Vβ1; yellow – Vβ2; red – Vβ3. Clones which are expanded in multiple birds are identified with an asterisk next to the CDR3 amino acid sequence. Background colours indicate the immunisation regime identity: red – infection only; dark red – single vaccination and infection; purple – double vaccination and infection.

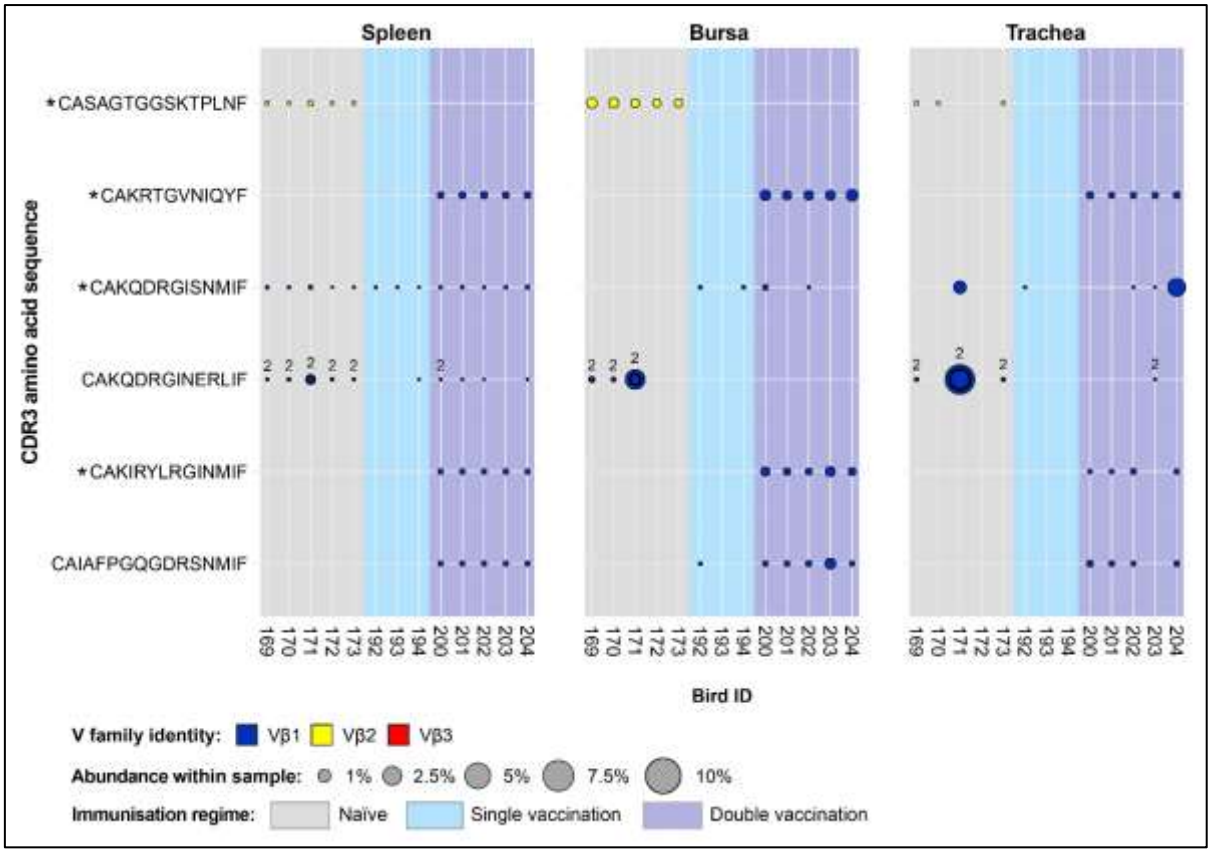

Figure 5. 16: *TCRβ clonal expansions in the restricted repertoire of uninfected birds.*

Circles indicate the presence of clones with a specific CDR3 amino acid sequence and are proportional to the abundance within each bird's tissue clonal compartment. Overlapping circles and adjacent numbers indicate different clones based on nucleotide sequence which share the same CDR3 amino acid sequence and are found in the same sample. The plot shows only the clones which are expanded in the uninfected treatment groups (at or above 0.5% and at less than 0.5% in any of the infected). Clones which are expanded in multiple birds are identified with an asterisk next to the CDR3 amino acid sequence. The colour of the circles indicates V family identity: blue – Vβ1; yellow – Vβ2. Background colours indicate the immunisation regime identity: grey – naïve; light blue – single vaccination; dark blue – double vaccination.

Out of the 13 clones that were identified as expanded in the vaccinated groups but absent or below the expansion threshold in the unvaccinated groups (**Figure 5.17**), 8 were previously found in the above to be restricted to infection, and 3 were restricted to the uninfected birds. The two remaining CDR3 sequences that are found expanded in members

of both infected and uninfected groups are identified with Vβ2 (CDR3: CASSLGDRNMIF) and Vβ3 (CAASDRDRGTPLNF) family genes, but not with Vβ1.

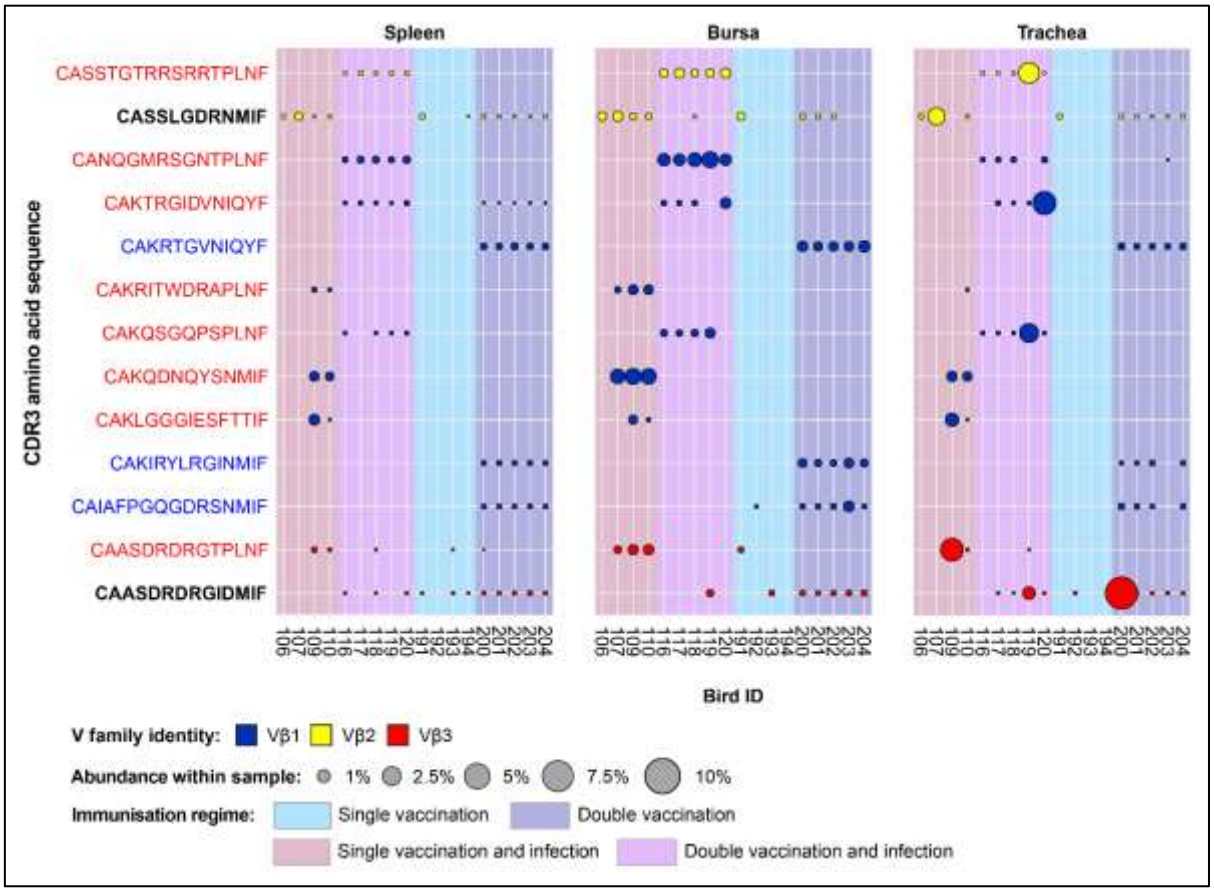

Figure 5. 17: *TCRβ clonal expansions in the restricted repertoire of vaccinated birds.*

Circles indicate the presence of clones with a specific CDR3 amino acid sequence and are proportional to the abundance within each bird's tissue clonal compartment. The plot shows only the clones which are expanded in the vaccinated treatment groups (at or above 0.5% and at less than 0.5% in any of the naïve or infection only groups). CDR3 amino acid sequences which coincide with clones restricted to infected and uninfected birds are shown in red and blue, respectively. The colour of the circles indicates V family identity: blue – Vβ1; yellow – Vβ2; red – Vβ3. Background colours indicate the immunisation regime identity: light blue – single vaccination; dark blue – double vaccination, dark red – single vaccination and infection; purple – double vaccination and infection.

V.4. Discussion

T cells are known to play important roles in protecting the host against infectious challenge [90,109,210]. In chickens, H9N2 infection has previously been shown to drive both CD4+ and CD8+ T cell responses, suggesting that both lineages may fulfil important roles in viral clearance [89,90]. The results presented herein consider the clonal dynamics of chicken T cells as revealed by high depth TCRβ repertoire sequencing during vaccination, infection, and combinations of these regimes.

The TCRβ repertoire was profoundly influenced by immunisations, in a tissue-dependent manner. The analysis included the spleen as a major secondary lymphoid organ where stimulation and proliferation of the adaptive immune system occurs, following antigenic stimulation [76]. Furthermore, the spleen could potentially substitute some of the roles of lymph nodes, given their absence in chickens, therefore concentrating a substantial part of the antigen-dependent responses to vaccination and/or infection [75]. Indeed, in the spleen, the analysis revealed patterns of clonal homeostasis which indicate a greater focus on larger clones for all the infected groups, thereby being indicative of antigen-specific expansions. As only the infected groups exhibited differences to the naïve treatment, there is a strong suggestion that vaccination exerts less influence on the TCRβ diversity and clonal homeostasis than infection in the spleen. This is also mirrored in the splenic repertoire diversity, although significant differences to the naïve birds were only found in the two groups which received both infection and vaccination(s), potentially due to the greater antigenic stimulation (number of exposures and overall amount of antigen). The effects of multiple antigenic stimulation are also apparent on the splenic TCRβ composition in terms of public and private clones (discussed in more detail below), with the repertoires of the multiply immunised birds exhibited larger public compartments than the naïve birds. This pattern suggests that the number of immunisations, irrespective of their nature (vaccination and/or infection) is a major determinant in the public vs. private composition of the TCRβ CDR3 repertoire in the spleen. As such, although infection rather than vaccination(s) is suggested to be a stronger driver of the diversity landscape in the spleen, an increased number of antigenic stimulations apparently dictates the balance in favour of public rather than private clonal responses within the spleens of H9N2-immunised birds. This could be

explained by multiple antigenic stimulations resulting in convergent expansions of public T cells with specific CDR3 sequences [211]. Support for this statement is also provided by the significantly higher levels of private rather than public clones in the naïve, single vaccination, and infection only groups. Parallels to these observations can be drawn from influenza studies in humans and mice, as repeated exposures throughout the lifetime of an individual can lead to clonal focusing and a more limited number of antigen-specific CD8 and (although less pronounced) CD4 expansions in elderly individuals [120,212,213]. Although immune senescence was the major focus of most studies, this explanation is unlikely to be relevant for the current study as the birds were only 35 days of age. However, it is plausible that multiple antigenic stimulation can focus the T cell responses towards oligoclonal expansions in spite of the overall high diversity expected in a young individual, thus biasing the immune response towards particular antigens in subsequent exposures. Given the high degree of clonal sharing (publicness) between individual chickens (see below and **Chapter II**), the effects of this phenomenon may be more pronounced in species which exhibit higher levels of public TCRs within their repertoires.

As the respiratory tract serves as a major site of AIV infection, the trachea was included in the analysis to serve as a proxy for tissues that are directly challenged by viral infection [214]. However, the results revealed that vaccination with an inactivated H9N2 vaccine in the absence of infection can also affect the T cell repertoire in this organ. Indeed, the analyses strongly suggest that both infection and vaccination are able to increase the TCRβ diversity in the trachea, with the clonal homeostasis focusing on smaller (and more diverse) clones. Intriguingly, the opposite pattern would be expected if TCRβ clones expand in response to antigenic challenge. A possible explanation for this pattern is that broad T cell mobilisation and migration to tissues occurs in response to chemokines or other signalling factors, following antigenic stimulation. Although initially (apparently) non-specific, this phenomenon would increase the chances of antigen-specific T cells to become activated following interactions with MHC class I and class II antigen-presenting cells in affected tissues. Indeed, as chickens lack lymph nodes, such a response may compensate for the absence of specialised sites of immune interactions, therefore promoting a more rapid activation of the adaptive immune response. This phenomenon would also be expected to be more pronounced in infected tissues such as the trachea, as more T cells would be

recruited in response to antigenic challenge [215]. Indeed, in terms of the diversity of dominant clones (D_2) in the trachea, it is only the infected groups that maintained the significant differences to the naïve birds. This indicates that the TCRβ clones may have undergone expansions following initial non-specific mobilisation, leading to a diverse polyclonal antigen-specific response. Furthermore, as all groups aside from the infection only birds exhibited higher proportions of public rather than private clones in the trachea, this suggests that infection drives individual-restricted TCRβ responses in this tissue. The infection only group also exhibited higher levels of private clones and lower levels of public clones than the naïve group, further providing support for this hypothesis. Interestingly, both groups that received a single vaccination (with or without infection) also had fewer public clones and more private clones than the naïve, albeit these differences weren't as pronounced. It was only the groups that received a double vaccination that had comparable levels of public and private clones to the naïve. The higher levels of tracheal public clones in these treatment groups may be a consequence of convergent clonal expansions which occur after immunisations with the same antigen, in a manner described above for the spleen. Whereas a single vaccination may stimulate clones which remain at low frequencies (and were deemed private by the current analysis), subsequent vaccination(s) can lead to further clonal expansions of the already primed low frequency antigen-specific T cells which would then be detected as public. This hypothesis deserves further investigation, and the comparison between deep sequencing results of bird groups that were immunised several times may provide answers. If indeed true, subsequent infections and/or vaccinations of the same individuals may also lead to higher public responses, and such findings may improve vaccination practices through the targeted delivery of specific antigens that stimulate public clones.

Unexpectedly, in the bursa, vaccination at a distant subcutaneous site was found to increase the TCRβ diversity for the groups that were immunised with one or two doses of inactivated H9N2 vaccine. Interestingly, this did not happen for any of the infected groups, irrespective of them receiving a vaccination prior to infection. As the bursa is the primary lymphoid site for B cell development in birds and is not traditionally associated with antigen-specific responses, the observed patterns suggest that antigenic stimulation via inactivated vaccines might lead to responses in this organ [77]. A developing B cell response

could then support expansions of cognate antigen specific CD4+ T cells. Although further studies are needed to examine the biology of these events, the observation of clonal expansions in the bursa raises important questions about what determines TCRβ diversity changes in this organ. Previous studies have revealed that αβ T cells can infiltrate this organ and expand in response to local pathological conditions such as infectious bursal disease virus (IBDV) infection [148,158,159], but we are unaware of changes being recorded associated with distant antigenic challenge. Relatedly, our previous findings (see **Chapter II**) concerning the bursal TCRβ repertoire have also revealed a diverse repertoire in spite of the relatively low proportion T cells in this organ (up to 4% of bursal lymphocytes) [104,148]. The functions of bursal αβ T cells in antigen-specific responses was also suggested by the differences between birds with an intact gut microbiota and their germfree counterparts. Given the importance of this organ in shaping B cell development and the fact that T cells had been previously identified in this organ [77], our work suggests that the bursal T cell population may be involved in supporting development of B cells or even in the selection of recently developed B cells for early engagement in an immunologic response. Moreover, the groups that received two or three immunisations had more public than private clones and these groups also exhibited significantly higher proportions of public clones than the naïve, further suggesting that the T cell population in this organ may be involved in antigen-specific responses. This is an interesting hypothesis and further studies might elucidate the functions of bursal T cells in more detail.

Although tissue type and immunisation regime influenced the contribution of public vs. private clonal composition of the repertoires of the analysed birds, the overall proportion of public clones was very high. The observed differences between the public compartments of birds belonging to different groups were mostly attributable to the rare public clones, shared between two and up to 50% of the birds included in this analysis. The more common clones were found at very low levels throughout the tissues, and although some significant differences were present in the ubiquitous public clones, the very small contribution to the repertoire does not allow for biologically meaningful statements to be made regarding the observed patterns in the current analysis. The fact that the most pronounced differences between the immunisation regimes were found in the rare public clones could be explained by the genetic heterogeneity between individuals. Given that the birds in this experiment

were from an outbred chicken line, less TCRβ rearrangements might be expected to be shared across all birds. Regardless, there was a substantial contribution to the repertoire of clones which are shared to some extent between individuals.

The previous analysis of the influences of the microbiome on the TCRβ repertoire (see **Chapter II**) hypothesised several mechanisms through which such a substantial proportion of the repertoire can be, to some extent public. These included the presence of non-classical T cells such as iNKT cells or MAIT cells, and the higher overall proportions in the tracheal tissues might reflect this phenomenon, given the increased presence of these lymphocytes in mucosal tissues [166,167]. However, given the high proportions of public clones observable in the spleen and bursa, it is likely that other factors such as the more compact genomic organisation of the TCRβ locus [87] or even the genetic mechanisms in involved in TCR diversification impose constraints on the realised repertoire in chickens, thereby biasing it towards a higher prevalence of public clones. Furthermore, the consequences of the more compact and dominantly expressed MHC class I and class II genes in the chicken (the "Minimal Essential MHC") [165] may also play a role during T cell development. Given that MHC molecules in chickens have been classified as "fastidious" and "promiscuous" in light of the diversity of peptides which they are able to bind and present to T cells (for a review, see [88]), this may exert important influences on the repertoire and directly affect the degree of clonal publicness in individual birds.

Interestingly, the comparison between the recovered TCRβ sequences in the current analysis and other studies, including the HTS analysis presented in **Chapter II** revealed that a substantial number of sequences are to some extent public, even some that were regarded private in the current experiment. Moreover, as many more sequences were found to be shared between two or more individuals in the current analysis than in the microbiota experiment, it is plausible that the total chicken TCRβ repertoire could be revealed. As the current H9N2 immunisation experiment included data from 29 birds as opposed to only 10 in the microbiota experiment, this strongly suggests that the repertoire analysis of more individuals could exhaust the diversity potential of TCRβ rearrangements, therefore providing a "full picture" of the total chicken repertoire. This is a very intriguing hypothesis, especially as the diversity potential of TCRβ rearrangement in chickens is considered slightly smaller yet still comparable to humans ($>10^{11}$ unique TCRβ rearrangements [109]).

Indeed, future repertoire work in the chicken alongside comparisons with published HTS databases might provide an answer to this question and reveal the implications in antigen-specific responses to pathogenic challenge and vaccination.

Tissue-specific TCRβ clones were also influenced by the H9N2 immunisation regimes in terms of their J gene and V family usage. Moreover, differences in the gene usages between the groups were also apparent when the private and public clonal compartments were considered. Generally, the proportions of Vβ1 clones are highest, followed by the Vβ2 and Vβ3 clones. As found previously (see Chapter II), the majority of Vβ3 clones are public, potentially indicating the limited diversity potential following gene rearrangement, as only one Vβ3 family gene is present in the chicken genome [111]. At the same time, the higher proportion of Vβ1 genes as opposed to Vβ2 genes may also be a consequence of more Vβ1 family genes being available (10 Vβ1 vs. 4 Vβ2) [76]. In the spleen, most differences observable in Vβ1 gene usage between the vaccinated and/or infected birds was due to higher proportions of Vβ1 public clones in these groups. At the same time, all of these groups also exhibited lower proportions of Vβ2 private clones in the spleen, which suggests that clonal expansions following immunisation(s) with vaccination and/or infectious challenge may have shifted the balance of Vβ2 private clones in favour of Vβ1 clones. Interestingly, the same pattern was observable in the bursa, but only for the bird groups that were subjected to more than one immunisation, either through double vaccination or vaccination(s) and infection. This further suggests that the bursa may be involved in an antigen-specific response, and that the TCRβ repertoire changes in this organ are dependent on the amount of antigenic stimulus to which the birds were subjected to.

Less clear patterns in terms of Vβ family usage were observable when considering the tracheal samples. By contrast, the only differences regarding overall Jβ family usage were present in the trachea, with naïve birds generally exhibiting less Jβ1 and Jβ3 clones and more Jβ2 clones than the vaccinated and/or infected groups. Furthermore, when considering the public vs. private clonal contributions of these Jβ families, the differences in Jβ2 were mirrored in the public clones, whereas the other Jβ families showed higher contributions of private clones in the H9N2 antigenically stimulated birds. Together, the differences indicate that different H9N2 immunisation regimes influence tissue-specific

TCRβ clonal compositions in terms of their VDJ rearrangements, with both V and J gene usage being affected in a tissue-dependent manner.

Several clonal expansions were found restricted to groups that were subjected to particular immunisation treatments. Interestingly, all of the group-restricted and expanded clones were public, the majority of which being mostly detected within the birds of a single group. Infection-restricted expanded sequences were found across chickens from all three infection groups, but the majority showed consistent expansions in one of the immunisation groups and not the others. The same pattern was observed in the clonal expansions restricted to the uninfected birds. Environmental factors are unlikely to explain these patterns, as the bird groups were housed together until the infection on day 21, when the single vaccination and infection group and the double vaccination and infection group were moved to one isolator, and the infection only group was moved to another. The uninfected groups remained together throughout the experiment. As such, environmental factors alone cannot account for the group-specific expansions. At the same time, cross-contamination is unlikely to explain these patterns given that multiple groups were processed at the same time and precautionary measures were taken to minimise the chances for sample contamination to occur.

A more plausible explanation for the group-specific clonal expansions is that particular immunisation regimes (and thus particular antigenic stimuli) bias the TCRβ repertoire in a consistent manner across multiple birds. Furthermore, as fewer clones were found to be restricted to the uninfected groups as opposed to the infected groups, this suggests that infection is able to drive differential responses as opposed to immunisations with homologous H9N2 inactivated vaccine alone. This may relate to the different MHC antigen presentation pathways underpinning vaccination and infection, as the former mostly accesses the MHC class II pathway whilst the by-products of intracellular viral replication during infection can be presented via the MHC class I pathway as well. Indeed, AIV infection is known to induce better CD8+ T cell responses than vaccination with an inactivated vaccine, and this may be reflected in the more numerous infection-restricted clonal expansions which were observed in this analysis. Interestingly, two clones (CDR3 amino acid sequences: CASSLGDRNMIF and CAASDRDRGIDMIF) were found across birds from vaccinated groups both in the presence and absence of infection. These clones

may represent αβ T cells that react to both vaccination and infection, and their specificities could potentially target antigens derived under both immunisation scenarios. Identifying such T cell specificities (including the sequence of the TCRα chains) could facilitate the targeted delivery of antigens through vaccination that better stimulates T cell responses to infection. This is an interesting hypothesis, and future studies that will examine both TCRα and TCRβ repertoires (e.g. through single-cell sequencing) in response to infection and vaccination with H9N2 AIVs might identify candidates and ultimately improve vaccination practices against these pathogens.

Collectively, these results support the findings revealed by the IgM and IgY repertoire analyses (see **Chapter IV**), as both the number and nature of the immunisations influenced the characteristics of the repertoire. For all the analysed tissues, consistent patterns were found that mirror and/or complement the results of the IgM and IgY repertoires. Indeed, the analysis of the TCRβ repertoire of H9N2 vaccinated/and or infected chickens provides important information on the adaptive immune system and on how antigenic stimulation via vaccination or infection with AIV subtype H9N2 alters the characteristics of the adaptive immune receptor repertoire.

Chapter VI: Thesis Summary, General Discussion, and Conclusions

VI.1. Thesis and chapter summary

In this thesis, I have examined the adaptive immune responses of chickens that were subjected to AIV H9N2 infection and/or vaccination(s). The main focus of the thesis was the adaptive immune receptor repertoire, for which the diversity of the systemic antibody responses and T-cell mediated immunity were analysed. Important information about the avian tissue-specific T and B cell immunity was revealed in terms of the IgM, IgY, and TCRβ repertoires and their responses to H9N2 infection and vaccination. At the time of writing, no published works on the avian adaptive immune repertoire was carried out in the context of avian influenza immunisations, in spite of the global importance of this pathogen for the poultry sector and human and animal health more broadly.

In the first chapter, I provided a general introduction to influenza A viruses emphasising their biology, ecology, and the impacts which they cause worldwide by infecting their host species. From both wild and domestic animals, influenza A viruses can readily jump the species barrier and cause the pandemics and seasonal epidemics in humans, causing significant disease-associated morbidity and mortality. Given that the natural reservoir of influenza A viruses is in wild aquatic birds, the focus of this thesis were Avian Influenza Viruses (AIVs), as a better understanding of the immune systems of their avian hosts has the potential to improve current and future prevention and control strategies. In the second part of the first chapter, I reviewed the current knowledge of the avian immune system and the immune responses to AIV infections and vaccinations of avian hosts. In addition, I described some of the avian-specific features of the immune system and the species-specific differences that influence susceptibility and pathogenesis, given that some bird species (e.g. ducks) are more resistant than others (e.g. gallinaceous poultry). Although both innate and adaptive immune responses were described, focus was put on the latter, as the adaptive immune system exhibits immunological memory which constitutes the basis for vaccination against AIVs. I concluded the chapter with information about the avian T and B cell

immune receptor repertoire and presented some of the parallel work done in mice and humans during influenza virus infections and what the benefits of mirroring these studies in avian hosts could bring.

The second chapter of the thesis describes the reagents, methods, and custom-made laboratory and computational techniques used throughout the subsequent chapters. Two major protocol development sections are present in this chapter, with one describing a high-throughput flow cytometry staining methodology which was developed for analysing different splenic lymphocyte subpopulations in chickens. The other main protocol development section in this chapter presents the analysis of the chicken TCRβ repertoire in the context of microbial colonisation. Of note is that this protocol development section was initially intended to comprise an entire data chapter of the thesis. Indeed, the original plan for the thesis was to analyse the effects of microbial colonisation in combination with H9N2 infection and vaccination. Unfortunately, due to the COVID-19 pandemic and associated lab closures, the animal experiment that was intended to provide the necessary samples for this work was cancelled, and thus the structure of the thesis was reorganised in order to focus entirely on the H9N2 vaccination and/or infection scenarios. However, as the methodology for chicken repertoire analysis was optimised using the microbial colonisation experiment samples, the work was included as part of the thesis in the protocol development section. As such, this subsection constitutes the first published high-throughput sequencing analysis of the chicken TCRβ repertoire and provides important information on properties such as the tissue-specific diversity, V and J gene usage, and public vs. private TCRβ clonal composition and the influence of the intestinal microbiome on these features of the repertoire. Lastly, the second chapter contains a description of the H9N2 vaccination and challenge animal experiment from which the samples for the analyses in this thesis were derived.

Chapter III of the thesis constitutes the first main data chapter and within it I examine the basic immune responses of chickens to H9N2 infection and vaccination. For this, I measured the H9N2-specific serum IgM and IgY antibody responses as recorded by custom-made ELISAs, and their protective abilities via HI assays. In addition, for the samples of the last time point of the experiment (day 35), I utilised the custom-made high-throughput flow cytometry protocol to measure the lymphocyte frequency changes in the

chickens' spleens. The results revealed that H9N2-specific IgM and IgY antibody responses developed following vaccination(s) and/or infection, in a time-dependent manner whilst also being higher in the groups that received multiple immunisations. At the same time, given that an important part of the antibody responses to AIV infection or vaccination are directed against the immunodominant haemagglutinin (HA) protein, the haemagglutination inhibition (HI) potential of the serum was quantified and found to be correlated with the IgM and IgY responses. These results proved that the H9N2 vaccinations and/or infection of chickens triggered protective antibody immune responses. Furthermore, the qPCR results for the virus in during the course of infection revealed that previously vaccinated birds had a shorter duration of infection and exhibit less viral shedding on average than their unvaccinated counterparts. Lastly, the results of the flow cytometry staining analysis on the spleen samples of the day 35 birds (last time point of the experiment) revealed a significantly higher frequencies of B cells and CD4+ αβ T cells in all of the immunised groups when compared to the naïve birds, further supporting the development of antibody-mediated immunity in response to H9N2 vaccination and/or infectious challenge. At the same time, some immunisation regime-specific differences to the naïve birds were observable in some groups in terms of their γδ T cell splenic subpopulations, indicating that these lymphocytes may be involved in the adaptive immune responses to H9N2 vaccination and/or infection. Together, the results of Chapter III served both as a confirmation of the successful adaptive immune responses that were mounted against AIV H9N2 and as a basis for the repertoire analyses which were carried out in the subsequent chapters.

In Chapter IV, I examined the characteristics of the IgM and IgY repertoires of chickens that were vaccinated against and/or infected with H9N2 AIV. For this, I focused on the samples derived from the same birds on which the spleen flow cytometry analyses were performed in Chapter III. The IgM/IgY sequences were obtained from the trachea, spleen, and bursa of Fabricius that were harvested on the last day of the experiment (day 35). By using the computational methods described in Chapter II, I examined the group-specific clonal homeostasis, the diversity and the public vs. private IgM and IgY repertoire compositions in the analysed tissues. Furthermore, I analysed the clonal expansions that were restricted to specific immunisation conditions (vaccination, infection, or absence of

infection) and the CDR3 sequences that were found in both IgM and IgY forms within the samples. The results revealed that both nature of immunisations (vaccination or infection) and the number of immunisations received by the birds impacted the diversity profiles of the analysed tissues. Further support of these observations came from the analysis of the treatment-restricted clonal expansions the majority of which indicating consistent expansions of particular clones across the same groups. Lastly, a high overall proportion of public clones was identified in the IgM and IgY repertoires of the birds, a characteristic which was also influenced by group and tissue type. This suggested that the immunoglobulin diversification via gene conversion in birds may be less efficient than the RAG-dependent V(D)J rearrangement diversification mechanism in mammals and bias the repertoire towards specific CDR3 clones which are shared across individuals. Together, the results of the IgM and IgY repertoire analysis in Chapter IV provided important information about the chicken systemic antibody repertoires and the modifications that occur following H9N2 infection and/or vaccination.

The TCRβ repertoires of the birds was also examined in Chapter V, which constituted the last main data chapter of the thesis. This was partly because the flow cytometry results of Chapter III revealed important differences in the CD4+ αβ T cell populations of the groups, suggesting that the specific H9N2 immunisation regimes stimulated their αβ T cells. The analysis proceeded similarly as for the microbial colonisation experiment presented in the protocol development section of Chapter II, analysing the diversity, V family and J gene usage, public vs. private compositions, and treatment-restricted expansions of the TCRβ repertoires. The results revealed tissue-specific influences of particular immunisation regimes, including differences in diversity and specific V family and J gene usages. These TCRβ observations were consistent with the IgM and IgY repertoires analysed in Chapter IV, and further suggested that both nature and number of immunisations are important in determining the composition of the repertoire within the analysed tissues. At the same time, a high proportion of the TCRβ repertoire was found to be public, results which supported the findings of the TCRβ analysis that was carried out during the protocol development presented in Chapter II. Indeed, when the two databases were compared, a large number of sequences both at the nucleotide and at the amino acid levels were found to be shared. These also included CDR3 sequences which were deemed private when the databases from

the two experiments were considered on their own. Furthermore, the relative proportions of public vs. private clones in the groups were influenced by the particular immunisation regime to which the birds were subjected. These findings, together with the IgM and IgY repertoire results from Chapter IV, are indicative of the "public nature" of the chicken adaptive immune repertoire, with many CDR3 sequences being shared by multiple individuals. Given the importance of T and B cell responses in protecting their avian hosts against infection and the implications of the current findings on practices such as vaccination, the results of the thesis have provided a detailed insight into the immune repertoires of chickens which serves as a solid foundation for future research on the avian adaptive immune system.

VI.2. Main findings and general discussion

The repertoire analysis presented in this thesis focused on sequences derived from chicken tissues which are immunologically relevant in B and/or T cell responses. The protocol development of the repertoire analysis included the spleen, bursa, and 3 other mucosal tissues which were part of the intestinal tract: jejunum, caecum, and colon. These tissues were used because of their relevance in microbial colonisation and were thus included in order to reveal differences between germ-free birds and their conventional counterparts. However, the H9N2 chapters of the thesis focused on the spleen, bursa of Fabricius, and the trachea. As for the protocol development, the spleen was chosen given its importance in antigen-specific immune responses, with this organ harbouring large populations of T and B lymphocytes [76]. As chickens lack lymph nodes, the spleen is both a major site where antigen presentation to T cells occurs and where B cell germinal centres are formed in response to antigenic challenge [104]. Furthermore, the spleen also harbours a large proportion of naïve T cells, with their CDR3 sequences allowing for a more in-depth exploration of the naïve repertoire. The bursa was chosen because of its role in B cell development, as this is the primary lymphoid organ of birds where B cell diversification occurs via gene conversion [112]. Moreover, given that more than 96% of lymphocytes in the bursa are B cells [104,148], T cell repertoire sequences from this organ were initially intended as a negative control. Lastly, the trachea was selected given its relevance during

H9N2 AIV infection, as it is a major site where viral replication occurs [214]. Although the T and B cell populations in this tissue are not large, changes in the TCR and BCR repertoires were expected to occur following infection with H9N2 and thus potentially revealing antigen-specific CDR3 sequences that respond to viral challenge. As such, the repertoire analyses of spleens, bursas, and tracheas of chickens had the potential to reveal the way in which the avian adaptive immune repertoire is impacted by H9N2 infection and/or vaccination. Indeed, the results showed important differences to the naïve chickens, in a both tissue- and group-specific manners.

As the largest secondary lymphoid organ, the splenic repertoires were significantly affected by both the nature (vaccination and/or infection) and number of H9N2 immunisations that the birds received. The effects of antigenic stimulation were observable in both the TCRβ and IgM and IgY repertoires when the immunised groups were compared to the naïve birds. Interestingly, for the TCRβ repertoire, H9N2 infection was suggested to drive the diversity landscape towards higher clonal dominance more than vaccination(s). This was also more evident in the groups that were vaccinated either once or twice before infection, which indicated that the higher antigenic load in those groups might also be a factor. Indeed, the multiple immunisation (either by vaccinations or vaccination(s) and infection) groups had higher proportions of public clones, a pattern which is suggestive of clonal focusing on particular antigens. Similar observations were made regarding the splenic IgM and IgY repertoires, which exhibited more dominant clones than the naïve but only in the multiply immunised groups. However, the higher proportions of public TCRβ clones in the multiply immunised groups was not mirrored in the IgM and IgY repertoires, although the double vaccinated group (in the absence of infection) did exhibit more public clones than the naïve chickens. Overall, less clear patterns concerning the differences between the groups were observed in the splenic IgM and IgY repertoires when contrasted to the TCRβ repertoire. Regardless, these were still suggestive of antigen-driven effects, with both nature and number of immunisations dictating the outcome on the repertoire. Indeed, the cumulative results of the repertoire analyses performed on the spleen samples confirmed expectations and also revealed that antigen-specific responses are mounted in response to vaccination and/or infection, with particular infection-restricted or vaccination-restricted clones being found at expanded levels across multiple birds,

especially within the same group. This was observable in both the TCRβ and the IgM and IgY repertoires, with the same expanded clones being found across multiple individuals which generally belonged to the same group. Furthermore, the pattern was observable across all the analysed tissues, not just for the spleen samples. These findings strongly support that sequential antigenic stimulations differentially dictate the adaptive immune responses in the spleen based on their nature and numbers.

An important finding of the thesis was the suggested involvement of the bursa of Fabricius in antigen-specific adaptive immune responses. Although this organ is not classically associated with antigen-specific responses [77], B cell expansions in response to antigen were suggested by the IgY+ population present in the bursa, alongside expanded clones in both IgM and IgY repertoires. The antigen-specific expansions following H9N2 vaccination(s) and/or infection were further suggested by the IgM and IgY differences between the of the immunised groups and the naïve birds in terms of diversities and public vs. private compositions of the repertoires. Interestingly, this was also observable in TCRβ repertoire of the bursa, in spite of the very low proportion of T cells found in this organ (up to 4%) [104,148]. As B cells comprise the majority of bursal lymphocytes, the function of the bursal T cells remains unknown [77,112]. It is not unlikely that both the B and T cells present in the bursa may interact with and expand in response to exogenous antigens derived from the gastrointestinal tract, given the connection that the bursa has with the intestines via the bursal duct. Indeed, this was suggested by the TCRβ repertoire analysis that was carried out as part of the protocol development section in Chapter II, where I performed the TCRβ repertoire analysis of germ free and conventional chickens. However, in the H9N2 experiment, given that differences to the naïve birds were found in the vaccinated and/or infected groups, the bursa may contribute to the adaptive immune responses to a much greater extent than previously believed. Future research examining the involvement of the Bursa during antigen-specific responses coupled with analyses of the bursal T cells may provide additional insight into the immunological roles of this avian lymphoid organ.

Although a major site of viral replication [214], the tracheal repertoires of the vaccinated groups (in the absence of infection) also showed changes to the naïve birds. In addition, both infection and vaccination (either alone or in combination) increased the diversity of

the TCRβ, IgM, and IgY repertoires. These are interesting patterns, especially given the fact that H9N2 infection in the trachea would be expected to drive antigen-specific expansions and thus decrease the clonal diversity in this tissue [215]. However, I hypothesised that in the absence of lymph nodes, a broad lymphocyte mobilisation might occur in birds as a response to antigenic stimulation. This initially nonspecific response would maximise the chances of both antigen presentation to T cells and activation of antigen-specific T and B cells. Such a scenario also explains why the infected birds generally exhibited a higher diversity in terms of dominant clones, as more antigen-specific T and B cells would undergo expansion and be recruited to the site of viral challenge. The tracheal samples also exhibited the largest proportions of public clones in the TCRβ, IgM, and IgY repertoires of all the analysed tissues, suggesting that (at basal levels) the lymphocytes present in this tissue have CDR3 sequences that respond to antigenic stimuli that are shared between individuals. However, the infection only group was generally the only one with a higher proportion of private clones when compared to the naïve, indicating that infection drives individual-restricted T and B cell responses in those tissues. The effects were not observable in the groups that were vaccinated prior to infection, potentially because the multiple antigenic stimulation resulted in convergent expansions across multiple individuals. As such, although the trachea seems to be populated with T and B lymphocytes which possess CDR3 sequences which are shared between birds, antigenic stimulation may trigger a broad migration of lymphocytes in the body which can localise expanded, individually-restricted (i.e. private) clones in this tissue if antigens are indeed present (e.g. during infection). This deserves further investigation, and future studies that examine the lymphocyte migrations in response to antigens coupled with repertoire sequencing might confirm the aforementioned hypothesis.

One of the most important findings of the thesis was the high contribution of public CDR3 sequences to the chicken adaptive immune repertoire. Interestingly, this applied not only for IgM and IgY repertoires, but also for the TCRβ repertoire. These results raise important questions about the total repertoire diversity potential in chickens, and strongly suggest that intrinsic factors constrain both the TCR and BCR repertoires towards specific CDR3 sequences that are shared across multiple individuals. In Chapters II, IV, and V, I have discussed some of the mechanisms that could potentially be at play in generating the high

degree of public clones, both for TCRβ and IgM/IgY. The particularities of the avian immune system are the most likely candidate, and several possible explanations were put forward. For the antibody repertoire, I hypothesised that the process of gene conversion may not be as efficient in diversifying the immunoglobulins as the RAG-dependent V(D)J rearrangement process observable in mammals. However, V(D)J somatic rearrangement is also used by birds in the diversification of their TCR repertoires [77], which also showed a high proportion of public clones (at least for the TCRβ). Although less Vβ and Jβ genes are available in chickens as opposed to mice and humans, the TCRβ diversity theoretically attainable in avian species is still of comparable orders of magnitude. Other hypotheses for the high proportions of public TCRβ clones included the consequences of the avian "single dominant MHC" [88,165], a potentially higher presence of non-classical T cells in the analysed tissues [166,167], and even the results of birds being species with high circulating frequencies of γδ T cells [76,78,79] (and thus a possibly higher importance of this T cell lineage). However, these hypotheses either explain indirectly or fail to account for the high degree of public immunoglobulins, and it is therefore likely that the above-mentioned factors contribute jointly to the observed high proportions of public IgM, IgY, and TCRβ clones.

An intriguing hypothesis was suggested given that an even higher number of TCRβ clones were found to be shared between individuals when the sequence databases of the H9N2 experiment and the microbial colonisation analysis presented in Chapter II were compared. As TCRβ clones that were regarded as private within each experiment were found to be public when the two databases were taken together, this indicates that many of the private sequences may in fact be public and thus be shared between multiple individuals, at least to a certain degree. If this hypothesis holds, then the repertoire sequencing of more individuals would eventually plateau in terms of the total number of unique clones being identified. This scenario may also apply to the IgM and IgY repertoires, given that high proportions of public clones were found within the birds of the H9N2 experiment, irrespective of their immunisation status. However, more sequence data would be required to test this hypothesis, and unfortunately this was unavailable at the time of writing the thesis.

Lastly, the chicken TCRβ repertoire analyses performed as part of the thesis research have also revealed a previously undescribed contribution of the Vβ3 family [111] clones within

specific tissues, particularly in the intestinal samples that were obtained from conventional microbiota and germ-free chickens. Intriguingly, the majority of these clones were highly public, suggesting that a limited potential for rearrangement exists for the Vβ3 family. Given that only one Vβ3 gene is available for somatic rearrangement, this may simply be a consequence of the genomic organisation and preferential rearrangements that occur following VDJ recombination. Regardless, unravelling the functional implications of Vβ3 clones given their high degree of publicness and preferential localisation in specific tissues remains an interesting topic for future studies, for which this thesis has provided a useful starting point.

VI.3. Caveats and future directions

The repertoire analysis of the chicken TCRβ, IgM, and IgY that was carried out as part of this thesis work provided important information about the adaptive immune responses in the context of H9N2 vaccination and/or infection at a very high resolution, reaching the level of individual clones. However, it is worth noting some of the caveats of the current research, and presenting the reasoning behind the design, methodology, and flowthrough of the thesis analyses in more detail.

The design of the animal experiment from which the samples were derived from included multiple conditions which enabled the analysis of vaccination against H9N2 in a single or double dose and infection itself. In addition the chicken groups also included combinations between these immunisation regimes, thus controlling for treatment-specific effects which would have not otherwise been captured. This necessarily implied adjusting the group sizes to lower numbers of individuals for logistical reasons. Indeed, although larger sample sizes would have been useful in controlling more of the individual-specific heterogeneity, the patterns that were observed were generally consistent both within and between the groups, indicating that the results were not simply the result of stochasticity. Although future research can focus on specific conditions in more detail (e.g. either infection or vaccination) and thus can include more individuals per treatment group, the analyses carried out as part of this thesis have not only revealed that significant changes occur in the repertoires of

birds after H9N2 vaccination and/or infection, but also provided a solid foundation for future research that will examine these processes in more detail.

The repertoire analysis presented in this thesis focused on the bulk sequencing of lymphocyte receptors. As opposed to single-cell repertoire sequencing, this approach did not allow for the pairing of TCR and BCR light and heavy chains, which also had the potential of identifying the antigen specificities of those receptors. However, bulk sequencing provided a general overview and a much higher sequencing depth of the repertoire landscapes, whilst permitting the examination of expanded clones that were only found under particular immunisation conditions, thus revealing potential correlations to antigen-specific responses. Even if the immunoglobulin light chain (IgL) or the TCRα repertoires would have been analysed, determining the exact light and heavy chain pairing is generally difficult to realise based on bulk sequence alone. However, if the same patterns of publicness apply to the IgL and/or TCRα, and expanded clones restricted to particular immunisation are found, the artificial pairing based on sequence data alone would be feasible. Although this was outside the scope of the current analysis, the bulk sequencing of the chicken repertoire presented in this thesis suggests that the artificial identification of antigen-specific light and heavy chain pairs is possible. If true, future studies that examine both the light and heavy chains of lymphocyte receptors can narrow the search for antigen specificity down to very few pairing options. Classical methods involving cloning the identified receptors and screening using antigens could subsequently determine the true antigen-specific T and B cell receptors, thus opening new avenues in avian immunological research, including the generation of monoclonal antibodies. This represents an interesting avenue to explore, for which the bulk repertoire sequencing methodology applied in this thesis has provided a solid foundation to build upon.

The IgM and IgY antibody repertoires were chosen given their importance during systemic responses. As a consequence, the IgA repertoire was not analysed as part of the thesis research. Although the IgA responses are important during infections with pathogens such as AIVs that infect via mucosal surfaces, immunisations with inactivated vaccines are known to be poor simulators of mucosal antigen-specific responses [42]. In addition, as opposed to the circulating IgM and IgY antibodies which can be measured through ELISA and HI assays, circulating IgA is found at very low levels, and is not known to contribute

towards systemic protection against viral challenge. Indeed, by focusing solely on the systemic IgM and IgY antibody responses and the corresponding immunoglobulin repertoires in the tissues of interest, a much more detailed picture of the avian humoral immune responses was provided during H9N2 infection and vaccination. As the experiment used an inactivated H9N2 vaccine after which weak IgA responses would be expected to develop, the focus on IgM and IgY responses was more appropriate in order for comparisons to be made across all the analysed groups.

Time constraints for completing the thesis research were also a factor with regards to the methodology and choice of samples. The initial experimental design included 2 additional cull points which were intended to evaluate the repertoires at the peak of infection (3 dpi) and one week following infectious challenge. Due to time constraints, the analysis focused only on the day 35 samples, which correspond to two days post infection. Indeed, future work carried out on the samples from the earlier time points will prove informative regarding time- and age-dependent changes in the TCR and BCR repertoires in the context of H9N2 vaccination and/or challenge. Another time constraint related to the optimisation of the custom flow cytometry protocol for cell sorting. Following repertoire sequencing of sorted cells, the phenotype identification of TCRβ sequences belonging to CD4+ and CD8+ αβT cells would have been possible. This being said, the focus of the work was a characterisation of the repertoire itself and not the functional involvement of the lymphocytes, with this topic remaining an interesting avenue for future research.

Several notable observations about the choice of the experimental design require contextualisation, particularly in terms of time constraints. Importantly, contingencies needed to be put in place due to the COVID-19 pandemic, as this delayed the progress of experimental work. These included the restructuring of the initial thesis aims and objectives as a consequence of laboratory closures and the cancellation of a planned animal experiment. The initial thesis plan was to examine the influence on the TCRβ repertoire of both the microbiota and antigenic challenge through vaccination and/or infection, by using H9N2 as a model pathogen. The animal experiment which did not materialise due to COVID-19 would have combined the two immunological conditions by including the administration of probiotics under similar conditions as for the animal experiment that was part of the repertoire work presented in this thesis. Given that this was not possible, the

thesis was refocused exclusively on the repertoire under H9N2 vaccination and/or challenge, and the IgM and IgY repertoires were included given the results of the flow cytometry carried out on the spleen samples that were harvested from the birds. Therefore, although the thesis was restructured given the constraints imposed by the pandemic, a much more in-depth analysis was performed on the chicken adaptive immune responses following H9N2 antigenic stimulation via vaccination(s) and/or infection.

As described previously, one of the main findings of the repertoire analysis performed in this thesis was the high proportions of public clones which were observable in the TCRβ and immunoglobulin repertoires. One of the potential features of the avian immune system that could explain such an interesting result is presence of a single dominant MHC in birds. This feature may impact T cell selection in the thymus, and also antigen presentation in the periphery, and thus restrict the potential of MHC-TCR interactions (including with B cells) which would consequentially lead to a reduction in the realised repertoires. As the chicken MHC molecules were previously classified into fastidious (specialist) and promiscuous (generalist) haplotypes, this could explain the high proportion of public clones, especially within the TCRβ repertoire. It is possible that if the birds used in the two experiments presented in the thesis all possess fastidious MHC molecules, a constraint in TCR thymic selection would have been imposed. As a consequence, this may in turn have led to a convergence between the repertoires of the birds. As such, the MHC typing of individuals would have provided information about the nature of the MHC of the birds and whether or not they share the same haplotype. However, this latter hypothesis is unlikely as the chickens from which the samples were derived from an outbred line (White Leghorn) as opposed to an inbred line which would be genetically very similar. Although MHC typing of individual birds and assessing the nature of their MHC haplotypes was outside the scope of the thesis, continuations of this research can provide the answers and improve our understanding of the avian adaptive immune repertoire.

VI.4. Conclusion

The analysis of the chicken adaptive immune repertoire presented in this thesis constitutes the first approach which uses high throughput sequencing technology for analysing the

TCR and BCR repertoire changes that occur following vaccination and/or infection with avian influenza virus subtype H9N2. At the same time, this research reveals important information about the biology of the chicken adaptive immune receptor repertoire which serves as a solid foundation for future work on avian immunology in the contexts of both health and disease. My findings include novel information about the T and B cell responses in avian hosts that could ultimately be harnessed in order to improve future practices in the poultry industry especially regarding the prevention and control of avian infectious diseases through vaccination.

Appendix I: Supplementary figures and information for the thesis data chapters

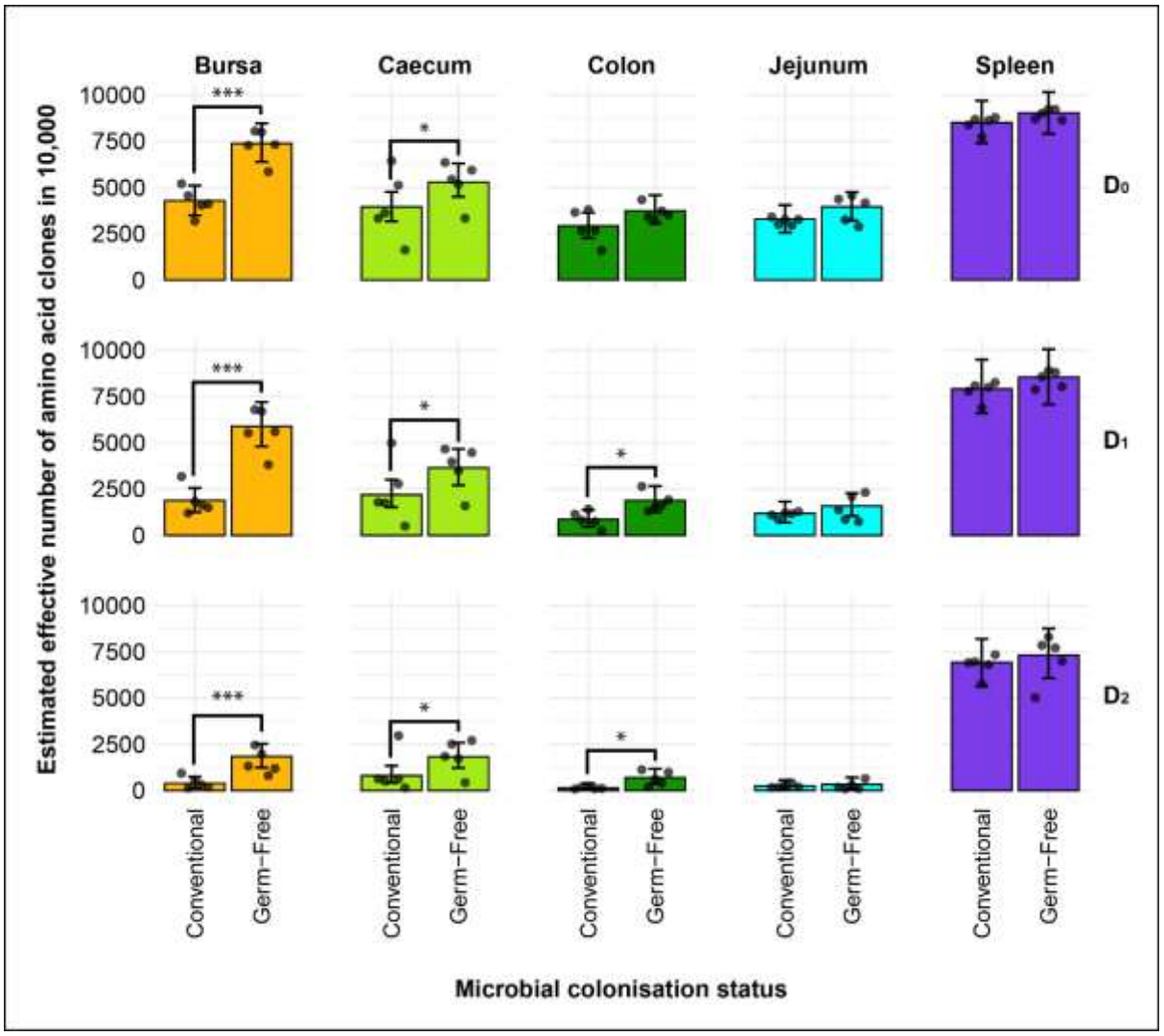

Figure A. 1: *Effective diversity within conventional and germ-free samples at the amino acid level.*

Different rows show the effective number of clones corresponding to clonal richness (D_0), the typical clones (D_1), and dominant clones (D_2). Tissues are colour coded for the bursa (orange), caecum (green), colon (dark green), jejunum (light blue), and spleen (purple). Dots represent individual bird observations of the effective number of species calculated in each tissue for the corresponding Hill number values. Error bars show the 95% bootstrap confidence intervals for the point estimates generated from 1000 simulations of the model. Statistically significant differences between the model estimates are depicted above the plots based on their corresponding p-values: * = $p < 0.05$; ** = $p < 0.01$, *** = $p < 0.001$.

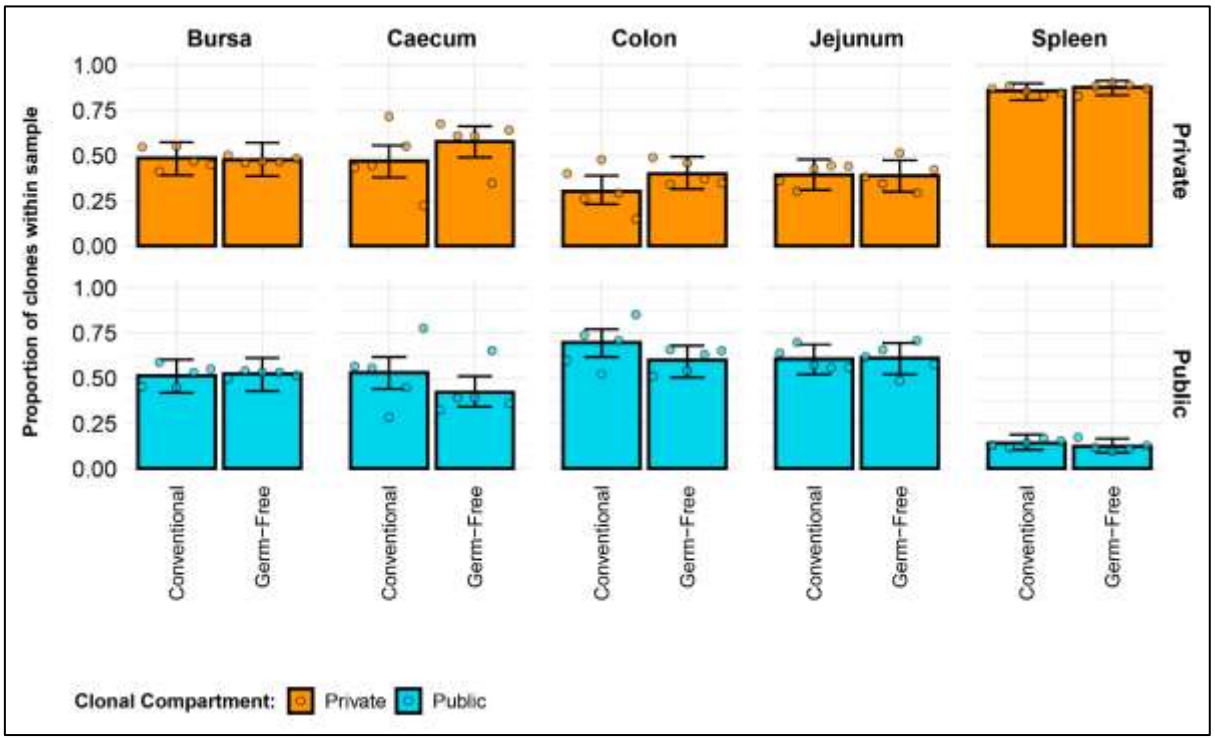

Figure A. 2: *Microbial status does not affect the proportional contribution of private and public CDR3 nucleotide sequences to the TCRβ repertoire.*

Private (individual-restricted) clones are shown in orange. Public clones (shared between two or more individuals) and are shown in light blue. Dots represent individual bird observations of public and private clonal compartments. Error bars represent 95% bootstrap confidence intervals for the point estimates generated from 1000 simulations of the model. Statistically significant differences between the model estimates are depicted above the plots based on their corresponding p-values: * = $p < 0.05$; ** = $p < 0.01$, *** = $p < 0.001$.

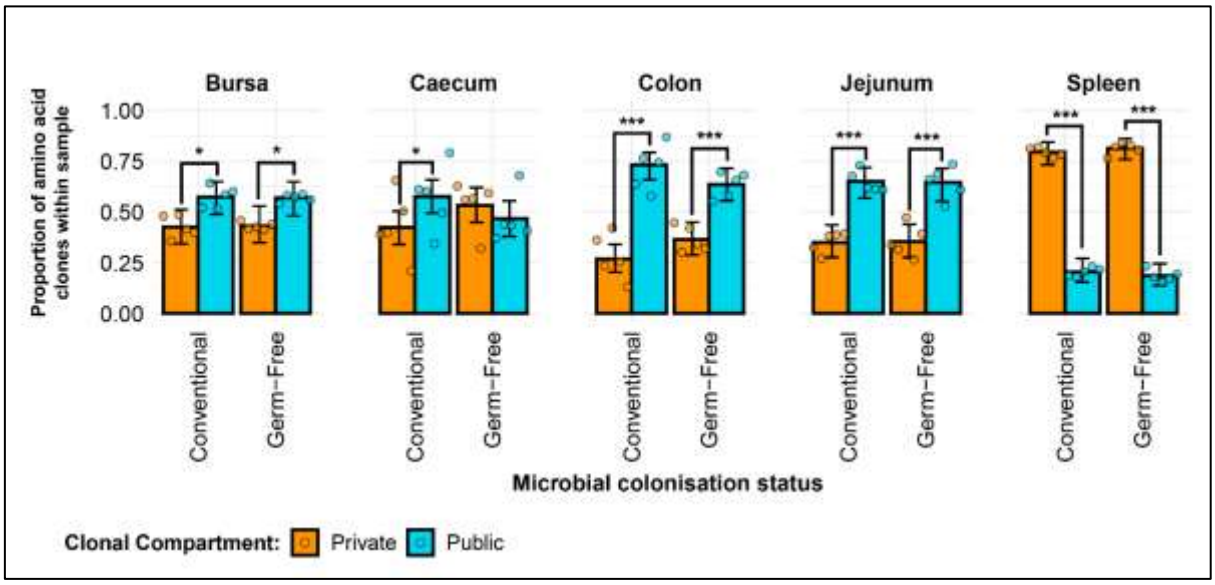

Figure A. 3: *TCRβ clone CDR3 amino acid public and private compartments.*

Private (individual-restricted) clones are shown in orange. Public clones (shared between two or more individuals) and are shown in light blue. Dots represent individual bird observations of public and private clonal compartments. Error bars represent 95% bootstrap confidence intervals for the point estimates generated from 1000 simulations of the model. Statistically significant differences between the model estimates are depicted above the plots based on their corresponding p-values: * = $p < 0.05$; ** = $p < 0.01$, *** = $p < 0.001$.

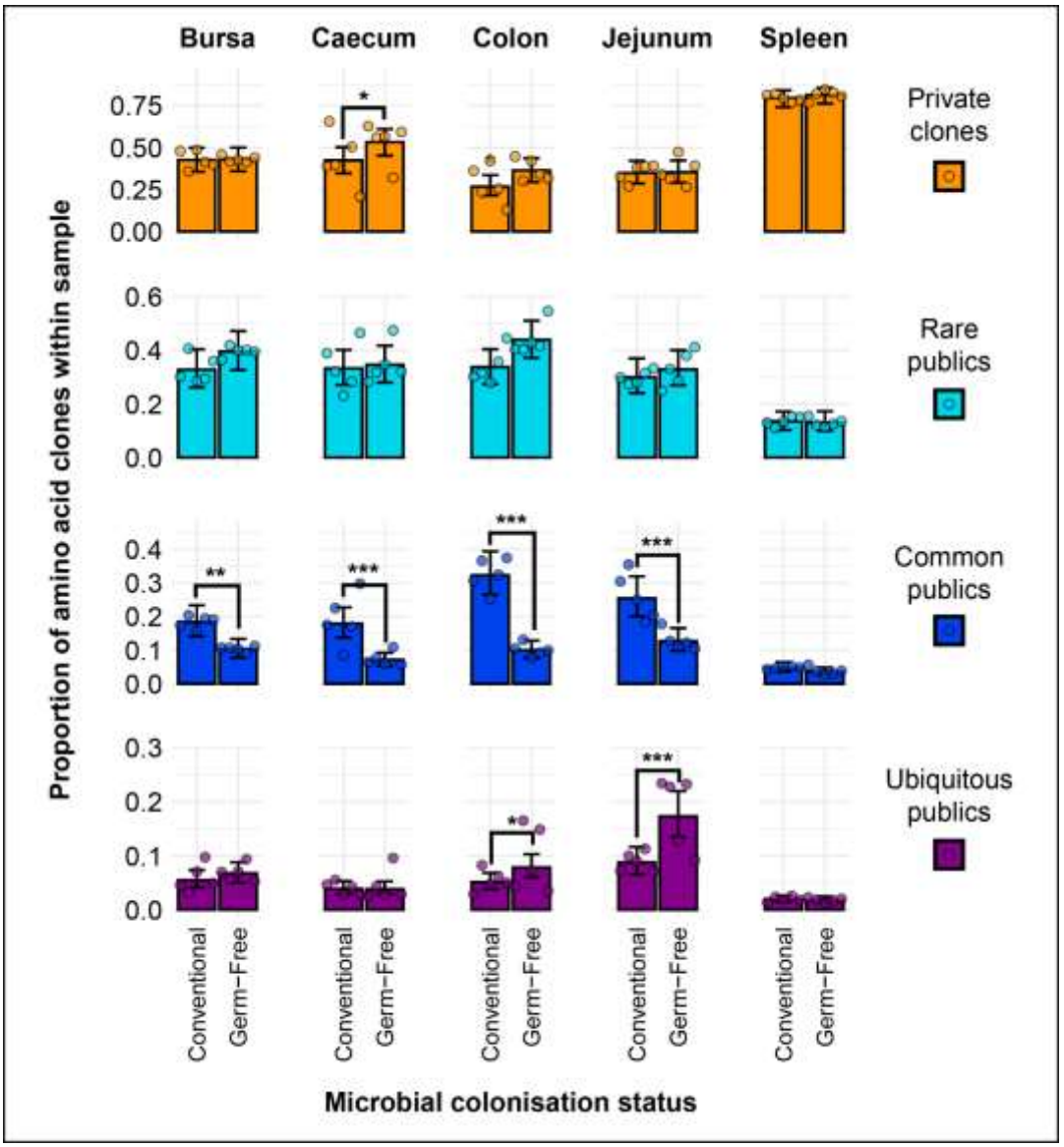

Figure A. 4: *TCRβ clone CDR3 amino acid private and public compartments based on different levels of clonal sharing between birds.*

Private (individual-restricted) clones are shown in orange. Rare publics (shared between ≥2 individuals and up to 5) and are shown in light blue. Common publics (shared between ≥5 and up to 9 birds) are shown in dark blue. Ubiquitous publics (found in all birds which were incorporated in the analysis) are shown in purple. Dots represent individual bird observations of private and distinct public clonal compartments. Error bars represent 95% bootstrap confidence intervals for the point estimates generated from 1000 simulations of the model. Statistically significant differences between the model estimates are depicted above the plots based on their corresponding p-values: * = $p < 0.05$; ** = $p < 0.01$, *** = $p < 0.001$.

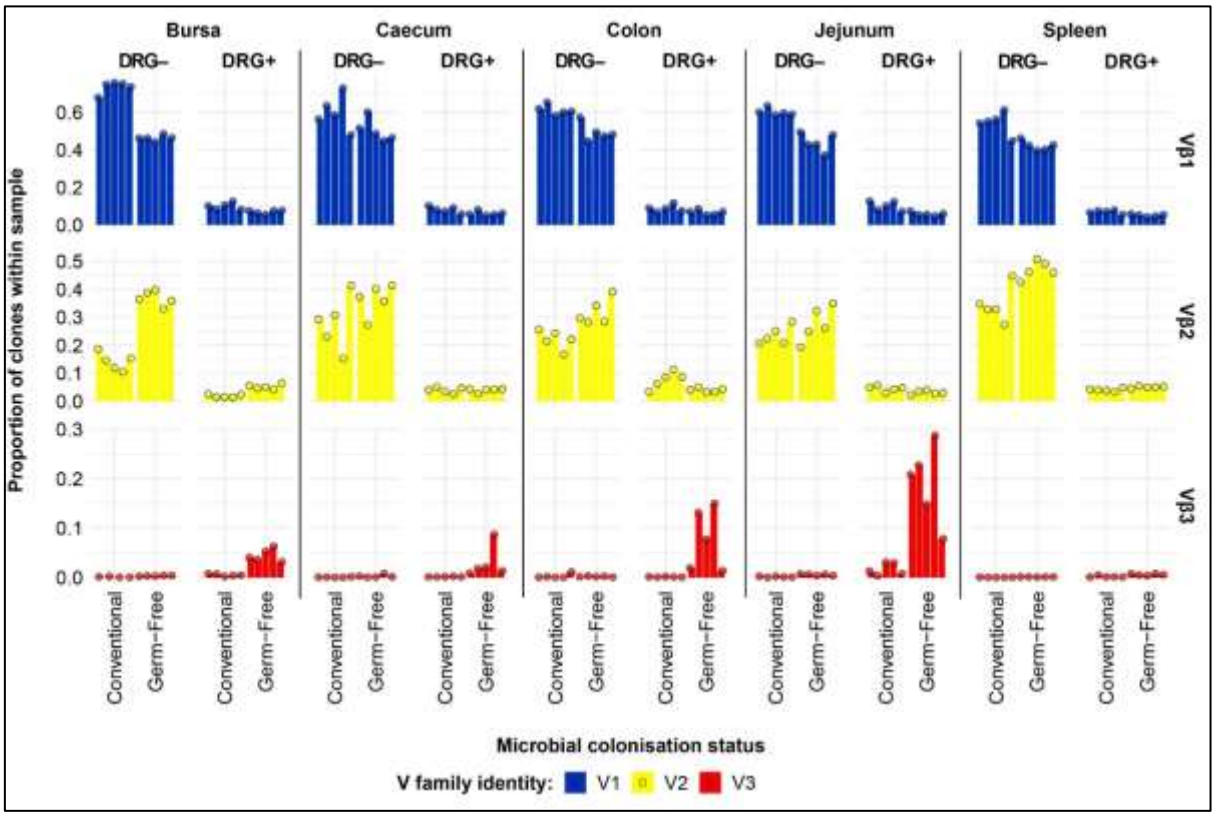

Figure A. 5: *Proportion of the repertoire occupied by clones with and without the DRG motif within their CDR3 by V family, tissue, and microbial status.*

V family identities are shown in blue (Vβ1), yellow (Vβ2), and red (Vβ3). Dots and bars represent individual bird observations.

	Vβ1	Vβ2	Vβ3
Conventional	10.5%	10.5%	49.5%
Germ-free	10.3%	9.7%	56.8%
Overall	10.2%	10.0%	53.9%

Figure A. 6: *Percentage of unique clones with the DRG motif within their CDR3 sequence.*

The numbers are rounded to one decimal point for convenience. Abundance within birds and sample is not represented in the figure, as only the unique clones were considered.

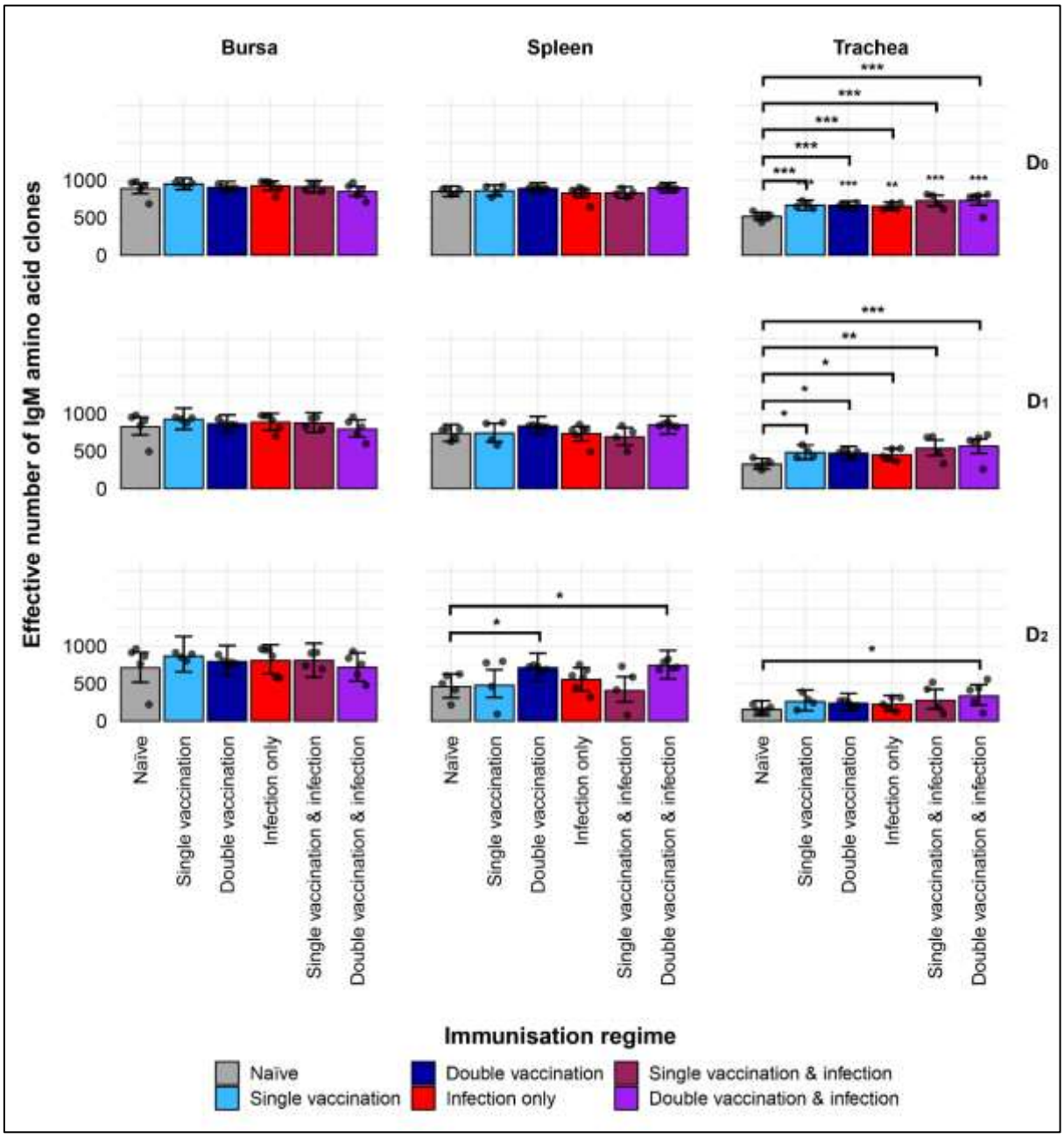

Figure A. 7: *IgM amino acid clonal diversity within samples.*

Different rows show the Hill numbers corresponding to clonal richness (D_0), the "typical" clones (D_1) and the "dominant" clones (D_2) in a theoretical sample of 1000 sequences. Immunisation regimes are colour coded and displayed on the x axes. Dots represent individual bird observations of the effective number of species calculated in each tissue for the corresponding H values. Error bars show the 95% bootstrap confidence intervals for the point estimates generated from 1000 simulations of the model. Statistically significant differences between the model estimates are depicted above the plots based on their corresponding p-values: * = $p < 0.05$; ** = $p < 0.01$; *** = $p < 0.001$.

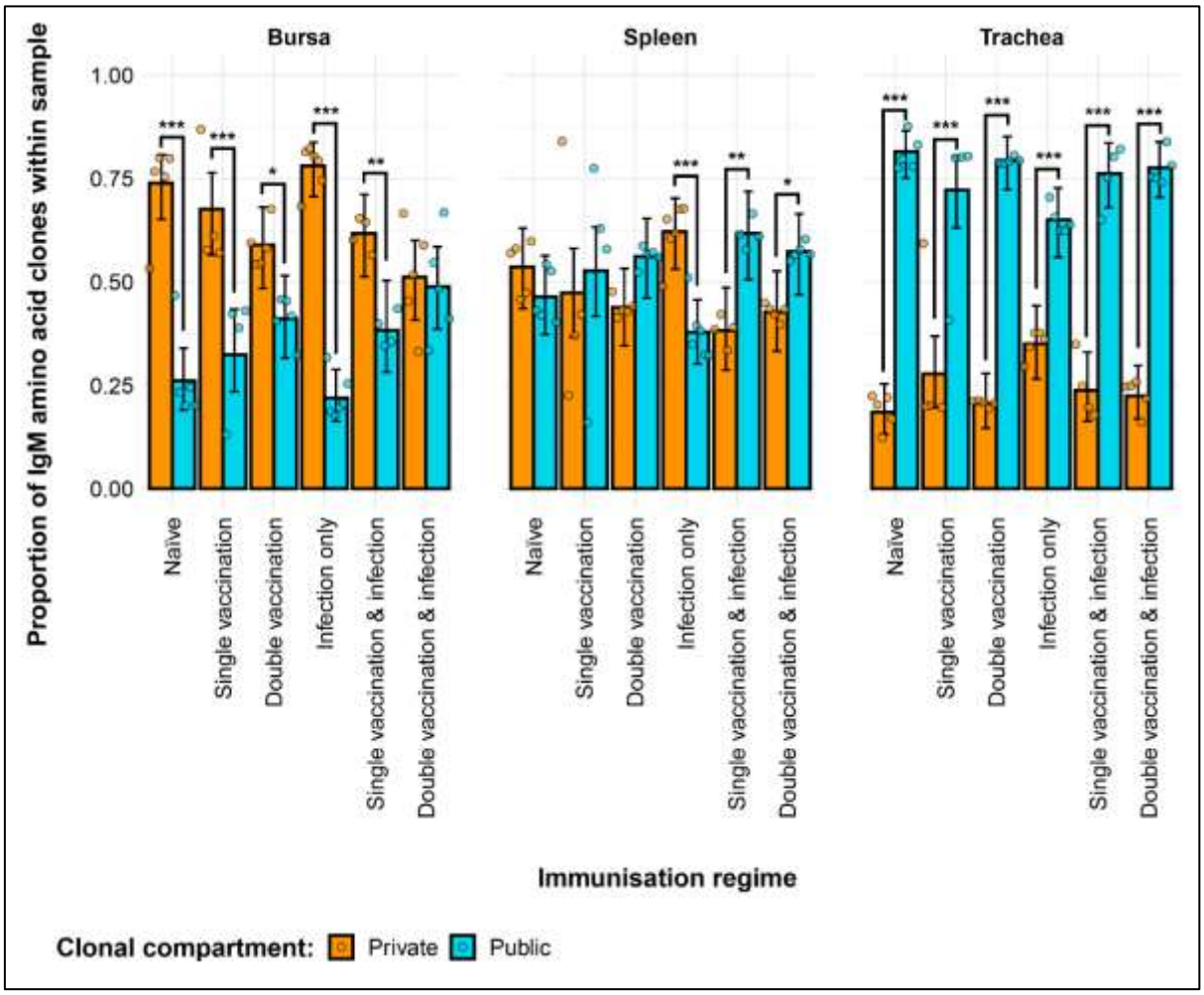

Figure A. 8: *Differences between the IgM amino acid public and private compartments under different H9N2 immunisation regimes based on clone CDR3 nucleotide structure.*

Private (individual-restricted) clones are shown in orange. Public clones (shared between more than two individuals) and are shown in light blue. Dots represent individual bird observations of public and private clonal compartments. Error bars represent 95% bootstrap confidence intervals for the point estimates generated from 1000 simulations of the model. Statistically significant differences between the model estimates are depicted above the plots based on their corresponding p-values: * = $p < 0.05$; ** = $p < 0.01$; *** = $p < 0.001$.

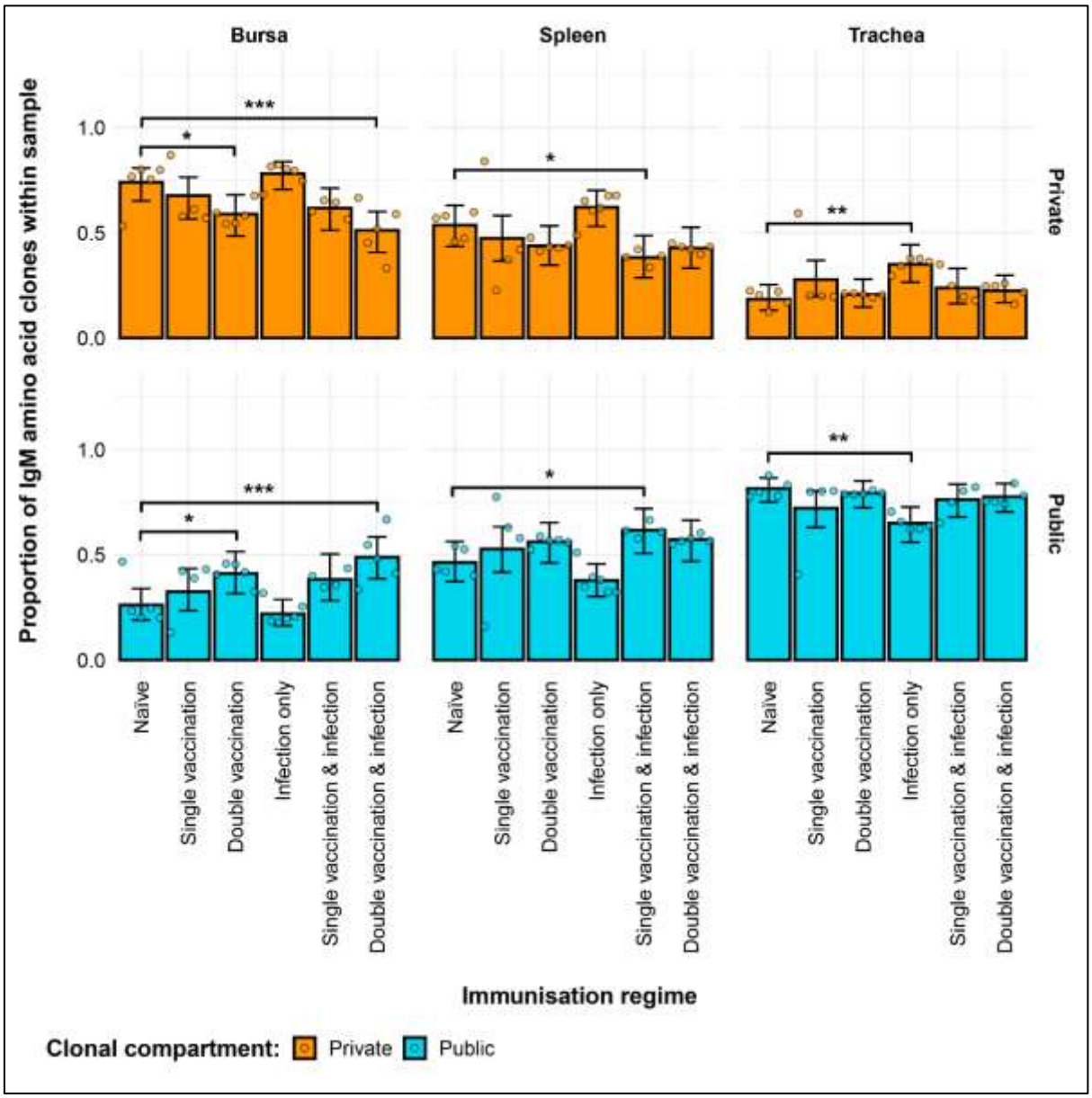

Figure A. 9: *Differences within the IgM amino acid public and private compartments under different H9N2 immunisation regimes based on clone CDR3 nucleotide structure.*

Private (individual-restricted) clones are shown in orange. Public clones (shared between more than two individuals) and are shown in light blue. Dots represent individual bird observations of public and private clonal compartments. Error bars represent 95% bootstrap confidence intervals for the point estimates generated from 1000 simulations of the model. Statistically significant differences between the model estimates are depicted above the plots based on their corresponding p-values: * = $p < 0.05$; ** = $p < 0.01$; *** = $p < 0.001$.

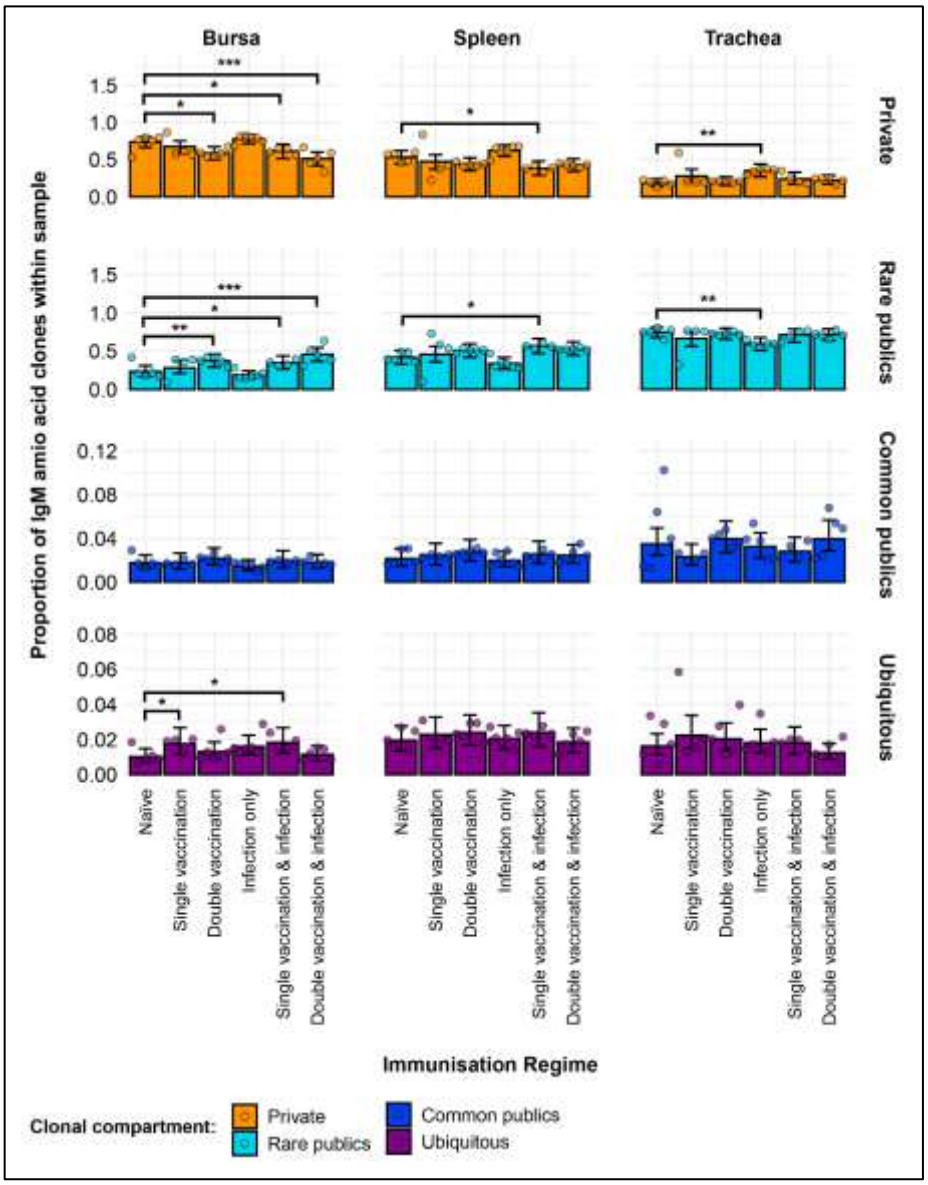

Figure A. 10: *Model estimates of IgM amino acid clone CDR3 private and public compartments based on different levels of clonal sharing.*

Private (individual-restricted) clones are shown in orange. Rare publics (shared between 2 or more than 2 individuals up to 50%) and are shown in light blue. Common publics (shared between more than 50% and up to 90% birds) are shown in dark blue. Ubiquitous publics (found in 90% or more of the birds which were incorporated in the analysis) are shown in purple. Dots represent individual bird observations of private and distinct public clonal compartments. Error bars represent 95% bootstrap confidence intervals for the point estimates generated from 1000 simulations of the model. Error bars represent 95% bootstrap confidence intervals for the point estimates generated from 1000 simulations of the model. Statistically significant differences between the model

estimates are depicted above the plots based on their corresponding p-values: * = $p < 0.05$; ** = $p < 0.01$; *** = $p < 0.001$.

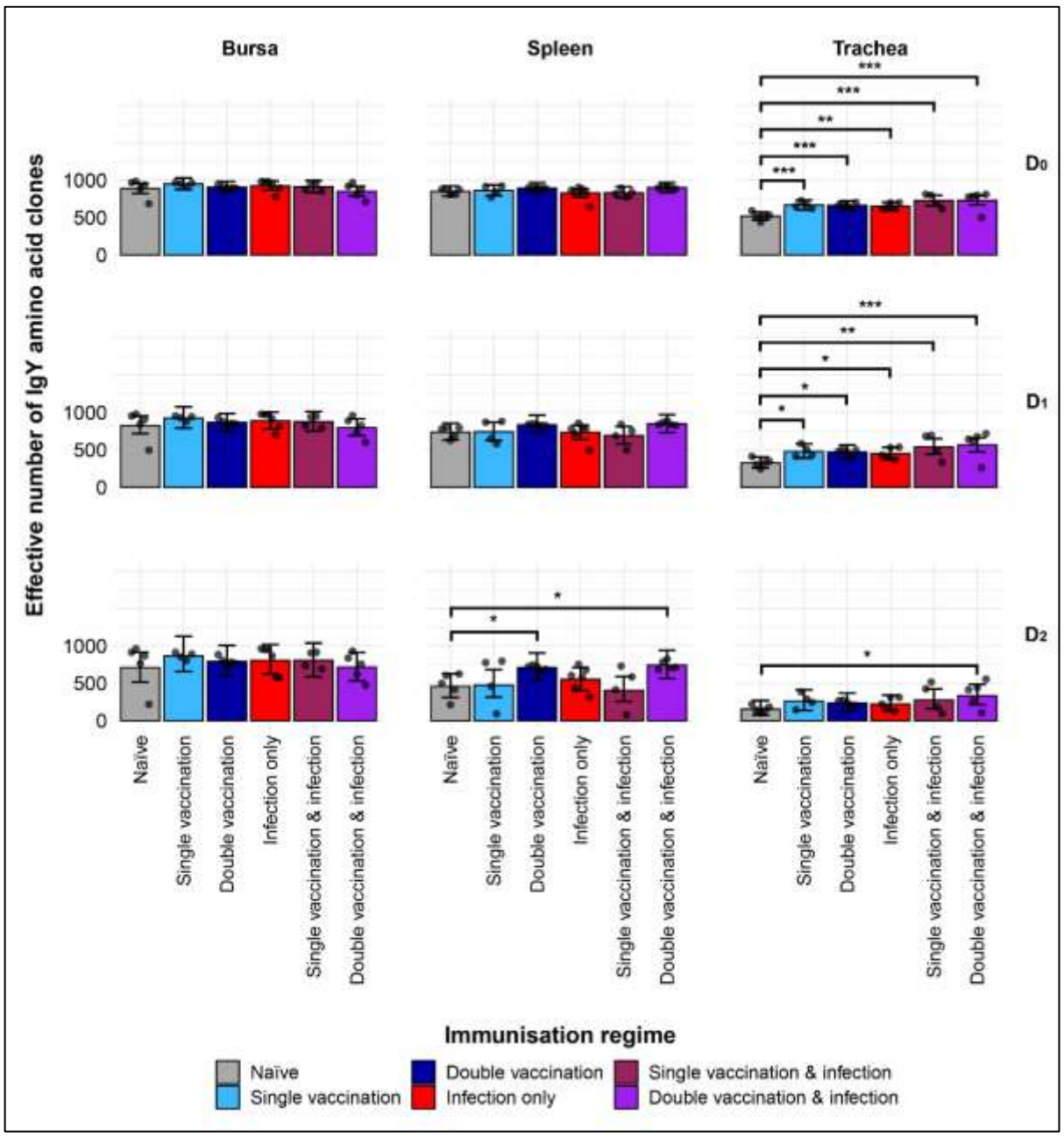

Figure A. 11: *IgY amino acid clonal diversity within samples.*

Different rows show the Hill numbers corresponding to clonal richness (D_0), the "typical" clones (D_1) and the "dominant" clones (D_2) in a theoretical sample of 1000 sequences. Immunisation regimes are colour coded and displayed on the x axes. Dots represent individual bird observations of the effective number of species calculated in each tissue for the corresponding H values. Error bars show the 95% bootstrap confidence intervals for the point estimates generated from 1000 simulations of the model. Statistically significant differences between the model estimates are

depicted above the plots based on their corresponding p-values: * = p < 0.05; ** = p < 0.01; *** = p < 0.001.

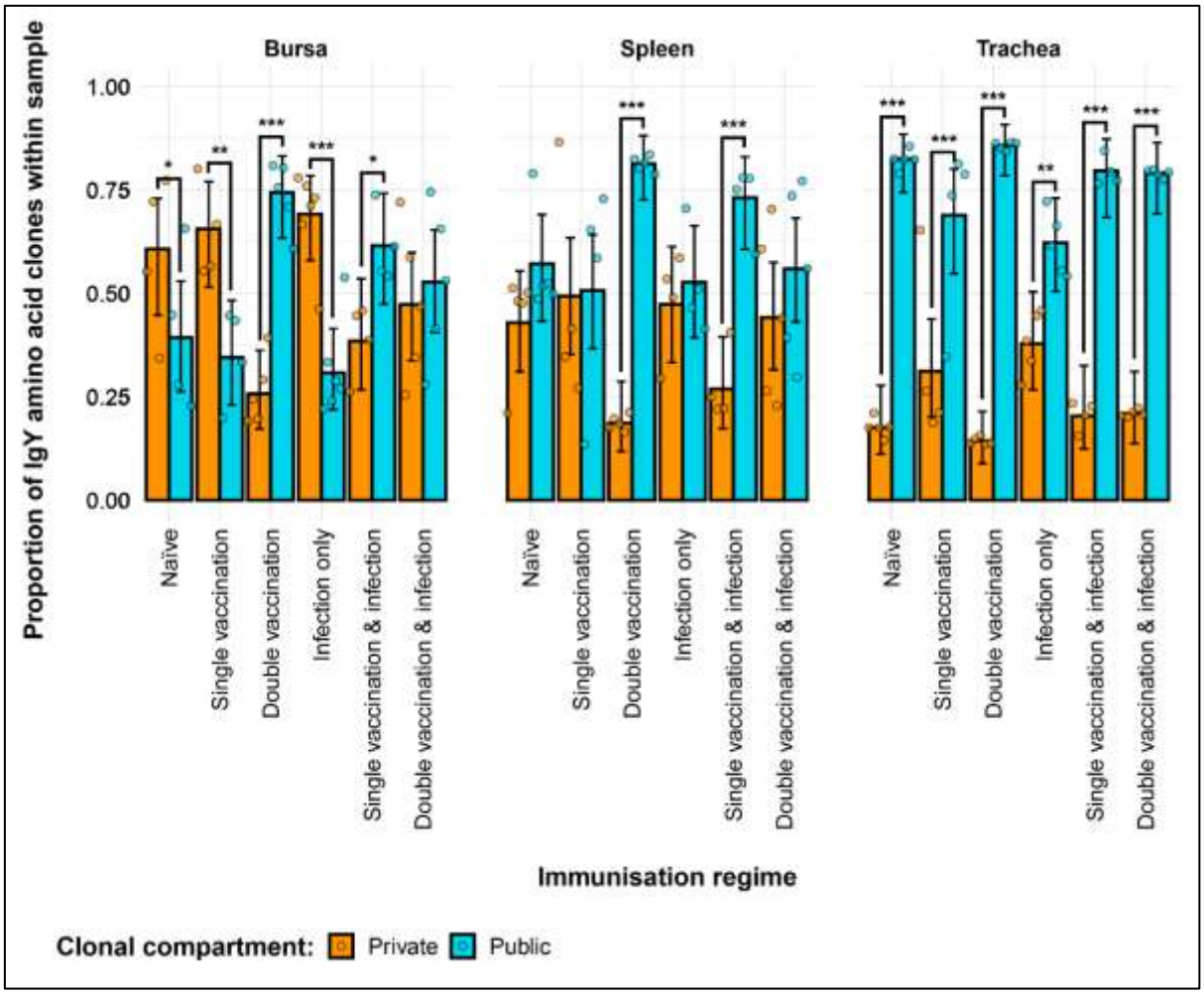

Figure A. 12: *Differences between the IgY amino acid public and private compartments under different H9N2 immunisation regimes based on clone CDR3 nucleotide structure.*

Private (individual-restricted) clones are shown in orange. Public clones (shared between more than two individuals) and are shown in light blue. Dots represent individual bird observations of public and private clonal compartments. Error bars represent 95% bootstrap confidence intervals for the point estimates generated from 1000 simulations of the model. Statistically significant differences between the model estimates are depicted above the plots based on their corresponding p-values: * = p < 0.05; ** = p < 0.01; *** = p < 0.001.

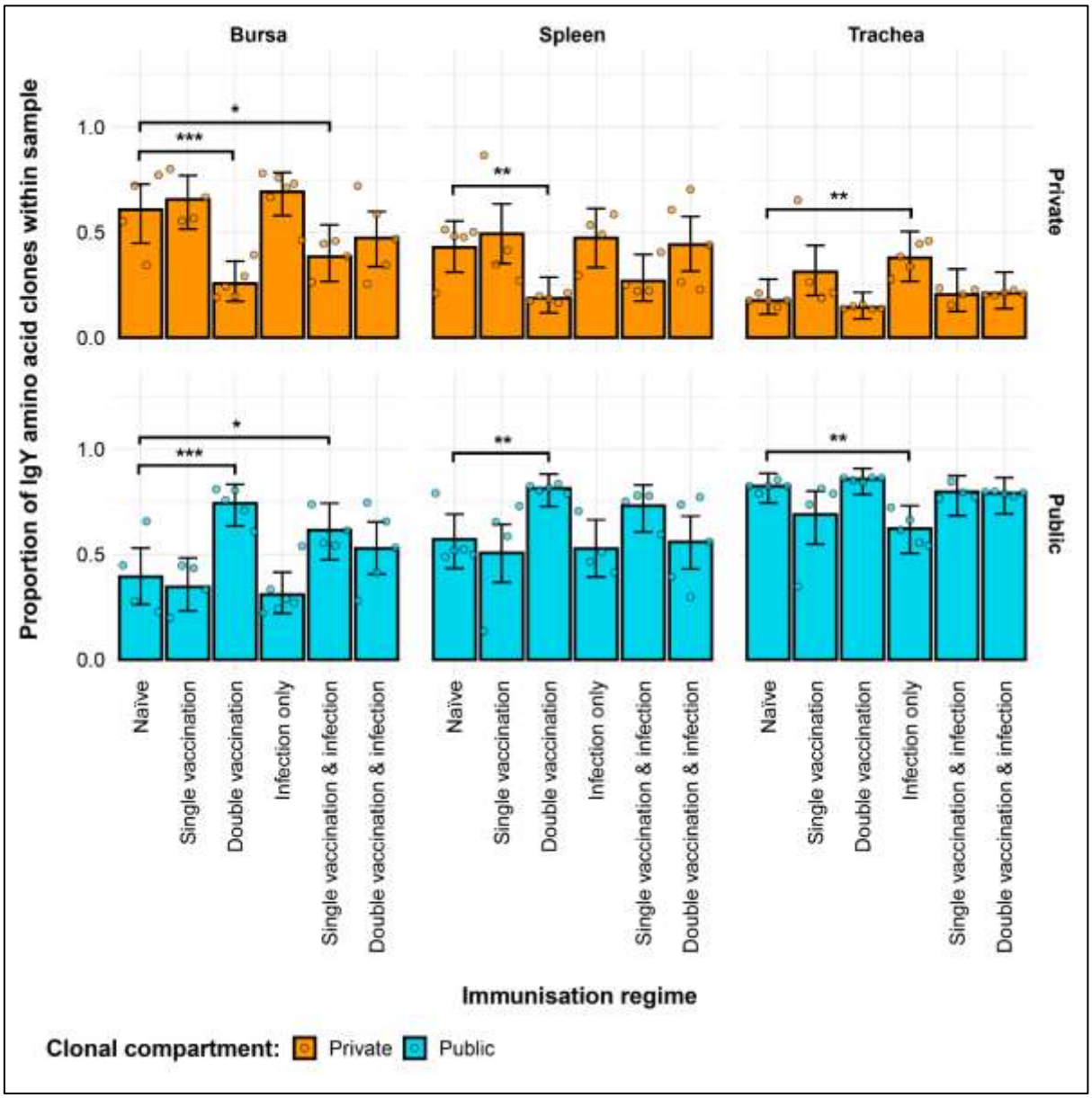

Figure A. 13: *Differences within the IgY amino acid public and private compartments under different H9N2 immunisation regimes based on clone CDR3 nucleotide structure.*

Private (individual-restricted) clones are shown in orange. Public clones (shared between more than two individuals) and are shown in light blue. Dots represent individual bird observations of public and private clonal compartments. Error bars represent 95% bootstrap confidence intervals for the point estimates generated from 1000 simulations of the model. Statistically significant differences between the model estimates are depicted above the plots based on their corresponding p-values: * = $p < 0.05$; ** = $p < 0.01$; *** = $p < 0.001$.

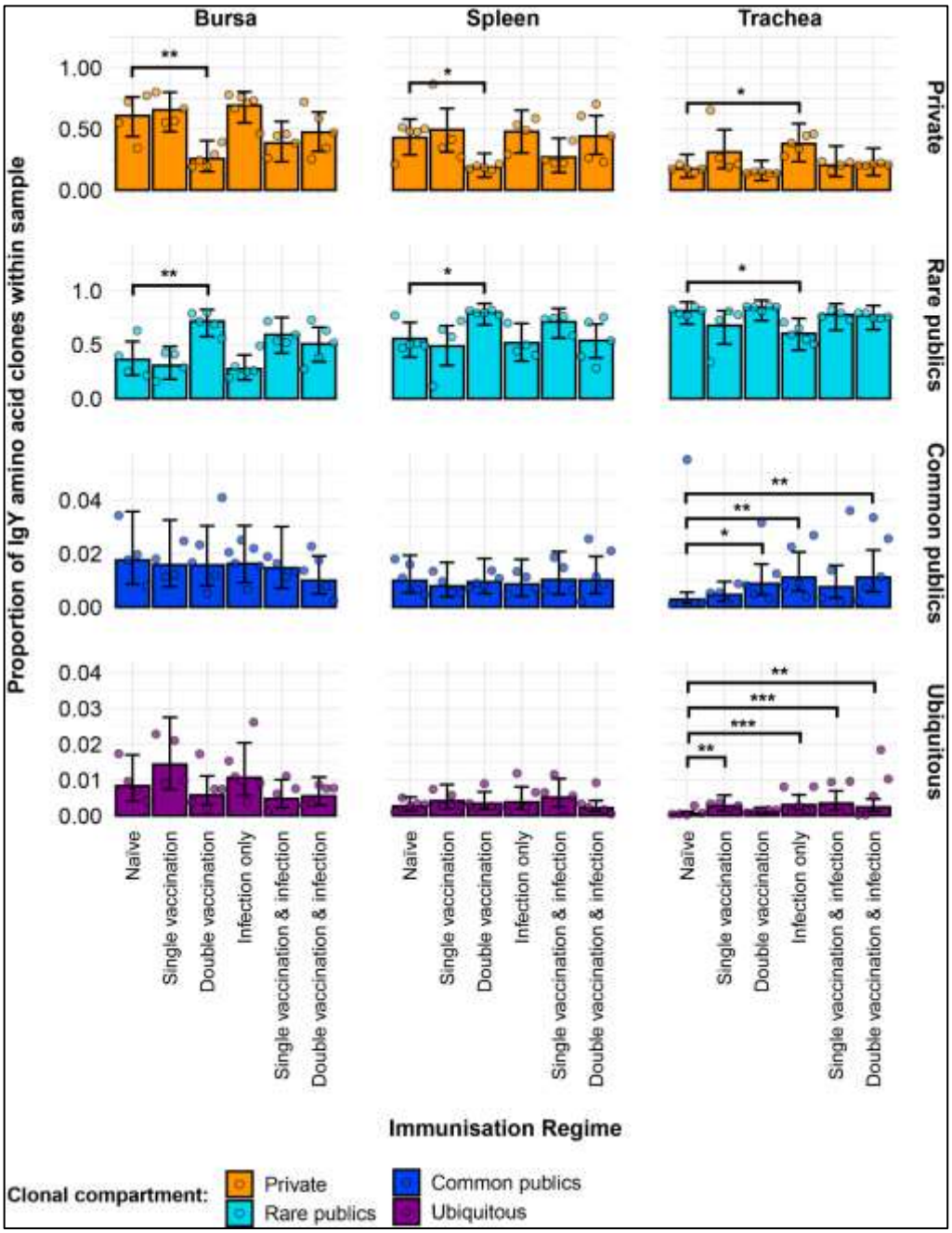

Figure A. 14: *Model estimates of IgY amino acid clone CDR3 nucleotide private and public compartments based on different levels of clonal sharing.*

Private (individual-restricted) clones are shown in orange. Rare publics (shared between 2 or more than 2 individuals up to 50%) and are shown in light blue. Common publics (shared between more than 50% and up to 90% birds) are shown in dark blue. Ubiquitous publics (found in 90% or more of the birds which were incorporated in the analysis) are shown in purple. Dots represent individual bird observations of private and distinct public clonal compartments. Error bars represent 95% bootstrap confidence intervals for the point estimates generated from 1000 simulations of the model. Statistically significant differences between the model estimates are depicted above the plots based on their corresponding p-values: * = $p < 0.05$; ** = $p < 0.01$; *** = $p < 0.001$.

-

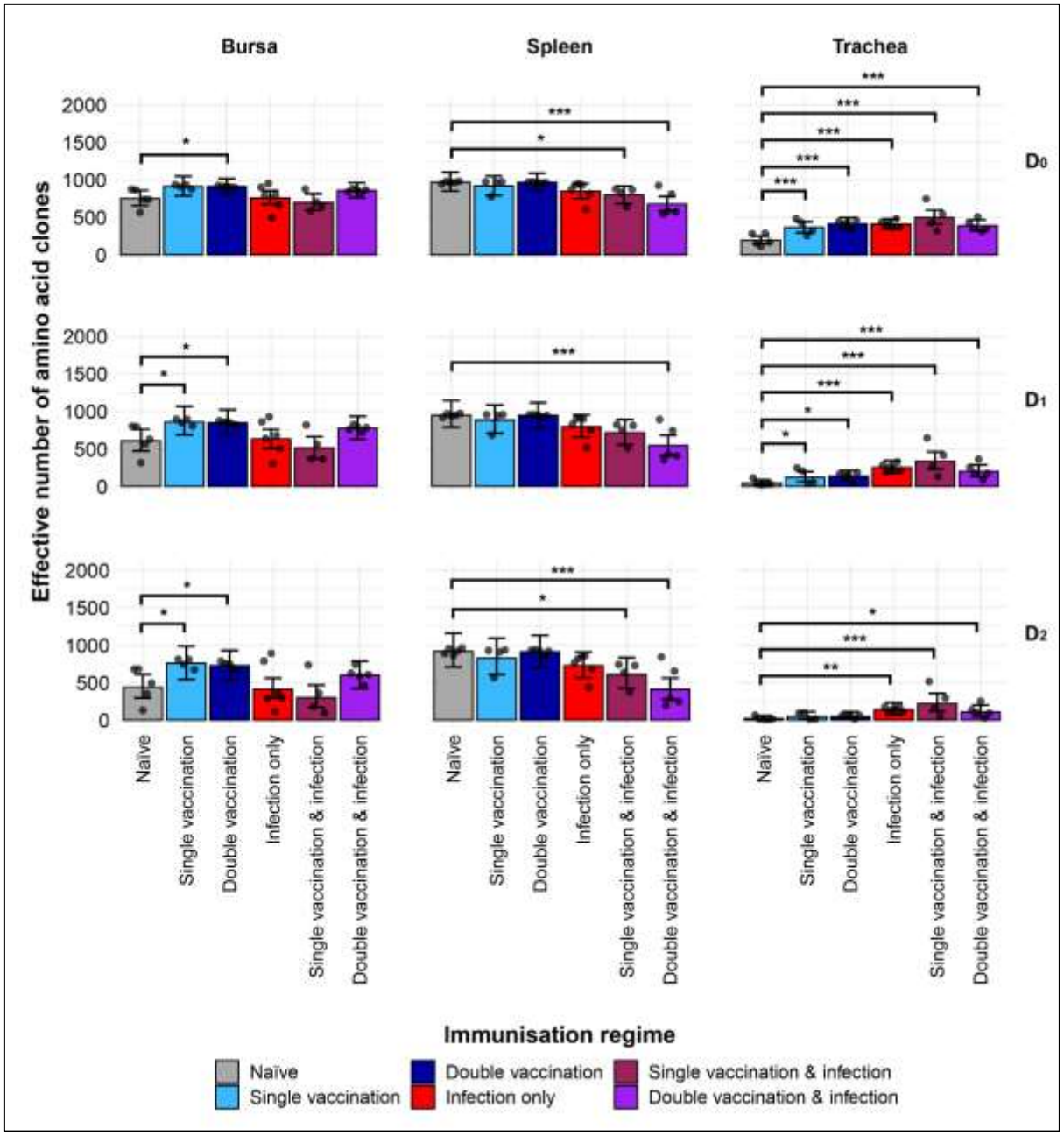

Figure A. 15: *TCRβ amino acid clonal diversity within samples.*

Different rows show the Hill numbers corresponding to clonal richness (D_0), the "typical" clones (D_1) and the "dominant" clones (D_2) in a theoretical sample of 1000 sequences. Immunisation regimes are colour coded and displayed on the x axes. Dots represent individual bird observations of the effective number of species calculated in each tissue for the corresponding H values. Error bars show the 95% bootstrap confidence intervals for the point estimates generated from 1000 simulations of the model. Statistically significant differences between the model estimates are depicted above the plots based on their corresponding p-values: * = $p < 0.05$; ** = $p < 0.01$; *** = $p < 0.001$.

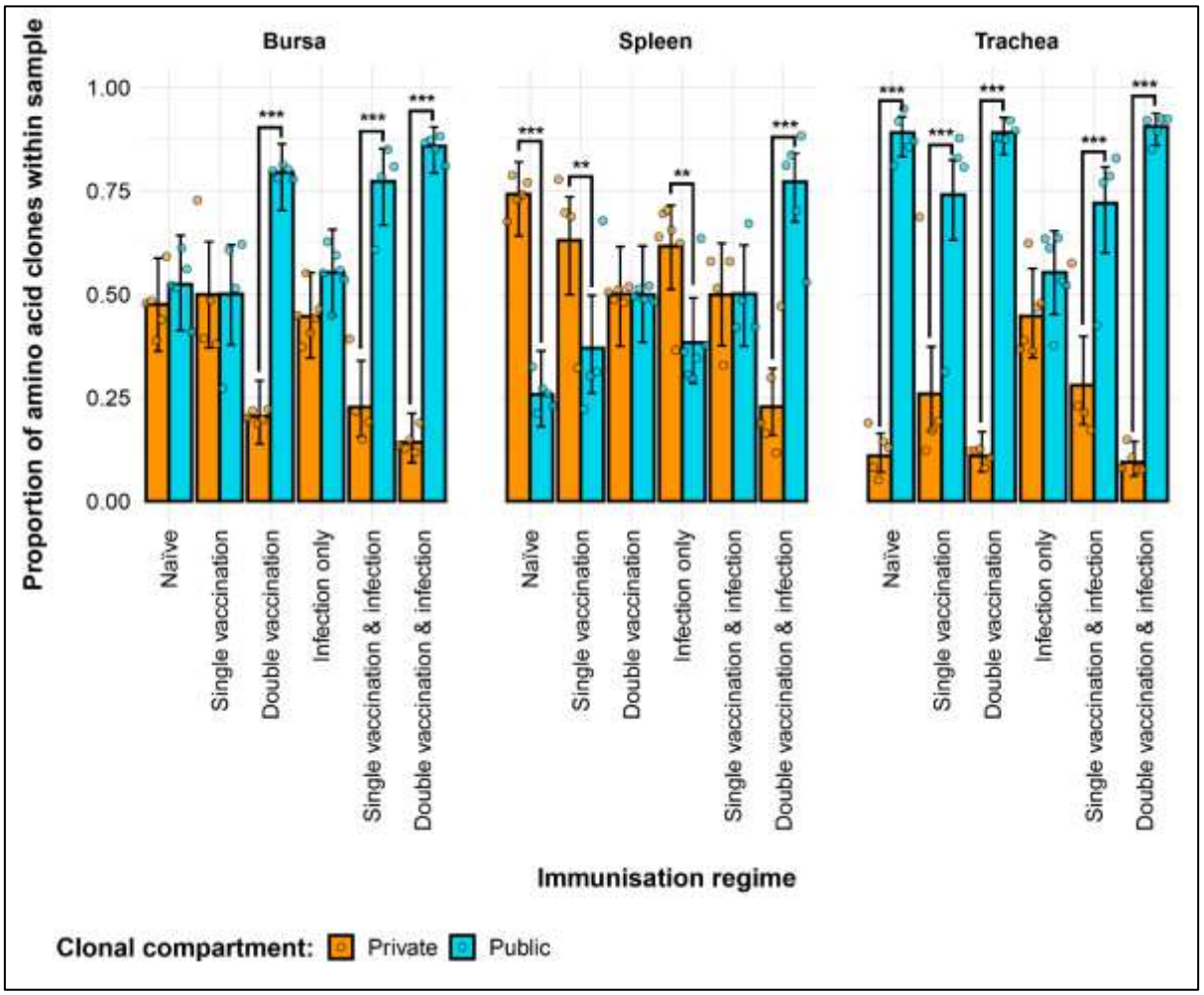

Figure A. 16: *Differences between the TCRβ public and private compartments under different H9N2 immunisation regimes based on clone CDR3 nucleotide structure.*

Private (individual-restricted) clones are shown in orange. Public clones (shared between more than two individuals) and are shown in light blue. Dots represent individual bird observations of public and private clonal compartments. Error bars represent 95% bootstrap confidence intervals for the point estimates generated from 1000 simulations of the model. Statistically significant differences between the model estimates are depicted above the plots based on their corresponding p-values: * = $p < 0.05$; ** = $p < 0.01$; *** = $p < 0.001$.

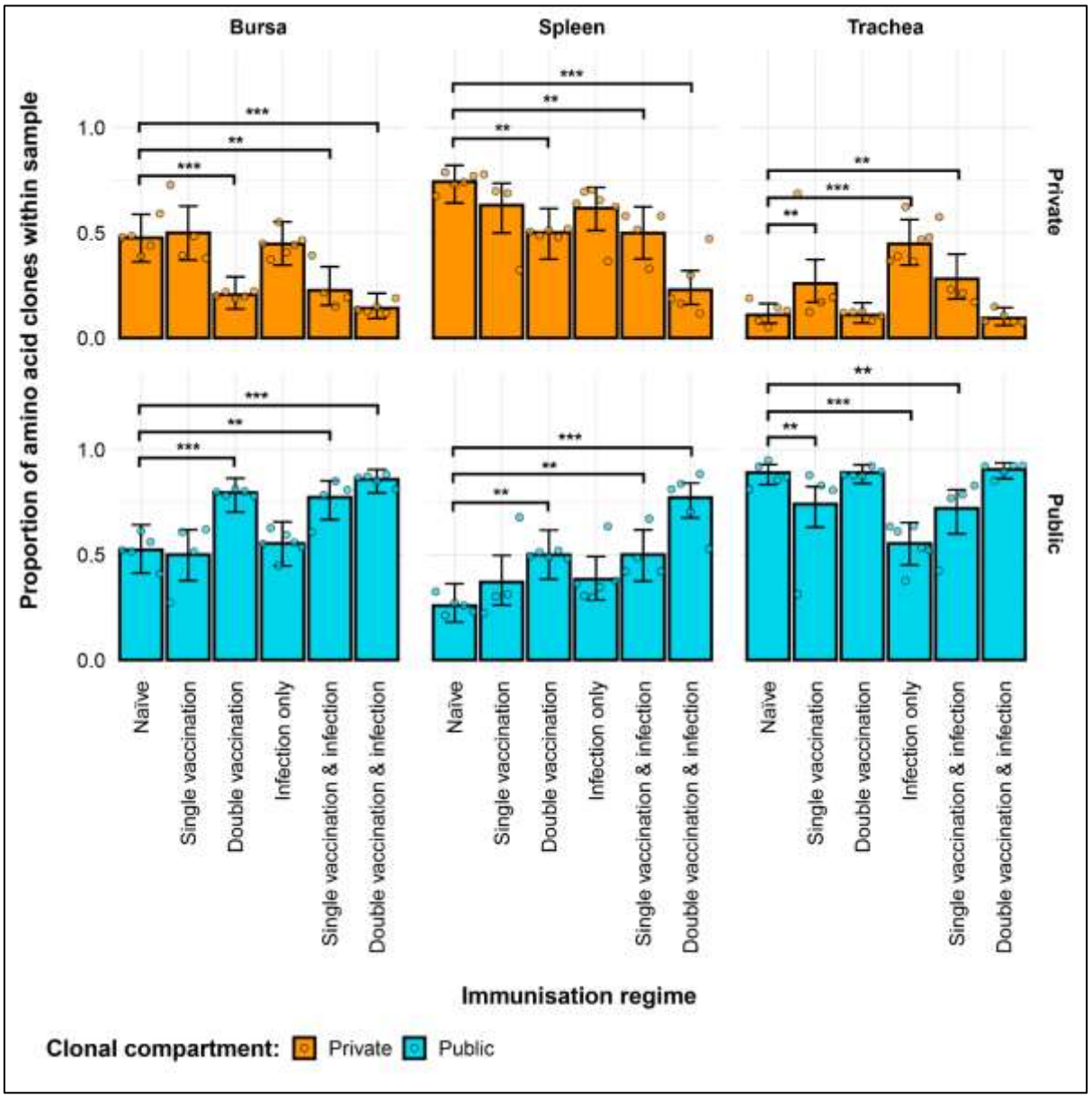

Figure A. 17: *Differences within the TCRβ public and private compartments under different H9N2 immunisation regimes based on clone CDR3 nucleotide structure.*

Private (individual-restricted) clones are shown in orange. Public clones (shared between more than two individuals) and are shown in light blue. Dots represent individual bird observations of public and private clonal compartments. Error bars represent 95% bootstrap confidence intervals for the point estimates generated from 1000 simulations of the model. Statistically significant differences between the model estimates are depicted above the plots based on their corresponding p-values: * = $p < 0.05$; ** = $p < 0.01$; *** = $p < 0.001$.

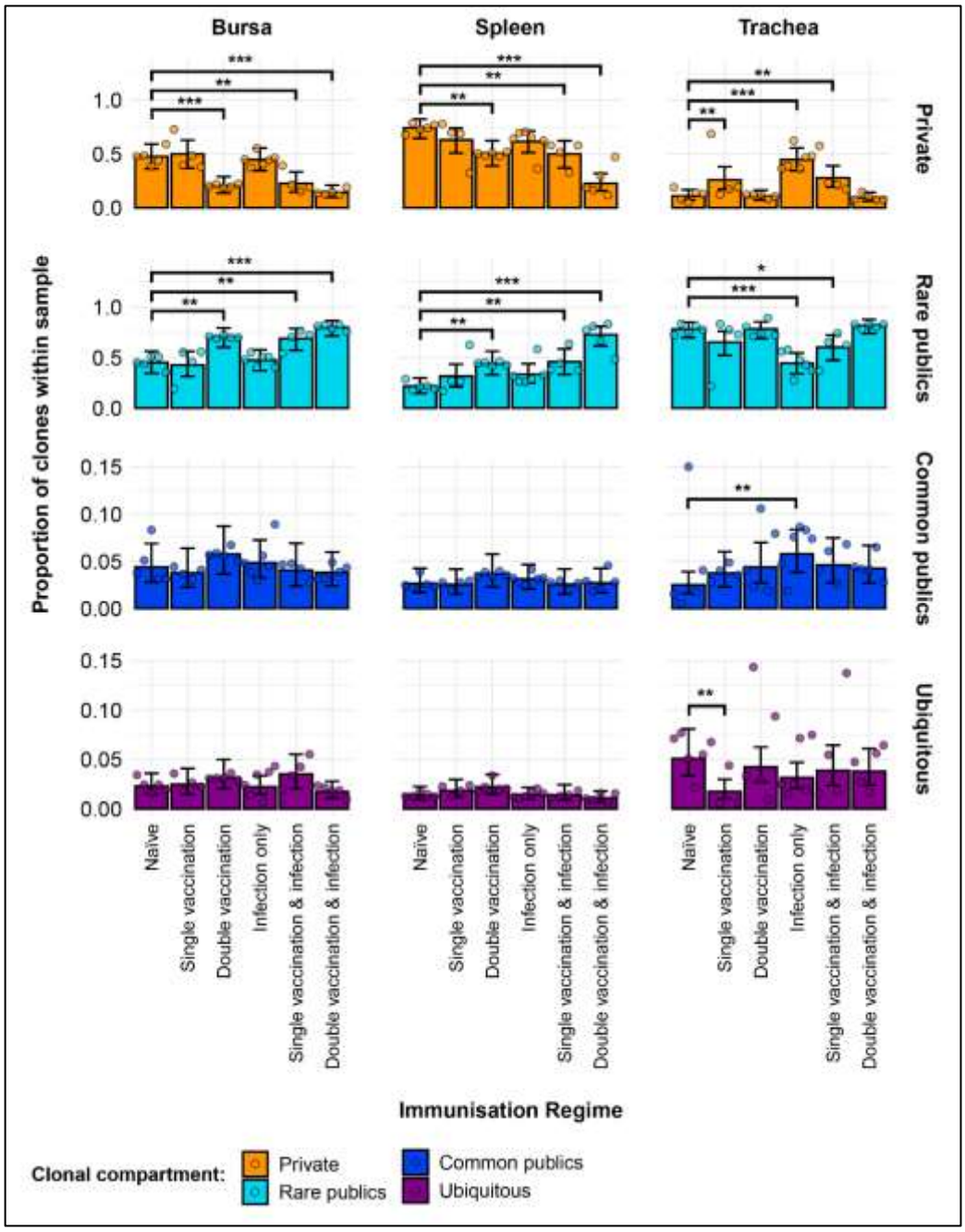

Figure A. 18: *Model estimates of TCRβ clone CDR3 nucleotide private and public compartments based on different levels of clonal sharing.*

Private (individual-restricted) clones are shown in orange. Rare publics (shared between 2 or more than 2 individuals up to 50%) and are shown in light blue. Common publics (shared between more than 50% and up to 90% birds) are shown in dark blue. Ubiquitous publics (found in 90% or more of the birds which were incorporated in the analysis) are shown in purple. Dots represent individual bird observations of private and distinct public clonal compartments. Error bars represent 95% bootstrap confidence intervals for the point estimates generated from 1000 simulations of the model. Statistically significant differences between the model estimates are depicted above the plots based on their corresponding p-values: * = $p < 0.05$; ** = $p < 0.01$; *** = $p < 0.001$.

Appendix II: COVID-19 research and public health work

Over the course of my doctoral studies, I have devoted a substantial part of my time to public health research and other healthcare-related activities, predominantly in Romania, my country of origin. Importantly, during the COVID-19 pandemic I was at the forefront of science communication and healthcare research and policy work in Romania, activities through which I contributed to mitigating the impacts of the then ongoing pandemic.

My COVID-19 communication activities began in early 2020, when I was invited on national television and radio broadcasts to discuss the pandemic. Since then, I have participated in hundreds of such broadcasts, where I provided scientific explanations of biological phenomena in a manner accessible to a non-specialist audience. At first, these activities mostly focused on providing information about infectious diseases, how the immune system responds to infection, and why it is important to abide by the measures aimed at containing the spread of the virus, such as social distancing and wearing face coverings. Informing the public was not limited to the territory of Romania, but also involved activities with its diaspora. In the UK, I was contacted by the Romanian embassy to participate in a series of live online broadcasts, where I addressed the concerns of the public and provided information about SARS-CoV-2 infection and the immune system. For my contributions, I received an official letter of gratitude from the Ambassador of Romania to the Court of St James's, which was also sent to my Department and College. Later on, as vaccines became available, my communication activities included explanations about how vaccines work and why it is important to get vaccinated in order to prevent severe forms of the disease and loss of life.

Low vaccine acceptance is a major problem in Romania, as I described in my first academic paper about the 2016 measles epidemic[1]. Indeed, improving the trust of the population in

[1] **Dascalu S***. (2019) Measles Epidemics in Romania: Implications for Public Health and Future Policy. *Front. Public Health* 7:98. doi:10.3389/fpubh.2019.00098

vaccines required a great deal of effort during the COVID-19 pandemic. In December 2020, I was invited by the coordinator of the vaccination campaign to become one of the main communicators of the immunisation efforts. At the same time, I helped to improve the national COVID-19 vaccination strategy. My most notable activity was coordinating the drafting of an academic paper[2] which highlighted the main challenges of vaccine implementation in Romania whilst also providing a set of recommendations that could help overcome them. This paper, co-authored with some of the most prominent figures in Romanian public health, was featured on the official website of the Ministry of Health and also received extensive media coverage. Consequently, for my involvement in the COVID-19 efforts in Romania, I received an honorary recognition from the Romanian Ministry of Health in early 2021.

Academically, I was also involved in theoretical work in epidemiology and public health. For instance, alongside my colleague Mahan Ghafari from Oxford, I contributed to an analysis of the early epidemic situation in Iran[3]. I also contributed to Mahan's opinion piece about the vaccination policy in Iran, which was featured on the BMJ website[4]. Similarly, motivated by the near-critical epidemiological context in Romania, I reviewed the successes and failures of the initial pandemic response, providing the international research community with the only comprehensive reference work on this topic[5]. Indeed, this publication attracted significant attention from academics and non-academics alike, and I was soon invited to join an international academic network under the patronage of the Romanian Embassy in Germany, which led to several fruitful collaborations that have continued to this day. Later on, alongside an international team of researchers, I wrote an

[2] **Dascalu S***, Geambasu O, Covaciu O, Chereches RM, Diaconu G, Dumitra GG, Gheroghita V, Popovici ED. (2021) Prospects of COVID-19 Vaccination in Romania: Challenges and Potential Solutions. *Front Public Heal* 9:644538. 10.3389/fpubh.2021.644538

[3] Ghafari M*, Hejazi B, Karshenas A, **Dascalu S** , Kadivar A, Khosravi MA, Abbasalipour M, Heydari M, Zeinali S, Ferretti L, Ledda A, Katzourakis A*. (2021) Lessons for preparedness and reasons for concern from the early COVID-19 epidemic in Iran. *Epidemics* 36:100472. doi.org/10.1016/j.epidem.2021.100472

[4] Ghafari M*, Rezaee-Zavareh MS, **Dascalu S** , Katzourakis A*. (2021) Iran's COVID-19 vaccination programme: using transparency to build public trust in immunisation. *BMJ opinion*. Available at: https://blogs.bmj.com/bmj/2021/08/03/irans-covid-19-vaccination-programme-using-transparency-to-build-public-trust-in-immunisation/

[5] **Dascalu S***. (2020) The Successes and Failures of the Initial COVID-19 Pandemic Response in Romania. *Front. Public Health* 8:344. doi:10.3389/fpubh.2020.00344.

opinion piece[6] about what went wrong following the implementation of the COVID-19 vaccination campaign in Romania, as very few of the previously highlighted issues were addressed properly by the national authorities, thus leading to a low vaccination coverage and a consequently high COVID-19 associated mortality. Additionally, I participated as a keynote speaker in several national conferences, including the National Conference of General Practitioners and the Romanian Healthcare Communication Forum. In recognition of my academic involvement, I was invited to become a Fellow of the Romanian Society for Epidemiology, a position which honours me greatly. Furthermore, in 2022 I was awarded a Knighthood of the "Order of Cultural Merit, Category H – Scientific Research" from the President of Romania, His Excellency Klaus Werner Iohannis. I was also rewarded with the title of "COVID Hero" by the League of Romanian Students Abroad and included in Newsweek Romania's "Top 100 Romanians Abroad".

Finally, perhaps my most impactful activity aimed at mitigating COVID-19 was engaging with religious institutions in Romania, which is the most religious country in Europe, in order to raise public compliance with the official guidelines and also tackle the issue of vaccine hesitancy. Extensive dialogue with church officials often led to measures being taken by this institution before official guidelines were released by the national authorities. Additionally, I was the first person ever to be invited on the official TV station of the Romanian Orthodox Church to talk about vaccination and its benefits. Moreover, I was asked to become an associate expert for FoRB Romania, an interdisciplinary community focused on topics related to freedom of religion and belief. These activities served as a basis for an academic publication[7] on the involvement of religious institutions during public health crises which I drafted with the help of an interdisciplinary team of researchers from the University of Oxford. Furthermore, with the support of the University of Oxford Ian Ramsey Centre for Science and Religion, I organised a conference entitled "Fighting Pandemics in a Life of Faith – Interdisciplinary Approaches to Public Health" which

[6] **Dascalu S***, Geambasu O, Raiu CV, Azoicai D, Popovici ED, Apetrei C*. (2021) COVID-19 in Romania: What Went Wrong? *Front. Public Health* 9:813941. doi:10.3389/fpubh.2021.813941

[7] **Dascalu S***, Flammer PG, Ghafari M, Henson SC, Nascimento R, Bonsall MB*. (2021) Engaging religious institutions and faith-based communities in public health initiatives: A case study of the Romanian Orthodox Church during the COVID-19 pandemic. *Front. Public Health* 9:768091. doi:10.3389/fpubh.2021.768091

brought together researchers and stakeholders from various fields of expertise, including theology, political sciences, medicine, public health, and biology. For my contributions to public health and for promoting interdisciplinary activities alongside religious communities and institutions, I was awarded the "Order of the Holy Brâncoveanu Martyrs", one of the highest distinctions of the Romanian Orthodox Church, from His Beatitude Patriarch Daniel.

As a scientist, I believe that the true impact of my studies needs to extend beyond the classical methods of disseminating results in academia. Moreover, as my DPhil is in Interdisciplinary Bioscience, I aimed to channel the potential of interdisciplinarity in order to improve public health and the wellbeing of people more broadly. Although not directly related to my DPhil research, I am happy knowing that I was able to contribute, at least in part, to mitigating the impacts of the pandemic and bettering people's lives.

References

[1] Shaw ML, Palese P. Orthomyxoviridae. In: Knipe DM, Howley PM, editors. Fields Virol. 6th ed., Wolters Kluwer Health; 2013.

[2] Barberis I, Myles P, Ault SK, Bragazzi NL, Martini M. History and evolution of influenza control through vaccination: from the first monovalent vaccine to universal vaccines. J Prev Med Hyg 2016;57:E115.

[3] Pappas G, Kiriaze IJ, Falagas ME. Insights into infectious disease in the era of Hippocrates. Int J Infect Dis 2008;12:347–50. https://doi.org/10.1016/J.IJID.2007.11.003.

[4] Webster RG. Influenza: An emerging disease. Emerg. Infect. Dis., vol. 4, Centers for Disease Control and Prevention; 1998, p. 436–41. https://doi.org/10.3201/eid0403.980325.

[5] Knipe DM, Howley PM, editors. Orthomyxoviruses. Fields Virol. 6th ed., Wolters Kluwer Health; 2013.

[6] Long JS, Mistry B, Haslam SM, Barclay WS. Host and viral determinants of influenza A virus species specificity. Nat Rev Microbiol 2019;17:67–81. https://doi.org/10.1038/s41579-018-0115-z.

[7] Chen J, Deng YM. Influenza virus antigenic variation, host antibody production and new approach to control epidemics. Virol J 2009;6:1–3. https://doi.org/10.1186/1743-422X-6-30.

[8] Alexander DJ. An overview of the epidemiology of avian influenza. Vaccine 2007;25:5637–44. https://doi.org/10.1016/j.vaccine.2006.10.051.

[9] Chen W, Calvo PA, Malide D, Gibbs J, Schubert U, Bacik I, et al. A novel influenza A virus mitochondrial protein that induces cell death. Nat Med 2001;7:1306–12. https://doi.org/10.1038/nm1201-1306.

[10] Herold S, Becker C, Ridge KM, Budinger GRS. Influenza virus-induced lung injury: Pathogenesis and implications for treatment. Eur Respir J 2015;45:1463–78. https://doi.org/10.1183/09031936.00186214.

[11] Cattoli G, Milani A, Temperton N, Zecchin B, Buratin A, Molesti E, et al. Antigenic Drift in H5N1 Avian Influenza Virus in Poultry Is Driven by Mutations in Major Antigenic Sites of the Hemagglutinin Molecule Analogous to Those for Human Influenza Virus. J Virol 2011;85:8718–24. https://doi.org/10.1128/jvi.02403-10.

[12] Cox NJ, Subbarao K. Global Epidemiology of Influenza: Past and Present. Https://DoiOrg/101146/AnnurevMed511407 2003;51:407–21. https://doi.org/10.1146/ANNUREV.MED.51.1.407.

[13] Taubenberger JK, Reid AH, Lourens RM, Wang R, Jin G, Fanning TG. Characterization of the 1918 influenza virus polymerase genes. Nature 2005;437:889–93. https://doi.org/10.1038/nature04230.

[14] Reid AH, Fanning TG, Janczewski TA, Taubenberger JK. Characterization of the 1918 "Spanish" influenza virus neuraminidase gene. Proc Natl Acad Sci U S A 2000;97:6785–90. https://doi.org/10.1073/pnas.100140097.

[15] Schäffr JR, Kawaoka Y, Bean WJ, Süss J, Senne D, Webster RG. Origin of the pandemic 1957 H2 influenza a virus and the persistence of its possible progenitors in the avian reservoir. Virology 1993;194:781–8. https://doi.org/10.1006/viro.1993.1319.

[16] Xu R, McBride R, Paulson JC, Basler CF, Wilson IA. Structure, Receptor Binding, and Antigenicity of Influenza Virus Hemagglutinins from the 1957 H2N2 Pandemic. J Virol 2010;84:1715–21. https://doi.org/10.1128/JVI.02162-09/SUPPL_FILE/WILSON_H2HA_SUPPINFO.DOC.

[17] Guan Y, Vijaykrishna D, Bahl J, Zhu H, Wang J, Smith GJD. The emergence of pandemic influenza viruses. Protein Cell 2010;1:9–13. https://doi.org/10.1007/s13238-010-0008-z.

[18] Pu J, Wang S, Yin Y, Zhang G, Carter RA, Wang J, et al. Evolution of the H9N2 influenza genotype that facilitated the genesis of the novel H7N9 virus. Proc Natl Acad Sci 2015;112:548–53. https://doi.org/10.1073/PNAS.1422456112.

[19] Alarcon P, Brouwer A, Venkatesh D, Duncan D, Dovas CI, Georgiades G, et al. Comparison of 2016–17 and previous epizootics of highly pathogenic avian influenza H5 Guangdong lineage in Europe. Emerg Infect Dis 2018;24:2270–83. https://doi.org/10.3201/eid2412.171860.

[20] Basuno E, Yusdja Y, Ilham N. Socio-economic impacts of avian influenza outbreaks on small-scale producers in Indonesia. Transbound Emerg Dis 2010;57:7–10. https://doi.org/10.1111/j.1865-1682.2010.01121.x.

[21] Govindaraj G, Sridevi R, Nandakumar SN, Vineet R, Rajeev P, Binu MK, et al. Economic impacts of avian influenza outbreaks in Kerala, India. Transbound Emerg Dis 2018;65:e361–72. https://doi.org/10.1111/tbed.12766.

[22] Ramos S, Maclachlan M, Melton A. A Report from the Economic Research Service A Report from the Economic Research Service Impacts of the 2014-2015 Highly Pathogenic Avian Influenza Outbreak on the U.S. Poultry Sector. USDA Econ Res Serv 2017:282–4.

[23] Çakır M, Boland MA, Wang Y. The Economic Impacts of 2015 Avian Influenza Outbreak on the U.S. Turkey Industry and the Loss Mitigating Role of Free Trade Agreements. Appl Econ Perspect Policy 2018;40:297–315. https://doi.org/10.1093/AEPP/PPX027.

[24] Webster RG, Rott R. Influenza virus a pathogenicity: The pivotal role of hemagglutinin. Cell 1987;50:665–6. https://doi.org/10.1016/0092-8674(87)90321-7.

[25] Beerens N, Heutink R, Harders F, Bossers A, Koch G, Peeters B. Emergence and Selection of a Highly Pathogenic Avian Influenza H7N3 Virus. J Virol 2020;94. https://doi.org/10.1128/JVI.01818-19.

[26] Alexander DJ. A review of avian influenza in different bird species. Vet. Microbiol., vol. 74, Vet Microbiol; 2000, p. 3–13. https://doi.org/10.1016/S0378-1135(00)00160-7.

[27] Abdelwhab ESM, Veits J, Mettenleiter TC. Genetic changes that accompanied shifts of low pathogenic avian influenza viruses toward higher pathogenicity in poultry. Virulence 2013;4:441. https://doi.org/10.4161/viru.25710.

[28] Lupiani B, Reddy SM. The history of avian influenza. Comp Immunol Microbiol Infect Dis 2009;32:311–23. https://doi.org/10.1016/j.cimid.2008.01.004.

[29] Alexander DJ, Brown IH. History of highly pathogenic avian influenza. OIE Rev Sci Tech 2009;28:19–38. https://doi.org/10.20506/rst.28.1.1856.

[30] Alexander DJ, Parsons G, Manvell RJ. Experimental Assessment Of The Pathogenicity Of Eight Avian Influenza A Viruses Of H5 Subtype For Chickens, Turkeys, Ducks And Quail. Avian Pathol 1986;15:647–62. https://doi.org/10.1080/03079458608436328.

[31] Chmielewski R, Swayne DE. Avian influenza: public health and food safety concerns. Annu Rev Food Sci Technol 2011;2:37–57. https://doi.org/10.1146/annurev-food-022510-133710.

[32] Wang Z, Loh L, Kedzierski L, Kedzierska K. Avian influenza viruses, inflammation, and CD8+ T cell immunity. Front Immunol 2016;7:1–10. https://doi.org/10.3389/fimmu.2016.00060.

[33] Peacock TP, James J, Sealy JE, Iqbal M. A Global Perspective on H9N2 Avian Influenza Virus. Viruses 2019;11:620. https://doi.org/10.3390/v11070620.

[34] Chen LJ, Lin XD, Guo WP, Tian JH, Wang W, Ying XH, et al. Diversity and evolution of avian influenza viruses in live poultry markets, free-range poultry and wild wetland birds in China. J Gen Virol 2016;97:844–54. https://doi.org/10.1099/jgv.0.000399.

[35] Zecchin B, Minoungou G, Fusaro A, Moctar S, Ouedraogo-Kaboré A, Schivo A, et al. Influenza a(H9N2) virus, Burkina faso. Emerg Infect Dis 2017;23:2118–9. https://doi.org/10.3201/eid2312.171294.

[36] Negovetich NJ, Feeroz MM, Jones-Engel L, Walker D, Alam SMR, Hasan K, et al. Live bird markets of bangladesh: H9n2 viruses and the near absence of highly

pathogenic h5n1 influenza. PLoS One 2011;6:e19311. https://doi.org/10.1371/journal.pone.0019311.

[37] Khan SU, Anderson BD, Heil GL, Liang S, Gray GC. A Systematic Review and Meta-Analysis of the Seroprevalence of Influenza A(H9N2) Infection among Humans. J Infect Dis 2015;212:562–9. https://doi.org/10.1093/infdis/jiv109.

[38] Hoa LNM, Tuan NA, My PH, Huong TTK, Chi NTY, Hau Thu TT, et al. Assessing evidence for avian-to-human transmission of influenza A/H9N2 virus in rural farming communities in northern vietnam. J Gen Virol 2017;98:2011–6. https://doi.org/10.1099/jgv.0.000877.

[39] Pawar SD, Tandale B V., Raut CG, Parkhi SS, Barde TD, Gurav YK, et al. Avian influenza H9N2 seroprevalence among poultry workers in Pune, India, 2010. PLoS One 2012;7:e36374. https://doi.org/10.1371/journal.pone.0036374.

[40] World Health Organization. Influenza at the human-animal interface summary and assessment, 28 February 2020. Emerg Situational Updat 2020. https://www.who.int/publications/m/item/influenza-at-the-human-animal-interface-summary-and-assessment-28-february-2020 (accessed August 2, 2021).

[41] World Health Organization. Influenza at the human-animal interface summary and assessment as of 3 March 2015. Emerg Situational Updat 2015. http://www.who.int/csr/don/8-february-2015-avian-influenza/en/ (accessed August 2, 2021).

[42] Swayne DE, Kapczynski D. Strategies and challenges for eliciting immunity against avian influenza virus in birds. Immunol Rev 2008;225:314–31. https://doi.org/10.1111/J.1600-065X.2008.00668.X.

[43] Todd C. Experiments on the Virus of Fowl-Plague. (II). Br J Exp Pathol 1928;9:101.

[44] Swayne DE. Avian influenza vaccines and therapies for poultry. Comp Immunol Microbiol Infect Dis 2009;32:351–63. https://doi.org/10.1016/J.CIMID.2008.01.006.

[45] OECD, Food, of the United Nations AO. OECD-FAO Agricultural Outlook 2022-2031. 2022. https://doi.org/https://doi.org/https://doi.org/10.1787/f1b0b29c-en.

[46] Statista. Production of eggs worldwide. Consum Goods FMCG; Food Nutr 2021. https://www.statista.com/statistics/263972/egg-production-worldwide-since-1990/ (accessed October 28, 2022).

[47] Chen H. Avian influenza vaccination: the experience in China. OIE Rev Sci Tech 2009;28:267–74. https://doi.org/10.20506/RST.28.1.1860.

[48] Sautto GA, Kirchenbaum GA, Ross TM. Towards a universal influenza vaccine:

Different approaches for one goal. Virol J 2018;15:1–12. https://doi.org/10.1186/s12985-017-0918-y.

[49] Young B, Sadarangani S, Jiang L, Wilder-Smith A, Chen MIC. Duration of influenza vaccine effectiveness: A systematic review, meta-analysis, and meta-regression of test- negative design case-control studies. J Infect Dis 2018;217:731–41. https://doi.org/10.1093/infdis/jix632.

[50] Peacock T, Reddy K, James J, Adamiak B, Barclay W, Shelton H, et al. Antigenic mapping of an H9N2 avian influenza virus reveals two discrete antigenic sites and a novel mechanism of immune escape. Sci Rep 2016;6:1–12. https://doi.org/10.1038/srep18745.

[51] Holzer B, Rijal P, McNee A, Paudyal B, Martini V, Clark B, et al. Protective porcine influenza virus-specific monoclonal antibodies recognize similar haemagglutinin epitopes as humans. PLoS Pathog 2021;17:e1009330. https://doi.org/10.1371/JOURNAL.PPAT.1009330.

[52] Rimi NA, Hassan MZ, Chowdhury S, Rahman M, Sultana R, Biswas PK, et al. A Decade of Avian Influenza in Bangladesh: Where Are We Now? Trop Med Infect Dis 2019, Vol 4, Page 119 2019;4:119. https://doi.org/10.3390/TROPICALMED4030119.

[53] Koutsakos M, Kedzierska K, Subbarao K. Immune Responses to Avian Influenza Viruses. J Immunol 2019;202:382–91. https://doi.org/10.4049/jimmunol.1801070.

[54] Davison F. The Importance of the Avian Immune System and its Unique Features. Avian Immunol 2014:1–9. https://doi.org/10.1016/B978-0-12-396965-1.00001-7.

[55] Evseev D, Magor KE. Innate Immune Responses to Avian Influenza Viruses in Ducks and Chickens. Vet Sci 2019, Vol 6, Page 5 2019;6:5. https://doi.org/10.3390/VETSCI6010005.

[56] Alick, Isaacs, Jean L. Virus interference. I. The interferon. Proc R Soc London Ser B - Biol Sci 1957;147:258–67. https://doi.org/10.1098/rspb.1957.0048.

[57] Taylor MW. Interferons. Viruses Man A Hist Interact 2014:101. https://doi.org/10.1007/978-3-319-07758-1_7.

[58] Vervelde L, Kapczynski DR. The innate and adaptive immune response to avian influenza virus. Anim Influ 2016:133–52. https://doi.org/10.1002/9781118924341.CH6.

[59] Barber MRW, Aldridge JR, Webster RG, Magor KE. Association of RIG-I with innate immunity of ducks to influenza. Proc Natl Acad Sci U S A 2010;107:5913–8. https://doi.org/10.1073/PNAS.1001755107/SUPPL_FILE/PNAS.201001755SI.PDF.

[60] Magor KE, Miranzo Navarro D, Barber MRW, Petkau K, Fleming-Canepa X,

Blyth GAD, et al. Defense genes missing from the flight division. Dev Comp Immunol 2013;41:377–88. https://doi.org/10.1016/J.DCI.2013.04.010.

[61] Iwasaki A, Pillai PS. Innate immunity to influenza virus infection. Nat Rev Immunol 2014;14:315–28. https://doi.org/10.1038/nri3665.

[62] Philbin VJ, Iqbal M, Boyd Y, Goodchild MJ, Beal RK, Bumstead N, et al. Identification and characterization of a functional, alternatively spliced Toll-like receptor 7 (TLR7) and genomic disruption of TLR8 in chickens. Immunology 2005;114:507–21. https://doi.org/10.1111/J.1365-2567.2005.02125.X.

[63] Kato H, Takeuchi O, Sato S, Yoneyama M, Yamamoto M, Matsui K, et al. Differential roles of MDA5 and RIG-I helicases in the recognition of RNA viruses. Nature 2006;441:101–5. https://doi.org/10.1038/NATURE04734.

[64] Loo Y-M, Fornek J, Crochet N, Bajwa G, Perwitasari O, Martinez-Sobrido L, et al. Distinct RIG-I and MDA5 Signaling by RNA Viruses in Innate Immunity. J Virol 2008;82:335–45. https://doi.org/10.1128/jvi.01080-07.

[65] Nakhaei P, Genin P, Civas A, Hiscott J. RIG-I-like receptors: Sensing and responding to RNA virus infection. Semin Immunol 2009;21:215–22. https://doi.org/10.1016/j.smim.2009.05.001.

[66] Yoneyama M, Fujita T. RNA recognition and signal transduction by RIG-I-like receptors. Immunol Rev 2009;227:54–65. https://doi.org/10.1111/J.1600-065X.2008.00727.X.

[67] Barber MRW, Aldridge JR, Fleming-Canepa X, Wang YD, Webster RG, Magor KE. Identification of avian RIG-I responsive genes during influenza infection. Mol Immunol 2013;54:89–97. https://doi.org/10.1016/j.molimm.2012.10.038.

[68] Lisi F, Zelikin AN, Chandrawati R. Nitric Oxide to Fight Viral Infections. Adv Sci 2021;8. https://doi.org/10.1002/advs.202003895.

[69] Burggraaf S, Bingham J, Payne J, Kimpton WG, Lowenthal JW, Bean AGD. Increased inducible nitric oxide synthase expression in organs is associated with a higher severity of H5N1 influenza virus infection. PLoS One 2011;6. https://doi.org/10.1371/journal.pone.0014561.

[70] Nogusa S, Ritz BW, Kassim SH, Jennings SR, Gardner EM. Characterization of age-related changes in natural killer cells during primary influenza infection in mice. Mech Ageing Dev 2008;129:223–30. https://doi.org/10.1016/J.MAD.2008.01.003.

[71] Stein-Streilein J, Guffee J, Fan W. Locally and systemically derived natural killer cells participate in defense against intranasally inoculated influenza virus. Reg Immunol 1988;1:100–5.

[72] Hamerman JA, Ogasawara K, Lanier LL. NK cells in innate immunity. Curr Opin Immunol 2005;17:29–35. https://doi.org/10.1016/J.COI.2004.11.001.

[73] Jansen CA, De Geus ED, Van Haarlem DA, Van De Haar PM, Löndt BZ, Graham SP, et al. Differential lung NK cell responses in avian influenza virus infected chickens correlate with pathogenicity. Sci Rep 2013;3. https://doi.org/10.1038/SREP02478.

[74] Vervelde L, Reemers SS, van Haarlem DA, Post J, Claassen E, Rebel JMJ, et al. Chicken dendritic cells are susceptible to highly pathogenic avian influenza viruses which induce strong cytokine responses. Dev Comp Immunol 2013;39:198–206. https://doi.org/10.1016/J.DCI.2012.10.011.

[75] Kwa S, Beverley P, Smith AL. Peyer's patches are required for the induction of rapid Th1 responses in the gut and mesenteric lymph nodes during an enteric infection. J Immunol 2006;176:7533–41. https://doi.org/10.4049/JIMMUNOL.176.12.7533.

[76] Smith AL, Göbel TW. Avian T Cells: Antigen Recognition and Lineages. Avian Immunol 2014:91–102. https://doi.org/10.1016/B978-0-12-396965-1.00005-4.

[77] Ratcliffe MJH, Härtle S. B Cells, the Bursa of Fabricius and the Generation of Antibody Repertoires. Avian Immunol., Academic Press; 2014, p. 65–89. https://doi.org/10.1016/B978-0-12-396965-1.00004-2.

[78] Pieper J, Methner U, Berndt A. Heterogeneity of avian γδ T cells. Vet Immunol Immunopathol 2008;124:241–52. https://doi.org/10.1016/j.vetimm.2008.03.008.

[79] Dixon R, Preston SG, Dascalu S, Flammer PG, Fiddaman SR, McLoughlin K, et al. Repertoire analysis of γδ T cells in the chicken enables functional annotation of the genomic region revealing highly variable pan-tissue TCR gamma V gene usage as well as identifying public and private repertoires. BMC Genomics 2021;22:1–19. https://doi.org/10.1186/s12864-021-08036-9.

[80] Hayday AC. γδ T Cell Update: Adaptate Orchestrators of Immune Surveillance. J Immunol 2019;203:311–20. https://doi.org/10.4049/JIMMUNOL.1800934.

[81] Ribot JC, Lopes N, Silva-Santos B. γδ T cells in tissue physiology and surveillance. Nat Rev Immunol 2021;21:221–32. https://doi.org/10.1038/s41577-020-00452-4.

[82] Zhang T, Li Q, Li X, Kang L, Jiang Y, Sun Y. Characterization of the chicken T cell receptor γ repertoire by high-throughput sequencing. BMC Genomics 2021;22:1–13. https://doi.org/10.1186/S12864-021-07975-7/FIGURES/9.

[83] Berndt A, Pieper J, Methner U. Circulating γδ T cells in response to Salmonella enterica serovar enteritidis exposure in chickens. Infect Immun 2006;74:3967–78. https://doi.org/10.1128/IAI.01128-05/ASSET/25BACC54-428A-4918-8051-8C19A6C9C903/ASSETS/GRAPHIC/ZII0070659800005.JPEG.

[84] Matsuyama-Kato A, Iseki H, Boodhoo N, Bavananthasivam J, Alqazlan N, Abdul-Careem MF, et al. Phenotypic characterization of gamma delta (γδ) T cells in chickens infected with or vaccinated against Marek's disease virus. Virology

2022;568:115–25. https://doi.org/10.1016/J.VIROL.2022.01.012.

[85] Fenzl L, Göbel TW, Neulen ML. γδ T cells represent a major spontaneously cytotoxic cell population in the chicken. Dev Comp Immunol 2017;73:175–83. https://doi.org/10.1016/J.DCI.2017.03.028.

[86] Chen L, Fakiola M, Staines K, Butter C, Kaufman J. Functional alleles of chicken BG genes, members of the butyrophilin gene family, in peripheral T cells. Front Immunol 2018;9:1–17. https://doi.org/10.3389/fimmu.2018.00930.

[87] Kind TJ, Osborn BA, Goldsby RA. Kuby Immunology. 8th ed. W. H. Freeman; 2007.

[88] Kaufman J. Generalists and Specialists : A New View of How MHC Class I Molecules Fight Infectious Pathogens. Trends Immunol 2018;39:367–79. https://doi.org/10.1016/j.it.2018.01.001.

[89] Song L, Xiong D, Hu M, Kang X, Pan Z, Jiao X. Enhanced humoural and cellular immune responses to influenza H7N9 antigen HA1-2 fused with flagellin in chickens. BMC Vet Res 2017;13:1–9. https://doi.org/10.1186/s12917-017-1106-4.

[90] Seo SH, Webster RG. Cross-reactive, cell-mediated immunity and protection of chickens from lethal H5N1 influenza virus infection in Hong Kong poultry markets. J Virol 2001;75:2516–25. https://doi.org/10.1128/JVI.75.6.2516-2525.2001.

[91] Xu C, Ye H, Qiu W, Lin H, Chen Y, Zhang H, et al. Phylogenetic classification of hemagglutinin gene of H9N2 avian influenza viruses isolated in China during 2012–2016 and evaluation of selected candidate vaccine strains. Poult Sci 2018;97:3023–30. https://doi.org/10.3382/PS/PEY154.

[92] Dai M, Li S, Keyi Shi, Sun H, Zhao L, Deshui Yu, et al. Comparative analysis of key immune protection factors in H9N2 avian influenza viruses infected and immunized specific pathogen–free chicken. Poult Sci 2021;100:39–46. https://doi.org/10.1016/j.psj.2020.09.080.

[93] Bi Y, Li J, Li S, Fu G, Jin T, Zhang C, et al. Dominant subtype switch in avian influenza viruses during 2016–2019 in China. Nat Commun 2020;11:1–12. https://doi.org/10.1038/s41467-020-19671-3.

[94] Cornelissen JBWJ, Vervelde L, Post J, Rebel JMJ. Differences in highly pathogenic avian influenza viral pathogenesis and associated early inflammatory response in chickens and ducks. Avian Pathol 2013;42:347–64. https://doi.org/10.1080/03079457.2013.807325.

[95] Anderson RW, Bennink JR, Yewdell JW, Maloy WL, Coligan JE. Influenza basic polymerase 2 peptides are recognized by influenza nucleoprotein-specific cytotoxic T lymphocytes. Mol Immunol 1992;29:1089–96. https://doi.org/10.1016/0161-5890(92)90041-U.

[96] Altstein AD, Gitelman AK, Smirnov YA, Piskareva LM, Zakharova LG, Pashvykina G V., et al. Immunization with influenza A NP-expressing vaccinia virus recombinant protects mice against experimental infection with human and avian influenza viruses. Arch Virol 2006;151:921–31. https://doi.org/10.1007/s00705-005-0676-9.

[97] Kreijtz JHCM, Fouchier RAM, Rimmelzwaan GF. Immune responses to influenza virus infection. Virus Res 2011;162:19–30. https://doi.org/10.1016/J.VIRUSRES.2011.09.022.

[98] Kreijtz JHCM, Mutsert G de, Baalen CA van, Fouchier RAM, Osterhaus ADME, Rimmelzwaan GF. Cross-Recognition of Avian H5N1 Influenza Virus by Human Cytotoxic T-Lymphocyte Populations Directed to Human Influenza A Virus. J Virol 2008;82:5161. https://doi.org/10.1128/JVI.02694-07.

[99] Wang Z, Wan Y, Qiu C, Quiñones-Parra S, Zhu Z, Loh L, et al. Recovery from severe H7N9 disease is associated with diverse response mechanisms dominated by CD8+ T cells. Nat Commun 2015;6:6833–6833. https://doi.org/10.1038/ncomms7833.

[100] Sridhar S, Begom S, Bermingham A, Hoschler K, Adamson W, Carman W, et al. Cellular immune correlates of protection against symptomatic pandemic influenza. Nat Med 2013;19:1305–12. https://doi.org/10.1038/nm.3350.

[101] Thomas PG, Keating R, Hulse-Post DJ, Doherty PC. Cell-mediated protection in influenza infection. Emerg Infect Dis 2006;12:48–54. https://doi.org/10.3201/eid1201.051237.

[102] Zhang H, Zheng H, Guo P, Hu L, Wang Z, Wang J, et al. Broadly Protective CD8 + T Cell Immunity to Highly Conserved Epitopes Elicited by Heat Shock Protein gp96-Adjuvanted Influenza Monovalent Split Vaccine. J Virol 2021;95:507–28. https://doi.org/10.1128/jvi.00507-21.

[103] Fellah JS, Jaffredo T, Nagy N, Dunon D. Development of the Avian Immune System. Avian Immunol 2014:45–63. https://doi.org/10.1016/B978-0-12-396965-1.00003-0.

[104] Oláh I, Nagy N, Vervelde L. Structure of the Avian Lymphoid System. Avian Immunol. Second Ed., Academic Press; 2013, p. 11–44. https://doi.org/10.1016/B978-0-12-396965-1.00002-9.

[105] Yang WT, Yang GL, Shi SH, Liu YY, Huang H Bin, Jiang YL, et al. Protection of chickens against H9N2 avian influenza virus challenge with recombinant Lactobacillus plantarum expressing conserved antigens. Appl Microbiol Biotechnol 2017;101:4593–603. https://doi.org/10.1007/s00253-017-8230-8.

[106] Schijns VEJC, van de Zande S, Lupiani B, Reddy SM. Practical Aspects of Poultry Vaccination. Avian Immunol 2014:345–62. https://doi.org/10.1016/B978-0-12-396965-1.00020-0.

[107] Magor KE. Immunoglobulin genetics and antibody responses to influenza in ducks. Dev Comp Immunol 2011;35:1008–17. https://doi.org/10.1016/j.dci.2011.02.011.

[108] Kim J-K, Seiler P, Forrest HL, Khalenkov AM, Franks J, Kumar M, et al. Pathogenicity and Vaccine Efficacy of Different Clades of Asian H5N1 Avian Influenza A Viruses in Domestic Ducks. J Virol 2008;82:11374–82. https://doi.org/10.1128/jvi.01176-08.

[109] Murphy KM. Janeway's Immunobiology. 8th ed. Garland Science; 2012.

[110] Lahti JM, Chen CL, Tjoelker LW, Pickel JM, Schat KA, Calnek BW, et al. Two distinct alpha beta T-cell lineages can be distinguished by the differential usage of T-cell receptor V beta gene segments. Proc Natl Acad Sci U S A 1991;88:10956–60. https://doi.org/10.1073/pnas.88.23.10956.

[111] Zhang T, Liu G, Wei Z, Wang Y, Kang L, Jiang Y, et al. Genomic organization of the chicken TCRβ locus originated by duplication of a Vβ segment combined with a trypsinogen gene. Vet Immunol Immunopathol 2020;219. https://doi.org/10.1016/j.vetimm.2019.109974.

[112] Glick B, Chang T, Science RJ-P, 1956 undefined. The bursa of Fabricius and antibody production. Elsevier n.d.

[113] Reynaud C -A, Anquez V, Weill J -C. The chicken D locus and its contribution to the immunoglobulin heavy chain repertoire. Eur J Immunol 1991;21:2661–70. https://doi.org/10.1002/eji.1830211104.

[114] Reynaud CA, Anquez V, Grimal H, Weill JC. A hyperconversion mechanism generates the chicken light chain preimmune repertoire. Cell 1987;48:379–88. https://doi.org/10.1016/0092-8674(87)90189-9.

[115] Friedensohn S, Khan TA, Reddy ST. Advanced Methodologies in High-Throughput Sequencing of Immune Repertoires. Trends Biotechnol 2017;35:203–14. https://doi.org/10.1016/j.tibtech.2016.09.010.

[116] Heather JM, Ismail M, Oakes T, Chain B. High-throughput sequencing of the T-cell receptor repertoire: Pitfalls and opportunities. Brief Bioinform 2018;19:554–65. https://doi.org/10.1093/bib/bbw138.

[117] Greiff V, Miho E, Menzel U, Reddy ST. Bioinformatic and Statistical Analysis of Adaptive Immune Repertoires. Trends Immunol 2015;36:738–49. https://doi.org/10.1016/j.it.2015.09.006.

[118] Lindau P, Robins HS. Advances and applications of immune receptor sequencing in systems immunology. Curr Opin Syst Biol 2017;1:62–8. https://doi.org/10.1016/j.coisb.2016.12.009.

[119] Sant S, Grzelak L, Wang Z, Pizzolla A, Koutsakos M, Crowe J, et al. Single-Cell Approach to Influenza-Specific CD8+ T Cell Receptor Repertoires Across

Different Age Groups, Tissues, and Following Influenza Virus Infection. Front Immunol 2018;9:1453.

[120] Gil A, Yassai MB, Naumov YN, Selin LK. Narrowing of Human Influenza A Virus-Specific T Cell Receptor α and β Repertoires with Increasing Age. J Virol 2015;89:4102 LP – 4116. https://doi.org/10.1128/JVI.03020-14.

[121] Ellebedy AH, Jackson KJL, Kissick HT, Nakaya HI, Davis CW, Roskin KM, et al. Defining antigen-specific plasmablast and memory B cell subsets in human blood after viral infection or vaccination. Nat Immunol 2016;17:1226.

[122] Jiang N, He J, Weinstein JA, Penland L, Sasaki S, He X-S, et al. Lineage Structure of the Human Antibody Repertoire in Response to Influenza Vaccination. Sci Transl Med 2013;5:171ra19 LP-171ra19. https://doi.org/10.1126/scitranslmed.3004794.

[123] Hou D, Ying T, Wang L, Chen C, Lu S, Wang Q, et al. Immune Repertoire Diversity Correlated with Mortality in Avian Influenza A (H7N9) Virus Infected Patients. Sci Rep 2016;6:33843. https://doi.org/10.1038/srep33843.

[124] Preston SG. Reptools: A suite of tools for annotating and processing immune repertoire data from Illumina sequencing n.d. https://github.com/sgp79/reptools (accessed June 13, 2022).

[125] Altschul SF, Gish W, Miller W, Myers EW, Lipman DJ. Basic local alignment search tool. J Mol Biol 1990;215:403–10. https://doi.org/10.1016/S0022-2836(05)80360-2.

[126] Smith TF, Waterman MS. Identification of common molecular subsequences. J Mol Biol 1981;147:195–7. https://doi.org/10.1016/0022-2836(81)90087-5.

[127] Rognes T. Faster Smith-Waterman database searches with inter-sequence SIMD parallelisation. BMC Bioinformatics 2011;12:1–11. https://doi.org/10.1186/1471-2105-12-221.

[128] R Core Team. R: A Language and Environment for Statistical Computing 2018.

[129] Holland S. Data Analysis in the Geosciences. Lect Notes, Dep Geol Univ Georg 2021. http://strata.uga.edu/8370/rtips/proportions.html (accessed June 13, 2022).

[130] CRAN - Package lmerTest n.d. https://cran.r-project.org/web/packages/lmerTest/index.html (accessed March 1, 2022).

[131] Douglas Bates, Martin Maechler BB. CRAN - Package lme4. CRAN 2014. https://cran.r-project.org/web/packages/lme4/index.html (accessed March 1, 2022).

[132] Chao A, Chiu CH, Jost L. Phylogenetic diversity measures based on Hill numbers. Philos Trans R Soc B Biol Sci 2010;365:3599–609. https://doi.org/10.1098/RSTB.2010.0272.

[133] Chao A, Gotelli NJ, Hsieh TC, Sander EL, Ma KH, Colwell RK, et al. Rarefaction and extrapolation with Hill numbers: A framework for sampling and estimation in species diversity studies. Ecol Monogr 2014;84:45–67. https://doi.org/10.1890/13-0133.1.

[134] Hsieh TC, Ma KH, Chao A. iNEXT: an R package for rarefaction and extrapolation of species diversity (Hill numbers). Methods Ecol Evol 2016;7:1451–6. https://doi.org/10.1111/2041-210X.12613.

[135] Sommer F, Bäckhed F. The gut microbiota — masters of host development and physiology. Nat Publ Gr 2013;11:227–38. https://doi.org/10.1038/nrmicro2974.

[136] Shang Y, Kumar S, Oakley B, Kim WK. Chicken gut microbiota: Importance and detection technology. Front Vet Sci 2018;5. https://doi.org/10.3389/fvets.2018.00254.

[137] Kabir SML. The role of probiotics in the poultry industry. Int J Mol Sci 2009;10:3531–46. https://doi.org/10.3390/ijms10083531.

[138] Oakley BB, Lillehoj HS, Kogut MH, Kim WK, Maurer JJ, Pedroso A, et al. The chicken gastrointestinal microbiome. FEMS Microbiol Lett 2014;360:100–12. https://doi.org/10.1111/1574-6968.12608.

[139] O'Hara AM, Shanahan F. The gut flora as a forgotten organ. EMBO Rep 2006;7:688–93. https://doi.org/10.1038/sj.embor.7400731.

[140] Hansen AK, Hansen CHF. The microbiome and rodent models of immune mediated diseases. Mamm Genome 2021;32:251. https://doi.org/10.1007/S00335-021-09866-4.

[141] Zheng D, Liwinski T, Elinav E. Interaction between microbiota and immunity in health and disease. Cell Res 2020 306 2020;30:492–506. https://doi.org/10.1038/s41422-020-0332-7.

[142] Muir WM, Wong GKS, Zhang Y, Wang J, Groenen MAM, Crooijmans RPMA, et al. Genome-wide assessment of worldwide chicken SNP genetic diversity indicates significant absence of rare alleles in commercial breeds. Proc Natl Acad Sci U S A 2008;105:17312–7. https://doi.org/10.1073/pnas.0806569105.

[143] Smith AL, Powers C, Beal RK. The Avian Enteric Immune System in Health and Disease. In: Schat KA, Kaspers B, Kaiser P, editors. Avian Immunol., Academic Press; 2014, p. 227–50.

[144] Mwangi WN, Beal RK, Powers C, Wu X, Humphrey T, Watson M, et al. Regional and global changes in TCRαβ T cell repertoires in the gut are dependent upon the complexity of the enteric microflora. Dev Comp Immunol 2010;34:406–17. https://doi.org/10.1016/j.dci.2009.11.009.

[145] Rosati E, Dowds CM, Liaskou E, Henriksen EKK, Karlsen TH, Franke A.

Overview of methodologies for T-cell receptor repertoire analysis. BMC Biotechnol 2017;17:1–16. https://doi.org/10.1186/s12896-017-0379-9.

[146] Woodsworth DJ, Castellarin M, Holt RA. Sequence analysis of T-cell repertoires in health and disease. Genome Med 2013;5:1. https://doi.org/10.1186/gm502.

[147] Padovan E, Casorati G, Dellabona P, Meyer S, Brockhaus M, Lanzavecchia A. Expression of two T cell receptor α chains: Dual receptor T cells. Science (80-) 1993;262:422–4. https://doi.org/10.1126/science.8211163.

[148] Kim I-J, You SK, Kim H, Yeh H-Y, Sharma JM. Characteristics of Bursal T Lymphocytes Induced by Infectious Bursal Disease Virus. J Virol 2000;74:8884. https://doi.org/10.1128/JVI.74.19.8884-8892.2000.

[149] Lefranc MP, Giudicelli V, Ginestoux C, Bodmer J, Müller W, Bontrop R, et al. IMGT, the international ImMunoGeneTics database. Nucleic Acids Res 1999;27:209–12. https://doi.org/10.1093/nar/27.1.209.

[150] Yu K, Shi J, Lu D, Yang Q. Comparative analysis of CDR3 regions in paired human αβ CD8 T cells. FEBS Open Bio 2019;9:1450–9. https://doi.org/10.1002/2211-5463.12690.

[151] Zamyatnin AA. Protein volume in solution. Prog Biophys Mol Biol 1972;24:107–23. https://doi.org/10.1016/0079-6107(72)90005-3.

[152] Kyte J, Doolittle RF. A simple method for displaying the hydropathic character of a protein. J Mol Biol 1982;157:105–32. https://doi.org/10.1016/0022-2836(82)90515-0.

[153] Rabia LA, Zhang Y, Ludwig SD, Julian MC, Tessier PM. Net charge of antibody complementarity-determining regions is a key predictor of specificity. Protein Eng Des Sel 2018;31:409–18. https://doi.org/10.1093/protein/gzz002.

[154] Mwangi WN, Smith LP, Baigent SJ, Beal RK, Nair V, Smith AL. Clonal Structure of Rapid-Onset MDV-Driven CD4+ Lymphomas and Responding CD8+ T Cells. PLoS Pathog 2011;7. https://doi.org/10.1371/journal.ppat.1001337.

[155] Ren C, Yin G, Qin M, Suo J, Lv Q, Xie L, et al. CDR3 analysis of TCR Vβ repertoire of CD8+ T cells from chickens infected with Eimeria maxima. Exp Parasitol 2014;143:1–4. https://doi.org/10.1016/j.exppara.2014.04.016.

[156] Brisbin JT, Gong J, Sharif S. Interactions between commensal bacteria and the gut-associated immune system of the chicken. Anim Heal Res Rev 2008;9:101–10. https://doi.org/10.1017/S146625230800145X.

[157] Wickramasuriya SS, Park I, Lee K, Lee Y, Kim WH, Nam H, et al. Role of Physiology, Immunity, Microbiota, and Infectious Diseases in the Gut Health of Poultry. Vaccines 2022;10:172. https://doi.org/10.3390/vaccines10020172.

[158] Rautenschlein S, von Samson-Himmelstjerna G, Haase C. A comparison of

immune responses to infection with virulent infectious bursal disease virus (IBDV) between specific-pathogen-free chickens infected at 12 and 28 days of age. Vet Immunol Immunopathol 2007;115:251–60. https://doi.org/10.1016/J.VETIMM.2006.11.002.

[159] Tanimura N, Sharma JM. Appearance of T cells in the bursa of Fabricius and cecal tonsils during the acute phase of infectious bursal disease virus infection in chickens. Avian Dis 1997;41:638–45. https://doi.org/10.2307/1592155.

[160] Laydon DJ, Bangham CRM, Asquith B. Estimating T-cell repertoire diversity: limitations of classical estimators and a new approach. Philos Trans R Soc B Biol Sci 2015;370. https://doi.org/10.1098/RSTB.2014.0291.

[161] Shugay M, Bolotin DA, Putintseva E V., Pogorelyy M V., Mamedov IZ, Chudakov DM. Huge overlap of individual TCR beta repertoires. Front Immunol 2013;4:466. https://doi.org/10.3389/fimmu.2013.00466.

[162] Zajonc DM, Girardi E. Recognition of microbial glycolipids by Natural Killer T cells. Front Immunol 2015;6:400. https://doi.org/10.3389/fimmu.2015.00400.

[163] Tweedie S, Braschi B, Gray K, Jones TEM, Seal RL, Yates B, et al. Genenames.org: The HGNC and VGNC resources in 2021. Nucleic Acids Res 2021;49:D939–46. https://doi.org/10.1093/nar/gkaa980.

[164] Pennington DJ, Vermijlen D, Wise EL, Clarke SL, Tigelaar RE, Hayday AC. The integration of conventional and unconventional T cells that characterizes cell-mediated responses. Adv Immunol 2005;87:27–59. https://doi.org/10.1016/S0065-2776(05)87002-6.

[165] Kaufman J, Milne S, Göbel TWF, Walker BA, Jacob JP, Auffray C, et al. The chicken B locus is a minimal essential major histocompatibility complex. Nature 1999;401:923–5. https://doi.org/10.1038/44856.

[166] Godfrey DI, Koay HF, McCluskey J, Gherardin NA. The biology and functional importance of MAIT cells. Nat Immunol 2019;20:1110–28. https://doi.org/10.1038/s41590-019-0444-8.

[167] Brennan PJ, Brigl M, Brenner MB. Invariant natural killer T cells: an innate activation scheme linked to diverse effector functions. Nat Rev Immunol 2013 132 2013;13:101–17. https://doi.org/10.1038/nri3369.

[168] Salomonsen J, Sørensen MR, Marston DA, Rogers SL, Collen T, Van Hateren A, et al. Two CD1 genes map to the chicken MHC, indicating that CD1 genes are ancient and likely to have been present in the primordial MHC. Proc Natl Acad Sci U S A 2005;102:8668–73. https://doi.org/10.1073/pnas.0409213102.

[169] Maruoka T, Tanabe H, Chiba M, Kasahara M. Chicken CD1 genes are located in the MHC: CD1 and endothelial protein C receptor genes constitute a distinct subfamily of class-I-like genes that predates the emergence of mammals.

Immunogenetics 2005;57:590–600. https://doi.org/10.1007/s00251-005-0016-y.

[170] Dalgaard TS, Norup LR, Pedersen AR, Handberg KJ, Jørgensen PH, Juul-Madsen HR. Flow cytometric assessment of chicken T cell-mediated immune responses after Newcastle disease virus vaccination and challenge. Vaccine 2010;28:4506–14. https://doi.org/10.1016/j.vaccine.2010.04.044.

[171] Han Y, Gu Y, Zhang AC, Lo YH. Review: Imaging technologies for flow cytometry. Lab Chip 2016;16:4639–47. https://doi.org/10.1039/c6lc01063f.

[172] Mouse Anti-Chicken Bu-1 Technical Bulletin. South Biotech n.d.

[173] Mouse Anti-Chicken TCRαβ/Vβ1 Technical Bulletin. South Biotech n.d.:8–9.

[174] Mouse Anti-Chicken TCRαβ/Vβ2 Technical Bulletin. South Biotech n.d.:8–9.

[175] Mouse Anti-Chicken TCRγδ Technical Bulletin. South Biotech n.d.:8–9.

[176] Mouse Anti-Chicken CD3 Technical Bulletin. South Biotech n.d.:8–9.

[177] Mouse Anti-Chicken CD8α Technical Bulletin. South Biotech n.d.:8–9.

[178] Mouse Anti-Chicken CD8β Technical Bulletin. South Biotech n.d.

[179] Mouse Anti-Chicken CD4 Technical Bulletin. South Biotech n.d.

[180] Hoffmann E, Neumann G, Kawaoka Y, Hobom G, Webster RG. A DNA transfection system for generation of influenza A virus from eight plasmids. Proc Natl Acad Sci 2000;97:6108–13. https://doi.org/10.1073/PNAS.100133697.

[181] Lone NA, Spackman E, Kapczynski D. Immunologic evaluation of 10 different adjuvants for use in vaccines for chickens against highly pathogenic avian influenza virus. Vaccine 2017;35:3401–8. https://doi.org/10.1016/j.vaccine.2017.05.010.

[182] WHO Global Influenza Programme Surveillance and Epidemiology team. WHO Global Influenza Surveillance Network Manual for the laboratory diagnosis and virological surveillance of influenza. 2011.

[183] Sridhar S, Brokstad KA, Cox RJ. Influenza Vaccination Strategies: Comparing Inactivated and Live Attenuated Influenza Vaccines. Vaccines 2015;3. https://doi.org/10.3390/VACCINES3020373.

[184] Kotey E, Lukosaityte D, Quaye O, Ampofo W, Awandare G, Iqbal M. Current and novel approaches in influenza management. Vaccines 2019;7. https://doi.org/10.3390/vaccines7020053.

[185] Kruskal WH, Wallis WA. Use of Ranks in One-Criterion Variance Analysis. J Am Stat Assoc 1952;47:583–621. https://doi.org/10.1080/01621459.1952.10483441.

[186] Benjamini Y, Hochberg Y. Controlling the False Discovery Rate: A Practical and

Powerful Approach to Multiple Testing. J R Stat Soc Ser B 1995;57:289–300. https://doi.org/10.1111/j.2517-6161.1995.tb02031.x.

[187] Conover WJ, Iman RL. On Multiple-Comparisons Procedures. Tech Rep LA-7677-MS, Los Alamos Sci Lab 1979.

[188] Burnham KP, Anderson DR. Model Selection and Multimodel Inference. Springer New York; 2004. https://doi.org/10.1007/B97636.

[189] James J, Howard W, Iqbal M, Nair VK, Barclay WS, Shelton H. Influenza a virus PB1-F2 protein prolongs viral shedding in chickens lengthening the transmission window. J Gen Virol 2016;97:2516–27. https://doi.org/10.1099/jgv.0.000584.

[190] Iqbal M, Yaqub T, Mukhtar N, Shabbir MZ, McCauley JW. Infectivity and transmissibility of H9N2 avian influenza virus in chickens and wild terrestrial birds. Vet Res 2013;44:100. https://doi.org/10.1186/1297-9716-44-100.

[191] Hernandez-Vargas EA. Modeling Influenza Virus Infection. In: Sánchez E, editor. Model. Control Infect. Dis. Host, Academic Press; 2019, p. 65–84. https://doi.org/10.1016/b978-0-12-813052-0.00015-4.

[192] Lee HY, Topham DJ, Park SY, Hollenbaugh J, Treanor J, Mosmann TR, et al. Simulation and Prediction of the Adaptive Immune Response to Influenza A Virus Infection. J Virol 2009;83:7151–65. https://doi.org/10.1128/JVI.00098-09.

[193] Lage H, Pirlot JF, Reynard F, Den T Van, Ferreira HL, Jean AD, et al. Immune Responses and Protection Against H5N1 Highly Pathogenic Avian Influenza Virus Induced by the Newcastle Disease Virus H5 Vaccine in Ducks Berg , Michel Bublot and Bénédicte Lambrecht Source : Avian Diseases , Vol . 56 , No . 4 , Supplement : Proceed 2019;56.

[194] Spackman E, editor. Animal Influenza Virus 2020;2123. https://doi.org/10.1007/978-1-0716-0346-8.

[195] Van Der Goot JA, Koch G, De Jong MCM, Van Boven M. Quantification of the effect of vaccination on transmission of avian influenza (H7N7) in chickens. Proc Natl Acad Sci U S A 2005;102:18141–6. https://doi.org/10.1073/PNAS.0505098102/SUPPL_FILE/05098TABLE13.DOC.

[196] Boyle DB, Selleck P, Heine HG. Vaccinating chickens against avian influenza with fowlpox recombinants expressing the H7 haemagglutinin. Aust Vet J 2000;78:44–8. https://doi.org/10.1111/j.1751-0813.2000.tb10359.x.

[197] Astill J, Alkie T, Yitbarek A, Taha-Abdelaziz K, Bavananthasivam J, Nagy É, et al. Induction of immune response in chickens primed in ovo with an inactivated H9N2 avian influenza virus vaccine. BMC Res Notes 2018;11:428. https://doi.org/10.1186/s13104-018-3537-9.

[198] Davelaar FG, Kouwenhoven B. Influence of maternal antibodies on vaccination of chicks of different ages against infectious bronchitis. Avian Pathol 1977;6:41–50. https://doi.org/10.1080/03079457708418211.

[199] Hao X, Li S, Chen L, Dong M, Wang J, Hu J, et al. Establishing a multicolor flow cytometry to characterize cellular immune response in chickens following h7n9 avian influenza virus infection. Viruses 2020;12:1396. https://doi.org/10.3390/v12121396.

[200] Degen WGJ, Van Daal N, Rothwell L, Kaiser P, Schijns VEJC. Th1/Th2 polarization by viral and helminth infection in birds. Vet Microbiol 2005;105:163–7. https://doi.org/10.1016/j.vetmic.2004.12.001.

[201] Seo SH, Peiris M, Webster RG. Protective Cross-Reactive Cellular Immunity to Lethal A/Goose/Guangdong/1/96-Like H5N1 Influenza Virus Is Correlated with the Proportion of Pulmonary CD8 + T Cells Expressing Gamma Interferon. J Virol 2002;76:4886–90. https://doi.org/10.1128/jvi.76.10.4886-4890.2002.

[202] Kavazović I, Polić B, Wensveen FM. Cheating the hunger games; Mechanisms controlling clonal diversity of CD8 effector and memory populations. Front Immunol 2018;9:2831. https://doi.org/10.3389/fimmu.2018.02831.

[203] Vainio O, Koch C, Toivanen A. B-L antigens (Class II) of the chicken major histocompatibility complex control T-B cell interaction. Immunogenetics 1984;19:131–40. https://doi.org/10.1007/BF00387856.

[204] Dai M, Xu C, Chen W, Liao M. Progress on chicken T cell immunity to viruses. Cell Mol Life Sci 2019;76:2779–88. https://doi.org/10.1007/s00018-019-03117-1.

[205] Sowder JT, Chen CLH, Lanier Ager L, Chan MM, Cooper MD. A large subpopulation of avian T cells express a homologue of the mammalian T gamma/delta receptor. J Exp Med 1988;167:315–22. https://doi.org/10.1084/JEM.167.2.315.

[206] Suarez DL, Schultz-Cherry S. Immunology of avian influenza virus: A review. Dev Comp Immunol 2000;24:269–83. https://doi.org/10.1016/S0145-305X(99)00078-6.

[207] Kaufman J. The Avian MHC. Avian Immunol 2014:149–67. https://doi.org/10.1016/B978-0-12-396965-1.00008-X.

[208] Schijns VEJC, van de Zande S, Lupiani B, Reddy SM. Practical Aspects of Poultry Vaccination. Avian Immunol 2014:345–62. https://doi.org/10.1016/B978-0-12-396965-1.00020-0.

[209] Skinner MA. Avian Immunosuppressive Diseases and Immunoevasion. Avian Immunol 2014:275–97. https://doi.org/10.1016/B978-0-12-396965-1.00016-9.

[210] ROSE ME, HESKETH P. Immunity to coccidia in chickens: adoptive transfer

with peripheral blood lymphocytes and spleen cells. Parasite Immunol 1982;4:171–85. https://doi.org/10.1111/j.1365-3024.1982.tb00429.x.

[211] Qi Q, Liu Y, Cheng Y, Glanville J, Zhang D, Lee JY, et al. Diversity and clonal selection in the human T-cell repertoire. Proc Natl Acad Sci U S A 2014;111:13139–44. https://doi.org/10.1073/pnas.1409155111.

[212] Wack A, Cossarizza A, Heltai S, Barbieri D, D'Addato S, Fransceschi C, et al. Age-related modifications of the human αβ T cell repertoire due to different clonal expansions in the CD4+ and CD8+ subsets. Int Immunol 1998;10:1281–8. https://doi.org/10.1093/intimm/10.9.1281.

[213] Lanzer KG, Johnson LL, Woodland DL, Blackman MA. Impact of ageing on the response and repertoire of influenza virus-specific CD4 T cells. Immun Ageing 2014;11:1–10. https://doi.org/10.1186/1742-4933-11-9.

[214] Shen CI, Wang CH, Shen SC, Lee HC, Liao JW, Su HL. The infection of chicken tracheal epithelial cells with a H6N1 avian influenza virus. PLoS One 2011;6:e18894. https://doi.org/10.1371/journal.pone.0018894.

[215] Lambert Emo K, Hyun YM, Reilly E, Barilla C, Gerber S, Fowell D, et al. Live Imaging of Influenza Infection of the Trachea Reveals Dynamic Regulation of CD8+ T Cell Motility by Antigen. PLoS Pathog 2016;12:e1005881. https://doi.org/10.1371/journal.ppat.1005881.